Seismic Control of Partially Observed Building Frames using MR Dampers

By

Vishisht Bhaiya

DEPARTMENT OF CIVIL ENGINEERING

Prof. S. D. Bharti
(Supervisor)

Prof. M. K. Shrimali
(Supervisor)

Submitted

in fulfillment of the requirements of the degree of Doctor of Philosophy

to the

MALAVIYA NATIONAL INSTITUTE OF TECHNOLOGY JAIPUR

INDIA

July, 2018

DECLARATION

It is certified that the work contained in this thesis entitled "*Seismic Control of Partially Observed Building Frames Using MR Dampers*", is original work and has not been submitted elsewhere for a degree.

July 2018

VISHISHT BHAIYA

2013RCE9534

CERTIFICATE

It is certified that the work contained in this thesis entitled "*Seismic Control of Partially Observed Building Frames Using MR Dampers*", by Mr. Vishisht Bhaiya (2013RCE 9534), has been carried out under our joint supervision. This work has not been submitted elsewhere for a degree.

(S. D. Bharti)
Professor
Civil Engineering
MNIT Jaipur

(M. K. Shrimali)
Professor
Civil Engineering
MNIT Jaipur

ABSTRACT

Although extensive research has been carried out on the semi-active control of building frames using MR dampers, research is still continuing on the subject. The literature review shows that there are certain areas where more investigations are needed such as the development of effective control algorithms for partially observed structure taking into the special features of the control using MR dampers, optimal placement of a limited number of MR dampers and sensors for partially observed systems and effective hybrid control of building frames using MR dampers. With the above background in view, the present work is undertaken. As a consequence, the following studies are carried out using thesis.

A new control algorithm called velocity tracking control (VTC) is presented for the semi-active control of partially observed building frames using MR dampers. The control scheme does not require the information regarding the complete state estimated from the partial observation if the measurements are taken from strategic locations. Since the determination of the control force in the MR damper is governed by the velocity and displacement of the floors where MR dampers are placed, an obvious choice for the strategic locations are the floors where the MR dampers are placed. The algorithm is developed based on physical reasoning substantiated by the Lyapunov stability condition of the first order filter used in the modified Bouc wen model to decide the voltage to be applied to the MR damper. The efficiency of the control algorithm is compared with that of a few standard algorithms, namely, Linear Quadratic Gaussian (LQG) with the clipped algorithm (LQGCl), bang-bang control, sliding mode with the clipped algorithm (SMCCl) and passive-on. The response quantities of interest for which percentage reduction in responses is compared include peak top floor displacement, peak inter story drift and maximum base shear for a number of real and two synthetically generated earthquakes.

Kalman filter works on the assumption that both excitation and measurement noise are Gaussian white. However, in reality, the excitations are non-white. Therefore, a new structural system is formulated by augmenting the state space equations of the structural system with the double filter equations whose output variable matches the desired excitation to the structural system. The input to the double filter is the Gaussian white noise. Thus, the assumptions inherent in the use of Kalman filter are strictly satisfied, and at the same time, by adjusting the filter parameters, the desired site-specific ground motion can be achieved. For online application of the control scheme, the

measured ground motion is fed into an ANN; the output from the ANN is the white noise that goes as input excitation to the augmented system for analyzing the control problem at hand. The responses of the new structural system are controlled using a limited number of MR dampers and observation sensors. Two types of random ground motions consistent with broadband and narrowband PSDFs of ground motions representing hard soil and soft soil conditions respectively are used as excitations to the structure. Three control algorithms, namely, LQG with clipped optimal control, bang-bang control and sliding mode with clipped optimal control are modified to determine the voltage to be applied to the MR damper. The results of the proposed formulation are compared with those of the conventional formulation in which the ground motion is directly used as input to the base of the building frame. Further, a sensitivity analysis is carried out to show how the error in the state estimation and hence, the control of responses varies with the assumed values of covariance of excitation and the noise used in the Kalman filter. The results of the sensitivity analysis help in the proper selection of the assumed values of the covariance of the excitation and the noise for online application of the control strategy.

An optimal placement strategy of MR dampers and sensors is presented for maximum reductions in response quantities of interest, namely, top floor displacement, maximum drift and base shear. The genetic algorithm is used to determine the optimal locations of sensors and dampers. The objective functions selected are the response quantities of interest. Two strategies for placement of measurements sensors are considered. In the first strategy, out of the available sensors, velocity sensors equal to the number of MR dampers are placed at locations of MR dampers and rest sensors are optimally placed. In the second strategy, no such condition is imposed on the placement of sensors. Optimal placements of MR dampers and sensors are obtained for bang bang and LQG with clipped optimal control.

A few hybrid control strategies comprising of different types of combinations of MR dampers and TMDs are attempted to either reduce the number of MR dampers to be employed to obtain the comparable reductions in the responses or alleviate the response reductions substantially compared to the use of MR dampers alone. They include i) STMD at the top floor and one MR damper at the first floor (STMDMR); ii) TMD at the top floor and two MR dampers placed at first and second floor (TMDMR2); and iii) three MR dampers placed at bottommost three floors and a TMD at the top floor (TMDMR3). The response parameters investigated in the study are the maximum top floor

displacement, maximum base shear, and maximum inter-story drift. Response reductions achieved with MR dampers alone are taken as the reference for comparison. Some of the control algorithms, namely LQR with the clipped algorithm, VTC and passive on presented in previous chapters are used for obtaining the controlled responses.

ACKNOWLEDGMENT

I am grateful to Professors S. D. Bharti, M. K. Shrimali and T K Datta at MNIT Jaipur, for their invaluable guidance and continuous support throughout the course of my Doctoral Programme. They have been an infinite source of encouragement for me, and their technical prowess nourished this thesis. I express my sincere gratitude towards Mr. Nishant Roy, who always remains available for technical discussions and guidance. He has always been, and will be, a source of inspiration for me, both on technical and personal fronts.

I would also like to express sincere gratitude towards my teachers, friends, faculty members, and staff members, at MNIT Jaipur. Their unending encouragement has been a source of positive energy, which helped me to have a better outlook, not only in terms of technical matters, but also in interpersonal learning and growth. The peer group at MNIT Jaipur, especially, Mr. Arnav Anuj Kasar, Mr. Shashi Narayan, Mr. Mohit Bhandari, and Mr. Mahdi Abdeddaim are acknowledged.

I am grateful to my parents and brother for all their love and support. Their trust in me has been the primary driving force and support for this work. No words can describe my gratitude towards my family and friends, who have always been there for me. Their unstinted and constant support has made this cruise enjoyable. At last, I would like to express gratitude towards almighty God, for showering grace on me, by giving an opportunity to pursue this enriching journey…

TABLE OF CONTENTS

LIST OF TABLES

LIST OF FIGURES

NOMENCLATURE

Notations	Description
U	MR damper force
$\dot{x}_v$	Pseudo relative velocity of damper
u_d	Relative displacement of the floor at which MR damper is placed
z_0	Evolutionary variable that describes the hysteretic behaviour of the damper
k_0	Stiffness at large velocity
x_0	Initial displacement of the accumulator
c_0	Viscous damping at large velocity
c_1	Viscous damping at low velocities for the force roll-off
k_1	Stiffness of the accumulator
α_0	Evolutionary coefficient of the dynamic model of MR damper
α, β, n and A_m	Shape parameters of the hysteresis loop
U_0	Output of first order filter of MR damper
V	Voltage applied to the MR damper
[M]	Mass matrix of the system VB-1
[C]	Damping matrix of the system VB-1
[K]	Stiffness matrix of the system VB-1
[G]	Damper location matrix
[z]	Displacement vector with respect to the ground
[r]	Influence coefficient vector
$\ddot{u}_g$	Earthquake ground acceleration
[A]	System matrix of state space of VB-1
[B]	Control matrix of state space of VB-1
[E]	Disturbance (excitation) matrix of state space of VB-1
[C]	Measurement matrix of state space of VB-1
[D]	Matrix multiplied by control force state space of VB-1
[x]	State vector of displacement and velocity
[y]	Vector of measured outputs

$\mathbf{[v]}$	Measurement noise vector
w	White noise
$\mathbf{I}$	Identity matrix
$\mathbf{O}$	Zeros matrix
d_i^r	Displacement of the piston of the r^{th} damper at the i^{th} time step.
v_i^r	Velocity of the piston of the r^{th} damper at the i^{th} time step
$\dot{x}^r$	Displacement of the r^{th} floor
$\hat{\mathbf{x}}(t)$	Estimated full state of the system
$\mathbf{K}(t)$	Kalman gain
$\mathbf{P}(t)$	Matrix associated with kalman gain
$\mathbf{V}$	Covariance matrices of white gaussian measurement noise
$\mathbf{W}$	Covariance matrices of excitation.
$\mathbf{L}(t)$	Feedback gain
$\mathbf{S}(t)$	Matrix associated with feed back gain
$\mathbf{Q}$	Weighing matrix multiplied with state vector in LQR cost function
$\mathbf{R}$	Weighing matrix multiplied with control force in LQR cost function
F_d	Desired control force obtained from LQR/ LQG/ sliding mode control algorithm
F_{mr}	MR damper force generated at the previous time step
V_{max}	Maximum voltage applied to the MR damper
H	Heaviside function
L	Lyapunov function
$\mathbf{P_L}$	Lyapunov matrix
$\mathbf{Q_P}$	Constant matrix multiplied associated with Lypaunov function in bang bang algorithm
$\mathbf{S}$	Vector of sliding variables
$\mathbf{M}$	Matrix associated with sliding variables
$\mathbf{P}$	Transformation matrix in sliding mode control algorithm
$\mathbf{B_1}$ and $\mathbf{B_2}$	Sub matrices obtained by the partition of B matrix
$\mathbf{x_n}$	Transformed state space vector in sliding mode control
$\mathbf{Q_S}$	Positive weighing definite matrix in sliding mode control

	algorithm
$\boldsymbol{\Delta}, \boldsymbol{\lambda}$	Matrices associated with calculation of control force in sliding mode control
$\boldsymbol{\delta}$	Matrix of sliding margin
ω_g , ξ_g , ω_s and ξ_s	Double Filter coefficients
$E[\sigma_{ui}]$ and $E[\sigma_{ci}]$;	Expected rms value of uncontrolled and controlled responses
$E[P_{ui}]$ and $E[P_{ci}]$	Expected uncontrolled and controlled absolute peak responses
Re	Percentage control of the response quantities of interest per unit control
P_r	Percentage reduction in response quantity
F_n	Normalized peak control force
s_s	Output of first filter
S_o	Ordinate of the PSDF of white noise w
[Av]	System matrix of state space of VB-2
[Bv]	Control matrix of state space of VB-2
[Ev]	Disturbance (excitation) matrix of state space of VB-2
[Cv]	Measurement matrix of state space of VB-2
[Dv]	Matrix multiplied by control force state space of VB-2
[Xv]	State vector of displacement and velocity of VB-2
[Uv]	MR damper force vector of VB-2
[AT]	System matrix of combined system of TMD and MR damper
[BT]	Control matrix of combined system of TMD and MR damper
[ET]	Disturbance (excitation) matrix combined system of TMD and MR damper
[CT]	Measurement matrix of combined system of TMD and MR damper
[DT]	Matrix multiplied by control force state space of combined system of TMD and MR damper
[XT]	State vector of displacement and velocity of combined system of TMD and MR damper

Chapter-1

Introduction

1.1 General

The safety of the civil engineering structures against hazards such as cyclones, tsunami, blast, and earthquakes are a rapidly expanding field of research. The conventional design of a structure depends on the inherent ductility of the structure to dissipate induced vibration energy while undergoing some degree of structural damage. An alternative approach, structural control is a well-established design philosophy in which a structure is not designed for vibration induced forces; in fact, the control system integrated with the structure takes care of the induced forces by providing the counter-acting forces or by dissipating the energy induced in the structure and thus preventing a catastrophic failure of the structural system.

Structural control is broadly classified into passive control, active control, semi-active control and hybrid control. In the passive control systems, there is no requirement of an external power source. However, the energy dissipation of a passively controlled structural system cannot be increased by the passive control devices, i.e. only a limited control can be achieved through the passive control systems. Passive devices such as base isolation, tuned mass damper, tuned liquid damper, visco-elastic damper, viscous fluid damper, friction damper, and metallic damper reduce the seismic response of the structure by partially absorbing the energy induced in the structure due to the excitations. The passive devices are simple in design and easy to install. However, the effectiveness of passive devices is always limited due to the passive nature of the devices and the random nature of earthquake events.

In the active control systems, control forces are generated using an external power source and applied to the structure through actuators/ controllers according to a predetermined control algorithm like the linear quadratic regulator (LQR), sliding mode, H_2/linear quadratic Gaussian (LQG), pole placement etc. With the help of the active control, a desired level of reduction of responses can be achieved. The active control strategies deliver force into the structure to counteract the energy of the dynamic loading and have the ability to control different vibration modes and to accommodate different loading conditions. Some examples of active systems are active mass damper, active tuned mass damper, and active tendon system. The dependency of active control systems

on the external energy source is a disadvantage as power failure can occur during strong earthquakes.

Semi-active control systems exploit the advantages of both passive and active control systems. The order of the power requirement of semi-active control systems are very small as compared to the power requirement of active control systems and they can generate control forces of the same order as produced by active control systems. The counteractive control forces in semi-active control are generated by reactive devices having variable damping and/or stiffness characteristics. Since the energy requirement of the semi active control system is very less, it can operate during large intensity earthquakes. These devices are characterized by their ability to dynamically change the structural properties, without adding energy to the controlled system. The semi-active control devices include semi-active stiffness control device, semi-active tuned liquid dampers, hydraulic damper, ER and MR dampers, and friction control device. Preliminary studies indicate that the semi-active system can achieve the majority of the performance of fully active systems, thus allowing for the possibility of effective response reduction for a broad class of seismic events. MR damper is one of the promising devices for vibration mitigation in structures and is being extensively used by researchers in the field of semi active control of structures.

The hybrid control scheme is developed by combining passive, active and semi-active control systems with the goal of enhancing the performance of structures against severe hazards. Hybrid mass dampers (HMDs), viscoelastic dampers (VEDs), active/semi-active base isolation systems, actuators and passive dampers, and semi-active tuned liquid dampers with passive dampers are some examples of hybrid control schemes. In hybrid control, active control is combined with passive control to supplement and improve the performance of a passive control system and to decrease the energy requirement of the active control system. In the case of power failure or failure of any component of the active control system, the passive component of the hybrid control system still offers a certain degree of protection; hence, the hybrid system is system fail-safe.

Since late 1990's, a number of review papers on passive and active control of structures have been published (Soong,1988, Jangid and Datta,1995, Housner et al.,1997). Further, in the recent years, extensive reviews on semi-active control and hybrid control of structures have also been made (Symans and Constantinou,1999, Spencer Jr and Nagarajaiah,2003, Fisco and Adeli,2011a, Fisco and Adeli,2011b). The present study

deals with the semi-active and hybrid control of structures using MR dampers; hence, a very brief review of the literature on seismic control of structures using semi-active control (MR dampers) and hybrid control is included here to highlight the need for the present study. Detail review of literature is presented in chapter 2.

1.1.1 Semi-active control with MR damper

Semi-active control using MR dampers is different from other control strategies in terms of following attributes (i) actuation of MR damper is governed by the structure and the force developed is primarily dependent upon the velocity of the piston ii) the application of voltage at any instant of time i.e. the time history of voltage is a discontinuous function iii) a maximum voltage (positive) can be applied to the damper iv) maximum control force that can be developed is limited by the maximum voltage applied to the damper and v) feedback information required to predict the control force is the states which control the actuation of the damper pistons. Above attributes have led to the formulation of different types of algorithm. Most of them consist of i) estimation of full state from the observed ones ii) an active control algorithm to find a reference force and iii) a clipping algorithm to apply voltage to the MR damper.

Semi-active control using the MR damper has become a topical subject of research. For implementing MR dampers in structural control, various analytical models have been proposed. A phenomenological model of a typical MR damper, based on Bouc–Wen hysteresis model, was proposed by Spencer et al. (1997). Yang et al. (2002) proposed two quasi-static models, an axi-symmetric and a parallel-plate model, for the force–velocity relationship of the MR dampers. The authors found that the models are useful for the device design but are not sufficient to describe the dynamic behavior of MR dampers. In the consecutive study, a new MR damper model system was introduced to describe the MR damper behaviour under the dynamic loading (Yang et al.,2004).

Wang et al. (2001) developed a theoretical model for predicting the behavior of electro-rheological (ER) and magneto-rheological (MR) dampers using the Herschel-Bulkley constitutive equation. Jimenez et al. (2005) presented a dynamic model for MR damper based on a modified LuGre dynamic friction model. Xia (2003) has constructed an inverse model of MR damper by using a multi-layer perceptron optimal neural network. Chang et al. (2002) used a recurrent neural network to represent the inverse dynamics of MR damper.

Control force produced from MR damper is a function of the relative displacement and velocity, and the current supplied to the damper. The current supplied to the MR damper depends on the voltage applied and hence, in the past, a number of semi-active control strategies have been developed for MR damper for deciding the voltage. Dyke et al. (1996b) proposed a clipped optimal control algorithm with acceleration feedback and demonstrated the application of this algorithm to control a seismically excited three storey scaled building model. Further modifications of clipped-optimal control were done by Yoshida and Dyke (2004) and also by Jung et al. (2006). Cho et al. (2005) proposed a modal control scheme applied along with Kalman filter and a low pass filter for vibration control of large structural systems, which may involve hundreds or even thousands of degrees of freedom. Leitmann (1994) presented a control strategy based on Lyapunov stability theory (bang-bang control) for ER dampers. The goal of this algorithm is to reduce the responses by minimizing the rate of change of a Lyapunov function. McClamroch and Gavin (1995) used a similar approach to develop a decentralized bang-bang controller for ER dampers. This control algorithm acts to minimize the total energy in the structure. Jansen and Dyke (2000) presented the maximum energy dissipation algorithm as a variation of the decentralized bang–bang approach proposed by McClamroch and Gavin (1995). The modulated homogeneous friction algorithm was originally proposed for the controller using a variable friction damper was modified for MR dampers by Jansen and Dyke (2000). Terasawa and Sano (2005) developed an adaptive control scheme using a simple mathematical model of the MR damper to express its hysteresis behavior of nonlinear dynamic friction mechanism of the MR fluid. Xu et al. (2000) proposed two optimal displacement control strategies for semi-active control of seismic response of frame structures using MR or ER dampers.

The use of a stochastic semi-active control strategy using ER/MR dampers was first proposed by Ying et al. (2003). A structural system excited by random loading and controlled by using ER/MR dampers is modelled as a dissipated Hamiltonian system. The control forces generated by ER/MR dampers are split into a passive part and an active part. The stochastic averaging method is applied to obtain partially completed averaged Ito stochastic differential equations for the quasi-Hamiltonian systems developed above. The response of a semi-active controlled system is obtained from solving the final dynamical programming equation and the FPK equation associated with the fully completed averaged Ito equations. Following nearly the same technique, a number of structural systems were controlled by using MR dampers by a few researchers (Dong et

al.,2004, Zhu et al.,2004, Cheng et al.,2006, Hu et al.,2016) and it was shown that the efficiency of the above control scheme is more than the linear-quadratic-Gaussian (LQG) control algorithm.

Full-scale and laboratory model experiments on MR dampers were carried out by a number of researchers. Yang et al. (2002) developed and tested a 20-t MR damper, suitable for full-scale applications, by subjecting it to quasi-static actuation. Christenson et al. (2008) carried out real-time hybrid simulations to physically test three large-scale 200 KN MR fluid dampers while simulating the seismic response of a three-story steel frame structure. Kim et al. (2006) carried out full-scale experiments on a single-degree-of-freedom mass that is equipped with a hybrid base isolation system. Cha et al. (2014) validated the performances of four semi-active control algorithms for the control of a large-scale realistic moment-resisting frame using a large-scale 200-kN MR damper. As far as laboratory model experiments are concerned, Yoshida et al. (2003) conducted tests on two-story building model with an asymmetric stiffness distribution using MR dampers and clipped-optimal control algorithm. Sun et al. (2003) performed an experimental modal analysis of a three storey model with the help of a closed-loop controller. Sahasrabudhe and Nagarajaiah (2005) studied the effectiveness of variable damping, provided by MR dampers in reducing the response of sliding isolated buildings. Xu et al. (2005) tested two building models, with podium structures and connected by the MR damper which are driven by a multilevel logic control algorithm. A prototype MR damper composed of a fixed orifice damper filled with MR fluid was developed and tested by Dyke et al. (1996b). Yi et al. (2001) conducted experiments on a six-story test structure to demonstrate the effectiveness of multi-input control strategies using both a Lyapunov and a clipped-optimal controller. Yoshioka et al. (2002) conducted experiments on a two-mass model to study the effectiveness of base-isolation strategy using clipped-optimal control.

1.1.2 Optimal structural Control using Genetic Algorithm (GA)

In recent times, genetic algorithm has found wide applications in the field of structural control, especially in active control of structures. Rao et al. (1991) used the genetic algorithm (GA) to find the optimum location of active controllers for a two bay truss by minimizing the dissipation energy of active controller as the objective function. Furuya and Haftka (1995) applied GA using an integer and binary coding to find the optimal location of actuators for large space structures. Dhingra and Lee (1995), Abdullah

et al. (2001) used a hybrid optimization scheme based on GA and gradient based technique to solve a multi-objective optimization problem for the determination of the optimum location of actuators/sensors. Li et al. (2000) proposed a multilevel genetic algorithm to determine the optimum number and location of actuators for active control under wind load. Ahlawat and Ramaswamy (2002) proposed a multi objective genetic algorithm to determine optimal configurations of a hybrid control system. Li et al. (2004) proposed a two level genetic algorithm to determine the optimal number and position of actuators in active control structures. Cha et al. (2013) proposed a multilevel genetic algorithm to determine the optimal number and location of active devices and sensors for a 20 story benchmark structure.

1.1.3 Hybrid control of Structure

Different hybrid control schemes have been developed and tried to enhance the control of structures for dynamic loading. Design of hybrid mass dampers (HMD) has been investigated by various researchers (Kawatani et al.,1994, Shing et al.,1994, Spencer Jr et al.,1994, Tamura et al.,1994, Adhikari and Yamaguchi,1997). Hybrid base-isolation system has also been considered as a viable hybrid control system. (Yang et al.,1991, Feng,1993, Reinhorn and Riley,1994, Yang et al.,1994a). Since base-isolation systems exhibit either hysteretic or nonlinear behaviour, researchers have developed various non-linear/hysteretic control strategies including fuzzy control (Nagarajaiah,1994), neural network based control (Venini and Wen,1994), dynamic linearization (Yang et al.,1994a) adaptive non-linear control (Rodellar et al.,1994). Inaudi and Kelly (1993) and Tzan and Pantelides (1994) developed a hybrid control system by combining viscolelastic dampers (VEDs) and active control systems. Meirovitch and Stemple (1997) proposed a nonlinear control method to mitigate the effect of earthquake by using base isolation and feedback control. Effectiveness of the performance of an active vibration absorber (AVA) in conjunction with a passive isolator system under seismic excitation was studied by Lee-Glauser et al. (1997). Symans and Kelly (1999) proposed an intelligent hybrid isolation system containing semi-active dampers for seismic protection of a bridge structure. Zhao et al. (2000) investigated the application of the sliding mode control (SMC) strategies for building structures with base isolation hybrid protective system. Nagashima et al. (2001) developed a hybrid mass damper (HMD) system and studied its application to a 36-storey building. Saito et al. (2001) developed a large-scale HMD system consisting of an auxiliary mass supported by multi-stagem rubber bearings and actuators. Yang and

Agrawal (2002) studied the safety performances of various types of hybrid control systems for nonlinear buildings against near-field earthquakes. Hybrid control systems consisted of mainly the base isolation system and either the passive control device or the semi-active damper or a combination of them. Park et al. (2003) investigated a hybrid control composed of a passive control system to reduce the earthquake-induced forces in the structure and an active control system to further reduce the bridge responses, especially deck displacements. Kim and Adeli (2004) presented a hybrid feedback least mean square (LMS) model for control of structures through integration of a feedback control strategy such as the LQR or LQG algorithm and the filtered-x LMS algorithm. Soneji and Jangid (2007) formulated a passive hybrid system consisting of a viscous fluid damper in association with elastomeric and sliding isolation system. Lin et al. (2005) proposed a semi-active tuned mass damper (STMD) for building control. Semi active tuned mass damper (STMD) combine a passive tuned mass damper (TMD) and a semi active damper. Cai et al. (2007) explored the TMD-MR damper system for cable vibration mitigation through an experimental approach. Kang et al. (2011) studied the effectiveness of semi-active tuned mass dampers (STMDs) for the response control of a wind-excited tall building.

1.2 Need for the present study

MR damper is a very costly device, and therefore, only a limited number of dampers can be used in practice. Moreover, numbers of sensors which are installed in the frame in practice are also limited. Thus, the semi-active control problem with MR dampers becomes a problem of finding optimum control of responses for a partially observed system by a suitable placement of MR dampers and sensors. In the literature, optimal placements of control devices are addressed for active and passive control of structures for fully observed systems. Very little literature exists where semi active optimal control of partially observed structures with a limited number of MR dampers and sensors is reported. Further, although there is a number of control algorithms developed for semi-active control of partially observed building frames, none of these algorithms are developed by taking advantage of the special features of semi-active control of structures with MR dampers. Studies on related issues of full state estimation from partial observations for site specific earthquakes modelled as random ground motions are not also well established in the literature. Finally, studies on the enhanced

response control of structures using hybrid control strategy combining semi active MR dampers and passive dampers need further investigation.

1.3 Scope and objectives of the work

Keeping the above gaps in view, the present study is undertaken. Semi active control of partially observed building frame under both random and recorded ground motions is performed using MR dampers. A new control algorithm is developed by taking advantage of the special features of MR damper control with a limited number of measurement sensors and dampers. Further, optimal placement of MR dampers and sensors for best reductions in responses is obtained using genetic algorithm (GA) based optimization technique and special features of MR damper control. A new formulation is also presented for non-white ground excitation for semi-active control of partially observed building frame in which use of Kalman filter for state estimation is accomplished with complete rigor. Finally, a hybrid control using a combination of TMD and MR dampers is investigated in order to obtain increased response reduction compared to the semi-active control using MR dampers only. Specific objectives of the study include:

1. To develop a new control algorithm based on tracking the measured responses of building frame and finding time history of the voltage to be applied to MR dampers directly without requiring state estimation.
2. To develop feedback control strategies, namely, LQG with clipped optimal control, bang-bang control, sliding mode control with clipped optimal control in MATLAB environment in order to compare the results of the proposed algorithm stated in the first objective.
3. To develop a semi-active control scheme using MR dampers for site-specific random excitation for partially observed building frame augmented with filter equations for including more rigor in the use of Kalman filter for state estimation.
4. To develop a genetically optimized control strategy for partially observed building frames using limited numbers of MR dampers and sensors.
5. To develop a hybrid control scheme for building frames using semi-active MR damper and TMD for a number of ground motion records.
6. To carry out a large number of numerical studies to investigate i) the relative performances of different control schemes used and developed for the study; and

ii) the effect of different parameters on the response reduction achieved by semi-active and hybrid control of building frames using MR dampers.

1.4 Organization of the thesis

For the fulfilment of the above objectives, the work is divided into seven chapters. **Chapter 2** provides an extensive literature review on semi-active control and hybrid control and application of genetic algorithm in structural control. The review work is broadly divided into two sections – semi-active control and hybrid control. The section on semi-active control is further sub-divided into two subsections, namely, experimental research and analytical research. In the experimental research, both full-scale and laboratory model experiments are reviewed. In the analytical research, the available literature on MR damper models and semi-active control algorithms are reviewed. The former includes a review on different MR damper models, their theoretical development, the features or advantages of these models and their applications in structural control problems. The latter covers a brief review of the control algorithms developed for semi-active control of structures, bringing out the theoretical basis, their salient features and the applications of each one of them. In the end, a brief review of the available literature on the hybrid control of structures is presented. The different combinations of passive, active and semi-active techniques used in developing the hybrid methods, the devices implemented, the algorithms developed to control these devices are discussed in this review section.

In **Chapter 3**, different semi active control strategies for partially observed building frame under random and deterministic ground motions using MR dampers are presented. The control of response is achieved with the help of a limited number of MR dampers and observation sensors. Since semi active control using the MR damper is inherently nonlinear, a simulation procedure is adopted for obtaining the expected peak and root mean square (r.m.s.) value of responses for random ground motion as the stochastic averaging technique used for stochastic control of responses with the help of MR dampers fails to predict expected peak value of responses. Five control algorithms, namely, LQR with clipped optimal control, bang-bang control, sliding mode with clipped optimal control, velocity tracking control and passive on control are used to find the voltage requirement in the MR dampers. State estimation is done using Kalman filter. The control of a ten storey building frame with three MR dampers and three observation

sensors is taken as the example problem. The controlled responses of interest are top floor displacement, maximum drift and base shear of the building frame.

Chapter 4 deals with the development of semi-active control algorithms for partially observed frames for site-specific ground motion represented by Clough and Penzin double filter power spectral density function of ground motion. Kalman filter works on the assumption that both excitation and measurement noise are Gaussian white. However, in reality, the excitations are non-white. Therefore, a new structural system is formulated by augmenting the state space equations of the structural system with the double filter equations whose output variable matches the desired excitation to the structural system. The input to the double filter is the Gaussian white noise. Thus, the assumptions inherent in the use of Kalman filter are strictly satisfied and at the same time, by adjusting the filter parameters, the desired site-specific ground motion can be achieved. For online application of the control scheme, measured ground motion is fed into an ANN; the output from the ANN is the white noise that goes as input excitation to the augmented system for analyzing the control problem at hand. The responses of the new structural system are controlled using a limited number of MR dampers and observation sensors. Two types of random ground motions consistent with broadband and narrowband PSDFs of ground motions representing hard soil and soft soil conditions, respectively, are used as excitations to the same ten storey building frame. Previously used three control algorithms, namely, LQR with clipped optimal control, bang-bang control and sliding mode with clipped optimal control, velocity tracking control and passive on control are modified to determine the voltage. Then, a sensitivity analysis is carried out to show how the error in the state estimation and hence, the control of responses varies with the assumed values of covariance of excitation and the noise used in the Kalman filter. The results of the sensitivity analysis help in the proper selection of the assumed values of the covariance of the excitation and the noise for online application of the control strategy.

Chapter 5 describes the optimal placement of MR dampers and sensors to obtain the best reductions in response quantities of interest, namely, top floor displacement, maximum drift and base shear. A single objective genetic algorithm is used to determine the optimal locations of sensors and dampers. Two optimal placement strategies of dampers and sensors are presented. The objective functions selected are the response quantities of interest. Optimal placements are obtained for the building frame used in Chapter 3. Time histories of the voltage supplied to the MR damper are obtained by using

bang-bang and LQG with clipped optimal control algorithms for a number of earthquakes. The ten-story frame in chapter 3 is solved for a number of cases to investigate the effect of algorithms, earthquakes and the control schemes on the optimal number and placement of MR dampers and sensors.

Chapter 6 deals with the development of a hybrid control scheme using MR dampers and a TMD. Combined equations of the motion of the building frame with MR dampers and the TMD under seismic excitation are written in the state-space form for the purpose of analysis. Three hybrid control strategies are attempted, namely, i) two MR dampers in the bottom two stories and a TMD at top floor; ii) three MR dampers in the bottom three stories and a TMD at top floor; and iii) one MR damper at the bottom storey and a semi-active tuned mass damper (STMD) at the top floor. The results of the analysis are compared with those of three and four MR dampers placed in the bottom stories of the frame for a number of earthquakes and a number of control strategies used in the previous chapters.

Chapter 7 gives the overall summary of the important conclusions drawn from the present study. Recommendations for future work in the field of semi-active control of structures as an extension of the present study are also included in this chapter.

Chapter 2

Literature Review

2.1 Introduction

Protections of structures against natural hazards like earthquakes, tsunami and cyclones have always been a major concern. In the last three decades, considerable attention has been paid by researchers to the concept of structural control, which is an effective technology for hazard mitigation. Depending upon the amount of external energy required, a control system can be divided into four categories – active, semi-active, hybrid and passive control systems. These methods can be defined as follows:

Passive Control – A passive control system does not require an external power source. Passive control system imparts forces that are developed in response to the motion of the structure. The energy in a passively controlled system, including the passive devices, cannot be increased by the passive control devices. A passive control system may be used to increase the energy dissipation capacity of a structure through localized, discrete energy dissipation devices located either within a seismic isolation system or over the height of the structure. Such systems may be referred to as supplemental energy dissipation systems. Supplemental energy dissipation devices may take many forms and dissipate energy through a variety of mechanisms, including base isolation devices, metallic yield dampers, friction dampers, viscoelastic dampers, viscous fluid dampers, tuned mass dampers and tuned liquid dampers. Out of these, base isolation devices have been widely implemented in practice.

Active Control – An active control system is one in which an external source of power supplies energy for actuators that apply forces to the structure in a prescribed manner. These forces can be used to both add and dissipate energy in the structure. In an active feedback control system, the signals sent to control the actuators are a function of the response of the system measured with sensors (displacement/velocity/acceleration measurement) and therefore, applied control force can be manipulated according to the response of the structure to optimize the energy requirements. In active control, active mass/tuned mass dampers (ATMD), active tendon systems, actuators/controllers have been used (Yang,1975, Yang et al.,1992, Rofooei and Tadjbakhsh,1993, Dyke et al.,1996a). Out of these, active mass/tuned mass dampers have been implemented for the response reduction of tall buildings in controlling wind-induced vibrations.

Semi-active Control – Semi-active control devices also use the measured structural responses to determine the control force required. However, they do not require large power sources as active devices do. Even with the help of a battery, the semi-active control devices can be operated. This is especially advantageous during power disruptions caused by the earthquake damage. These devices have properties that can be adjusted in real time and can only absorb or dissipate energy, therefore guaranteeing system stability. They are also found to be more energy-efficient than active control and more effective in reducing structural responses than passive control (Dyke et al.,1996b, Jansen and Dyke,2000). In addition, they are reliable since they act as passive devices in the case of power or mechanical failure. In semi-active control, the use of electro-rheological/ magneto-rheological dampers, fluid viscous dampers, and semi active tuned mass dampers have drawn considerable interest among researchers.

Hybrid Control – The common usage of the term "hybrid control" implies the combined use of active and passive control systems. For example, a structure equipped with viscoelastic damper supplemented with an active mass damper on the top of the structure, or a base isolated structure with actuators actively controlled to enhance the control level. In hybrid control, various combinations of passive, active and semi-active devices have been investigated. Amongst them, the concepts using base isolation and ATMD, and visco-elastic dampers and ATMD, and MR damper and TMD have drawn considerable interest.

Passive and semi-active controls are preferred over active control due to their reliability and inherent stability. Active control system sometimes develops asynchronous control forces due to time delays, thus making the structure unstable. Out of semi-active, passive and hybrid control, semi-active control has attracted more attention because it can provide a large reduction in the response of the structure using less external power.

A number of state-of-the-art papers on structural control have been published. These reviews provide a good overview of different structural control strategies developed and implemented in practice. They include state-of-the-art reviews on base isolation of structures by Kelly (1986) and by Jangid and Datta (1995), state-of-the-art reviews on active structural control by Soong (1988) and by Datta (2003) and a comprehensive review on structural control by Housner et al. (1997). For semi-active control, the state-of the-art review was published by Symans and Constantinou (1999), by Spencer Jr and Nagarajaiah (2003), and by Fisco and Adeli (2011a). Soong and Reinhorn (1993) and Fisco and Adeli (2011b) have done a review of research in the area of hybrid

control systems. A study of the above review papers shows that extensive researches in the areas of passive, active, semi-active and hybrid control have been carried out. Since the present study deals primarily with the semi-active control using MR dampers, the review of literature is mostly confined to the papers published in this area. Some of the very recent studies on genetic algorithm which are applied for optimum active and semi-active control of structures are included in this review.

2.2 Semi-active Control

The semi-active control originates from the passive control system, modified to allow the adjustment of mechanical properties based on feedback from the excitation or the measured response. As an active control system, it monitors the feedback measurement, and generates an appropriate command signal. As a passive control system, control forces are developed as a result of the motion of the structure. Control forces primarily act to oppose the motion and are developed through appropriate control algorithms. Generation of forces through the control devices require a small amount of external power for operation. Different types of semi-active control devices include:

1) **Stiffness control devices** – These devices are utilized to modify the stiffness, and hence, the natural frequency of the system. This establishes a new resonant condition during earthquakes. The devices used are stiffness bracings, which are engaged or released so as to include or not to include the additional stiffness in the system, and operate through fluid control within tubes by valves (Yang et al.,1996, He et al.,2001).
2) **Electrorheological dampers/ magnetorheological dampers** – They consist of a hydraulic cylinder containing micron-size dielectric particles suspended within a fluid. In the presence of current, particles polarize and offer an increased resistance to flow (change from viscous fluid to yielding solid within milliseconds). The magnetorheological dampers are magnetic analogues of electrorheological dampers, and have electromagnets located within the piston head which generate the magnetic field (Ehrgott and Masri,1992, Dyke et al.,1996b, Dyke et al.,1997, Spencer et al.,1997).
3) **Friction control devices** – They are energy dissipaters within the lateral bracing of a structure, or as components within the sliding isolation system. The coefficient friction of sliding is controlled by the modulus of fluid pressure in a pneumatic vessel (Akbay and Aktan,1991, Feng et al.,1993)

4) **Fluid viscous devices** – They consist of a hydraulic cylinder, with a piston dividing it into two sides. The cycling piston forces oil through an orifice, creating the output force. The output force is modulated by an external control valve which connects two sides of the cylinder (Sack et al.,1994, Symans and Constantinou,1997).

5) **STMDs and STLDs** – The dynamic characteristics of the TMDs are controlled by external current. In TLDs, the length of the hydraulic tanks is modified by adjusting the rotation of the buffles in the tank, and thus, the sloshing frequencies of the fluid are changed. In STMDs, the damping device is replaced by MR damper.

The literature for semi-active control is reviewed under two heads, namely, experimental work and theoretical work.

2.2.1 Experimental Studies

Significant experimental studies on MR dampers have been carried out to understand their working and interaction with the structural systems. The experimental studies are conducted on scaled models of bridges and building frames, as well as on full-scale structures. It is shown that MR dampers significantly outperform comparable passive damping configurations, while their requirement of energy is only a fraction of the energy needed by the active controller.

Full Scale Experiments

Yang et al. (2002) developed and tested a 20 ton MR damper for full-scale applications. The damper uses a particularly simple geometry in which the outer cylindrical housing is part of the magnetic circuit. The effective fluid orifice is the entire annular space between the piston outside diameter and the inside of the damper cylinder housing. Movement of the piston causes fluid to flow through this entire annular region. The damper is double-ended, i.e., the piston is supported by a shaft at both ends. The electromagnetic coils are wired in three sections on the piston. This result in four effective valve regions as the fluid flows past the piston. The complete damper is approximately 1 m long, has a mass of 250 kg, and contains approximately 6 litres of MR fluid. Quasi-static experiment was conducted and the experimental results had shown that MR dampers can provide large controllable damping forces, while requiring only a small amount of energy.

Kim et al. (2006) conducted full-scale experiments on a single degree of freedom (SDOF) mass which was equipped with a hybrid base isolation system. The hybrid system consists of a set of four friction pendulum system (FPS) bearings that serve as the base isolation system and an MR damper. The SDOF mass and its hybrid isolation system are subjected to various intensities of near- and far-fault earthquakes on a large shake table. The proposed fuzzy controller modulates resistance of the semi-active damper based on the feedbacks received from displacement or acceleration transducers attached to the structure. The authors compared several types of passive and semi-active control strategies. The study shows that a combination of FPS bearings and an adjustable MR damper can provide robust control of vibration for a large full-scale structure undergoing a wide variety of seismic loads.

Christenson et al. (2008) carried out real-time hybrid simulations to test three large-scale 200 KN MR fluid dampers while simulating the seismic response of three-story steel frame structure. The performance of the MR dampers were experimentally verified as applied to a structure allowed to yield under severe dynamic loading. The real-time hybrid simulations provided a cost-effective means for large-scale testing of the critical components in a semi-active controlled structure. Virtual coupling was shown to increase the stability while maintaining performance. The results showed that the large-scale MR dampers placed at each floor of the three storeys steel framed structure can provide significant response reduction.

Cha et al. (2014) validated the performances of four semi-active control algorithms for the control of a large-scale realistic moment-resisting frame using a large-scale 200-kN MR damper. For conducting the test, a large-scale damper-braced steel frame was designed and fabricated. The overall dimensions of the prototype structure are 45.7 m (150 ft) by 45.7 m (150 ft) in plan and 11.43 m (37.5 ft) in elevation. Four semi-active controllers, namely (1) passive on, (2) clipped optimal controller, (3) decentralized output feedback polynomial controller, and (4) Lyapunov stability based controller, were designed for this frame. Real-time hybrid simulations (RTHS) were carried out for these controllers using three recorded earthquakes. The comparative performance of these controllers was investigated using both RTHS and numerical simulations in terms of reductions in the maximum interstory drifts, displacements, absolute accelerations, and control forces. RTHS and simulation results both show that semi-active controllers are effective in reducing response quantities of the large scale building frame.

Laboratory Model Experiments

Dyke et al. (1996b) developed a prototype of MR damper, composed of a fixed orifice damper filled with MR fluid. The main cylinder of the damper is 3.8 cm in diameter and is 21.5 cm long in its extended position. The main cylinder consists of piston, magnetic circuit, and accumulator and 50 ml of MR fluid. The length of the stroke of damper was ±2.5 cm and can develop up to 3000 N force. A sinusoid of amplitude 1.5 cm and of frequency 2.5 Hz, at four constant voltage levels, namely, 0 V, 0.75 V, 1.5 V and 2.25 V were applied for testing the damper.

Yi et al. (2001) conducted experimental study test on a six-story test structure to demonstrate the effectiveness of multiple MR dampers for structural control. The test structure was subjected to scaled versions of the 1940 El Centro earthquake. Two control algorithms, Lyapunov and clipped-optimal controller were used to control the structure, and four MR dampers were employed, each of capacity 29 N. Tests conducted at various excitation levels demonstrated the ability of the MR damper to surpass the performance of a comparable passive system in a variety of situations.

Yoshioka et al. (2002) installed a sponge-type MR damper between the base and the ground, resulting in a "smart" base isolation strategy. The test structure consisted of a two-mass model supported by laminated rubber bearings. The mass of the isolated base and of the superstructure were 10.5 kg and 57.5 kg. The damper had a maximum force capacity of 50 N, and it was modeled with the help of the analytical expressions developed by Spencer et al. (1997). Clipped-optimal controller employing the H_2/LQG strategy was used to reduce structural responses and the smart base isolation system was found to be effective for both far-field and near-field earthquake excitations.

Yoshida et al. (2003) proposed a semi-active control system to reduce the coupled lateral and torsional motions in the asymmetric building subjected to horizontal seismic excitation. A two-story building model with an asymmetric stiffness distribution, having floor mass of 23.3 kg was tested. Magnetorheological (MR) dampers were applied as semi-active control devices and the voltage was determined based on a clipped-optimal control algorithm with the H_2/LQG controller, which used absolute acceleration feedback. Shear mode MR dampers (Lord Corporation), having maximum force range of 20 – 25 N, were used. For predicting the behaviour of a prototype shear-mode MR damper the Bouc-Wen model was used. The experimental results demonstrated that the performance of the semi-active controller using MR dampers was significantly better than the passive control system where constant voltages were applied to the MR dampers.

Sun et al. (2003) conducted experimental modal analysis of a three-storey model. The dynamic parameters of the model, including natural frequencies, damping ratios and vibration mode shapes, were identified through impact hammer tests. The MR damper was placed between the ground and the first floor of the structure. A four-parameter non-linear hysteretic biviscous MR damper model was proposed. It was concluded that the semi-active system could achieve a significant reduction in the responses. Furthermore, comparisons of the semi-active system with passive control configurations demonstrated that the performance of the semi-active system exceeded that of comparable passive systems.

Sahasrabudhe and Nagarajaiah (2005) studied the effectiveness of variable damping, provided by MR dampers, in reducing the response of sliding isolated buildings during near-fault earthquakes. A 1:5 scale two-story building model, weight of each floor being 5.8 kN, was tested. The MR dampers used were of the range of 50-300 lbs and a Lyapunov-based control algorithm was developed for the control of the MR damper. The MR damper was found to reduce the bearing displacements more than the passive high and low damping cases, while maintaining the isolation level forces less than the passive high damping case. The semi-active controlled case also maintained the superstructure interstory drift and acceleration responses within the bounds of the passive high and low damping cases.

Xu et al. (2005) carried out experimental studies on a scaled model of building with podium structure. The multistory building was constructed as a slender 12-story building model and the podium structure was built as a relatively stiff three-story building model. A MR damper, which had a force capacity of more than 150 N, together with a current controller was used to link the three-story building to the 12-story building. The two building models without any connection, with the rigid connection, and connected by an MR damper were tested under the scaled El Centro 1940 north–south ground motion. The MR damper was manipulated by a multilevel logic control algorithm. Experimental results demonstrated the effectiveness of MR dampers in totally eliminating the whipping effect due to the sudden change of building lateral stiffness and mass at the top of these structures and also in reducing the seismic response of the structure.

Analytical Research

MR Damper Models

Initially, research started with modeling of ER dampers and in one of those early works; the ER damper was analytical modeled using Bingham viscoplastic model (Stanway et al.,1987), which was later extended to a viscoelastic-plastic model in the consequent study (Gamota and Filisko,1991).

Spencer et al. (1997) proposed a phenomenological model of an MR damper, based on Bouc–Wen hysteresis model. The proposed model overcomes different shortcomings of the earlier models; it is numerically tractable and it can effectively exhibit a wide variety of hysteretic behaviour. When compared with experimental results, the model was found to be in good agreement over a wide range of operating conditions. The proposed model consists of a dashpot in series with the Bouc-Wen model and the arrangement could effectively portray the non-linear force roll-off in the region where the velocity approaches zero. The stiffness of the accumulator present in a damper is accounted for by an additional spring element. To obtain a model that reproduces the behaviour of the damper with varying magnetic fields, three parameters are assumed to vary with the applied voltage. A first-order filter has also been incorporated to account for the dynamics involved in driving a damper's electromagnet and in the MR fluid reaching equilibrium.

Wang and Gordaninejad (2001) proposed an MR damper model based on fluid mechanics and the Herschel-Bulkley constitutive equation. The effect of fluid compressibility within the damper was considered by the inclusion of the effective bulk modulus in the proposed model. The theoretical model presented is validated by comparing the analytical results with experimental data for a prototype MR fluid damper. It was demonstrated that the proposed fluid mechanics based model can accurately predict the dynamic response of an MR damper over a wide range of operating conditions. The major advantage of the proposed model is its dependency on only the geometric and material properties of the device.

Yang et al. (2002) developed two quasi-static models, an axisymmetric and a parallel-plate model to describe the force–velocity relationship of the MR damper. In axisymmetric model, the pressure gradient along the flow is resisted by the fluid shear stress that is governed by the Navier–Stokes equation. For analyzing the quasi-static motion of the flow inside the damper, the fluid inertia is neglected. The yield stress in the axisymmetic model is related to the radial coordinate due to the radial distribution of the magnetic field in the gap. In the parallel-plate model, because of the small ratio between the flow gap and the diameter of the damper piston, the axisymmetric flow field found in

the damper can be approximated as flow through a parallel duct. The parameters were modified so as to make this model analogous to the axisymmetric model. In the parallel-plate model, the yield stress was assumed to be a constant. The simpler parallel-plate model, however, was found to be adequate for practical design.

Jin et al. (2002) developed the ridgenet estimation technique for the modeling of the MR dampers. Compared to wavelet-based algorithms, the new approach constructs the nonlinear mapping by a ridgenet network instead of multidimensional wavelets. The advantage of the proposed model is that the number of basis functions is significantly reduced, so that the algorithm is better positioned for the biasvariance design trade-off.

Yang et al. (2004) upgraded the phenomenological model proposed by Spencer et al. (1997) in a consequent study in order to consider the MR fluid stiction phenomenon, as well as inertial and shear thinning effects. The proposed dynamic model comprised of a dynamic model of the power supply and a dynamic model of the MR damper. Because the previous studies have demonstrated that a current-driven power supply can substantially reduce the MR damper response time, this study employs a current driver to power the MR damper. Results of the study show that use of a current driven power supply can dramatically reduce the MR damper response time. To describe the MR fluid shear thinning effect which results in the force roll-off of the damper resisting force in the low velocity region, the damping coefficient in this model is defined as a mono-decreasing function with respect to absolute velocity. Compared with other types of models based on the Bouc–Wen model, the proposed model has been shown to be more effective, especially in describing the force roll-off in the low velocity region, force overshoots when velocity changes in sign, and two clockwise hysteresis loops at the velocity extremes. It was also shown through experimental results that a current-driver can significantly reduce the MR damper response time.

Jiménez and Álvarez-Icaza (2005) proposed a dynamic model for magnetorheological dampers based on a modified LuGre dynamic friction model. For establishing the model structure, a set of experiments with controlled displacement and current were performed. Based on these experiments, an expression to predict the force exerted by the magnetorheological damper was proposed. The resultant model uses the relative velocity between damper ends, the internal state of the dynamic friction model and the current level at the coil of the damper as inputs to predict the force exerted by the damper. After this initial approximation, experiments with random displacement and current were also performed to validate the model. Because the structure of the model is

linear in the parameters, it was possible to use standard recursive parameter identification algorithms to fit the model parameters to the experimental data. For improving the quality of the predicted force, a closed-loop observer to estimate the internal state of the dynamic friction model was included. Analysis regarding the convergence of this observer was presented. The results obtained, based on the experimental data, showed a good level of accuracy between the predicted and measured forces, despite some small discrepancies at low velocities.

Tse and Chang (2004) developed an inverse model to determine the command signal required by dampers to produce the desirable control forces. The model is based on Bouc-Wen model and it is based on the assumption that the MR fluid always behaves in the post-yielding region. Experimental results showed that the inverse model can provide a smoother tracing of the target force as compared to the clipped model. The inverse model, however, requires accurate parameters from the Bouc-Wen model that must be obtained a priori by laboratory testing and numerical computation.

Zahrai and Salehi (2014) examined the performance of semi-active control of structures using MR dampers. Two models of 9 and 20-story buildings were selected for parametric study and Simulink (MATLAB) was used for simulations. Clipped optimal algorithm was considered as control algorithm and optimal classic linear control method was used to determine desirable control power. Based on the obtained results, it was observed that the used control strategy significantly decreases structure responses. Two mechanisms were suggested to improve the function of dampers and their performance. The proposed mechanism was shown to be effective in reducing the capacity and number of dampers required.

Control Algorithms

For application of MR dampers as semi-active control systems for applications in building frames and bridges various control algorithms have been developed. Most widely reported control algorithms are reviewed below:

Dyke et al. (1996a) proposed clipped-optimal control strategy, based on acceleration feedback. The control strategy was found to be effective in controlling structures using MR dampers. In this method, the desired control force is predicted using H_2/LQG control algorithm. When the desired control force at the current time step is less than the applied force of the previous time step then the voltage is set to zero and when the desired control force at the current time step is greater than the applied force of the previous time step then the voltage is set to maximum.

In the original clipped-optimal control algorithm, the command voltage takes on the value of either zero or the maximum. In some situations when the dominant frequencies of the system under control are low, large changes in the forces applied to the structure may result in high local acceleration values. Yoshida and Dyke (2004) proposed a modification to the original clipped-optimal control algorithm to reduce this effect. In the modified version of the algorithm, the control voltage can be any value between zero and the maximum. The control voltage is determined using a linear relationship between the applied voltage and the maximum force of MR damper. When the desired force is larger than the maximum force that the device can produce, the maximum voltage is applied. They showed that the modified clipped-optimal control algorithm is typically able to achieve a significant reduction in the peak accelerations over that of the original clipped-optimal control algorithm. Although the modified clipped-optimal control algorithm could reduce the peak accelerations, the modification of the original clipped optimal control algorithm might increase the peak drifts slightly.

Jung et al. (2006) proposed another modification to solve the problem of an increase in the peak drifts. In this, the command voltage input to the MR damper is the maximum inside the region where the difference between the desired control force and the actual control force is quite large. Otherwise, the command signal is calculated according to the modified algorithm. That is, this revised version represents a compromise between the original and the modified clipped optimal control algorithms.

Cho et al. (2005) presented a modal control scheme which was applied together with a Kalman filter and a low-pass filter. Modal control reshapes the motion of a structure by merely controlling a few selected vibration modes. Hence, in the designing phase of a controller, the size of weighting matrix was reduced because the lowest one or at best two modes were controlled. This control technique was developed taking into consideration the vibration control of a civil engineering structure, which is usually a large structural system that may involve hundreds or even thousands of degrees of freedom. The numerical results indicated that the motion of the structure was effectively suppressed by merely controlling a few lowest modes, although resulting responses varied greatly depending on the choice of measurements available and weightings.

Leitmann (1994) developed control algorithms using Lyapunov's stability theory (bang-bang control). This approach requires the use of a Lyapunov function, which must be a positive definite function of the states of the system. Assuming the origin to be a stable equilibrium point, if the rate of change of the Lyapunov function is negative

semidefinite, then the origin is stable in the sense of Lyapunov. Thus, the goal of this control strategy was to choose control input, which makes the derivative of the Lyapunov function as negative as possible. The Lyapunov function may be chosen in many different ways, thus resulting in a variety of control laws. These control strategies are also referred to as a bang-bang (also as two-stage or bi-state or on-off) algorithm.

McClamroch and Gavin (1995) using a similar approach developed another control law, called the decentralized bang-bang control law. It was developed for use with an electrorheological damper. In this approach, the Lyapunov function was chosen to represent the total vibratory energy in the structure (kinetic plus potential energy). As is done in the case of bang-bang control, the goal of this controller is to make the derivative of the Lyapunov function as large and negative as possible (maximizing the rate at which energy is dissipated).

Maximum energy dissipation theory is a variation of the decentralized bang-bang approach proposed by McClamroch and Gavin (1995). Unlike the decentralized bang-bang control, where the Lyapunov function is chosen to represent the total vibratory energy of the structure, in this approach it represents the relative vibratory energy in the structure (i.e., without including the velocity of the ground in the kinetic energy term). This control law commands the maximum voltage when the measured force and relative velocity are dissipating energy (producing large dissipative forces) and commands the minimum voltage when energy is not being dissipated (producing small forces when the force is not dissipative).

Inaudi (1997) proposed the modulated homogeneous friction algorithm for a variable fiction damper. Since there are strong similarities between the behavior of a variable friction device and the MR damper, this algorithm was modified for MR dampers by Jansen and Dyke (2000).

Terasawa and Sano (2005) developed an adaptive control scheme using a simple mathematical model of the MR damper to express its hysteresis behavior of nonlinear dynamic friction mechanism of the MR fluid. The model parameters are identified by using an adaptive observer, and the identified model is effectively used to synthesize an adaptive inverse controller to attain linearization of the nonlinear behaviour of the MR damper, which generates the necessary voltage input to the MR damper so that the desirable damping force can be added to the structure. The desired damping force can also be designed so that the behavior of the structure may coincide with a desired reference dynamics even when the structure model involves uncertain parameters.

Xu et al. (2000) proposed two optimal displacement control strategies for semi-active control of seismic response of frame structures using MR or ER dampers. The stiffness of brace system supporting the smart damper is taken into consideration. The force-displacement relationship of an MR or ER damper based on a parallel-plate model is first extended to include the stiffness of chevron brace supporting the smart damper. The equations of motion of a multi-storey frame structure with smart damper-brace systems are then established. The clipped optimal displacement control strategy, which is parallel to the clipped optimal force control strategy, and the optimal displacement control strategy with the controller-structure interaction considered are proposed for seismically excited frame structures with MR or ER dampers. The results show that for a given structure under a given ground motion, no matter which control strategy is used, there exist the optimal values of the maximum yielding shear stress and the Newtonian viscosity of smart fluids, by which the maximum seismic response reduction can be achieved.

Jing et al. (2002) proposed a multilevel logic control algorithm, which avoids the requirement of the accurate mathematical models for the control system and the MR damper. Only the velocity and displacement between the two ends of the MR damper are considered as feedbacks for the determination of control force by complying with the logic rules of PanBoolean algebra. The core concept of the logic control is to switch the control damper force to a corresponding prespecified actuated force region based on different states of feedback responses by either increase or decrease of applied current. The magnitude of control force is thus a function of the level of deviation of structure from its static equilibrium. The larger the magnitude of deviation, the greater the damper force that is applied.

Classical stochastic control strategies included the use of LQG control developed by Athans (1971). The controlled equation of motion is written in discrete difference form and the variables are treated as Markov process. Relatively recent works on the development of control strategies for random excitation use Fokker–Planck–Kolmogorov (FPK) equation extensively. Ying et al. (2003) proposed a stochastic semi-active control strategy using ER/MR dampers for randomly excited systems. A structural system excited by random loading and controlled by using ER/MR dampers is modelled as a dissipated Hamiltonian system with n degrees of freedom. The control forces generated by ER/MR dampers are split into a passive part and an active part. The stochastic averaging method is applied to obtain partially completed averaged Ito stochastic differential equations for

the quasi-Hamiltonian systems developed above. Then, the stochastic dynamical programming principle is applied to the partially averaged Ito equations to establish a dynamical programming equation. Finally, the response of semi-actively controlled system is obtained from solving the final dynamical programming equation and the FPK equation associated with the fully completed averaged Ito equations of the system.

Zhu et al. (2004) applied the above developed semi-active control strategy for the control of structures subject to wind load. The power spectral density (PSD) matrix of the fluctuating part of wind velocity vector is diagonalized in the eigenvector space. Each element of the diagonalized PSD matrix is modelled as a set of second-order linear filter driven by white noise. The stochastic averaging method is applied to obtain a set of partially averaged Ito equations for controlled modal energies. The stochastic dynamical programming principle is used to obtain the optimal control law which can be implemented by the MR/ER dampers. The response of semi-active controlled structures is predicted by using the reduced FPK equation associated with fully averaged Ito equations of the controlled structures.

Dong et al. (2004) modified the previously proposed stochastic optimal semi-active control strategy for application to a nonlinear oscillator subjected to Gaussian white noise excitations. The control force generated by the MR damper is split into a passive part and a semi-active part. For a nonlinear non-hysteretic stochastic control system, an Itô stochastic differential equation for total energy is derived by using the stochastic averaging method of energy envelope. A dynamical programming equation for the controlled total energy is established based on the stochastic dynamical programming principle. The optimal control law is obtained by minimizing the dynamical programming equation. Finally, the response of semi-actively controlled system is obtained from solving the final dynamical programming equation and the Fokker-Planck-Kolmogorov (FPK) equation associated with the fully averaged Itô equation.

In recent years, a few algorithms have been proposed which are variants of Lypaunov stability criteria or LQR/LQG control. Cha and Agrawal (2013b) presented a novel turbo-Lyapunov control strategy for the semi-active control of a nonlinear highway bridge. The control strategy is based on the fact that the optimal control signal is strongly dependent on the velocity across MR damper. In this approach, the control signal is calculated using an integrated traditional Lyapunov function and a turbo-function. This turbo-function adds or subtracts additional voltage depending on the change in the

absolute velocity across an MR damper. The performance of the proposed controller has been investigated in reducing response quantities of the highway bridge benchmark model. The results show that the proposed turbo-Lyapunov control strategy is quite competitive with respect to numerous other control approaches in reducing response quantities of the benchmark bridge model.

Cha and Agrawal (2013a) presented another novel decentralized output feedback control strategy for the active and semi-active controls of the highway bridge benchmark phases I and II problems. The control force is calculated using two third-order polynomial equations expressing a direct relationship between displacement and velocity of the control device and the control force. An advanced implicit redundant representation genetic algorithm is utilized to determine optimal coefficients of the two polynomial equations by minimizing the sum of three evaluation criteria for six prescribed earthquakes. The results show that the proposed decentralized output feedback polynomial control strategy can achieve significant response reductions in the bridge system, and it is evidently superior to sample control strategies and other suggested active and semi-active controls for the phase I problem and is quite competitive with respect to the sample and other semi-active control approaches for the fully isolated phase II problem.

Mohajer Rahbari et al. (2013) proposed a direct semi-active control method to mitigate the seismic responses of structures equipped with magnetorheological (MR) dampers. Bouc–Wen model is utilized to model the nonlinear behavior of the MR dampers, and a controller is proposed based on this model features. In the proposed semi active control algorithm, for generating the MR damper control force close to the estimated optimal control force at any moment, the optimal magnitude of current voltage that is applied to produce a magnetic field in the MR damper is calculated through the use of linear quadratic regulator optimal control algorithm. The algorithm is used to control seismic vibrations of a three-story and an 11-story sample shear building that have been equipped with the MR dampers.

Hazaveh et al. (2015) presented a semi active control strategy for determining MR damper force, using three algorithms namely, discrete wavelet transform (DWT), linear quadratic regulator (LQR), and clipped-optimal control algorithm. DWT is used to obtain the local energy distribution of the motivation over the frequency bands to modify conventional LQR. The clipped-optimal control algorithm is used to get the MR damper control force to approach the desired optimal force obtained from modified LQR. Bouc-

Wen phenomenological model is utilized to capture the observed nonlinear behaviour of MR dampers. Time history analysis for a single degree of freedom (SDOF) with periods of T= 0.2-5.0 sec is utilized to compare the impact of using classic and modified LQR in controlling the MR damper force under 20 design level earthquakes of the SAC (SEAOC-ATC-CUREE) project. Performance is assessed by comparing the maximum displacement (Sd), total base shear (Fb) and the controller energy. This study shows the proposed modified LQR is more effective at reducing displacement response than conventional LQR. The modified LQR method reduces the median value of uncontrolled Sd by approximately 40% to 88%, over all periods to 5.0 seconds. Moreover, the modified LQR uses about 45% less energy than conventional LQR. Overall, these results indicate the robustness of the proposed method to mitigate structural response using MR dampers.

Control using genetic Algorithm

Researchers in recent years have also used the genetic algorithm extensively in the field of structural control. The primary advantage of these "intelligent" controllers is that they obviate the need for development of any control strategy analytically. Genetic algorithm introduced by Holland (1975b) has been used quite extensively in the structural control.

Rao et al. (1991) formulated a zero-one optimization problem for the discrete optimal actuator location selection problem in actively controlled structures. A genetic algorithmic approach is developed to solve this zero-one optimization problem. The feasibility of the proposed method is demonstrated for the example problem of two-bay truss. The number of actuators is assumed to be three. The optimal linear quadratic regulator is applied to solve the optimal control gain. The dissipation energy of active controller is used as the objective function for maximization. Results were obtained with different crossover probability (from 1.0 to 0.6) and mutation probability (from 0.001 to 0.005). The number of function evaluations in 10 generations varies from 18 to 35. Most of them find the global optimal solution (1,3,5).

Furuya and Haftka (1995) compared several variants of genetic algorithms for optimal placement of actuators on large space structures. By using a simple formulation for the effectiveness of the actuators, the authors perform the millions of evaluations required for comparing the different algorithms as well as the effects of changing mutation rates and population sizes. Results show that the disruptive reproduction operators, such as uniform crossover performed better than single point crossover.

Furthermore, the use of integer coding was more advantageous than binary coding for the example problem. However, even the best algorithm required hundreds of thousands of evaluations for obtaining near optimal designs.

Dhingra and Lee (1995) formulated a multi-objective optimization problem for flexible space structures. The structural weight, controlled system energy, stability robustness index, and the damping augmentation provided by the active controller are considered as objective functions of the design problem. The solution methodology was based on cooperative game theory which permits an integrated determination of optimum feedback gains and optimum locations of actuators/sensors while simultaneously optimizing five different objective functions. The numerical optimizer is based on a hybrid optimization scheme which is synergistic blend of artificial genetic search and gradient-based search techniques. For the single and multiobjective optimization problems which were solved, it was seen that the optimum solutions obtained using the hybrid optimization method frequently outperform the optimum solutions obtained using gradient-based search procedures. The results indicate that the hybrid optimizer has the potential to solve other design optimization problems with mixed discrete-continuous variables with similar efficiency.

Li et al. (2000) proposed a multilevel genetic algorithm to determine the optimum number and location of actuators for active control under wind load. The optimization problem considering the number, the position of actuators and the control algorithms simultaneously in actively controlled structures can be described as a multi-level optimal design model naturally. This problem has the properties of non-linearity, non-continuous, discreteness and multi-modal objective function. The multi-level design model and the formulation in each level proposed give a natural and distinct description for the optimization problem. The multi-level genetic algorithm proposed has been proved to be an effective algorithm for solving the multi-level optimization problem. Furthermore, MLGA is a powerful global search technique that can be used in the analysis and design of structural control systems. Moreover, the optimal position of actuators depends on the control algorithm. In other words, different control algorithms or different controllers yield different positions of actuators.

Abdullah et al. (2001) used a hybrid optimization scheme based on GA and gradient based technique to solve a multi-objective optimization problem for the determination of the optimum location of actuators/sensors. The proposed method of

optimizing the placement of sensor/actuator pairs and their respective gains while using direct velocity feedback as a control law is an effective, simple, and inexpensive method of designing a control system for high-rise structures. The proposed genetic algorithm with selective updating procedures allows the algorithm to quickly converge to the fittest generation. For the example forty-storey structure, the average cost function value varies more from the initial generation to the final generation because there are fewer controllers in comparison to the total number of floors, thus placement has more of an effect on the average cost function value. The decision variables in this optimization problem are greatly dependent on the weighting matrices of LQR method.

Ahlawat and Ramaswamy (2002) proposed a multi objective genetic algorithm to determine optimal configurations of a hybrid control system. A tuned mass damper (TMD) and an active mass driver (AMD) have been used as the passive and active control components of the hybrid control system, respectively. A fuzzy logic controller (FLC) has been used to drive the AMD. The genetic algorithm has been used for the optimization of the control system. Peak acceleration and displacement responses non-dimensionalized with respect to the uncontrolled peak acceleration and displacement responses, respectively, have been used as the two objectives of the multi-objective optimization problem. The proposed design approach for an optimum hybrid mass damper (HMD) system, driven by FLC has been demonstrated with the help of a numerical example. It was shown that the optimum values of the design parameters of the hybrid control system can be determined without specifying the modes to be controlled. The proposed FLC driven HMD has been found to be very effective for vibration control of seismically excited buildings in comparison with the available results for the same example structure but with a different optimal absorber.

Li et al. (2004) formulated the problem of optimal design of the numbers and positions of actuators in actively controlled structures as a three-level optimal design problem. A two-level genetic algorithm (TLGA) is proposed for solving this problem. The authors presented a case study in which a building is subjected to earthquake excitation and controlled by active tendon actuators. Results of this study show that: (1) the design problem for optimizing number and configuration of actuators simultaneously in actively controlled structures has the features of non-linearity, mixed-discreteness and multi-modality; (2) a three-level design model can give a reasonable description for this kind of design. Wongprasert and Symans (2004) used genetic algorithm with integer representation to determine the optimal damper locations for seismic control of a 20-story

benchmark building. Both H_2- and H∞ norms of the linear system transfer function were utilized as the objective functions. Moreover, frequency weighting was incorporated into the objective functions so that the genetic algorithm emphasized minimization of the response in the second mode of vibration instead of the dominant first mode. The results from numerical simulations of the nonlinear benchmark building show that, depending on the objective function used, the optimal damper locations can vary significantly. However, most of dampers tend to be concentrated in the lowermost and uppermost stories. In general, the damper configurations evaluated herein performed well in terms of reducing the seismic response of the benchmark building in comparison to the uncontrolled building

Cha et al. (2013) proposed a gene manipulation, multi-objective genetic algorithm to optimize the placement of active devices and sensors in frame structures to reduce active control cost and increase the structural control strategy's effectiveness. Gene manipulation uses engineering judgment to modify the encoded variable information defining the number of devices and sensors per floor in selected Pareto-optimal front individuals. The proposed methodology evolves Pareto-optimal layouts that minimize the number of devices/sensors used while also minimizing the building interstory drift for a 20-story steel-frame building under earthquake loading. The results indicate that the number and location of the devices and sensors in the layouts obtained strongly depends on the desired maximum drift. Also, the location of the sensors significantly impacts the efficiency of the active controller in reducing interstory drifts. In simulation trials, the proposed gene manipulation method obtained layouts that distributed devices and sensors more evenly over the building height than layouts obtained using standard multi-objective methods, resulting in greater control efficiency. The primary benefit of implementing the proposed gene manipulation was in reducing the number of multi-objective genetic algorithm generations required by up to 40% without negatively impacting the quality of Pareto-optimal device/sensor layout solutions obtained.

2.3 Hybrid Control

The hybrid control system is generally defined as one that employs a combination of passive and active devices or passive and semi-active devices. As multiple control devices are operating in hybrid control systems, some of the restrictions and limitations of each system when they act alone can be alleviated. Additionally, the resulting hybrid control system is more reliable than a fully active system, although it is also often

somewhat more complicated. Research in the area of hybrid control systems has focussed primarily on two classification systems, hybrid mass damper systems, and (ii) active base isolation. The hybrid mass damper (HMD) is a combination of a tuned mass damper (TMD) and an active mass driver/active control actuator. Active base-isolation system consists of a passive base isolation system combined with a control actuator to supplement the effects of the base isolation system. In addition to these, some other passive devices like visco-elastic dampers, tuned liquid column dampers are combined with the active control device like active mass driver/active control actuator. Soong and Reinhorn (1993) presented a review of early research contributions in the area of hybrid control in Unites States. Review on structural control by Housner et al. (1997) and by Fisco and Adeli (2011b) also provides an overview of developments in the area of hybrid control.

Various control methods have been investigated for HMD controller design. Shing et al. (1994), Kawatani et al. (1994) and Spencer Jr et al. (1994) considered optimal control methods for HMD control design. Tamura et al. (1994) proposed a gain scheduling technique in which the control gains vary with the excitation level to account for stroke and control force limitations. Adhikari and Yamaguchi (1994) applied sliding mode theory to control structures with HMD systems.

Active base-isolation system has been investigated by many researchers. Some of the early contributions in this area are by Yang et al. (1991), Yang et al. (1992), Nagarajaiah et al. (1993). Several small-scale experiments have been performed to verify the effectiveness of this class of systems in reducing the structural responses. Reinhorn and Riley (1994) performed experimental and analytical studies on a small scale bridge installed with a sliding hybrid isolation system. The control actuator of the hybrid system was employed between the sliding surface and the ground to supplement the base-isolation system. Feng et al. (1993) presented another type of hybrid base-isolation system having semi-active friction-controller fluid bearings in the isolation system. The pressure in the fluid could be varied to control the amount of friction at the isolation surface. As base-isolation systems exhibit either hysteretic or nonlinear behaviour, researchers have also developed various non-linear/hysteretic control strategies including fuzzy control (Nagarajaiah,1994), neural network based control (Venini and Wen,1994), dynamic linearization (Yang et al.,1994a) and adaptive non-linear control (Rodellar et al.,1994).

Some of the researchers have also investigated another category of the hybrid control systems consisting of viscoelastic dampers and the active control systems. Inaudi and Kelly (1993) presented a formulation for earthquake resistant design of optimum hybrid isolation systems for sensitive equipment protection. The hybrid system consisted of laminated rubber bearings, viscoelastic dampers and a set of actuators. The actuators were integrated into the main structural system, deliver forces on the basement of the isolated substructure mounted on the main structural system. An integral design procedure for the passive and active components of the isolation system was developed aiming at acceleration reduction under random excitation. The active component of the isolation system applied forces proportional to the absolute velocity of the isolated piece of equipment.

Tzan and Pantelides (1994) studied viscolelastic dampers (VEDs) and active control systems together as a hybrid system for their effectiveness in reducing the response of seismic structures. They examined the possibility of combining VEDs and active control systems to improve the performance of both systems. Viscoelastic dampers considered had properties which were both frequency and temperature dependent. Two control algorithms based on drift and velocity/acceleration feedback were compared with existing algorithms.

Meirovitch and Stemple (1997) presented the nonlinear control method to mitigate the effect of earthquake through base isolation and feedback control. The control law is a modified on-off with dead zone in conjunction with a direct feedback. The control design was found satisfactory, indicating that significant reduction in the acceleration of the structure can be achieved with the control force smaller than 1% of the weight of the structure.

Glauser et al. (1997) studied the effectiveness of the performance of an active vibration absorber (AVA) in conjunction with a passive isolator system under seismic excitation. The optimum AVA controller parameters are obtained by using the frequency matching method. It was observed that the hybrid and AVA controller could be designed to be highly effective in suppressing the structural vibration.

Symans and Kelly (1999) proposed an intelligent hybrid isolation system containing semi-active dampers for seismic protection of a bridge structure. The study showed that hybrid seismic isolation systems consisting of combined base isolation bearings and supplemental energy dissipation devices can be beneficial in reducing the seismic response of structures.

Zhao et al. (2000) investigated the application of the sliding mode control (SMC) strategies for reducing the dynamic responses of the building structures with base isolation hybrid protective system. They proposed the method for determining switching function and the closed loop (feedback) controllers based on the reaching law method of sliding mode control theory.

Nagashima et al. (2001) developed a hybrid mass damper (HMD) system and studied its application to a 36-storey building to improve the habitability of the building against strong winds. Two HMD systems were applied to control the transverse-torsional coupled vibration of the building. Variable gain feedback (VGF) control technique was also developed to fully utilize the capacity of the HMD system from weaker to stronger external excitations.

Saito et al. (2001) developed a large-scale hybrid mass damper (HMD) system to reduce building response during strong winds and earthquakes of upto medium strength. The HMD consisted of an auxiliary mass supported by multi-stage rubber bearings and actuators driven by AC servomotors. Two HMDs were installed on the top floor of a target building to suppress both translational and torsional vibrations.

Yang and Agrawal (2002) studied the safety performances of various types of hybrid control systems for nonlinear buildings against near-field earthquakes. Hybrid control systems consisted of mainly the base isolation system and either the passive control device or the semi-active dampers or the combination. Passive control systems involved viscous dampers and friction dampers and two newly proposed semi-active control systems were investigated including the resetting semi-active stiffness damper and the semi-active electromagnetic friction damper. Simulation studies were performed for control of base-isolated buildings subjected to various near-field earthquakes. Simulation results demonstrated that the proposed resetting semi-active stiffness damper and semi-active electromagnetic friction damper were quite effective in protecting the safety of building structures against near-field earthquake.

Park et al. (2003) investigated a hybrid control scheme composed of a passive control system to reduce the earthquake-induced forces in the structure and an active control system to further reduce the bridge responses, especially deck displacements. Lead rubber bearings (LRBs) are used for the passive control design. For the active control design, ideal hydraulic actuators are used and an H_2/ LQG control algorithm was adopted. A hybrid feedback-LMS model was presented for control of structures through integration of a feedback control strategy such as the LQR or LQG algorithm and the

filtered-x LMS algorithm (Kim and Adeli,2004). The algorithm was presented for control of structures through integration of a feedback control algorithm such as the LQR or LQG algorithm and the filtered-x LMS algorithm. The algorithm was applied to the active tuned mass damper system. It has been shown that the hybrid feedback-LMS algorithm minimizes vibrations over the entire frequency range and thus is less susceptible to modeling error and inherently more stable.

Soneji and Jangid (2007) proposed a passive hybrid system consisting of a viscous fluid damper (VFD), used as a passive supplemental energy dissipation device, and elastomeric sliding isolation systems. The seismic response of a simplified lumped-mass bridge model with passive hybrid systems was compared with the corresponding response of the bridge with only isolation systems, as well as with the uncontrolled bridge. The results of the investigation showed that the addition of supplemental damping in the form of a viscous fluid damper significantly reduces the earthquake response of an isolated cable-stayed bridge.

Chung et al. (2005) proposed a semi-active tuned mass damper (STMD) for building control. Semi active tuned mass damper (STMD) combine a passive tuned mass damper (TMD) and a semi active damper. The property of semi active damper is adjusted online to produce the desired control force. In their study, they used two kinds of semi active control devices, one is variable damping device and the other is MR damper to illustrate the control effect of STMD. They compare the control effect of the TMD and active tuned mass damper with that of the STMD. The numerical simulation results showed that the STMD improve the control efficiency of TMD.

Cai et al. (2007) explored the TMD-MR damper system for cable vibration mitigation through an experimental approach. The combination of the position flexibility of TMDs and the adjustability of MR dampers were the advantages of the proposed damper. The proposed damper system was attached to a 7.16-m-long cable to investigate its vibration reduction effectiveness and the dynamic properties of the combined cable-damper system. Experimental results show good vibration reduction effects of the TMD-MR system.

Kang et al. (2011) studied the effectiveness of semi-active tuned mass dampers (STMDs) for the response control of a wind-excited tall building. A 76-storey, 306 m benchmark building proposed for the city of Melbourne, Australia was used for this purpose. Across wind load, data from wind tunnel tests were employed as excitation. A variable damping device and a magneto rheological (MR) damper were used to compose

STMDs. A ground hook control algorithm was used to appropriately modulate the damping force of the semi-active damper. The robustness of the STMD was also investigated through the uncertainty in the building's stiffness. The numerical studies show that the STMD can reduce the structural responses similar to an ATMD, but with a significant reduction in power consumption. It was also shown that the STMD with a 50 kN capacity MR damper can effectively control a full-scale tall building subjected to wind excitation, and it can satisfy the design requirements and constraints of the benchmark problem.

Kim et al. (2015) studied the control performance of a semi-active TMD using an idealized variable damping device and a magnetorheological (MR) damper. These both systems are capable of changing the properties of TMDs in real time based on the dynamic responses of a structure. The control performance of STMD is investigated with respect to various types of excitation by numerical simulation. Groundhook control algorithm is used to appropriately modulate the damping force of semiactive dampers. The control effectiveness between STMD and a conventional passive TMD, both under harmonic and random excitations, is evaluated and compared for a single-degree-of-freedom (SDOF) structure. Excitations are applied to the structure as a dynamic force and ground motion, respectively. The numerical studies showed that the control effectiveness of STMD is significantly superior to that of the passive TMD, regardless of the type of excitations.

Kaveh et al. (2015) investigated the performance of semi-active tuned mass dampers (SATMD), in which a mass damper works parallel with a MR damper for response reduction of a ten story building for four earthquake excitations. Input voltage of the MR damper was calculated using a fuzzy controller optimized by charged system search (CSS) algorithm. The results showed better performance of the optimized fuzzy controller in comparison with conventional fuzzy controllers and passive TMD.

Bathaei et al. (2017) investigated the performance of a semi-active tuned mass damper with adaptive magnetorheological (MR) damper using two different types of fuzzy controllers for seismic control of a 11-DOF building frame. The TMD was installed on the roof and the MR damper was placed on the 11th story. The fuzzy system was designed based on the acceleration and velocity of the top floor. Hence, the input voltage needed to produce the control force was based on the movement of the structure. The seismic performance of semi-active type-2 controller, which considers the uncertainties related to input variables, is higher than that of the type-1 fuzzy controller. The type-2

fuzzy controller is capable of reducing further the maximum displacement, acceleration, and base shear of the structure by 11.7, 14, and 11.2%, respectively, compared to the type-1 fuzzy controller.

2.4 Concluding Remarks

From the above literature, it is seen that the optimized semi active control of responses using MR dampers and sensors is not well reported in the literature. Since the MR damper is a very costly device, a limited of them can be used in practice. Further, a limited number of response measurements are possible in practice for feedback control. As a consequence, optimized semi active control of partially observed structures using the MR damper forms an important subject of research.

Although, a large number of control algorithms are developed for semi-active control of partially observed building frames, all algorithms except passive-on use estimated state of the structure for obtaining the desired time history of voltage to be applied to the MR damper. This introduces some errors in the predicted control force and hence, controlled responses. There is a need for developing a control algorithm based on the measured responses only, in order to avoid these kinds of errors.

Further, it is seen from the literature review that the different control algorithms provide different response reductions for various excitations. However, an extensive comparative study on the performance of different control algorithms using the MR damper is lacking. Another area where not many studies are available in the literature is the nature of ground motion considered in the semi active control with MR damper. The topic is important in relation to the full state estimation from the observed ones. Kalman filter which is widely used for the state estimation is strictly valid for Gaussian white noise excitation. However, the ground motions (random or deterministic) considered in the studies are non-white. Thus, procedure for use of Kalman filter for partially observed systems under non-white excitations needs special attention.

Various combinations of control techniques and devices have been carried out by researchers in the field of hybrid control. There has been extensive use of hybrid mass dampers (HMDs), viscolelastic dampers (VEDs), active control systems and active or passive base isolation systems. Comparatively, fewer studies are conducted using a hybrid system consisting of semi-active MR dampers and passive TMDs in the form of STMD. Hybrid control of building frames has attracted the researchers but no significant research has been done on the optimal number and placement of the MR damper in the

hybrid control using TMD and MR dampers. With the above gap areas identified in the literature review, the objectives of the present study have been framed and have been stated at the end of the introduction chapter.

Chapter 3

Development of a New Algorithm for Partially Observed Building Frame Using MR Damper

3.1 Introduction

A comprehensive review of different studies on semi-active control using the MR damper is made in chapter two. The review shows that a large number of algorithms have been developed for the semi-active control of building frames using the MR damper. However, very few algorithms are developed where the control voltage to be applied to generate the desired control force is directly derived. Either control forces developed by standard algorithm are clipped or modified to accommodate the forces which could be generated by the MR damper within a limited voltage range. Further, very few control algorithms are developed by taking advantage of the special features of semi-active control with MR dampers, described in Chapter 1 and considering the requirements of good state estimation from the measured ones. Finally, no systematic comparison of the efficiency of different control algorithms under different types of ground motions for partially observed systems has been made in the past. Such comparison is useful in deciding the appropriate algorithm to be used for specific type of excitation. With this background in view, the study presented in this chapter is conducted.

In this study, first a direct control algorithm called velocity tracking control is proposed for semi-active control of building frames using a limited number of MR dampers and measurement of responses. Then, the efficiency of the proposed algorithm is compared with those of a number of widely used control algorithms for different types of earthquakes for partially observed system. The types of earthquakes include

i. Far field earthquakes
ii. Near field earthquakes
iii. Synthetically generated narrowband and broadband earthquakes

The new control algorithm uses a limited number of MR dampers and sensors to control the structural responses. The algorithm has two distinct features i) it does not require the knowledge of the full state ii) no reference control force is required for comparison, in order to decide the voltage to be applied during a time increment. Since the full state of the system is not required for the development of the algorithm, the state

estimation from the measured states can be eliminated, thus eliminating a major source of error in the algorithm developed.

3.2 Theory

First, the proposed algorithm called the velocity tracking algorithm (VTC) is developed. Then, four control strategies, which are well established, are briefly outlined. The algorithms are: i) LQG with clipped optimal control, ii) bang-bang control, iii) sliding mode control with clipped optimal control, and iv) passive–on control. The efficiency of the proposed algorithm is compared with those of the four algorithms mentioned above. Two observation schemes are considered for semi active control. First scheme is based on partial observation, i.e., a few number of responses (displacement or velocity feedback) are measured and the full state is estimated from the measured ones using Kalman filter. The other scheme is full state observation in which it is assumed that the full state (all floors displacements and velocities) are available for feedback and control force is calculated using them.

3.2.1 Generation of Control Forces using MR Damper

Force in the MR damper is generated based on the movement of the piston and the viscosity of the MR fluid which is manipulated by applying the voltage to the magnetic coil of the MR damper. While the actuation of the piston is governed by the vibration of the structure, the applied voltage is governed by the control algorithm. The modified bouc wen model is used for predicting the MR damper force. Inputs to the model are the inter-story drifts and velocities. The parameters of the MR damper are shown in Table 3.1 and the diagram of the model is given in Figure 3.1.

The MR damper force U predicted by the model is given as (Spencer et al.,1997):

$$U = c_1 \dot{x}_V + k_1 (u_d - x_0) \tag{3.1}$$

where, the evolutionary variable z_0 is given as

$$\dot{z}_0 = -\gamma \,|\, \dot{u}_d - \dot{x}_V \,|\, z_0 \,|\, z_0 \,|^{n-1} - \beta (\dot{u}_d - \dot{x}_V) \,|\, z_0 \,|^n + A_m (\dot{u}_d - \dot{x}_V) \tag{3.2}$$

and $\dot{x}_V$ is given as

$$\dot{x}_V = \left\{\frac{1}{c_0 + c_1}\right\}\{\alpha_0 z_0 + c_0 \dot{u}_d + k_0(u_d - x_V)\} \tag{3.3}$$

where, u_d and $\dot{u}_d$ are the relative displacement and relative velocity of the floor at which damper is placed; z_0 is the evolutionary variable that describes the hysteretic behaviour of the damper; k_1 is the accumulator stiffness; c_0 is the viscous damping at large velocities; c_1 is viscous damping for force roll-off at low velocities**;** k_0 is the stiffness at large velocities; and x_0 is the initial stiffness of spring k_1; α_0 is the evolutionary coefficient; and γ, β, η and A_m are shape parameters of the hysteresis loop. The model parameters dependent on command voltage, c_0, c_1, and α_0 are expressed as

$$c_0 = c_{0a} + c_{0b} U_0 \tag{3.4}$$

$$c_1 = c_{1a} + c_{1b} U_0 \tag{3.5}$$

$$\alpha_0 = \alpha_{0a} + \alpha_{0b} U_0 \tag{3.6}$$

where, U_0 is given as output of first order filter following the condition as below

$$\dot{U}_0 = \eta(U_0 - V) \tag{3.7}$$

Note that V is the voltage applied to the MR damper.

3.2.2 Velocity tracking control (VTC)

Velocity tracking algorithm is based on two premises i) force in the MR damper modelled by modified Bouc-wen model (Spencer et al.,1997) depends largely on the velocity and much less on the displacement of the piston and ii) when the voltage across the damper is changed then the direction of the force remains the same, while the magnitude of the force changes for a given set of piston displacement and velocity. The former is dictated by the relative movements between the two floors which in turn depend upon the control force. The latter is governed by the mechanical characteristics of the damper. These characteristics are responsible for limiting the maximum voltage that can be applied to the MR damper. Further, they lead to a saturation effect i.e. beyond a certain level of voltage; the increase in force in the MR damper with the increase in voltage is

marginal. To illustrate the saturation effect, MR damper force is generated using a set of relative displacement and relative velocity of first floor of the building used in the numerical study subjected to El Centro (1940) and Kobe (1995) earthquakes. The MR damper force is generated at different voltages, namely 0, 3, 6, 9 and 10 volt using modified bouc-wen model. A comparison of the MR damper force generated at different voltage is plotted in Figure 3.2. It is seen from the figure that as the voltage is increased from 0 to 10 volt, the MR damper force increases but the sign remains the same. Further, in the figure, the absolute maximum force generated in the MR damper saturates after 9 volt.

It was stated in the introduction that the use of filter for estimating the full state from the observed ones introduces some amount of error in the state estimation. Further, the filter constant matrices, used for finding the best state estimate, do not remain invariant of the nature of disturbance and measurement noises. Therefore, any control algorithm which does not require state estimation will be a preferred choice. The new control algorithm eliminates the use of filter by taking advantage of the features of semi-active control using MR damper namely,

i) The actuation of the pistons of MR dampers within the fluid is solely governed by the states of the floors between which MR dampers are placed.
ii) Voltage to be applied at an instant of time is either maximum or minimum (usually zero) determined by a control algorithm.
iii) Number of MR dampers is always limited from the consideration of cost and saturation effect; therefore, the information about the states required determining the control forces are limited.

Thus, velocity and displacement sensors are placed only at the floors whose states are to be known for the determination of the damper forces. Knowledge of the states i.e. displacement and velocities of other floors are redundant for feedback information if a direct control algorithm is formulated. The direct algorithm is defined as the one which obtains the voltage to be applied at every instant of time using the feedback information of the measured states only i.e. full state information is not required.

Consider the multi degree of freedom (MDOF) system represented by

$$[\mathbf{M}][\ddot{\mathbf{z}}]+[\mathbf{C}][\dot{\mathbf{z}}]+[\mathbf{K}][\mathbf{z}]=[\mathbf{G}][\mathbf{u}]-[\mathbf{M}][\mathbf{r}][\ddot{u}_g] \tag{3.8}$$

where, **M**, **C**, and **K** are the mass, damping and stiffness matrices of the system, respectively; **u** is the MR damper force vector; **G** is the damper location matrix of ones and zeroes; **z** is the displacement vector with respect to the ground; **r** is an influence coefficient vector; and $\ddot{\mathbf{u}}_{\mathbf{g}}$ is the earthquake ground acceleration. The governing equation (Equation 3.8) is expressed in the state-space form as below:

$$[\dot{\mathbf{x}}] = [\mathbf{A}][\mathbf{x}] + [\mathbf{B}][\mathbf{u}] + [\mathbf{E}][\ddot{u}_g] \tag{3.9}$$

$$[\mathbf{y}] = [\mathbf{C}][\mathbf{x}] + [\mathbf{D}][\mathbf{u}] + \mathbf{v} \tag{3.10}$$

where **A** is a 2n x 2n system matrix, **B** is a 2n x n_C control matrix, **E** is a 2n x 1 disturbance (excitation) matrix, **C** is a p x 2n measurement matrix, **D** is a p x n_c matrix, **x** is a 2n x 1 state vector, **y** is a p x 1 vector of measured outputs and **v** is a p x 1 measurement noise vector; n is the number of states, n_C is the number of controllers and p is the number of measurements of feedback responses. The **A, B** and **E** matrices are defined as

$$\mathbf{A} = \begin{bmatrix} \mathbf{O} & \mathbf{I} \\ -\mathbf{M}^{-1}\mathbf{K} & -\mathbf{M}^{-1}\mathbf{C} \end{bmatrix};\ \mathbf{B} = \begin{bmatrix} \mathbf{O} \\ -\mathbf{M}^{-1}\mathbf{G} \end{bmatrix};\ \mathbf{E} = \begin{bmatrix} \mathbf{O} \\ \mathbf{r} \end{bmatrix} \tag{3.11}$$

where, **I** and **O** are the identity and null matrices of size n x n, respectively.

The matrix **A**, **B**, **E**, **C** and **D** should be such that the controllability condition is satisfied i.e.

i. The pair **A** and **E** is stabilizable.

ii. The pair **A** and **B** is stabilizable; pair **C** and **A** is detectable.

Further, the observability condition should also holds good

$$\begin{bmatrix} \mathbf{B} \\ \mathbf{D} \end{bmatrix} \mathbf{D}^{\mathbf{T}} = \begin{bmatrix} \mathbf{O} \\ \mathbf{I} \end{bmatrix} \tag{3.12}$$

where **O** and **I** are the identity and null matrices.

Referring to Figure 3.3, consider n_a number of MR dampers placed as shown in the figure. The control algorithm is based on the closed loop feedback control. The

feedback information available at i^{th} time step is utilized to decide the voltage to be applied to r^{th} MR damper at $i+1^{th}$ time step. Let d_i^r and v_i^r be the displacement and velocity of the piston of the r^{th} damper at the i^{th} time step. Then the force generated by the damper is given by the equations 3.1-3.3 with u_d and $\dot{u}_d$ representing d_i^r and v_i^r.

It was shown in the Figure 3.2 that for a given set of d_i^r and v_i^r the damper force increases with increase in the voltage. Therefore, for maximizing the control action, V_{max} is applied to the r^{th} MR damper if the damper force acts opposite to the direction of movement of the r^{th} floor i.e. , it opposes $\dot{x}^r$. If both damper force and velocity of floor in the same direction, $V_{min.}$ (i.e. zero) is applied to the damper. These voltages act over the time interval Δt i.e. between t_{i+1} and t_i. The above condition may be mathematically represented by

$$\dot{x}_i^r f_i^r < 0, \;\; V_{i+1} = V_{max} (t_i < t \le t_{i+1}) \tag{3.13}$$

$$\dot{x}_i^r f_i^r > 0, \;\; V_{i+1} = V_{min} (t_i < t \le t_{i+1}) \tag{3.14}$$

The conditions represented by equations (3.13-14), correspond to the Lypaunov stability conditions of the first order filter (equation 3.7) of the modified Bouc Wen model. The proof is given in subsequent subsection. Note that this filter equation governs the relationship between the voltage applied to the MR damper and the force developed in it by way of modifying the properties of the fluid inside. The schematic diagram of VTC is shown in Figure 3.4.

Proof:

The Lypaunov function for the filter is represented by equation 3.15

$$L = \frac{1}{2} U_O^2 \tag{3.15}$$

The derivative of Lyapunov function is given as,

$$\dot{L} = U_0 \dot{U}_0 \tag{3.16}$$

Substituting $\dot{U}_0$ from equation 3.7 in equation 3.15 and establishing the Lyapunov condition as $\dot{L}$ to be negative,

$$U_0(U_0 - V) < 0 \tag{3.17}$$

Assuming both U_0 and V to be positive, the condition is satisfied for $U_0 < V$.

Since, V can assume Vmax or V_{min} (usually kept at zero), $V = V_{max}$ satisfies the condition given by equations 3.16-17. For V=0, the Lyapunov stability condition is not satisfied i.e.

$$U_0(U_0 - V) > 0 \tag{3.18}$$

Thus, equation 3.13 corresponds to Lyapunov stability condition of the filter used in the modified Bouc wen model. When the Lyapunov condition is not staisfied, equation 3.14 is used which is developed based on physical reasoning and which is meaningful in the sense that the magnitude of the force devloped is minimized by setting voltage at the minimum when the instability of the filter sets in.

3.2.3 Other standard algorithms used for comparing the results of VTC

Since first three algorithms require the full state estimation from the measured states, the state estimation using Kalman filter is described first. The control algorithms are derived using the separation principle i.e. the algorithm remains valid for the estimated and actual state.

Full State estimation using Kalman filter

For partially observed system, the full state $\hat{\mathbf{x}}(t)$ is estimated from the measurement $\mathbf{y}(t)$ by the equation (3.19)

$$\dot{\hat{\mathbf{x}}}(t) = \mathbf{A}\hat{\mathbf{x}}(t) + \mathbf{B}\mathbf{u}(t) + \mathbf{K}(t)\left(\mathbf{y}(t) - \mathbf{C}\hat{\mathbf{x}}(t)\right) \tag{3.19}$$

where $\mathbf{K}(t)$ is the Kalman gain associated with the Kalman filter. At each time step t, the Kalman gain estimates the state from past measurements and inputs. The Kalman gain is obtained from **A, B, V, W** matrices and $E(\mathbf{x}(\mathbf{0})\mathbf{x}^{\mathbf{T}}(\mathbf{0}))$ by solving the following Riccati equations (equations 3.20-21). **V** and **W** are the covariance matrices of white Gaussian noise $\mathbf{v}(t)$ and excitation $\mathbf{w}(t)$. Thus, excitation and measurement noise in equations 3.8-10 should ideally be white noise.

$$\dot{\mathbf{P}}(t) = \mathbf{P}(t)\mathbf{A} + \mathbf{P}(t)\mathbf{A}^{\mathbf{T}} + \mathbf{P}(t)\mathbf{C}^{\mathbf{T}}\mathbf{V}^{-1}\mathbf{C}\mathbf{P} + \mathbf{W} \tag{3.20}$$

K(t) in equation 3.20 called Kalman gain is given as:

$$\mathbf{K}(t) = \mathbf{P}(t)\mathbf{C}^{T}\mathbf{V}^{-1} \text{ and } \mathbf{P(0)} = E\left(\mathbf{x(0)x}^{T}\mathbf{(0)}\right) \tag{3.21}$$

LQG with Clipped Optimal Control (LQGCl)

The control force **u**(t) is obtained by LQR algorithm using estimated states $\hat{\mathbf{x}}(t)$ as shown below:

$$\mathbf{u}(t) = -\mathbf{L}(t)\hat{\mathbf{x}}(t) \tag{3.22}$$

where **L**(t) is the feedback gain matrix and it is defined using **A,B, Q, R** matrices and **F** by solving the following Riccati equations:

$$-\dot{\mathbf{S}}(t) = \mathbf{A}^{T}\mathbf{S}(t) + \mathbf{S}(t)\mathbf{A} - \mathbf{S}(t)\mathbf{B}^{T}\mathbf{R}^{-1}\mathbf{B}^{T}\mathbf{S}(t) + \mathbf{Q} \tag{3.23}$$

$$\mathbf{L}(t) = \mathbf{R}^{-1}\mathbf{B}^{T}\mathbf{S}(t) \text{ and } \mathbf{S}(T) = \mathbf{F} \tag{3.24}$$

The input voltage to the MR damper is obtained using clipped optimal law (Dyke et al.,1996a). When the absolute value of MR damper force is greater than the absolute value of LQR force, then the voltage is set to maximum, and when the absolute value of MR damper force is less than the absolute value of force, then the voltage is set to zero. The mathematical form of clipped optimal law is:

$$V = V_{max} H\left\{\left(F_d - F_{mr}\right)F_{mr}\right\} \tag{3.25}$$

where V is the input voltage to the MR damper, H is the Heaviside function, $V_{max}$is the maximum input voltage, F_d is the desired control force obtained from LQR control algorithm and F_{mr} is the MR damper force. The voltage is maximum when Heaviside function is one and zero when Heaviside function is zero. The schematic diagram of LQG with clipped optimal control for full state and partial state observation is shown in Figure 3.5.

Bang-Bang control

Bang-bang control is based on Lyapunov's stability theory (Leitmann,1994). The Lyapunov function denoted by **L{x̂}** is a positive definite function of the states of the system. According to the theory, when the rate of change of Lyapunov function (**L̇**) is negative semi-definite, the system is said to be stable. Hence, in developing the cotrol

algorithm the objective is to select control inputs such that the $\dot{\mathbf{L}}$ remains negative. For the bang-bang control, the following Lypaunov function is selected.

$$\mathbf{L}\{\hat{\mathbf{x}}\} = \frac{1}{2}\|\hat{\mathbf{x}}\|_{\mathrm{p}}^{2} \tag{3.26}$$

where $\|\{\hat{\mathbf{x}}\}\|_{\boldsymbol{p}}$ is the P-norm of state defined by

$$\|\hat{\mathbf{x}}\|_{\mathbf{p}} = \left[\{\hat{\mathbf{x}}^{\mathbf{T}}\}\{\mathbf{P_L}\}\{\hat{\mathbf{x}}\}\right]^{1\backslash 2} \tag{3.27}$$

where, $\mathbf{P_L}$ is real, symmetric, positive definite matrix. In the case of a linear system, to ensure $\dot{\mathbf{L}}$ is negative definite, $\mathbf{P_L}$ is found using the following Lyapunov equation for a positive definite matrix $\mathbf{Q_P}$,

$$[\mathbf{A}^{\mathbf{T}}][\mathbf{P_L}] + [\mathbf{P_L}][\mathbf{A}] = -[\mathbf{Q_P}] \tag{3.28}$$

The derivative of the Lyapunov function for the solution of the state-space equation given in equation (3.9) is

$$\dot{\mathbf{L}} = -\frac{1}{2}\{\hat{\mathbf{x}}^{\mathbf{T}}\}\{\mathbf{Q_P}\}\{\hat{\mathbf{x}}\} + \{\hat{\mathbf{x}}\}[\mathbf{P_L}][\mathbf{B}]\{\mathbf{f_m}\} + \{\hat{\mathbf{x}}^{\mathbf{T}}\}[\mathbf{P_L}][\mathbf{E}]\{\ddot{\mathrm{u}}_{\mathrm{g}}\} \tag{3.29}$$

where $\mathbf{f_m}$ is the MR damper force vector generated in the previous time step.

Thus the control law, which will minimize $\dot{L}$ is

$$\mathrm{V} = \mathrm{V}_{\max}\mathrm{H}\left(\{-\hat{\mathbf{x}}^{\mathbf{T}}\}\{\mathbf{P_L}\}\{\mathbf{B}\}\{\mathbf{f_m}\}\right) \tag{3.30}$$

where, H (.) is Heaviside step function. When H (.) is greater than zero, voltage applied to the damper is $V_{max,}$, otherwise, the voltage is set to zero. The schematic diagram of bang-bang control for full state and partial state observation is shown in Figure 3.6.

Sliding mode control with clipped optimal control (SMCCl)

Sliding mode control has been used for active control of structures by various researchers (Yang et al.,1994b, Sarbjeet and Datta,2000, Sarbjeet and Datta,2003). Sliding mode control consists of two stages: firstly, the sliding surfaces are designed and then the controllers are designed such that they drive the response trajectory on the sliding

surfaces. The external excitation is neglected for the design of sliding surfaces. However, it is taken into account for the design of controllers. For m number of controllers, m numbers of sliding surfaces, S_1, S_2…S_m are defined as given below

$$\mathbf{S} = [S_1, S_2, ...S_m]' \tag{3.31}$$

where **S** is a vector consisting of m sliding variables. **S** is defined as a linear combination of state variables as shown in equation (3.32)

$$\mathbf{S} = \mathbf{M}\hat{\mathbf{x}} \tag{3.32}$$

where **M** is a (m x 2n) matrix to be determined such that motion on the sliding surface is stable. For the response trajectory to stay on sliding surface it is required that $\dot{\mathbf{S}} = 0$. From equations (3.9) and (3.32) it follows that

$$\dot{\mathbf{S}} = \mathbf{M}(\mathbf{A}\hat{\mathbf{x}} + \mathbf{B}\mathbf{u}) = 0 \tag{3.33}$$

Solution of equation (3.33) for **u** gives the equivalent control force $\mathbf{u_{eq}}$ on the sliding surface as given below:

$$\mathbf{u_{eq}} = \mathbf{u} = -(\mathbf{MB})^{-1}\mathbf{MA} \tag{3.34}$$

Substitution of eq. (3.35) in eq. (3.9) gives the following relation when external excitation is neglected.

$$\dot{\hat{\mathbf{x}}} = \left[\mathbf{A} - \mathbf{B}(\mathbf{MB})^{-1}\mathbf{MA}\right]\hat{\mathbf{x}} \tag{3.35}$$

For the determination of **M** matrix, the state-space equation of motion, equation (3.9) is transformed into the so-called regular form (Yang et al.,1994b) as follow:

$$\mathbf{x_n} = \mathbf{P}\hat{\mathbf{x}} \tag{3.36}$$

where **P** is the transformation matrix given as below

$$\mathbf{P} = \begin{bmatrix} \mathbf{I}_{2n-m} & -\mathbf{B}_1\mathbf{B}_2^{-1} \\ \mathbf{O}_m & \mathbf{I}_m \end{bmatrix} \tag{3.37}$$

$\mathbf{I_{2n-m}}$ and $\mathbf{I_m}$ are the identity matrices of size 2n-m x 2n-m and m x m, respectively; $\mathbf{O_m}$ is the zeroes matrix of size m x m. $\mathbf{B_1}$ and $\mathbf{B_2}$ are the sub matrices of size 2n-m x m and m x m obtained by the partition of **B** matrix as follow

$$\mathbf{B} = \begin{bmatrix} \mathbf{B_1} \\ \mathbf{B_2} \end{bmatrix} \tag{3.38}$$

If the partition of **B** into $\mathbf{B_1}$ and $\mathbf{B_2}$ results in a singular $\mathbf{B_2}$ matrix then the original state equation is rearranged such that $\mathbf{B_2}$ matrix becomes non singular.

By substituting the transformation matrix **P**, the state equation (3.9) and sliding surface equation (3.32) becomes as follow

$$\dot{\mathbf{x}}_n = \bar{\mathbf{A}}\mathbf{x}_n + \bar{\mathbf{B}}\mathbf{u} \text{ and } \mathbf{S} = \bar{\mathbf{M}}\mathbf{x}_n \tag{3.39, 3.40}$$

$$\text{where } \bar{\mathbf{A}} = \mathbf{PAP}^{-1} = \begin{bmatrix} \bar{\mathbf{A}}_{11} & \bar{\mathbf{A}}_{12} \\ \bar{\mathbf{A}}_{21} & \bar{\mathbf{A}}_{22} \end{bmatrix};\ \bar{\mathbf{M}} = \mathbf{MP}^{-1};\ \bar{\mathbf{B}} = \begin{bmatrix} \mathbf{0} \\ \mathbf{B}_2 \end{bmatrix} \tag{3.41}$$

Eq. (3.40) is referred as regular form in which $\bar{\mathbf{B}}$ is given by eq. (3.41)

$\mathbf{x_n}$ and $\bar{\mathbf{M}}$ are partitioned as follow:

$$\mathbf{x}_n = \begin{bmatrix} \mathbf{x}_{n1} \\ \mathbf{x}_{n1} \end{bmatrix} \text{and } \bar{\mathbf{M}} = \begin{bmatrix} \bar{\mathbf{M}}_1 : \bar{\mathbf{M}}_2 \end{bmatrix} \tag{3.42}$$

where $\mathbf{x_{n1}}$ and $\mathbf{x_{n2}}$ are vectors of size 2n-m and m. $\bar{\mathbf{A}}_{11}$, $\bar{\mathbf{A}}_{22}$, $\bar{\mathbf{M}}_1$ and $\bar{\mathbf{M}}_2$ are matrices of size 2n-m x 2n-m, m x m, m x 2n-m, and m x m, respectively. Substituting equation (3.42) in equations (3.39) and (3.40), the following equations of motion on sliding surface are obtained,

$$\dot{\mathbf{x}}_n = \bar{\mathbf{A}}_{11}\mathbf{x}_{n1} + \bar{\mathbf{A}}_{12}\mathbf{x}_{n2} \tag{3.43}$$

$$\mathbf{S} = \bar{\mathbf{M}}_1\mathbf{x}_{n1} + \bar{\mathbf{M}}_2\mathbf{x}_{n2} = 0 \tag{3.44}$$

Assuming $\bar{\mathbf{M}}_2$ to be an identity matrix i.e. $\bar{\mathbf{M}}_2 = \mathbf{I_m}$ then using equation (3.43), $\mathbf{x_{n2}}$ is written in terms of $\mathbf{x_{n1}}$ as,

$$\mathbf{x}_{n2} = -\bar{\mathbf{M}}_1\mathbf{x}_{n1} \tag{3.45}$$

Substituting the value of $\mathbf{x_{n2}}$ in equation (3.43) gives the following 2n-m equations of motion on the sliding surface

$$\mathbf{x}_{n2} = \left(\bar{\mathbf{A}}_{11} - \bar{\mathbf{A}}_{12}\bar{\mathbf{M}}_1\right) \tag{3.46}$$

The matrix $\bar{\mathbf{M}}_1$ can be determined from equation (3.44) such that the motion $\mathbf{x_n}$ on the sliding surface is stable. Here, for obtaining the $\bar{\mathbf{M}}_1$ matrix, LQR approach is used. The design of the sliding surface $\mathbf{S} = \mathbf{M}\hat{\mathbf{x}} = 0$ is obtained by minimizing the integral of the quadratic function of the state vector given as

$$J = \int_0^\infty \hat{\mathbf{x}}'(t)\mathbf{Q}_s\hat{\mathbf{x}}(t)dt \tag{3.47}$$

where $\mathbf{Q_s}$ is a 2n x 2n positive definite weighting matrix. In terms of the transformed state vector $\mathbf{x_n}$, the performance index J becomes

$$J = \int_0^\infty \left[\mathbf{x}'_{n1}\mathbf{x}'_{n2}\right]'\bar{\mathbf{L}}\begin{bmatrix}\mathbf{x}_{n1}\\ \mathbf{x}_{n2}\end{bmatrix}dt \tag{3.48}$$

in which

$$\bar{\mathbf{L}} = (\mathbf{P}^{-1})'\mathbf{Q}_S\mathbf{P}^{-1};\ \bar{\mathbf{L}} = \begin{bmatrix}\bar{\mathbf{L}}_{11} & \bar{\mathbf{L}}_{12}\\ \bar{\mathbf{L}}_{21} & \bar{\mathbf{L}}_{22}\end{bmatrix} \tag{3.49}$$

where $\bar{\mathbf{L}}_{11}$ and $\bar{\mathbf{L}}_{22}$ are 2n-m x 2n-m and m x m matrices, respectively. The performance index in equation (3.48) is minimized with the constraints of eq. (3.43) of motion, and the $\mathbf{x_{n2}}$ is expressed in terms of $\mathbf{x_{n1}}$ as

$$\mathbf{x}_{n2} = -0.5\bar{\mathbf{L}}_{22}^{-1}((\bar{\mathbf{A}}_{12})'\hat{\mathbf{M}} + 2\bar{\mathbf{L}}_{21})\mathbf{x}_{n1} \tag{3.50}$$

where $\hat{\mathbf{M}}$ is a 2n-m x 2n-m Riccati matrix satisfying the following matrix Riccati equation

$$\hat{\mathbf{A}}'\hat{\mathbf{M}} + \hat{\mathbf{M}}\hat{\mathbf{A}} - 0.5\hat{\mathbf{M}}\bar{\mathbf{A}}_{12}\bar{\mathbf{L}}_{22}^{-1}(\bar{\mathbf{A}}_{12})'\hat{\mathbf{M}} = -2\left(\bar{\mathbf{L}}_{11} - \bar{\mathbf{L}}_{12}\bar{\mathbf{L}}_{22}^{-1}(\bar{\mathbf{L}}_{12})'\right) \tag{3.51}$$

in which

$$\hat{\mathbf{A}} = \bar{\mathbf{A}}_{11} - \bar{\mathbf{A}}_{12}\bar{\mathbf{L}}_{22}^{-1}\bar{\mathbf{L}}_{21} \tag{3.52}$$

$\bar{\mathbf{M}}_1$ is obtained from a comparison between the equations (3.45) and (3.50)

$$\bar{\mathbf{M}}_1 = 0.5\bar{\mathbf{L}}_{22}^{-1}\left((\bar{\mathbf{A}}_{12})'\hat{\mathbf{M}} + 2\bar{\mathbf{L}}_{21}\right) \tag{3.53}$$

The sliding surface vector **S** is obtained from equation (3.41) as

$$\mathbf{M} = \bar{\mathbf{M}}\mathbf{P} = \left[\bar{\mathbf{M}}_1 : \mathbf{I}_m\right]\mathbf{P} \tag{3.54}$$

The control forces are designed to bring the state trajectory to the sliding surface **S** = 0. To achieve this, a Lyapunov function **H** is considered.

$$\mathbf{H} = 0.5\mathbf{S'S} = 0.5\hat{\mathbf{x}}'\mathbf{M'M}\hat{\mathbf{x}} \tag{3.55}$$

The time derivative of the Lyapunov fumction (equation (3.55)) is

$$\dot{\mathbf{H}} = \mathbf{S'}\dot{\mathbf{S}} = \mathbf{S'M}\dot{\mathbf{x}} \tag{3.56}$$

And putting $\dot{\mathbf{x}}$ from equation (3.9), the equation (3.56) is written as

$$\dot{\mathbf{H}} = \mathbf{S'M}\left[\mathbf{[A][\hat{x}]+[B][u]+[E][}\mathrm{w}\mathbf{]}\right] \tag{3.57}$$

Equation (3.57), after algebraic manipulation, is written as

$$\dot{\mathbf{H}} = \boldsymbol{\lambda}(\mathbf{u} - \boldsymbol{\Delta}) \tag{3.58}$$

where $\boldsymbol{\lambda} = \mathbf{S'MB}$; $\boldsymbol{\Delta} = -(\mathbf{MB})^{-1}\mathbf{M}\left[\mathbf{[B][u]+[E][}\mathrm{w}\mathbf{]}\right]$ (3.59)

To guarantee the condition of Lypaunov stability, a diagonal matrix **δ**, named as the matrix of sliding margin, is chosen. For every $\delta_i \geq 0$ and assuming $\mathbf{u} = \boldsymbol{\Delta} - \boldsymbol{\delta\lambda'}$, the time derivative of Lyapunov function $\dot{H}$ is always less than zero, which is the required Lyapunov stability criteria. Thus by assuming a suitable **δ** matrix, **u** is calculated from the following equation.

$$\mathbf{u} = \boldsymbol{\Delta} - \boldsymbol{\delta\lambda'} \tag{3.60}$$

The clipped control law is used (equation 3.25) to calculate the required voltage to be applied to the MR damper. The schematic diagram of sliding mode with clipped optimal control for full state and partial state observation is shown in Figure 3.5.

3.2.4 Passive-on

Passive-on is the simplest form of semi–active control strategy used for MR dampers. The MR fluid has a unique property that when an electromagnetic field is applied across it, its viscosity increases and it turns into a viscoelastic solid from the liquid state. Hence, the yield stresses of the MR fluid can be changed by varying the intensity of the electromagnetic field i.e. voltage. In passive-on, the voltage applied to the MR damper is set to the maximum voltage and as a result, MR damper behaves purely as a passive device. As like passive devices, passive on strategy is reliable, and possess a fixed resistance to all types of loadings. However, due to the addition of a constant level

of energy to the system, there is a possibility that heat can be generated in the MR damper leading to the failure of the control system. The schematic diagram of passive-on control is shown in Figure 3.7.

3.3 Numerical Study

For the study, a ten story shear type building frame is used having a mass of each floor as 18000 kg and stiffness of each floor as 24965 KN/m. Three MR dampers, three displacement feedback sensors and three velocity feedback sensors are placed at the first three floors of the building frame. For full observation, it is assumed that states of all floors are known and available for the computation of control force. The building frame is subjected to two near field and two far field earthquakes. The summary of the selected earthquake data is given in Table 3.2. The ground acceleration data have been downloaded from COSMOS Virtual Data Center and PEER Berkeley Strong Motion Database. The time histories of the real ground excitations are shown in Figures 3.8-9.

In addition to real earthquakes, two random excitations, namely broadband and narrowband excitations are simulated from their power spectral density function (PSDF). The PSDFs of the random excitations are given by the following Clough and Penzin double filter PSDF equation(Clough and Penzien,1975)

$$\ddot{S}_{ug}(\omega) = S_0 * \frac{\left(1 + 4\xi_g^{\,2}\left(\frac{\omega}{\omega_g}\right)\right)}{\left(1 - \left(\frac{\omega}{\omega_g}\right)^2\right)^2 + 4\xi_g^2\left(\frac{\omega}{\omega_g}\right)^2} * \frac{\left(\frac{\omega}{\omega_s}\right)^4}{\left(1 - \left(\frac{\omega}{\omega_s}\right)^2\right)^2 + 4\xi_s^2\left(\frac{\omega}{\omega_s}\right)^2} \tag{3.61}$$

The different filter parameters used for the generation of PSDF for the narrowband excitation and broadband excitations are shown in the Figure 3.10. Note that in the figure the sharply peaked PSDF typifies a narrowband process (for soft soil condition) and the other PSDF signifies a broadband process (for firm ground condition).

Using the PSDFs, a set of twenty time histories is generated from each PSDF. The sample time history of broadband and narrowband excitation is shown in Figure 3.11. For each time history, responses are obtained and the results of the analysis are shown in the form of the following control measures:

$$P_{pi} = \frac{E[\sigma_{ui}] - E[\sigma_{ci}]}{E[\sigma_{ui}]} * 100 \tag{3.62}$$

$$P_{pi} = \frac{E[P_{ui}] - E[P_{ci}]}{E[P_{ui}]} * 100 \tag{3.63}$$

(i = 1, 2, 3; 1- top floor displacement; 2- maximum story drift; 3- base shear)

in which $E[\sigma_{ui}]$ and $E[\sigma_{ci}]$ are the expected rms value of uncontrolled and controlled responses; $E[P_{ui}]$ and $E[P_{ci}]$ are the expected uncontrolled and controlled absolute peak responses.

Figure 3.12 shows a comparison of percentage reductions in top floor displacement, maximum inter story drift and maximum base shear using El Centro (1940) earthquake for two observation strategies considered and for all the control algorithms. Note that for passive-on and VTC control strategies, knowledge of full state is not required; only with the help of the observed states, the control force generated in the MR damper can be directly obtained if the measurements are taken from the floors where MR dampers are placed. It is seen from the figure that the percentage reductions in responses generally differ between full state and partial state observation for LQGCl, SMCCl and bang bang algorithms. In certain cases, this difference is quite significant. This shows the effect of partial state observation on the control of responses for these algorithms. The reason for the difference is attributed to the difference between the estimated full state and the actual full state of the system. For the development of these algorithms, information of the full state is required for the generation of the reference control force for MR dampers. For the passive-on and VTC control algorithms, the response reductions remain the same for full state and partial state observations, since these algorithms generate the control force in MR damper using the measured states of the floors where MR dampers are placed.

When percentage reductions in responses are compared between different algorithms, it is seen that percentage reduction in maximum inter story drift is maximum for VTC algorithm. For other two response quantities, percentage reductions obtained by VTC algorithm are quite comparable (in some cases) to those obtained by other algorithms. Further, it is seen from the figure that the percentage reductions in base shear are generally less as compared to other two response quantities for all algorithms.

Figures 3.13-15 show the comparison between the response reductions obtained by different algorithms for Victotria, Spitak and Kobe earthquakes. Figures show nearly the same trend of results as observed for the El Centro earthquake.

Figures 3.16-19 depicts the percentage reductions in responses for simulated broadband and narrowband excitation. Response reductions are observed for both expected peak and rms values. It is seen from the figures that percentage reductions for both are nearly of the same order. The pattern of reductions shows the similar trend as that of the real earthquakes. Both VTC and passive-on control, consistently provide more reductions in maximum interstory drift compared to other algorithms.

Figure 3.20 shows the time history of control force of LQGCl, LQG and LQR control algorithms for the El Centro earthquake. It may be seen from the figure that the LQGCl, which depicts the time history of control force developed in the MR damper placed at first floor, is much less in comparison to the time history of reference control forces obtained by LQG and LQR. While the peak control force developed in the MR damper is of the order of 150 kN, those of the reference control forces obtained by the LQR and LQG are of the order of 450 kN and 5000 kN, respectively. Because of the limitation of the maximum voltage that can be applied to the MR damper, the reference control forces predicted by LQR and LQG can never be realized in the MR damper. The magnitude of this difference is large and this necessitates the development of an alternative control algorithm which can produce control force in the MR damper without the need of any reference or target control force like passive-on control system. The VTC control algorithm fulfils this need.

Figure 3.21 shows the same comparison between the time histories of control force obtained by LQGCl, LQG and LQR control algorithm for Spitak earthquake. Although, the nature of the time histories of the control force is distinctly different than those of the El Centro earthquake, the same magnitude of difference between the peak control forces actually developed in the MR damper and those obtained by LQG and LQR is observed.

Figures 3.22 and 3.23 show the time histories of the control forces developed in the first storey MR damper for different control algorithms for El Centro and Spitak earthquakes, respectively. The natures of the time histories of control forces for the different algorithms are different. Further, they are different for the two earthquakes. The peak values of the control force for both earthquakes are minimum for VTC algorithm.

Table 3.3 compares between the peak control forces developed in the first storey MR damper obtained by different control algorithms and for different earthquakes. It is seen from the table that for all earthquakes considered in the study, the VTC control algorithm provides the least value of peak control force.

Based on the values of peak control force recorded in Table 3.3, the percentage control of the response quantities of interest per unit control force denoted by factor Re is obtained. The factor Re is defined as

$$\mathrm{Re} = \frac{P_r}{F_n} \tag{3.64}$$

where P_r is the percentage reduction in response quantity and F_n is the normalized peak control force expressed as a percentage of the total weight of the frame.

The greater the value of Re, more is the efficiency of the control algorithm. Tables 3.4-6 show the values of Re for different response quantities of interest obtained by different algorithms for different earthquakes. It is seen from the tables that the values of Re are consistently higher for all response quantities of interest for the VTC algorithm for all earthquakes considered in the study.

3.4 Conclusions

A new semi active control strategy (VTC) for building frames using MR dampers subjected to both random excitation and real earthquake records is presented. The controlled responses are compared with those of a few standard algorithms, namely, i) LQG and sliding mode algorithms applied in conjunction with clipped optimal control; ii) Bang bang control and iii) Passive on control. Since the semi active control using the MR damper is inherently nonlinear, a simulation procedure is adopted for random excitations in order to retain the full nonlinearity. The Kalman filter is used for estimating the states. Three response quantities of interest are considered in the study, namely, peak top floor displacement, maximum drift and maximum base shear. The results of the numerical study lead to the following conclusions:

- Percentage reduction in different response quantities varies with earthquakes and control algorithms used.
- In VTC algorithm, there is no need to estimate the full state for the prediction of control voltage and hence, it is a direct algorithm in the sense that no reference control force is required to predict the control voltage.

- Except for the VTC and passive on control algorithms, prediction of the control of responses by other algorithms is less reliable because of the errors involved in state estimation.
- The VTC control algorithm provides a maximum percentage reduction in the peak inter story drift amongst all control algorithms considered. Percentage reductions in other two response quantities obtained by VTC control algorithms are quite comparable to those of other algorithms.
- Response reduction per unit control force denoted by factor Re is consistently higher for VTC algorithm for all earthquakes; from this consideration, VTC algorithm is most efficient among the algorithms considered in the study.

Table 3-1: Parameters for MR damper

Parameter	Value	Parameter	Value
c_{0a}	50.30 KN.sec/m	α_{0a}	8.70 KN/m
c_{0b}	48.70 KN.sec/m.V	α_{0b}	6.40 KN/m.V
k_0	0.0054 KN/m	γ	496 m^{-2}
c_{1a}	8106.2 KN.sec/m	β	496 m^{-2}
c_{1b}	7807.9 KN.sec/m.V	A	810.50
k_1	0.0087 KN/m	n	2
x_0	0.18 m	η	190 sec^{-1}

Table 3-2: Summary of earthquake time histories used

	Year	Earthquake	Recording Station	PGA, m/s^2
Far field	1940	Imperial valley (California)	El Centro array #9 (USGS)	3.1276
	1980	Victoria (Mexico)	Cucapah	0.6611
Near field	1995	Kobe (Japan)	Nishi	4.9320
	1988	Spitak (Armenia)	Gukasian	1.9521

Table 3-3: Peak control forces (kN) generated in the first storey MR damper

Earthquakes	**Control Algorithms**				
	Passive	Bang bang	LQGC	SMCC	VTC
El Centro	129	129	144	124	113
Victoria	72	75	71	70	64
Kobe	136	131	135	131	120
Spitak	132	133	154	132	104
Narrowband	105	101	107	104	94
Broadband	95	88	90	92	80

Table 3-4: Efficiencies of control algorithms measured by the factor Re (peak top floor displacement)

Earthquakes	**Control Algorithms**				
	Passive	Bang bang	LQGC	SMCC	VTC
El Centro	7.42	6.55	3.84	7.05	8.54
Victoria	6.79	7.21	10.35	9.07	10.60
Kobe	0.72	1.02	0.65	1.37	1.65
Spitak	4.77	4.72	3.20	5.29	6.20
Narrowband	5.92	5.62	4.88	5.65	6.93
Broadband	6.84	6.99	7.72	7.66	9.13

Table 3-5**:** Efficiencies of control algorithms measured by the factor Re (maximum drift)

Earthquakes	**Control Algorithms**				
	Passive	Bang bang	LQGC	SMCC	VTC
El Centro	7.71	6.89	3.93	5.50	8.73
Victoria	16.33	14.69	8.92	8.80	18.94
Kobe	4.08	4.24	3.61	2.48	5.08
Spitak	6.42	6.57	4.23	4.50	8.61
Narrowband	9.10	8.58	5.40	4.91	10.75
Broadband	11.37	11.59	7.67	7.83	14.25

Table 3-6: Efficiencies of control algorithms measured by the factor Re (maximum base shear)

Earthquakes	**Control Algorithms**				
	Passive	Bang bang	LQGCl	SMCCl	VTC
El Centro	6.13	5.38	1.93	5.44	6.98
Victoria	2.80	1.74	8.29	7.34	5.55
Kobe	1.22	1.79	0.88	1.92	2.55
Spitak	4.11	4.11	2.24	4.42	5.66
Narrowband	3.42	2.45	-0.30	3.64	4.35
Broadband	5.82	3.36	3.95	7.02	7.59

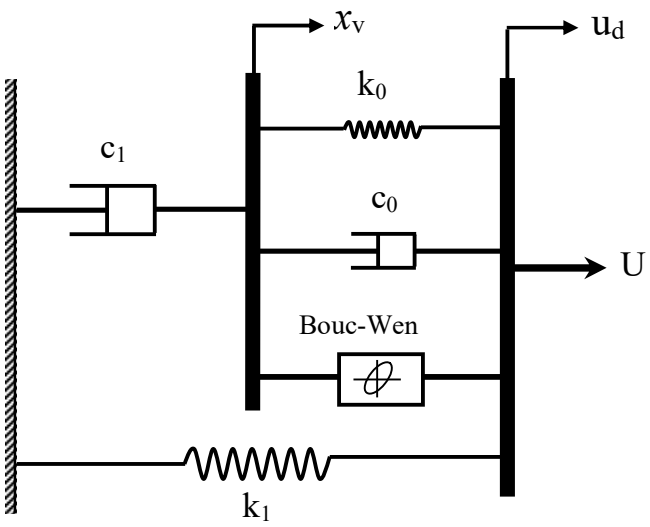

Figure 3-1: Modified Bouc-wen model for MR damper

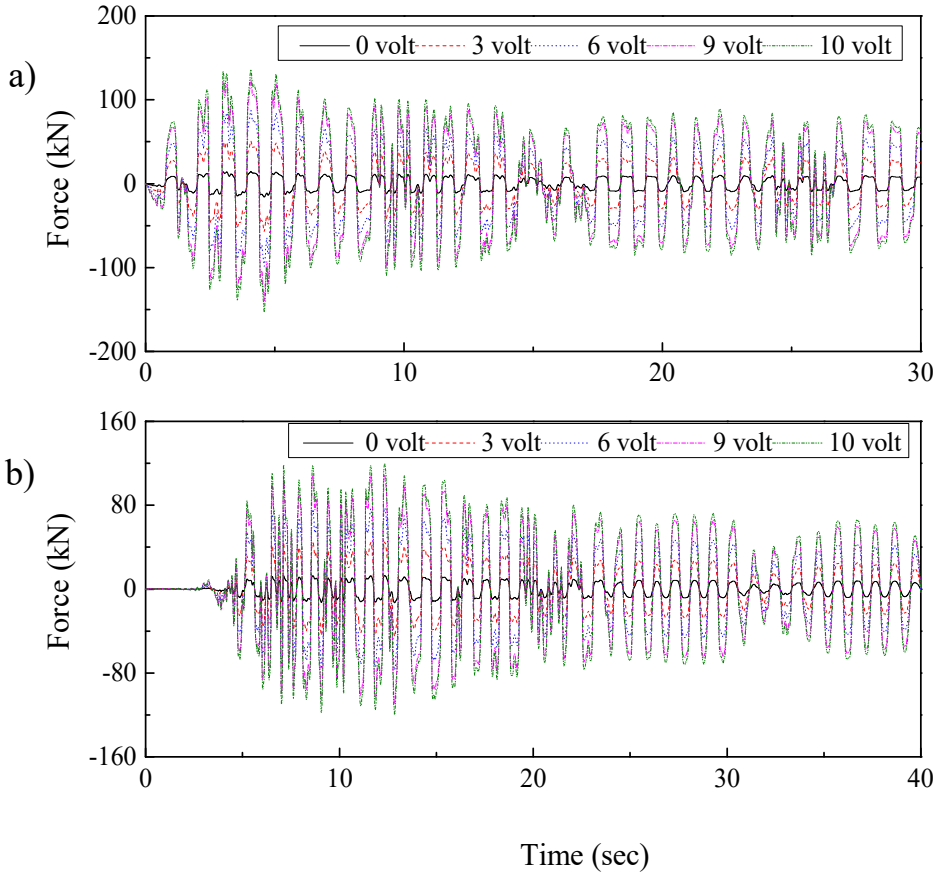

Figure 3-2: Comparison of force generated by modified bouc-wen model at different voltages for a) El Centro and b) Kobe earthquake

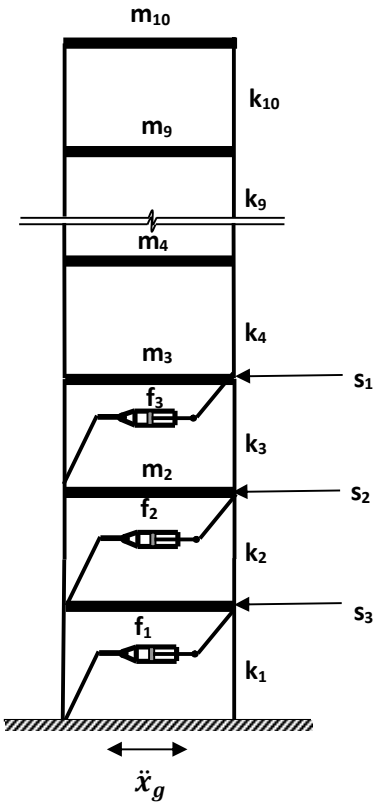

Figure 3-3: Building frame installed with three MR dampers and three displacement feedback sensors at the first three floors

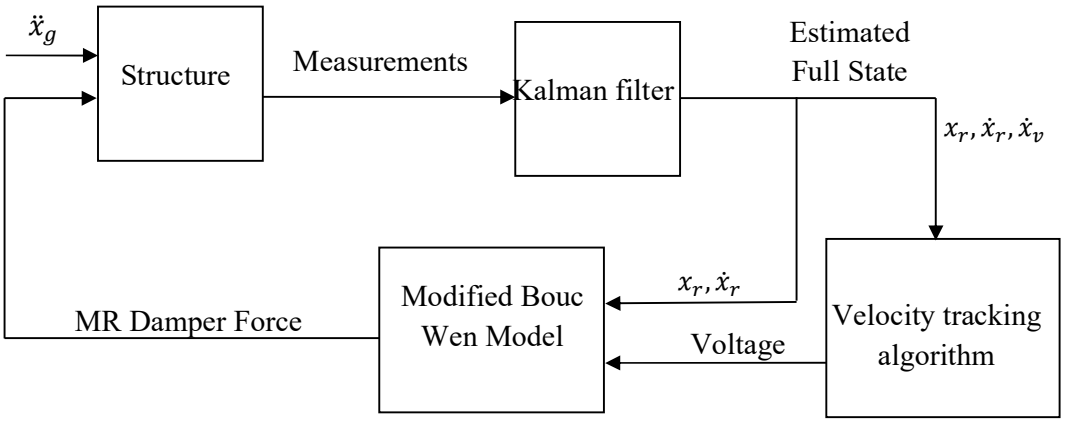

Figure 3-4: Schematic diagram of velocity tracking control for partial state observation based strategy

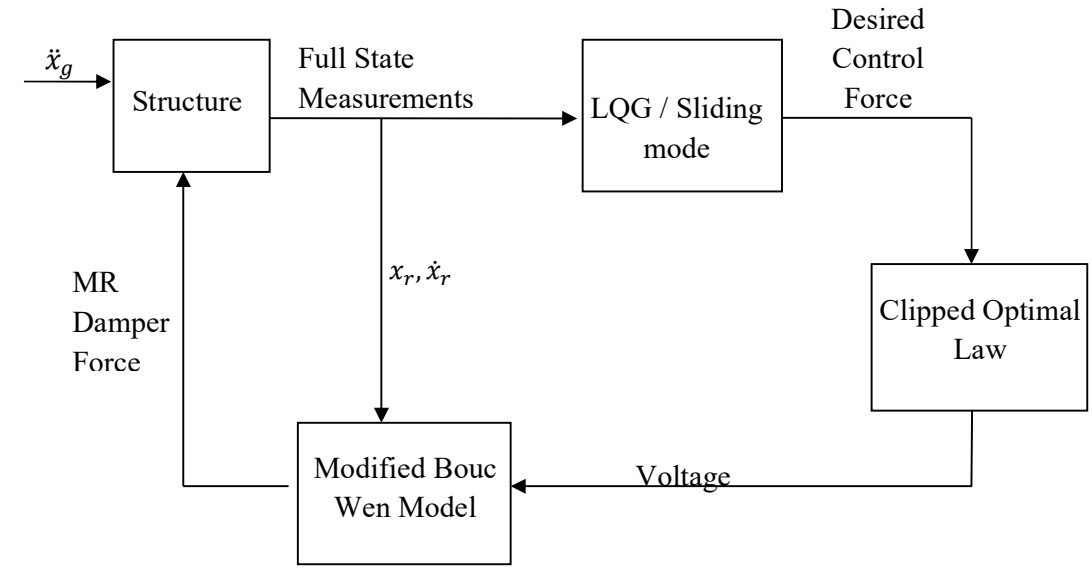

a)

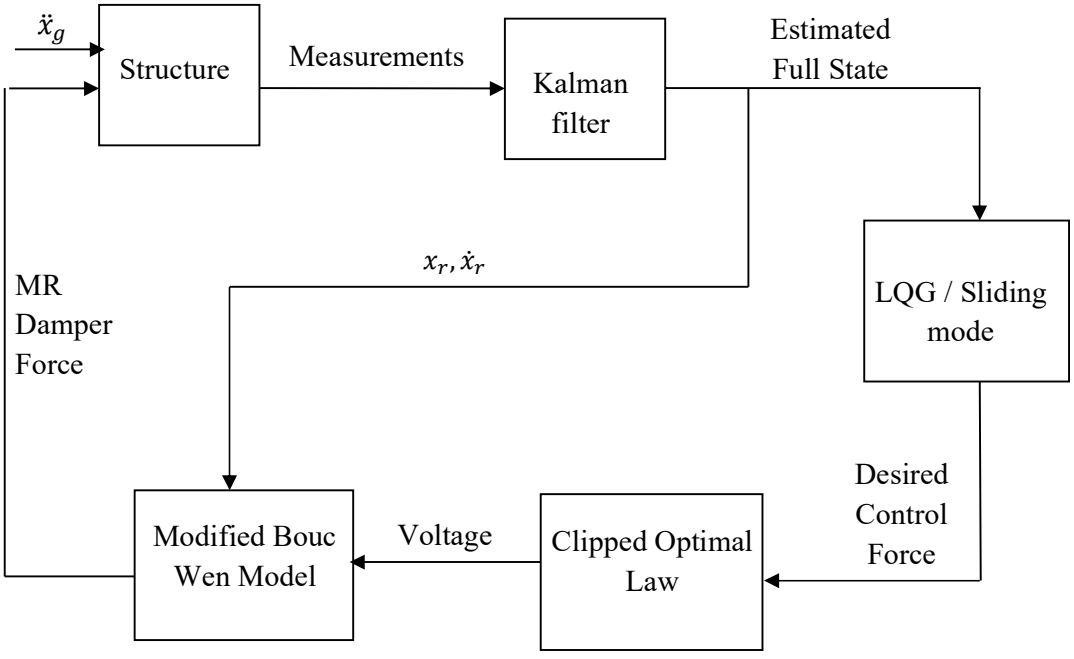

b)

Figure 3-5: Schematic diagram of LQG / Sliding mode with clipped optimal control for a) full state and b) partial state observation based strategy

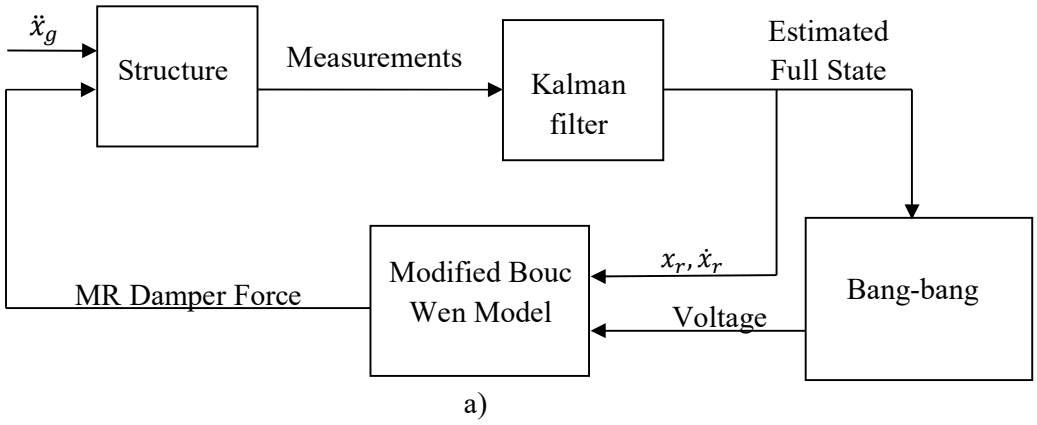

a)

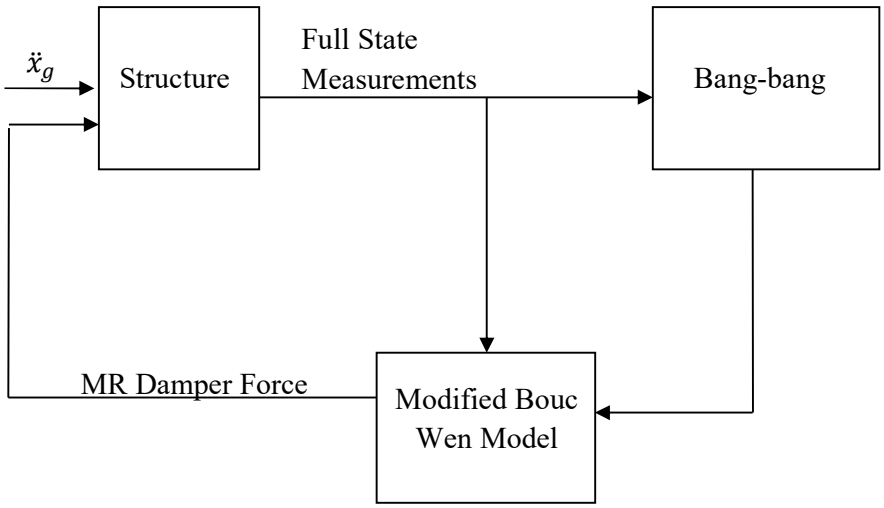

b)

Figure 3-6: Schematic diagram of bang-bang control for a) full state and b) partial state observation based strategy

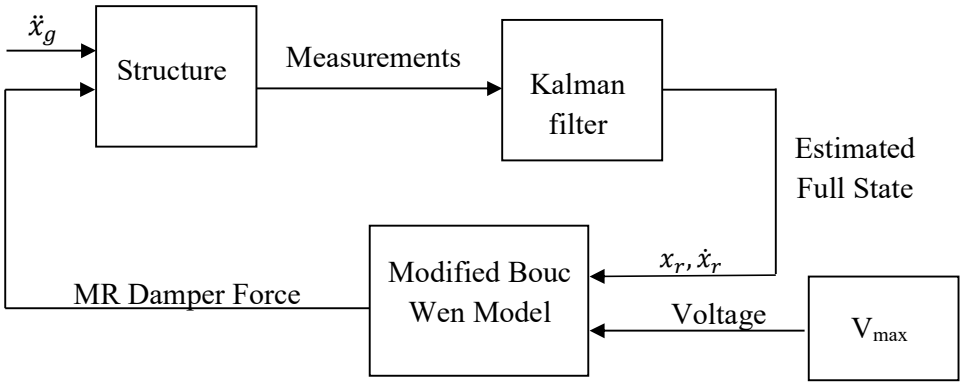

Figure 3-7: Schematic diagram of passive-on control for a) partial state and b) full state observation based strategy

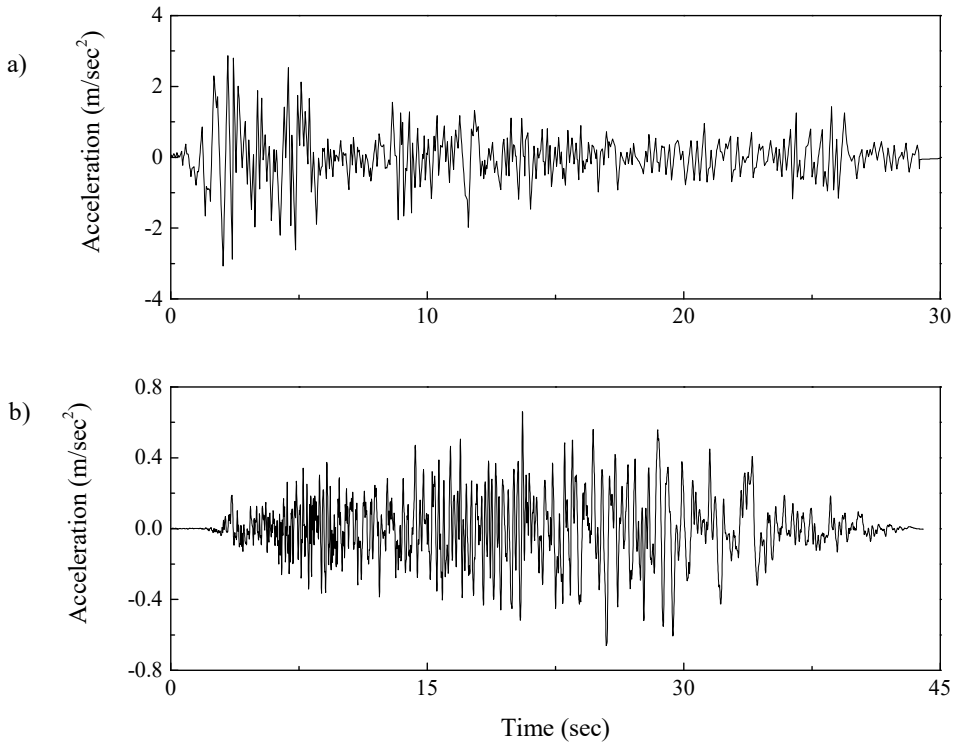

Figure 3-8: Ground acceleration time history plots of a) El Centro (1940) and b) Victoria (1980) earthquake

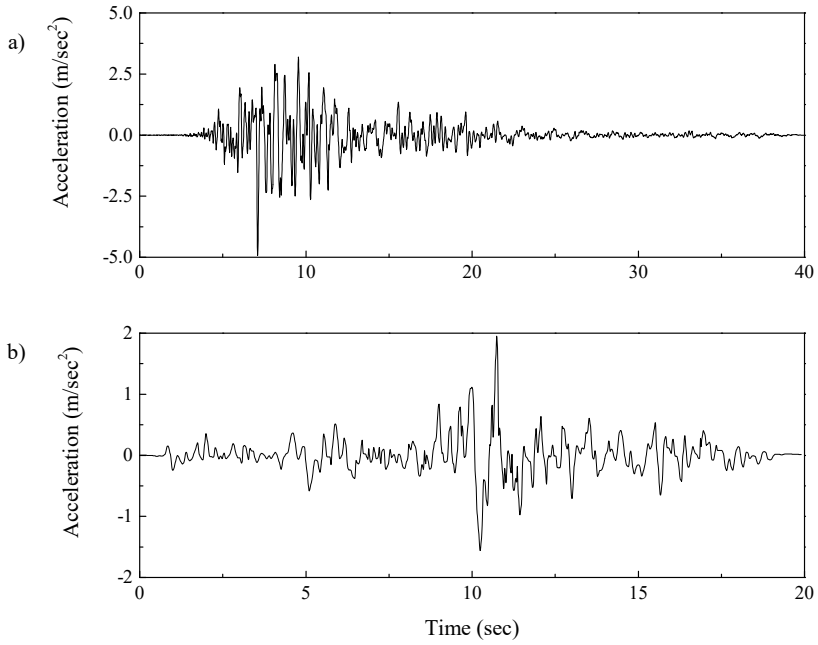

Figure 3-9: Ground acceleration time history plots of a) Kobe (1995) and b) Spitak (1988) earthquake

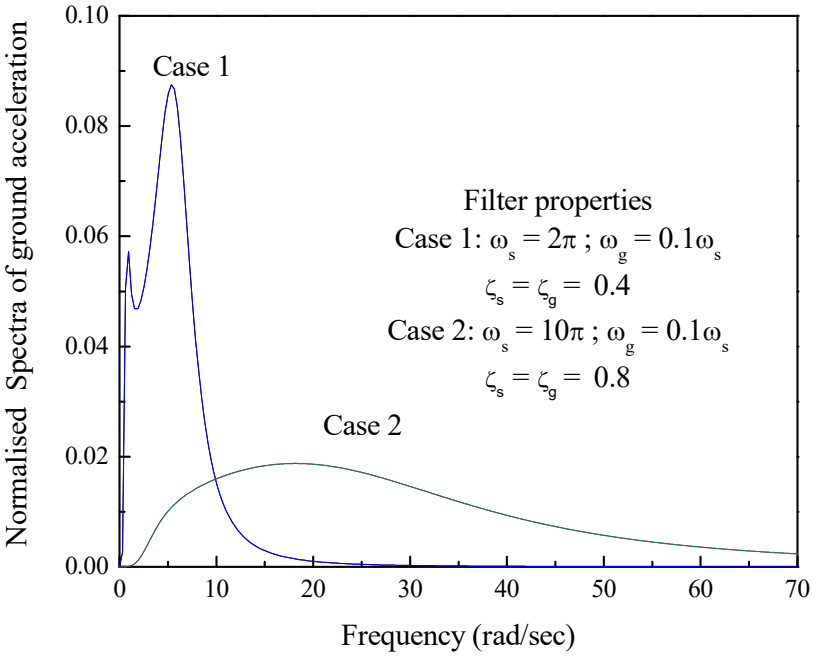

Figure 3-10: PSDF for the narrowband and broadband excitation

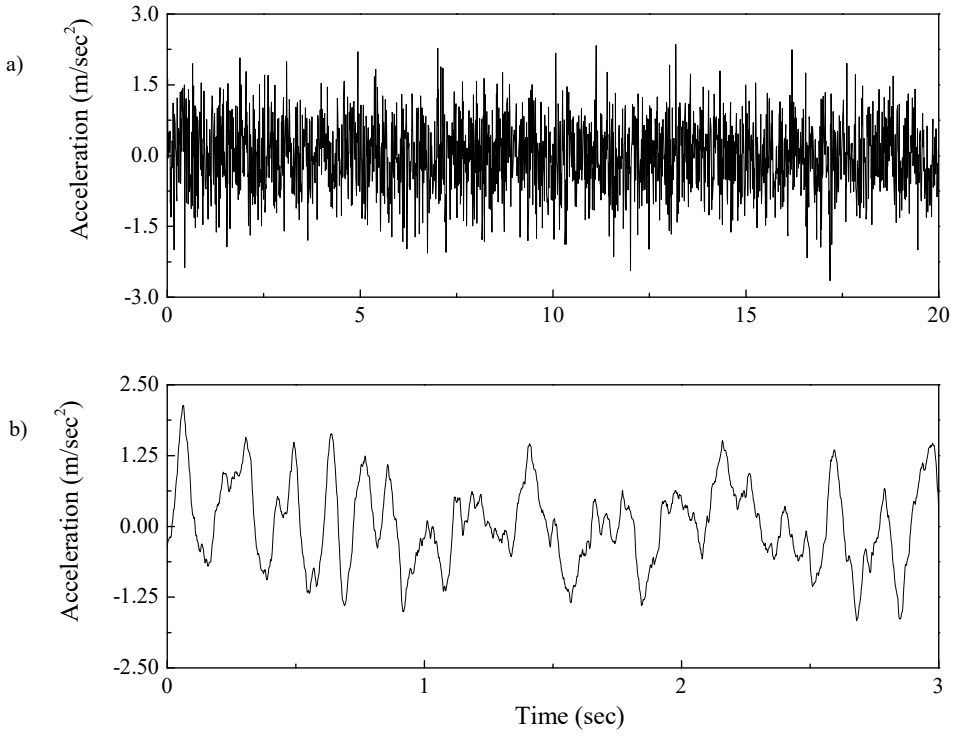

Figure 3-11: Ground acceleration time history plots of a sample of a) broadband and b) narrowband excitation

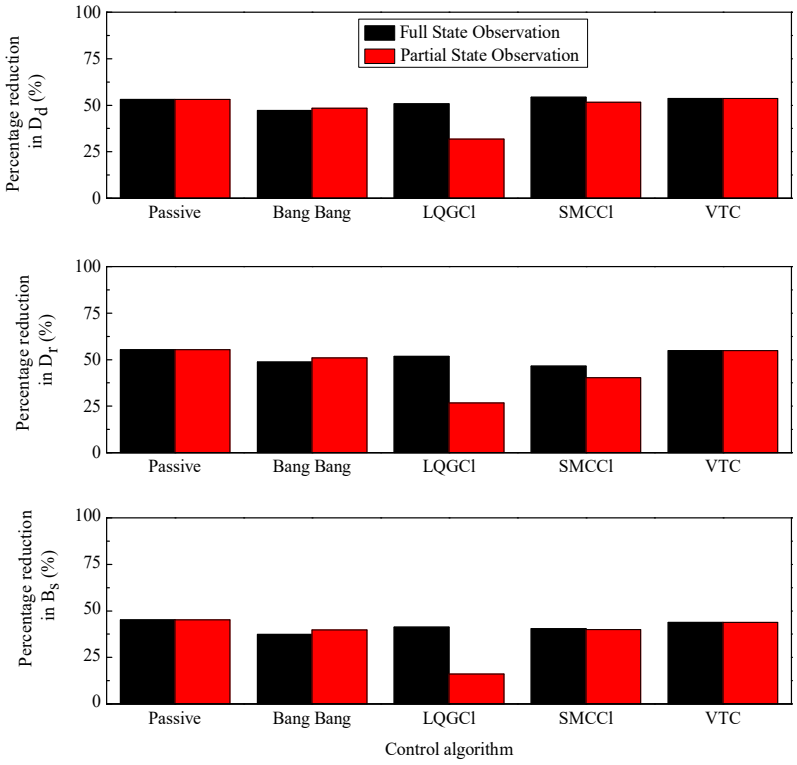

Figure 3-12: Comparison of percentage reduction in different response quantities for full state and partial state observations for El Centro (1940) earthquake

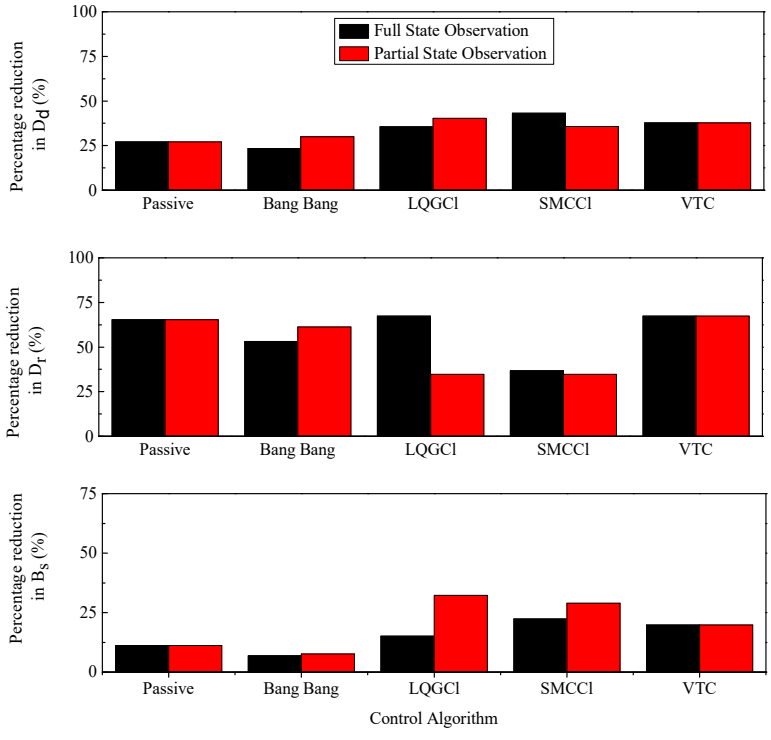

Figure 3-13: Comparison of percentage reduction in different response quantities for full state and partial state observations for Victoria (1980) earthquake

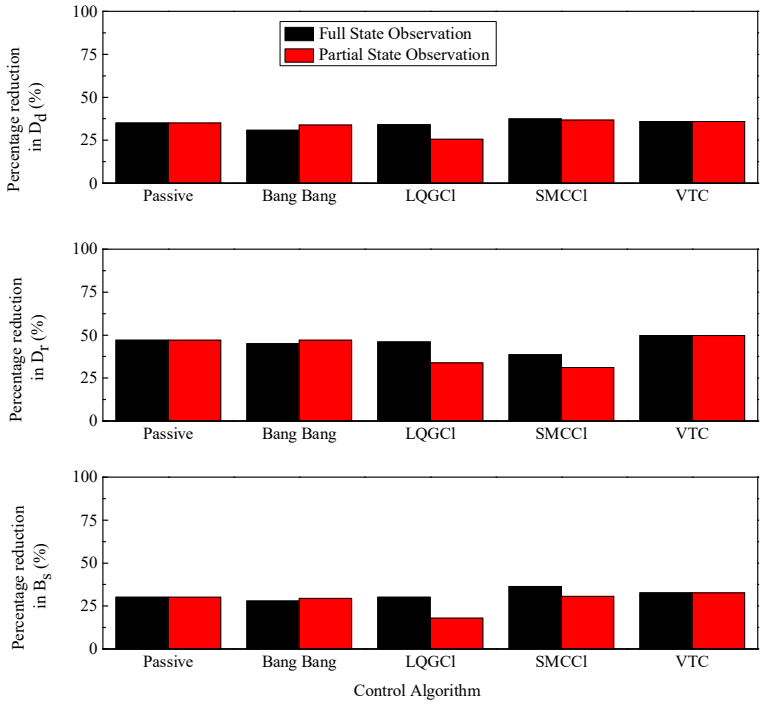

Figure 3-14: Comparison of percentage reduction in different response quantities for full state and partial state observations for Spitak (1988) earthquake

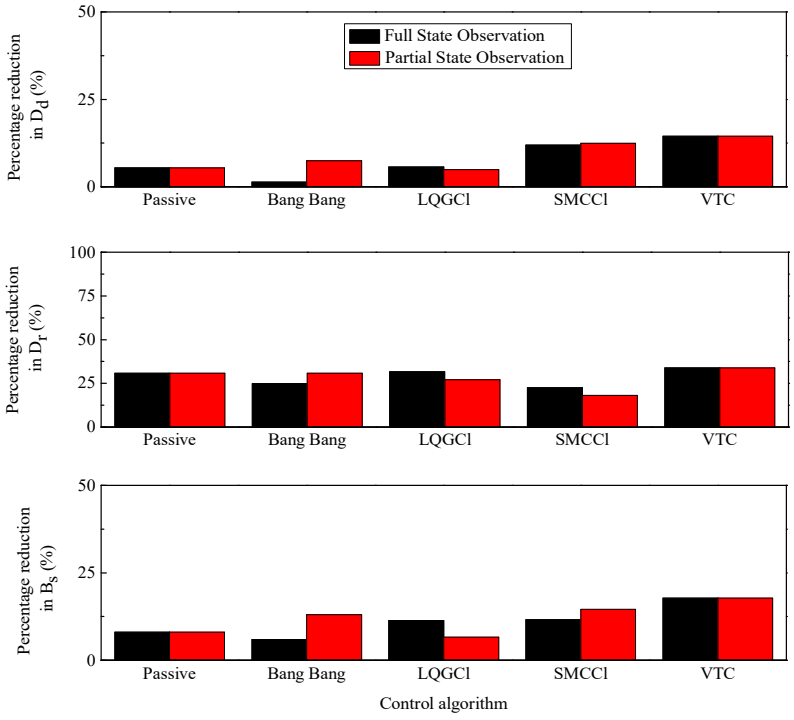

Figure 3-15: Comparison of percentage reduction in different response quantities for full state and partial state observations for Kobe (1995) earthquake

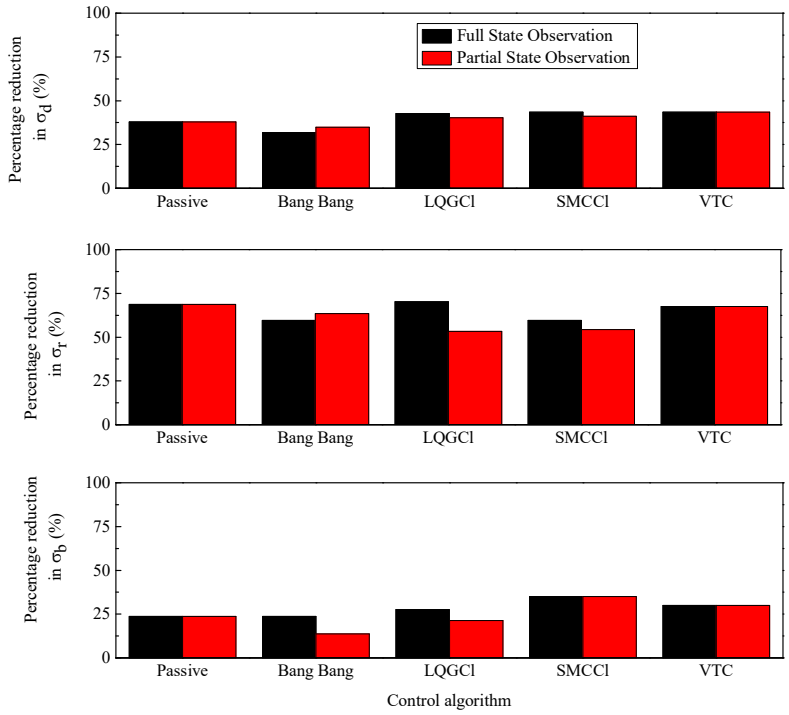

Figure 3-16: Comparison of percentage reduction in expected rms values of different response quantities for full state and partial state observations for broadband earthquake

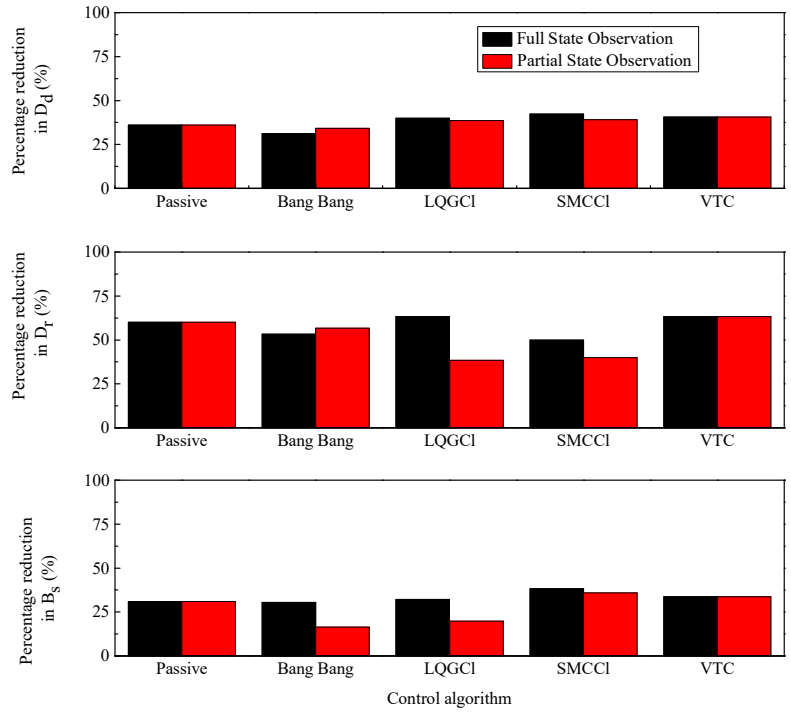

Figure 3-17: Comparison of percentage reduction in expected peak values of different response quantities for full state and partial state observations for broadband earthquake

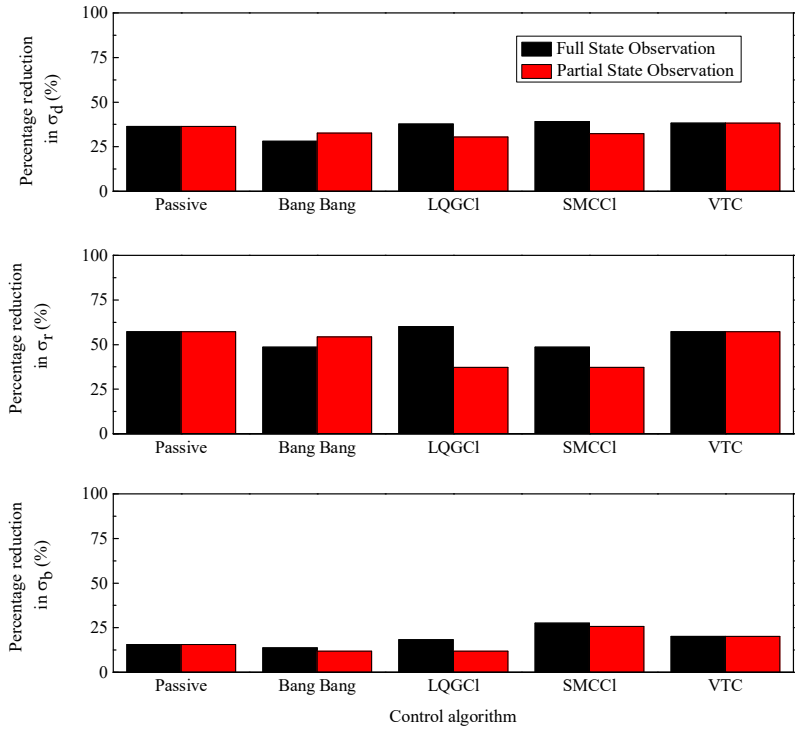

Figure 3-18: Comparison of percentage reduction in expected rms values of different response quantities for full state and partial state observations for narrowband earthquake

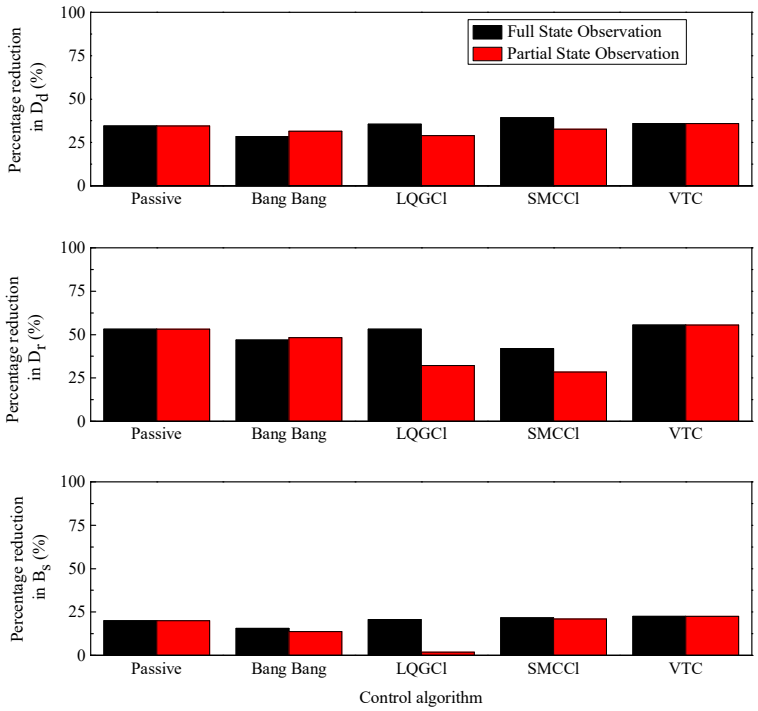

Figure 3-19: Comparison of percentage reduction in expected peak values of different response quantities for full state and partial state observations for narrowband earthquake

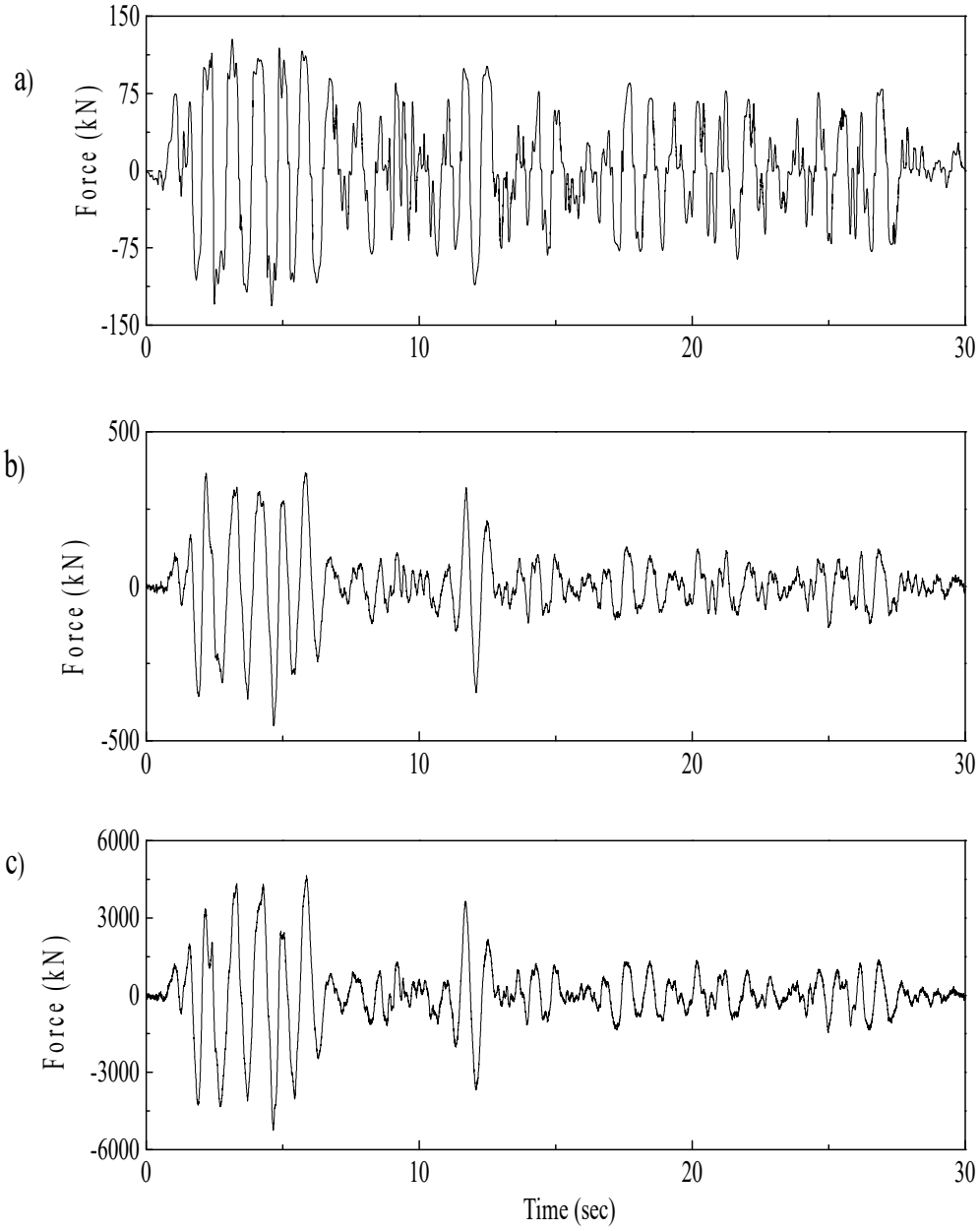

Figure 3-20: Comparison of control forces for first floor MR damper for a) LQGCl b) LQG and c) LQR for El Centro earthquake

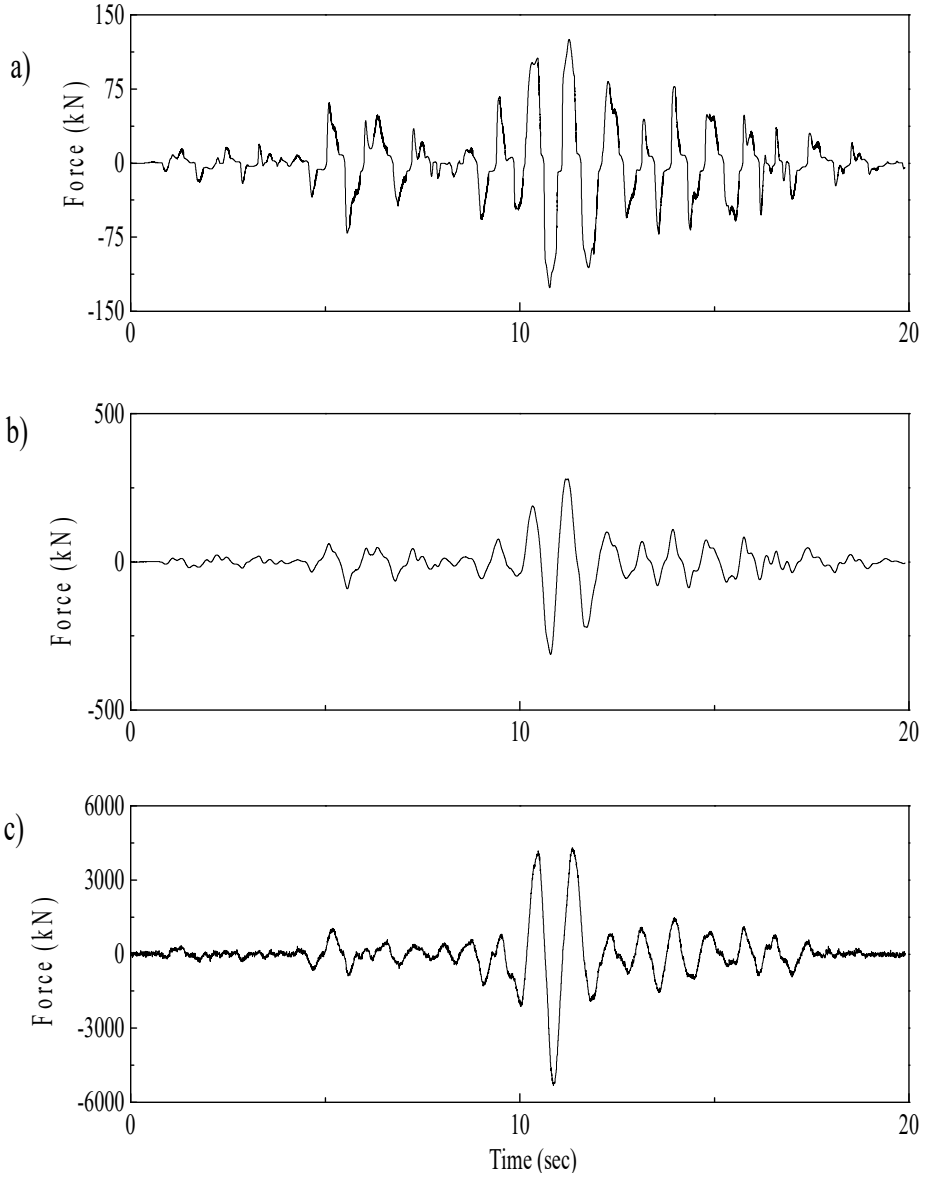

Figure 3-21: Comparison of control forces for first floor MR damper for a) LQGCl b) LQG and c) LQR for Spitak earthquake

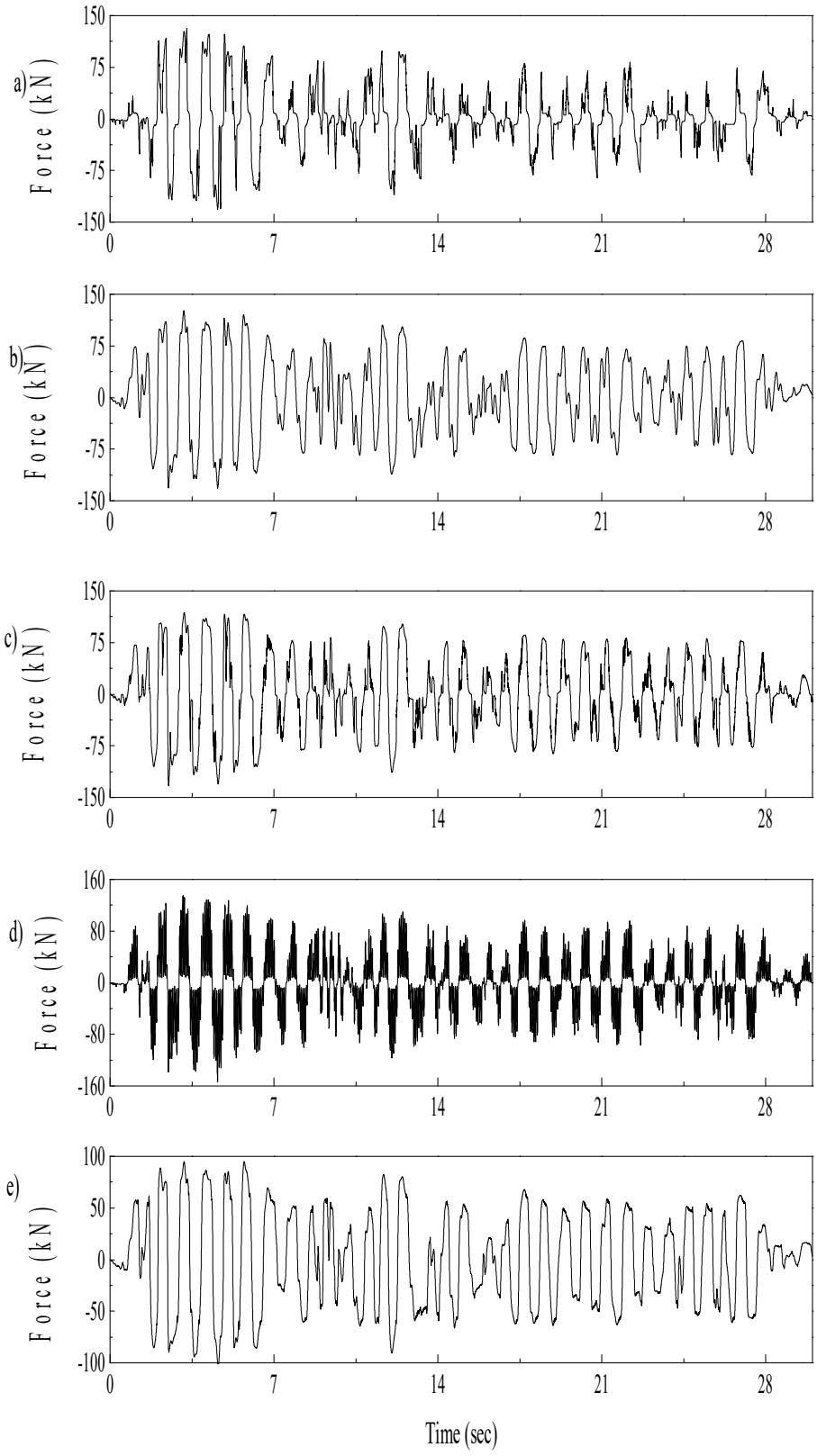

Figure 3-22: Comparison of first story MR damper forces obtained through a) SMCCl b) Passive c) Bang bang d) LQCCl and e) VTC for El Centro earthquake

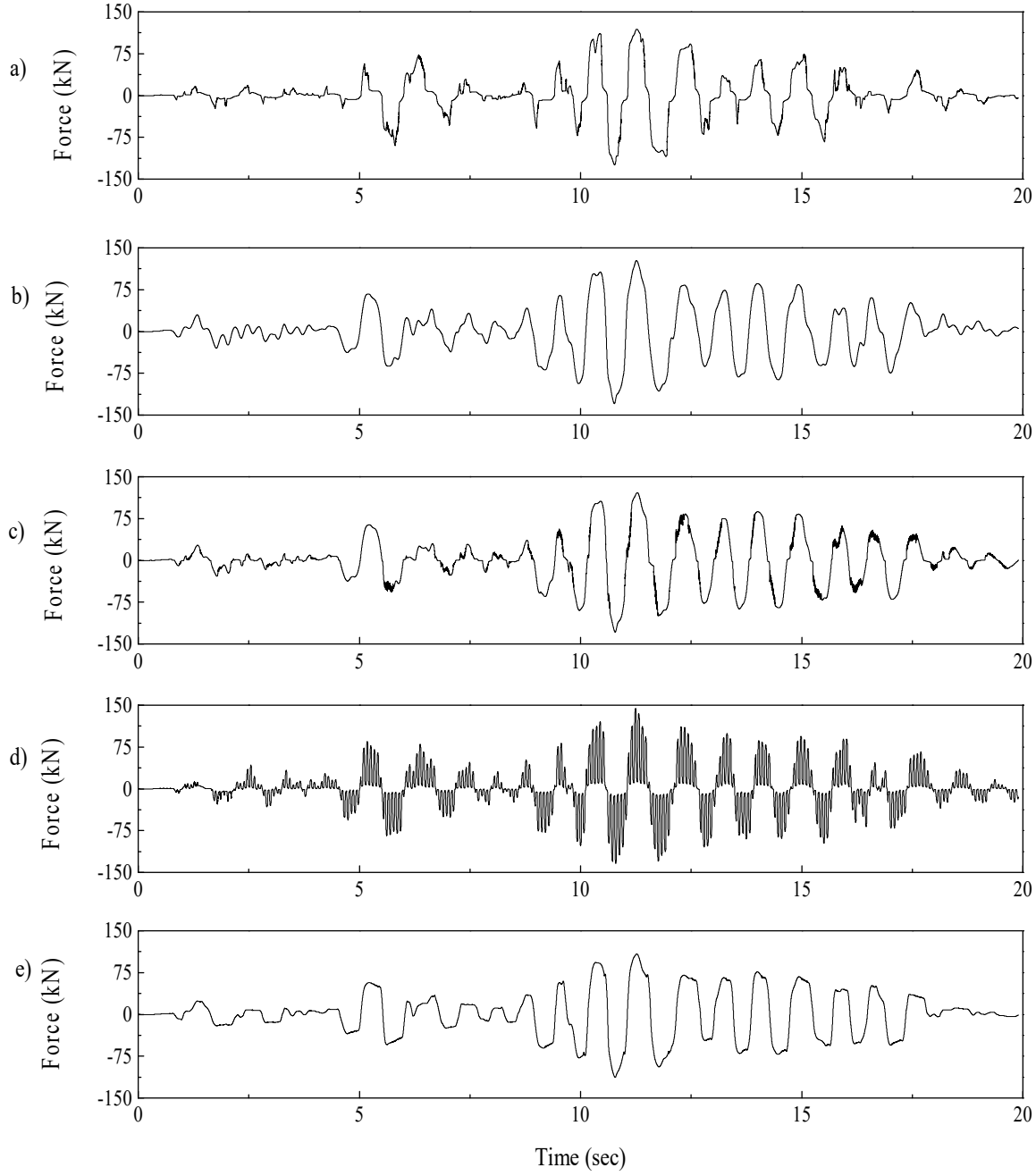

Figure 3-23: Comparison of first story MR damper forces obtained through a) SMCCl b) Passive c) Bang bang d) LQGCl and e) VTC for Spitak earthquake

Chapter 4

Modified Seismic Semi Active Control of Partially Observed Systems Using MR Dampers

4.1 Introduction

Although a large number of studies exist on the semi-active control of partially observed building frames using MR dampers, there is a lack of rigor in the formulations made. This is because that use of Kalman filter for state estimation requires that both process and measurement noises should ideally be Gaussian white. While the exact nature of measurement noises is unknown, it may be reasonable to assume it as Gaussian white, since many of the measurement noises are broad-band processes, if not white. This same assumption is not true for seismic excitation since, except for some ideal situations, seismic excitations are not white. However, Kalman filter is used for state estimation for non-white Gaussian seismic excitation for most of the partially observed control problems reported in the literature in Chapter 2. Since the Kalman filter requires only the values of covariance of the excitation and the measurement noises, the state estimation remains the same irrespective of the nature of excitation. Hence, the formulation of the problem lacks theoretical rigor if they are not white. Further, from the point of implementation, the methods have a major drawback that they assume a value of the covariance of ground motion as input to the Kalman filter without the knowledge of that of the ground motion measured in real-time application. Herein, an alternative formulation is presented in which the state variables are augmented by two filter variables. White noise is passed through the filters to obtain the desired type of seismic excitation to the structure. The system with augmented variables has Gaussian white noise as input excitation. The results of the proposed formulation are compared with those of the conventional formulation in which seismic excitation is directly prescribed as input to the structure. Further, a sensitivity analysis is carried out to investigate the effect of the variation of the covariance of the excitation and the noise on the state estimate and hence, on the control of responses. The study is useful in selecting proper values of the covariance of the excitation and the noise to be inputted to the Kalman filter for the real-time application of the control scheme. For the same, ANN is also trained to transform the measured ground motion to white noise which is considered as input to the control algorithm of the proposed formulation.

4.2 Theory

The state vector of the formulation (called VB-1) used in the previous chapter, contains only the structural displacement and velocity. Moreover, the ground motion is non- white and assumed as Gaussian. Since excitation is non- white, the full state estimation from the measured state using Kalman filter lacks theoretical rigor. In order to bring in the theoretical rigor, an alternative formulation (VB-2) is presented by augmenting the state vector of the structure by two filter variables. The VB-2 system is shown in Figure 4-1. The filter equations are coupled to the equations of motion of the structure in state space. A white noise is passed through the filters to obtain the desired non-white seismic excitation to the structure. The augmented system is analyzed for the control problem in which white noise forms the input excitation. For the formulation, the following set of filter equations (4.1-2) are augmented to the set of chapter 3, equations 3.9-10

$$\ddot{x}_g + 2\xi_g\omega_g\dot{x}_g + \omega_g^2 x_g = \ddot{s}_s + w \tag{4.1}$$

$$\ddot{s}_s + 2\xi_s\omega_s\dot{s}_s + \omega_s^2 s_s = -w \tag{4.2}$$

where x_g is the free field ground motion which is the output of second order filter; s_s is the output of first filter; w is the white noise; ω_g , ξ_g , ω_s and ξ_s are the filter coefficients. The power spectral density function (PSDF) of the ground acceleration as obtained from eqns. (4.1) and (4.2) is given by equation 3.61 (Clough and Penzien,1975) which is reproduced here.

$$\ddot{S}_{ug}(\omega) = S_0 * \frac{\left(1 + 4\xi_g^2\left(\frac{\omega}{\omega_g}\right)\right)}{\left(1 - \left(\frac{\omega}{\omega_g}\right)^2\right)^2 + 4\xi_g^2\left(\frac{\omega}{\omega_g}\right)^2} * \frac{\left(\frac{\omega}{\omega_s}\right)^4}{\left(1 - \left(\frac{\omega}{\omega_s}\right)^2\right)^2 + 4\xi_s^2\left(\frac{\omega}{\omega_s}\right)^2} \tag{3.61}$$

where S_o is the ordinate of the PSDF of white noise w in equation 4.1. When the equations 4.1 and 4.2 are substituted in equations 3.9 and 3.10, the following state space equations for the structure filter system are obtained.

$$[\dot{\mathbf{X}}_V] = [\mathbf{A}_V][\mathbf{X}_V] + [\mathbf{B}_V][\mathbf{U}_V] + [\mathbf{E}_V][w] \tag{4.3}$$

$$[\mathbf{Y}_V] = [\mathbf{C}_V][\mathbf{X}_V] + [\mathbf{D}_V][\mathbf{U}_V] + \mathbf{v} \tag{4.4}$$

where $[\mathbf{X_V}]^T = [\hat{\mathbf{x}}\ x_g s_s\ \dot{\hat{\mathbf{x}}}\ \dot{x}_g \dot{s}_s]$; $\hat{\mathbf{x}}$ is the estimated state; $\mathbf{A_V}$ is a 2(n+2) x 2(n+2) matrix whose elements are function of structure's characteristics and filter coefficients, $\mathbf{B_V}$ is a 2(n+2) x m damper force coefficient matrix, $\mathbf{E_V}$ is a 2(n+2) x 1 excitation coefficient matrix, $\mathbf{C_V}$ is a p x 2(n+2) measurement matrix, $\mathbf{D_V}$ is a p x m matrix of zeroes, $\mathbf{X_V}$ is a 2(n+2) x 1 state vector, $\mathbf{Y_V}$ is a p x 1 vector of measured outputs, **v** is a p x 1 measurement noise vector, w is the white noise excitation. For the formulation VB-2, the control strategies are developed in the similar way as developed for VB-1 given in previous chapter. Note that for VB-1, the excitation is the ground acceleration $\ddot{u}_g$ applied directly below the structure, while for VB-2, the excitation is the white noise applied at the support of first filter. The matrices $\mathbf{A_V}$, $\mathbf{B_V}$, etc. are defined below:

$$\mathbf{A_V} = \begin{bmatrix} \mathbf{O}_{n+2} & \mathbf{I}_{n+2} \\ -\mathbf{M_V^{-1}K_V} & -\mathbf{M_V^{-1}C_V} \end{bmatrix} \mathbf{B_V} = \begin{bmatrix} \mathbf{O}_{n+2} \\ -\mathbf{M_V^{-1}G_V} \end{bmatrix};\ \mathbf{E_V} = \begin{bmatrix} \mathbf{O}_{n+2} \\ -\mathbf{M_V^{-1}J_V} \end{bmatrix} \tag{4.5}$$

where, $\mathbf{I_{n+2}}$ and $\mathbf{O_{n+2}}$ are the identity and null matrices of size n + 2 x n + 2, respectively; and $\mathbf{J_V} = \begin{bmatrix} \mathbf{O}_n \\ -1 \\ 1 \end{bmatrix}$

Three standard semi-active control strategies are employed to obtain the controlled responses using MR dampers. They are i) LQG with clipped optimal control (LQGCC); ii) sliding mode with clipped optimal control (SMCC) and iii) bang bang control. Modified Bouc-Wen model described in previous chapter is used for generation of the control force using MR dampers. These control strategies are described in section 3.2.3 of chapter 3. A schematic diagram of the control strategy in real time is shown in Figure 4.1.

4.3 Real time application of the control method

For real-time application of the control strategy, white noise signal consistent with the measured ground motion is required. For this purpose, an ANN is trained offline and incorporated in the control scheme. For generating white noise input to the filters corresponding to the real ground excitation a neural network is trained. For training of neural network, a two-layered feed forward neural network is used for training. The input data and target data for the training of the neural network is the filtered excitation and the

corresponding white noise, respectively. The network is trained offline using twenty five sets of both broadband and narrowband filtered excitations and corresponding white noises consistent with the filter equations 4.1 and 4.2. Using the gensim command in MATLAB, a neural network function block of the trained neural network is created in SIMULINK of MATLAB. The function block of the neural network is then applied before the state space block in SIMULINK as shown in Fig. 4.2 and real excitation is given as input.

4.4 Numerical Study

For the study, the same ten story linear shear type building frame of chapter 3 having a mass of each floor as 18000 kg and stiffness of each floor as 24965 KN/m is considered. Controlled responses are obtained using VB-1 (Chapter 3), in which the state vector contains only structural displacements and velocities, and VB-2 (Fig. 4.1), in which the state vector contains filter variables, and the structural displacements and velocities. For the former, the excitation is the simulated ground acceleration from its PSDF, which is specified in chapter 3, Figure 3-10. For the latter, the excitation is the corresponding white noise, which produces the simulated ground acceleration when passed through the filters. For this purpose, two types of ground motions are considered, namely, narrow band and broad band excitations. The filter coefficients (Equations 4.1-2) used for generating two types of excitations are shown in Figure 3-10. The value of S_0 in equation 3.60 is so adjusted that the rms value of the white noise over a frequency band of 30 rad/sec is 0.05g. The corresponding covariance of excitations is 0.2 and 0.58, respectively. The corresponding PSDFs of both narrow and broadband excitations are shown in Chapter 3, Figure 3-10. Sample time histories of filtered narrow band and broad band excitations are shown in Chapter 3, Figure 3-11. The corresponding covariance of excitations is 0.2 and 0.58 respectively. Sample time history of corresponding white noise for narrow band and broad band filtered excitations is shown in Figure 4-3. The MR damper properties are given in Chapter 3, Table 3-1.

The control of responses is obtained with three MR dampers placed at first, second and third floors in a sequence. Since the placement of measurement sensors greatly influences the estimated state of the structure, their locations are decided based on best accurate estimate of the states of the floors where MR dampers are placed. As the control forces generated in the MR dampers largely depend on the velocities of the floors

where MR dampers are attached, placement of a velocity sensor at each of those floors is the obvious choice. If more than three sensors are used, the extra sensors are placed in locations so as to obtain the best results. In the present example problem, six sensors are used with three velocity sensors and three displacement sensors placed at bottom three floors where MR dampers are placed.

For VB-2, **W** is the covariance matrix of white noise having size 24 x 24. The last 12 diagonal terms contain the covariance of white noise. **V** matrix remains the same as that of VB-1. The values of matrices are selected based on the sensitivity analysis carried out in a subsequent section. **Q** and **R** matrices for the LQR algorithm are of size 24 x 24 and 3 x 3 respectively for the VB-2 system. **Q** and **R** matrices are adjusted for each earthquake to obtain the best results. Similarly, the $\mathbf{Q}_S$ matrix in the sliding mode control is adjusted for each earthquake to get the best results. An ensemble of twenty five time histories is used to find the response reductions and associated control force. The results of the analysis are shown in the form of the control measures explained by equations 3.62-63 in Chapter 3.

4.5 Comparison of Reductions in Responses obtained by Control Strategies VB-1 and VB-2

Figures 4.4-7 show comparison between the percentage reductions in peak and rms values of the response quantities of interest obtained by VB-1 and VB-2 using different control algorithms for broadband and narrowband excitations. It is seen from the figures that the response reductions in general are different for the two schemes (VB-1 and VB-2) and the difference varies with the response quantities of interest. Further, the difference is more pronounced for narrowband excitation; VB-2 provides more reduction in responses. In certain cases, VB-2 gives a much higher response reduction compared to VB-1. Comparison between the response reductions obtained by different algorithms shows that SMCCl and bang bang control generally provide more reduction in responses as compared to LQGCl. The maximum percentage reductions in drift and displacement are about 60%. The reduction in base shear is always less compared to other two response quantities; maximum reduction is of the order of 30%.

The peak control forces developed in the MR damper located in the first floor are compared for the two control schemes in Table-4-1. It is seen from the table that there is not much difference between the peak control forces required for the two control

schemes. The reason for this may be attributed to the limitation of the maximum voltage that can be applied to the MR dampers. Since the maximum voltage remains the same for the two schemes, it limits the control forces generated in the MR damper resulting in nearly the same peak control forces for the two.

Force-displacement and force-velocity plots of the first story MR damper are shown in Figures 4.8-19 for a sample time history of narrowband, broadband and corresponding white noise. It is seen from the figures that the nature of the plots is different for the two control schemes, VB-1 and VB-2. Further, they are different for different control algorithms.

4.6 Sensitivity study

For on-line application of the control schemes, the covariance matrices of noise and excitations are to be provided as inputs to the control algorithms. Since both are not actually known for future events, reasonable estimates of both are required for implementation of the schemes for adequate control of responses for future earthquakes. Therefore, a sensitivity study is required to properly adjust the values of the elements of the covariance matrices to obtain the desired control of responses and to ensure the numerical stability of the control schemes.

These covariance matrices function as constant matrices in Kalman filter for state estimation. The values of the matrices are adjusted to obtain the best results. Ideally, these values should be close to the measured values during earthquake. Therefore, the sensitivity analysis should be carried out within a range of values, consistent with the anticipated mean square value of the future earthquake in the region. Similarly, the values of the covariance matrix of measurement noise are adjusted within a range of expected values.

Adjusted values may differ from earthquake to earthquake, similar to those of $\mathbf{Q}_v$ and $\mathbf{R}_v$ matrices. With these backgrounds in view, the sensitivity study is carried out for the two control schemes, VB-1 and VB-2 for the broadband and narrowband excitation for all the three control algorithms. Note that for VB-1, the time histories of ground motion are generated from the PSDF of broadband and narrowband excitation shown in Figure 3-10, while those for VB-2 are the corresponding white noise excitations. Three values of covariance of noises, i.e. $vv^T = 10^{-7}$, 10^{-8} and 10^{-9} m^2/sec^4 are considered for the

study. The results of the analysis are shown in Figures 4-20-45. It is seen from the figures that as the vv^T increases from 10^{-9} to 10^{-7}, the critical value of the covariance of excitation, beyond which the numerical instability occurs, increases. The increase is about tenfold i.e. as vv^T increases from 10^{-9} to 10^{-8} for white noise corresponding to VB-2 system, the cut off value of the covariance of excitation increases from 0.066 to 0.66 for LQGCl, after which numerical instability takes place. Thus, covariance of noise and the critical value of excitation are correlated. Critical (cut off) values of covariance of excitation for three control algorithms and both excitations are shown in Table 4-2. Further, it is observed from the figures that for the same level of covariance of noise, the critical value of the covariance of excitation for broadband excitation which is input for VB-1 is less as compared to the white noise excitation, which is input to VB-2. This shows that the correlation between the covariance of excitation and covariance of noise depends upon the control scheme employed i.e. VB-1 and VB-2.

The result of the above study clearly shows that for the higher expected value of PGA of ground motion for a site, the covariance of noise to be selected for obtaining numerical stability of the control scheme is also higher. Further, it is seen from Figures 4.20-45 that once the level of covariance of noise is adjusted from the point of the numerical stability of control scheme, the percentage reduction in responses for covariance of excitation less than the critical value remains nearly the same.

With the increase in the covariance of noise, it is expected that state estimation will have more error leading to a less reliable reduction in responses for the control system. This is evident from the results presented in the Table 4-3. In the table, the difference between the percentage reductions in top floor displacement obtained using LQR and LQG control algorithms for the same ten storey building frame using one actuator at the top floor of the building is shown. For the LQG algorithm, six sensors (three displacements and three velocities) are employed at the floor levels where MR dampers are placed. In the LQR algorithm, it is assumed that the complete state is fully observed. Because of the error in the state estimation due to the presence of noise, the reductions in responses for the two algorithms are different; LQR provides more reduction in responses. The percentage difference in percentage reductions in top floor displacement is obtained by equation 4.6

$$\text{Percentage difference} = \frac{(D_D)_{LQR} - (D_D)_{LQG}}{(D_D)_{LQR}} \quad (4.6)$$

in which, $(D_D)_{LQR}$ is the percentage reduction in maximum top floor displacement obtained by LQR; $(D_D)_{LQG}$ is that obtained by LQG. Two values of the covariances of noises, i.e. $vv^T = 10^{-3}$ and 10^{-7} are considered along with covariance of excitation as 0.5 m^2/sec^4.

It is seen from the table that the percentage difference increases significantly as vv^T increases from 10^{-7} to 10^{-3} for active control with actuator. Thus, it is evident that adjustment of the covariance of noise at a higher level for achieving numerical stability of the control scheme for higher values of PGA of ground motion would lead to less reliable prediction of the controlled responses. For semi active control of structure with MR damper using LQGCl (VB-1), the error in the prediction of the controlled responses is considerably reduced due to the limitation of the maximum applied voltage in the MR dampers as shown in Table 4-4. Therefore, semi active control with MR damper is more reliable in predicting the controlled responses as compared to active and other semi active control schemes.

4.7 Conclusions

A modified semi active control of partially observed building frames under seismic excitation is presented. The new formulation incorporates more theoretical rigor in the analysis by making the input excitation to be Gaussian white with the help of a double filter incorporated in the structural system. Further, a sensitivity analysis is carried out which helps in selecting appropriate values of the covariance matrices, which are not known a priori, to be inputted to Kalman filter for state estimation for online applications. This is necessary for avoiding the onset of numerical instability in the control algorithm and hence, making it more robust. The results of the alternative formulation are compared with the conventional analysis. A ten story building frame is taken as an example problem. Three control algorithms are used for obtaining the time histories of the voltage to be applied to MR dampers. The control of responses for a ten story building frame is realized with the help of three MR dampers placed at the bottom three stories and the states of the system are observed with the help of six sensors. Numerical study leads to the following conclusions:

(1) Response reductions obtained by the proposed alternative formulation (VB-2) differ from those of the conventional formulation (VB-1) showing the need for improving the state estimation with more theoretical rigor; in general, the response reductions are found to be more for the VB-2 as compared toVB-1.

(2) Out of the three control algorithms employed, bang bang control and SMCCl generally provide better control of responses as compared to LQGCl.

(3) Critical covariance of excitation depends on the formulation (VB-1 and VB-2), and the covariance of noise; below the critical value, the response reductions are invariant of the value of the covariance matrix of excitation given as input to the Kalman filter. The covariance matrix of excitation inputted to the Kalman filter should be less than or equal to the critical covariance for numerical stability of the algorithm.

(4) Covariance of noise is to be set to a higher level in order to increase the critical covariance of excitation; thus, for the high anticipated PGA used in the design, adjusted covariance of noise is higher.

(5) For higher covariance of noise, predicted response reductions are less reliable because of the greater error introduced in the state estimation.

(6) For semi active control with MR damper, the differences in response reductions due to the change in formulation and in the parameters considered in the sensitivity analysis are narrowed down due to the limitation on maximum voltage that can be applied to the MR damper; in this sense, semi active control with MR damper merits an advantage.

Table 4-1: Peak control forces developed in the MR damper for different control strategies

Control Algorithm	**Broadband Excitation (kN)**		**Narrowband Excitation (kN)**	
	VB-1	**VB-2**	**VB-1**	**VB-2**
Bang Bang	101	92	88	87
LQGCl	107	95	91	93
SMCCl	104	97	92	92

Table 4-2: Critical values of covariance of excitation for different control algorithms under different excitations

Control Algorithms	**Broadband excitation (m^2/sec^4)**		**Narrowband excitation (m^2/sec^4)**	
	VB-1 ($vv^T= 10^{-7}$)	**VB-2 ($vv^T= 10^{-8}$)**	**VB-1 ($vv^T= 10^{-7}$)**	**VB-2 ($vv^T= 10^{-8}$)**
LQGCl	0.52	0.66	0.52	0.67
Bang Bang	1.1	0.71	0.53	0.71
SMCCl	1.17	0.71	0.51	0.71

Table 4-3: Percentage error in peak values of top floor displacement for LQG and LQR algorithm for three MR dampers and one actuator for different noise covariance's

Noise Covariance	Broadband Excitation		Narrowband Excitation	
vv^T	MR dampers (%)	Actuator (%)	MR dampers (%)	Actuator (%)
10^{-7}	2	10	9	1
10^{-3}	17	54	25	41

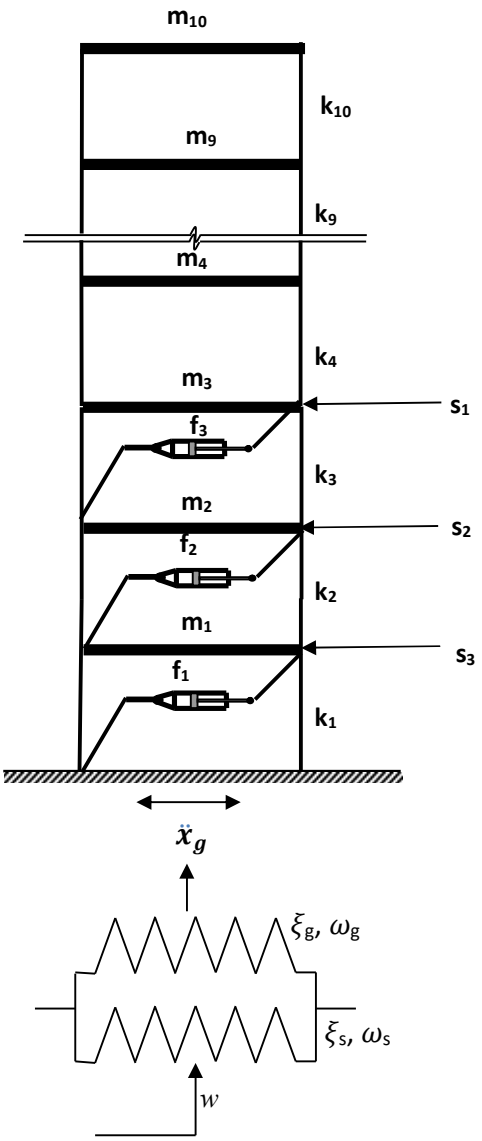

Figure 4-1: VB 2 system equipped with three MR dampers and six sensors

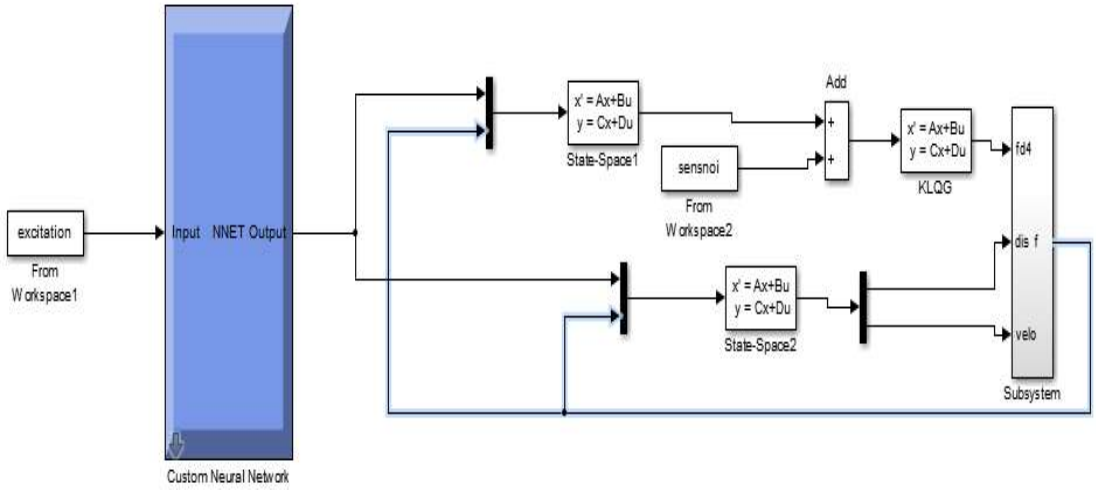

Figure 4-2: Use of ANN for online application of algorithm in SIMULINK

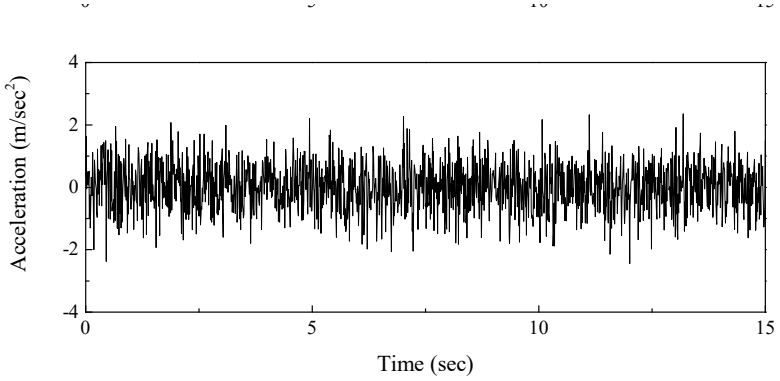

Figure 4-3: Sample time history of white noise

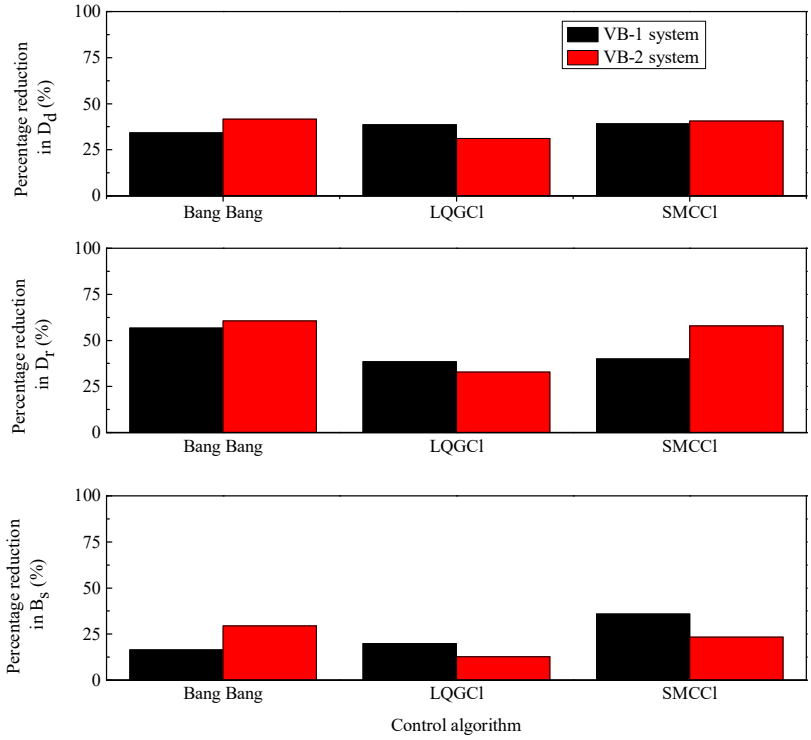

Figure 4-4: Comparison between percentage reductions in expected peak values of different response quantities obtained by VB-1 and VB-2 (broadband excitation)

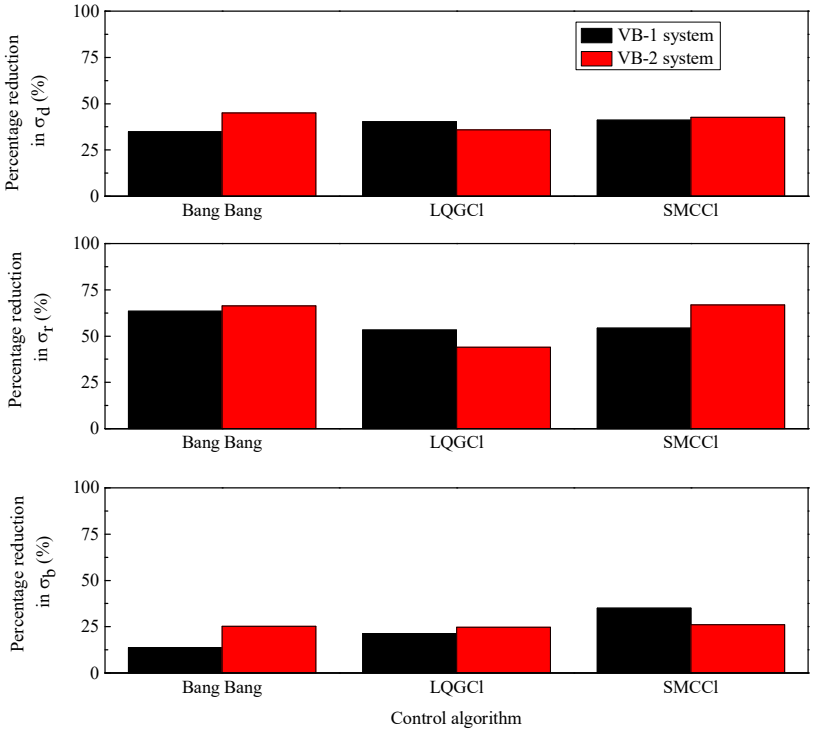

Figure 4-5: Comparison between percentage reductions in expected rms values of different response quantities obtained by VB-1 and VB-2 (broadband excitation)

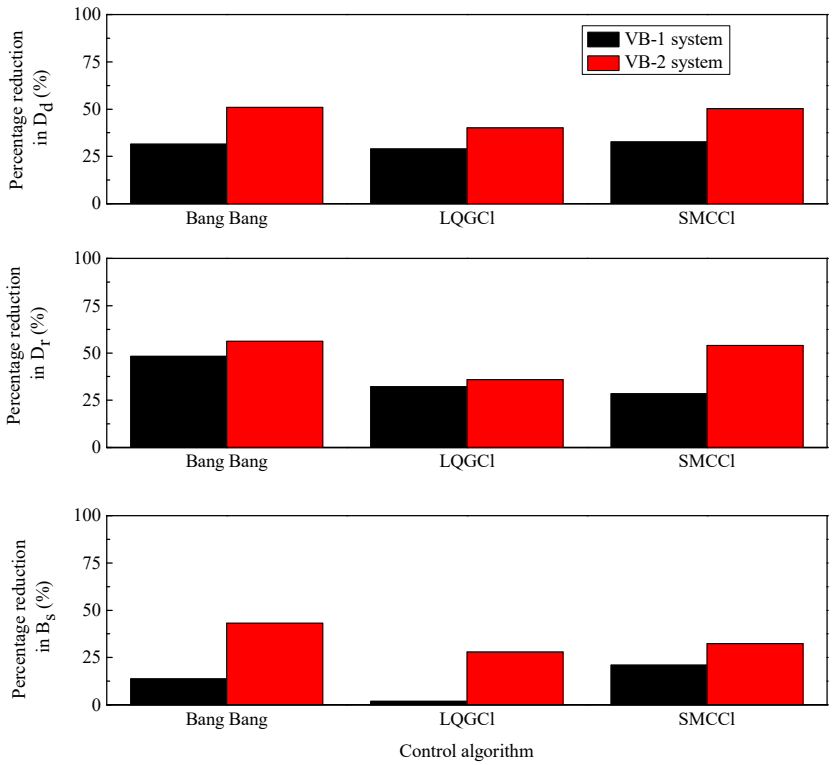

Figure 4-6: Comparison between percentage reductions in expected peak values of different response quantities obtained by VB-1 and VB-2 (narrowband excitation)

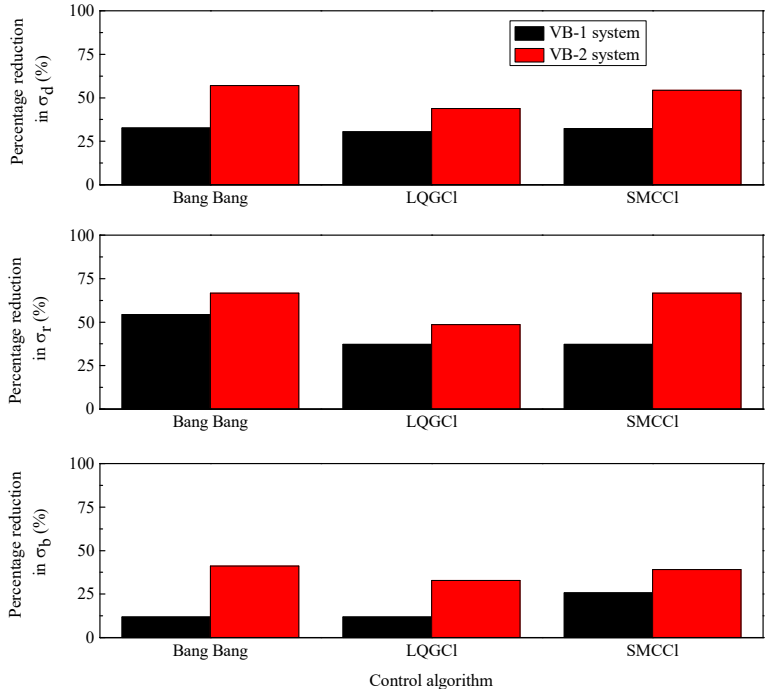

Figure 4-7: Comparison between percentage reductions in expected rms values of different response quantities obtained by VB-1 and VB-2 (narrowband excitation)

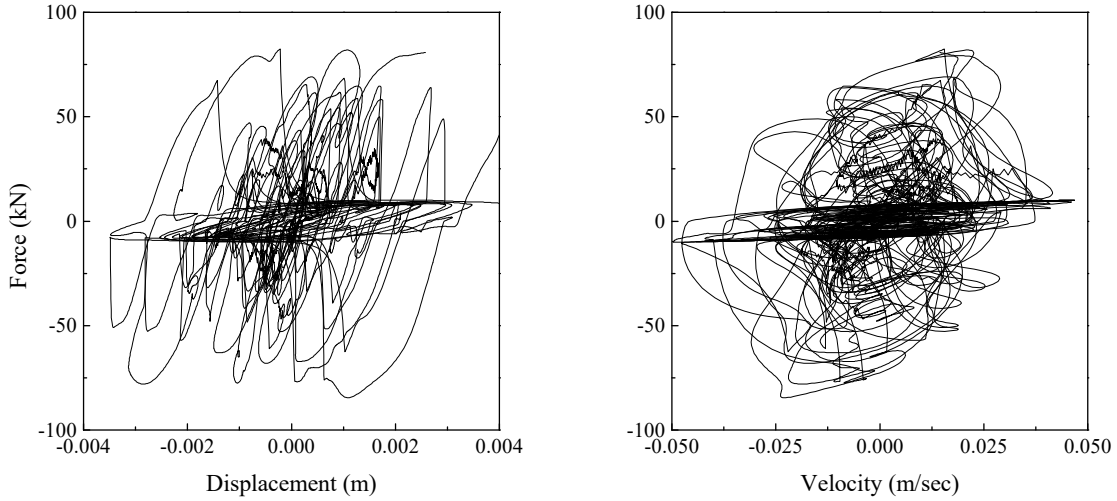

Figure 4-8: Force-displacement and force velocity plots of MR damper located at the first floor for LQGCl under broadband white noise (VB-2 system)

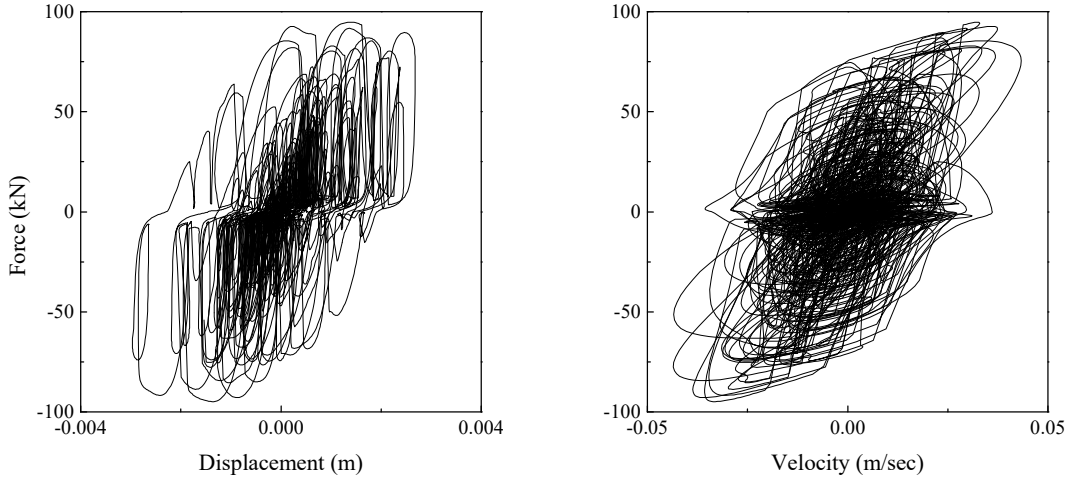

Figure 4-9: Force-displacement and force velocity plots of MR damper located at the first floor for LQGCl under broadband filtered excitation (VB-1 system)

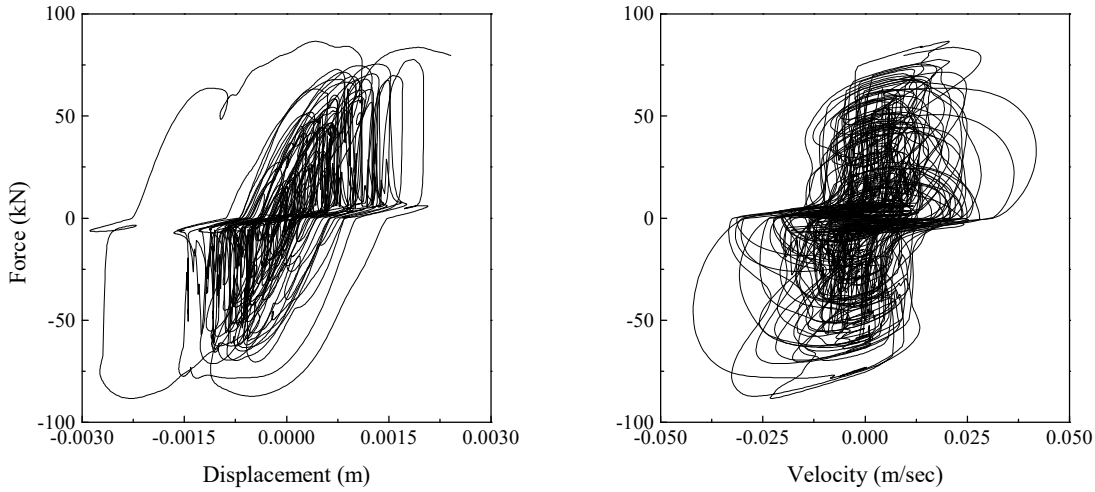

Figure 4-10: Force-displacement and force velocity plots of MR damper located at the first floor for bang bang control under broadband white noise (VB-2 system)

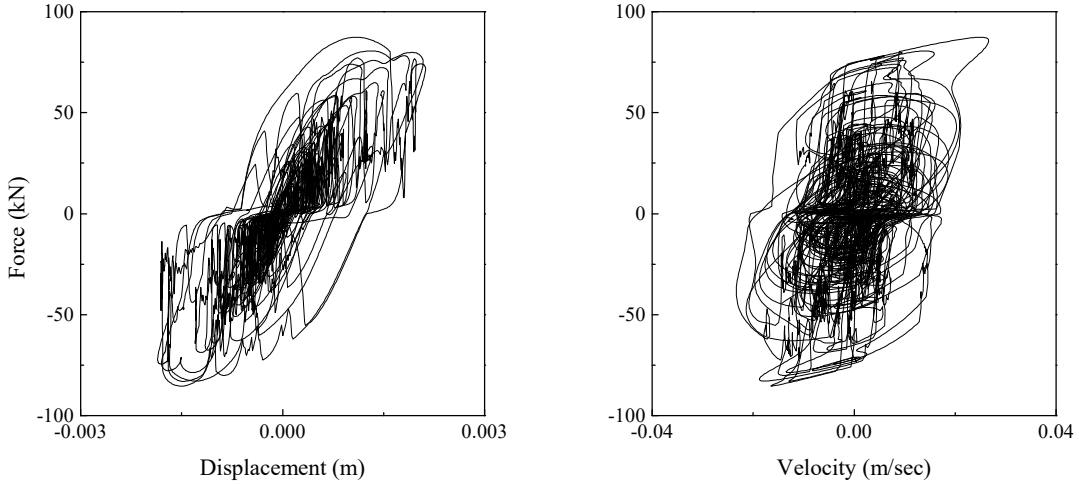

Figure 4-11: Force-displacement and force velocity plot of MR damper located at the first floor for bang bang control under broadband filtered excitation (VB-1 system)

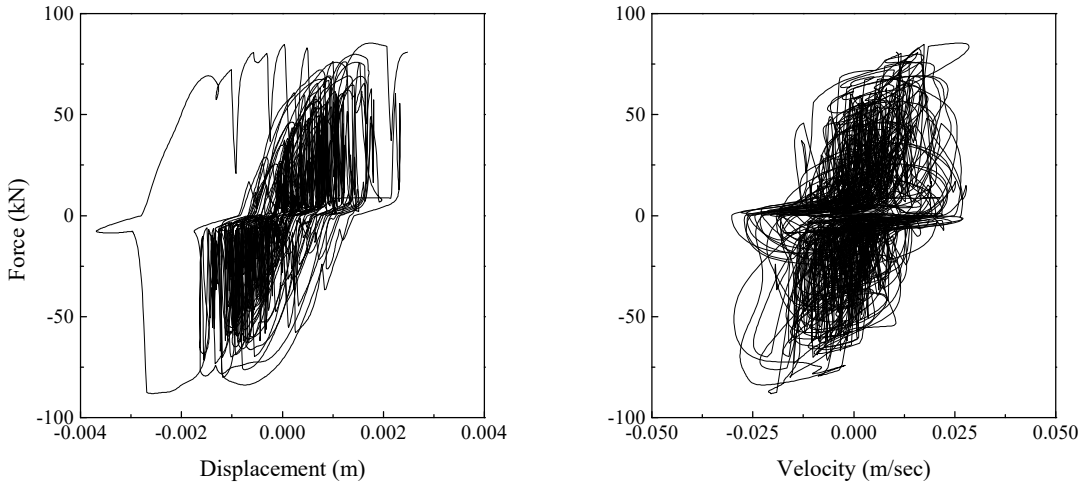

Figure 4-12: Force-displacement and force velocity plot of MR damper located at the first floor for SMCCl under broadband white noise (VB-2 system)

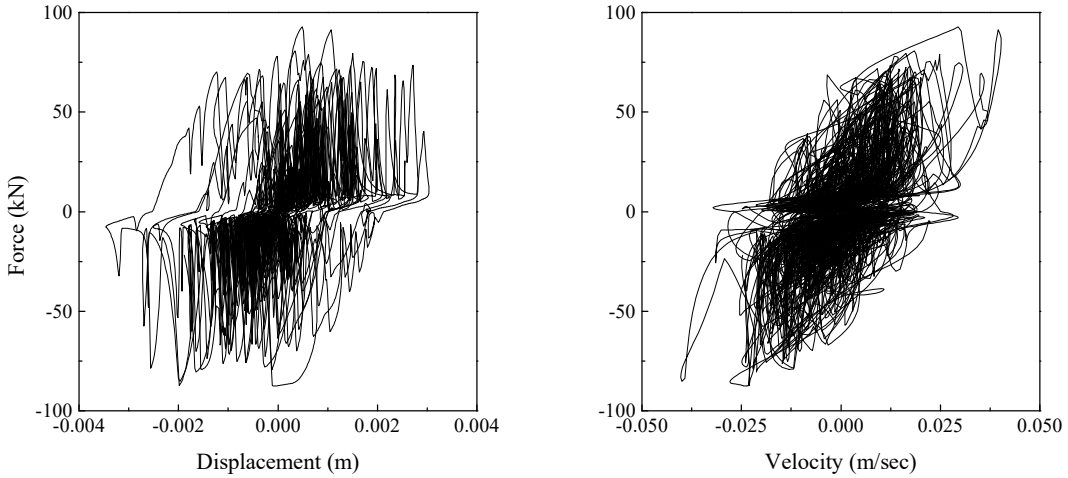

Figure 4-13: Force-displacement and force velocity plot of MR damper located at the first floor for SMCCl under broadband filtered excitation (VB-1 system)

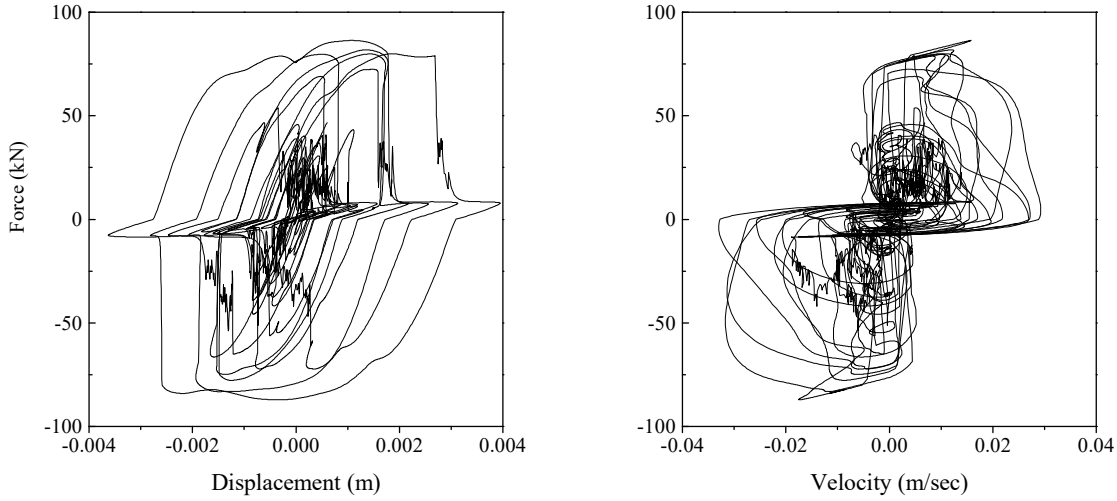

Figure 4-14: Force-displacement and force velocity plot of MR damper located at first floor for LQGCl under narrowband white noise (VB-2 system)

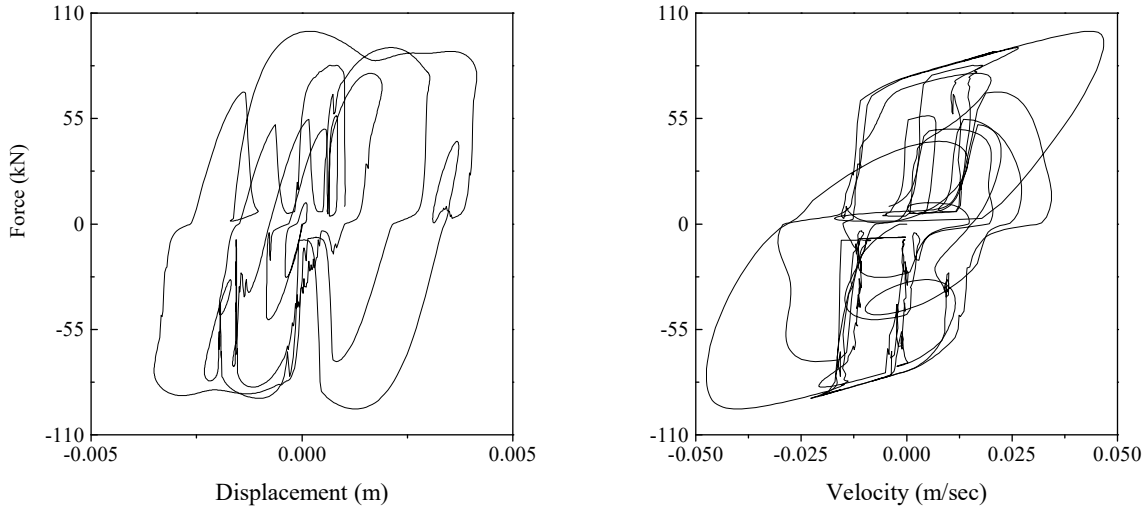

Figure 4-15: Force-displacement and force velocity plot of MR damper located at first floor for LQGCl under narrowband filtered excitation (VB-1 system)

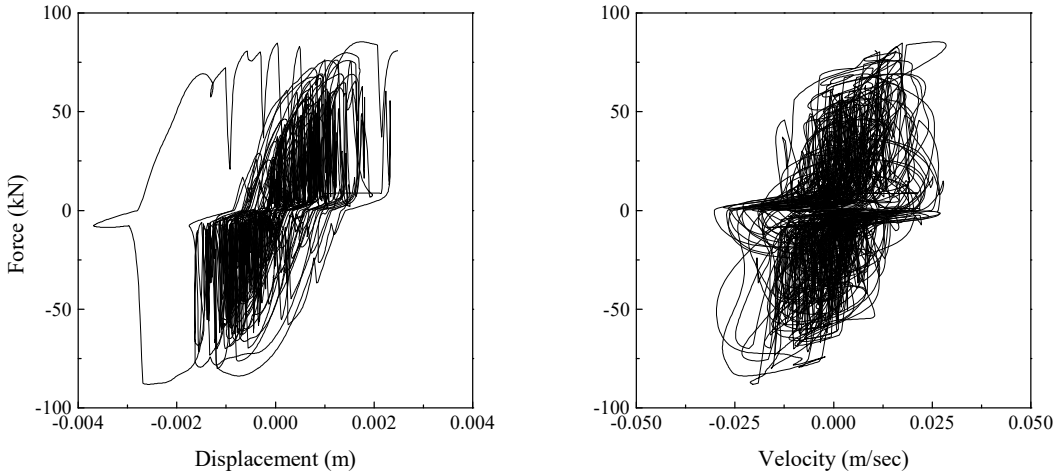

Figure 4-16: Force-displacement and force velocity plot of MR damper located at first floor for bang bang under narrowband white noise (VB-2 system)

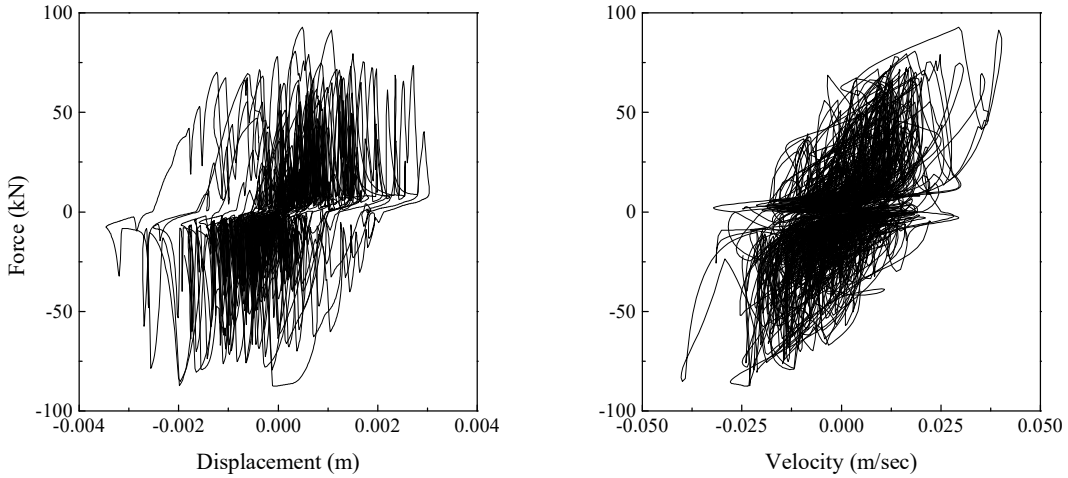

Figure 4-17: Force-displacement and force velocity plot of MR damper located at first floor for bang bang under narrowband filtered excitation (VB-1 system)

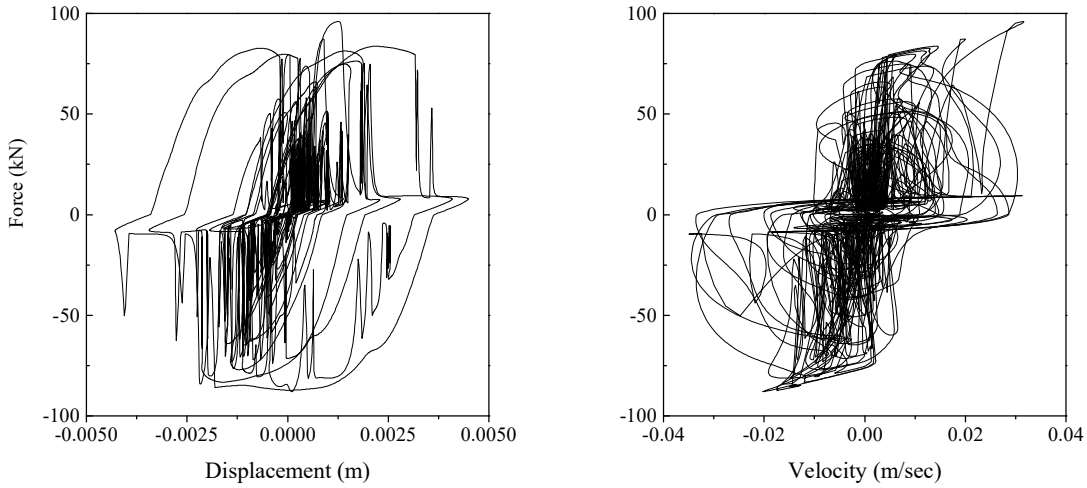

Figure 4-18: Force-displacement and force velocity plot of MR damper located at first floor for SMCCl under narrowband white noise (VB-2 system)

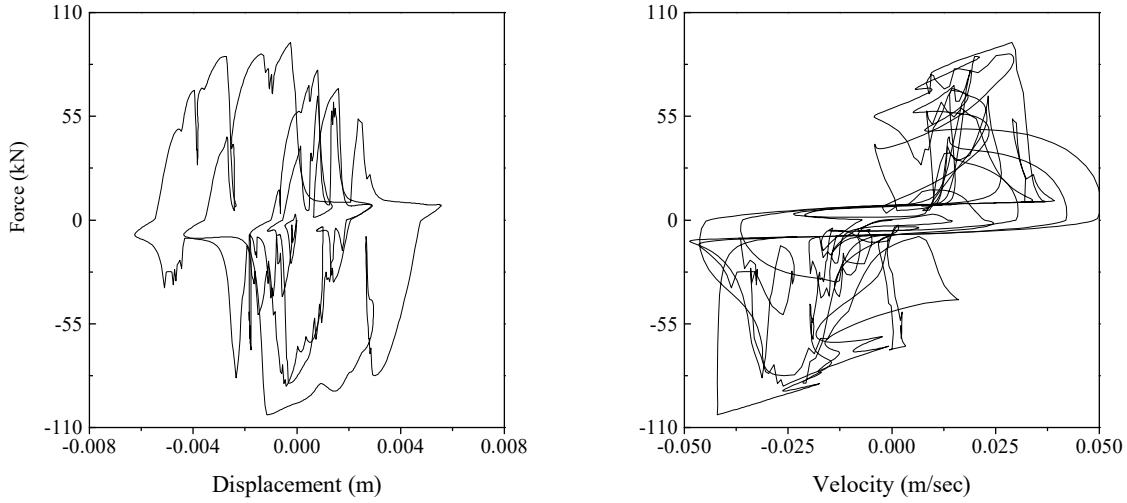

Figure 4-19: Force-displacement and force velocity plot of MR damper located at first floor for SMCCl under narrowband filtered excitation (VB-1 system)

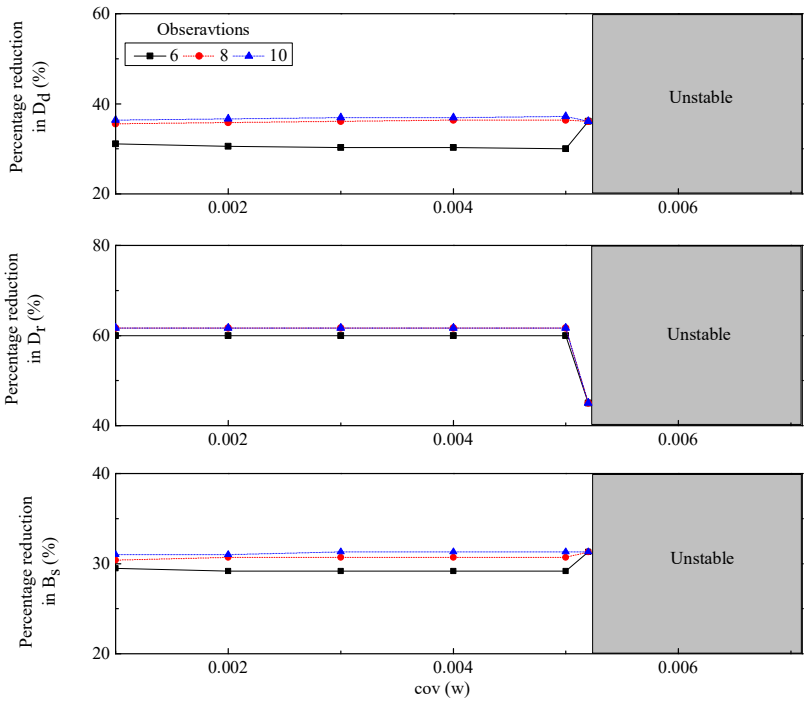

Figure 4-20: Variation of percentage reduction in different response quantities with covariance of excitation for LQGCl for broadband excitation at $vv^T = 10^{-9}$ m^2/sec^4 (VB-1)

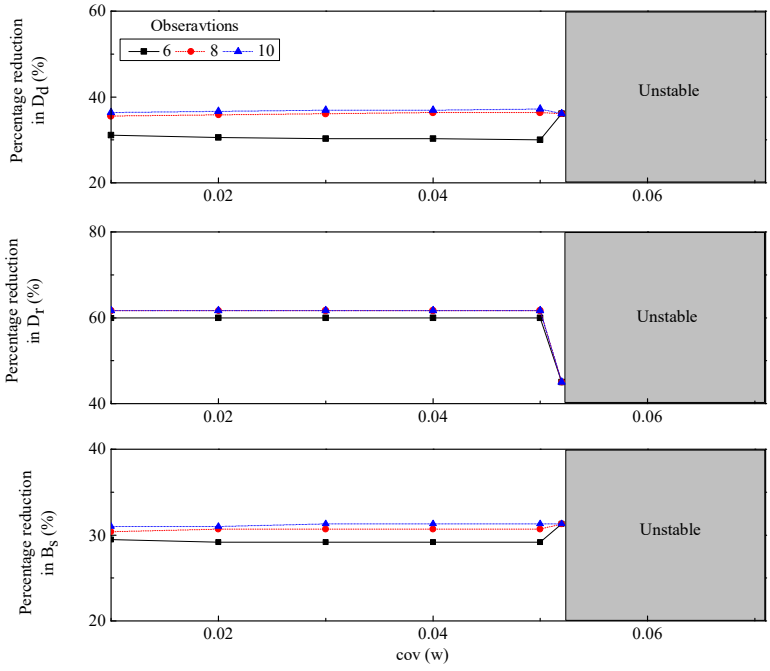

Figure 4-21: Variation of percentage reduction in different response quantities with covariance of excitation for LQGCl for broadband excitation at $vv^T = 10^{-8}$ m^2/sec^4 (VB-1)

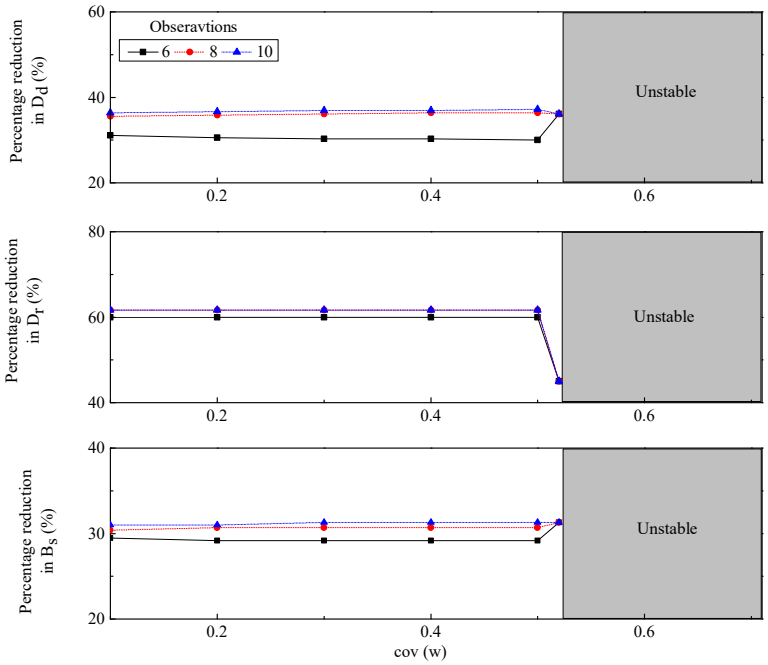

Figure 4-22: Variation of percentage reduction in different response quantities with covariance of excitation for LQGCl for broadband excitation at $vv^T = 10^{-7}$ m^2/sec^4 (VB-1)

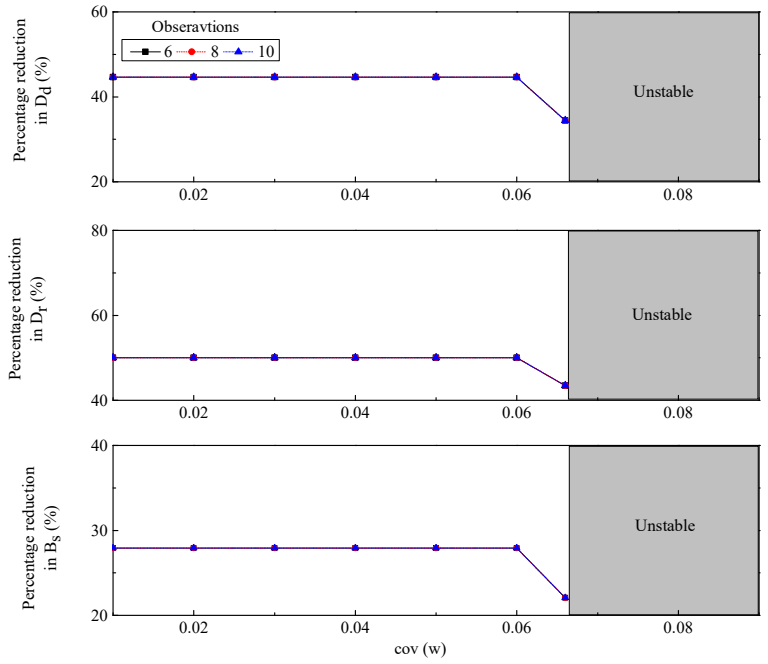

Figure 4-23: Variation of percentage reduction in different response quantities with covariance of excitation for white noise for LQGCl corresponding to broadband excitation at $vv^T = 10^{-9}$ m^2/sec^4 (VB-2)

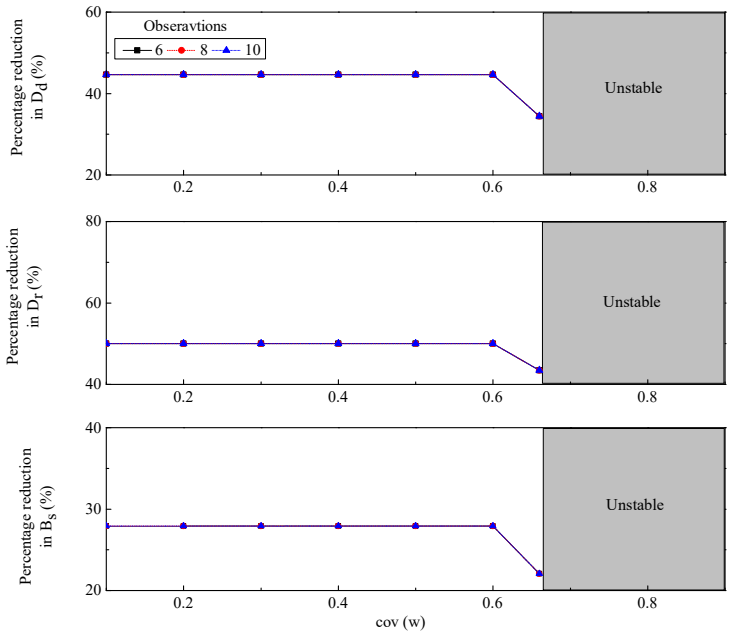

Figure 4-24: Variation of percentage reduction in different response quantities with covariance of excitation for white noise for LQGCl corresponding to broadband excitation at $vv^T = 10^{-8}$ m^2/sec^4 (VB-2)

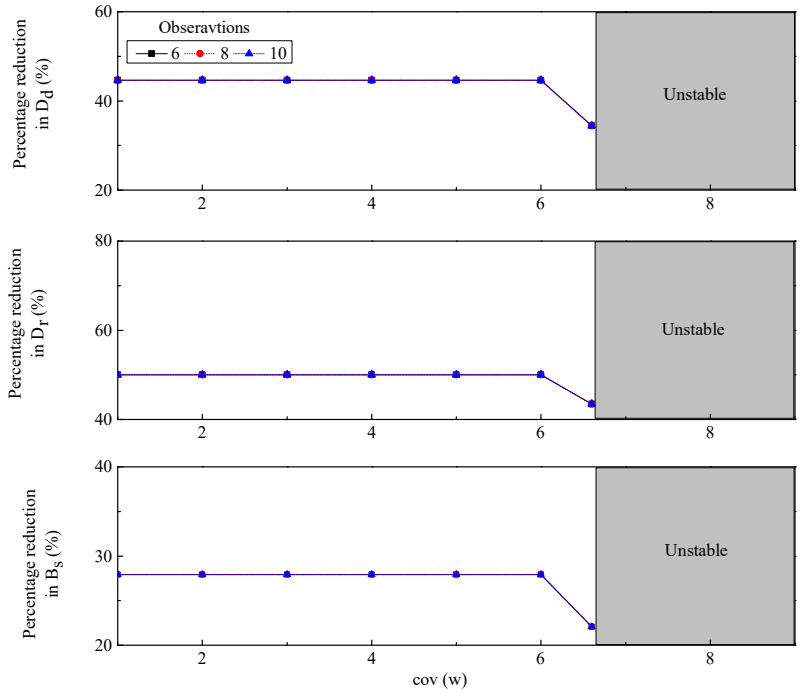

Figure 4-25: Variation of percentage reduction in different response quantities with covariance of excitation for white noise for LQGCl corresponding to broadband excitation at $vv^T = 10^{-7}$ m^2/sec^4 (VB-2)

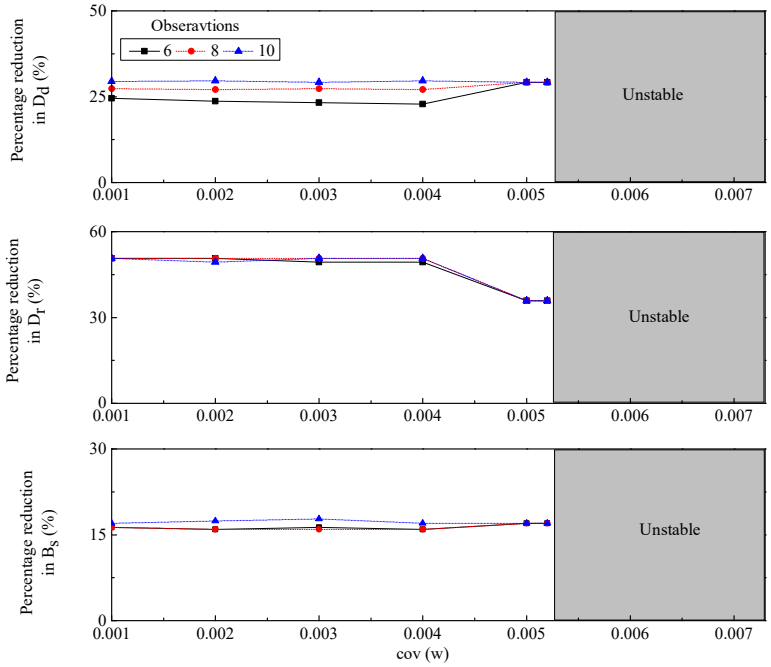

Figure 4-26: Variation of percentage reduction in different response quantities with covariance of excitation for LQGCl for narrowband excitation at $vv^T = 10^{-9}$ m^2/sec^4 (VB-1)

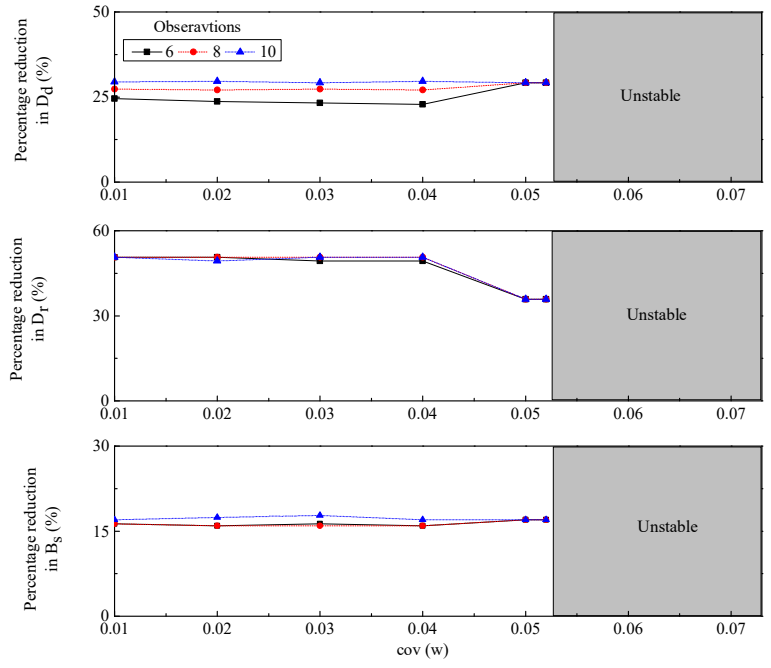

Figure 4-27: Variation of percentage reduction in different response quantities with covariance of excitation for LQGCl for narrowband excitation at $vv^T = 10^{-8}$ m^2/sec^4 (VB-1)

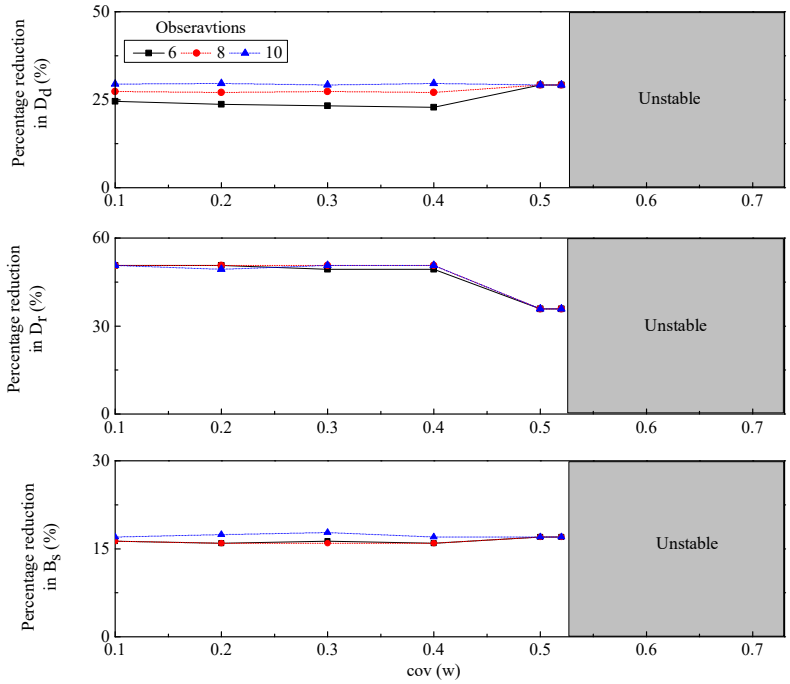

Figure 4-28: Variation of percentage reduction in different response quantities with covariance of excitation for LQGCl for narrowband excitation at $vv^T = 10^{-7}$ m^2/sec^4 (VB-1)

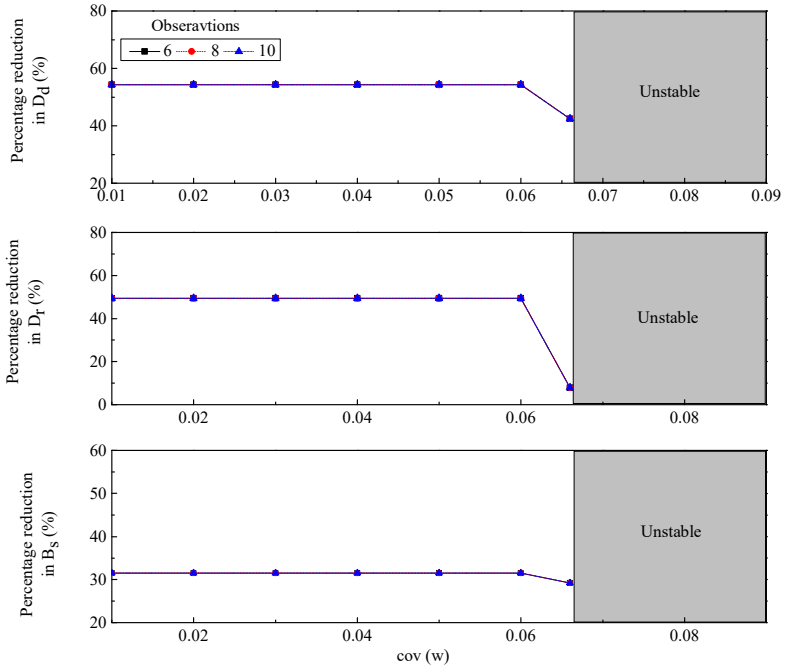

Figure 4-29: Variation of percentage reduction in different response quantities with covariance of excitation for white noise for LQGCl corresponding to narrowband excitation at $vv^T = 10^{-9}$ m^2/sec^4 (VB-2)

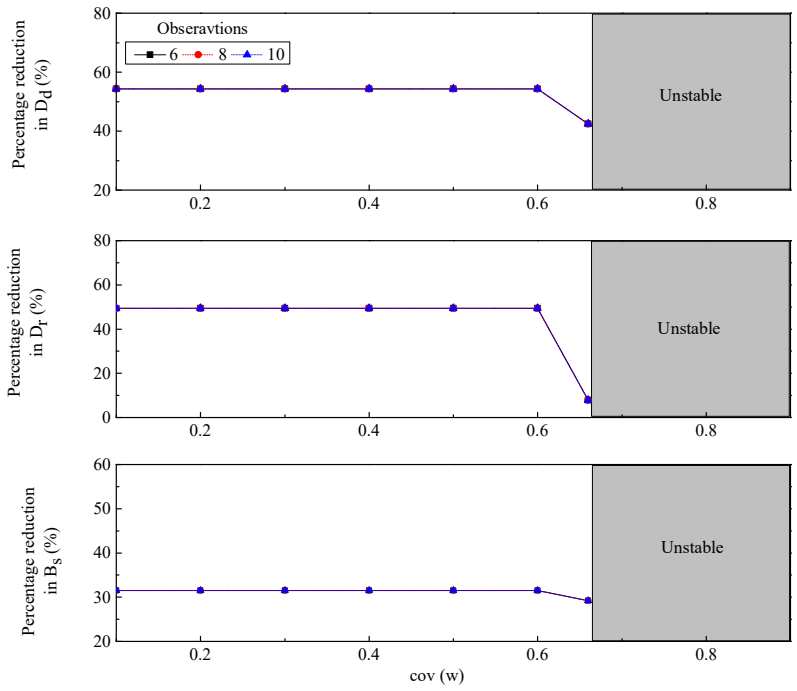

Figure 4-30: Variation of percentage reduction in different response quantities with covariance of excitation for white noise for LQGCl corresponding to narrowband excitation at $vv^T = 10^{-8}$ m^2/sec^4 (VB-2)

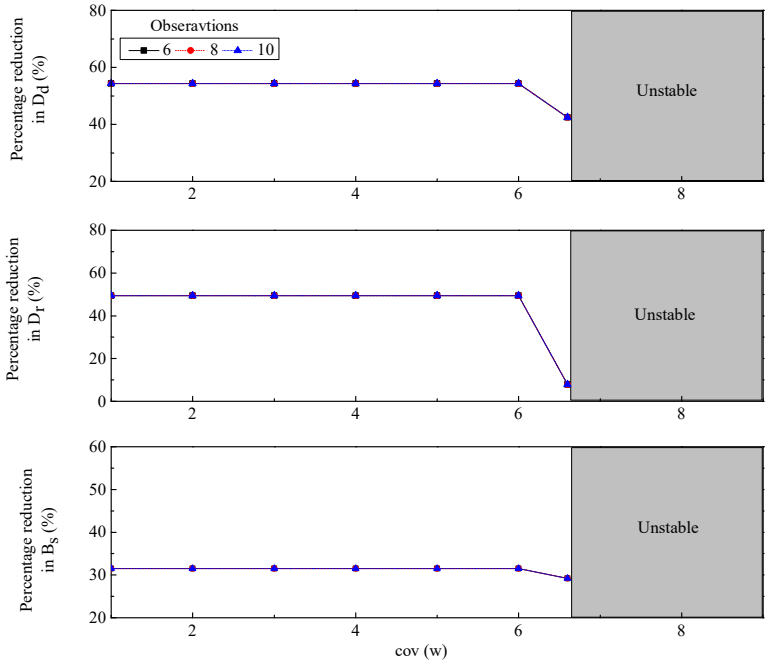

Figure 4-31: Variation of percentage reduction in different response quantities with covariance of excitation for white noise for LQGCl corresponding to narrowband excitation at $vv^T = 10^{-7}$ m^2/sec^4 (VB-2)

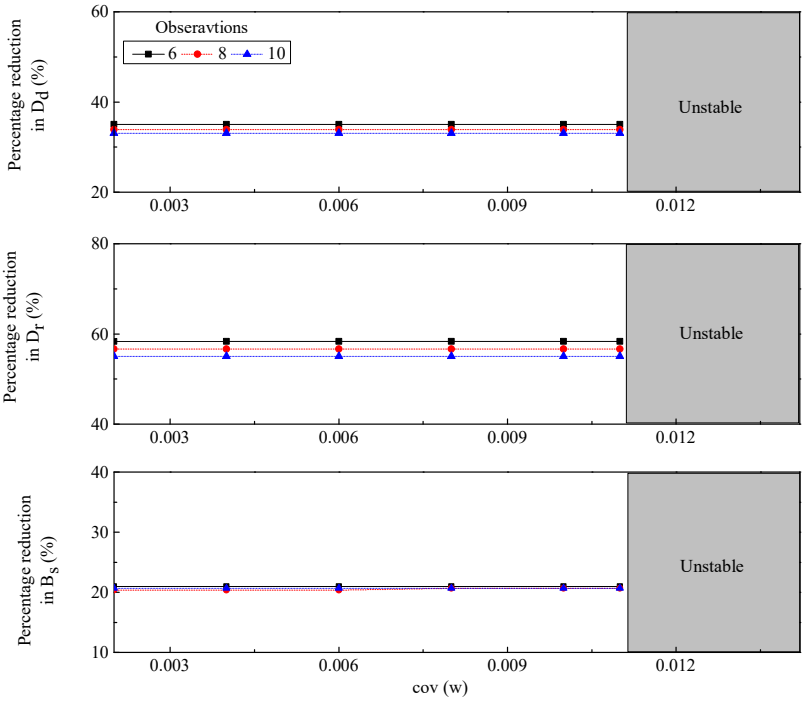

Figure 4-32: Variation of percentage reduction in different response quantities with covariance of excitation for bang bang for broadband excitation at $vv^T = 10^{-9}$ m^2/sec^4 (VB-1)

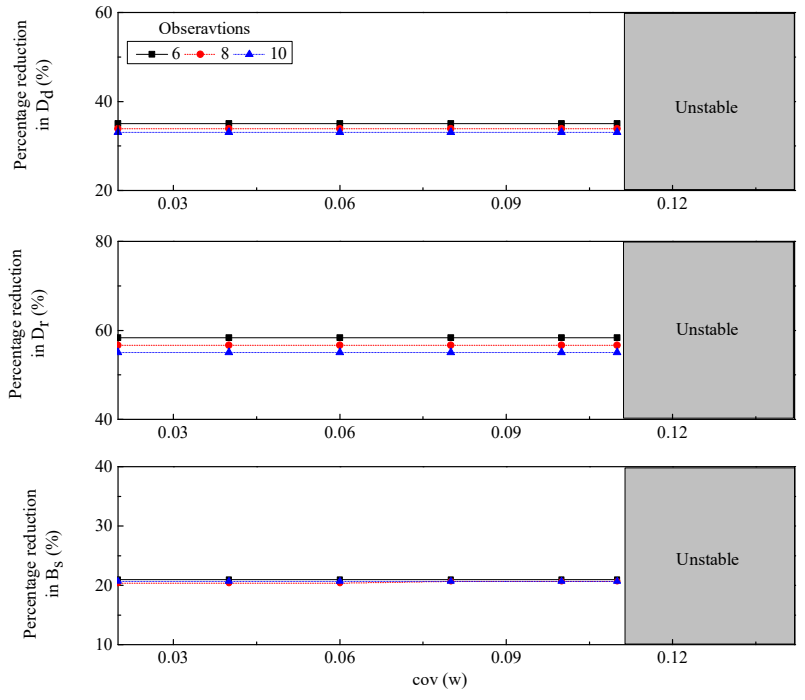

Figure 4-33: Variation of percentage reduction in different response quantities with covariance of excitation for bang bang for broadband excitation at $vv^T = 10^{-8}$ m^2/sec^4 (VB-1)

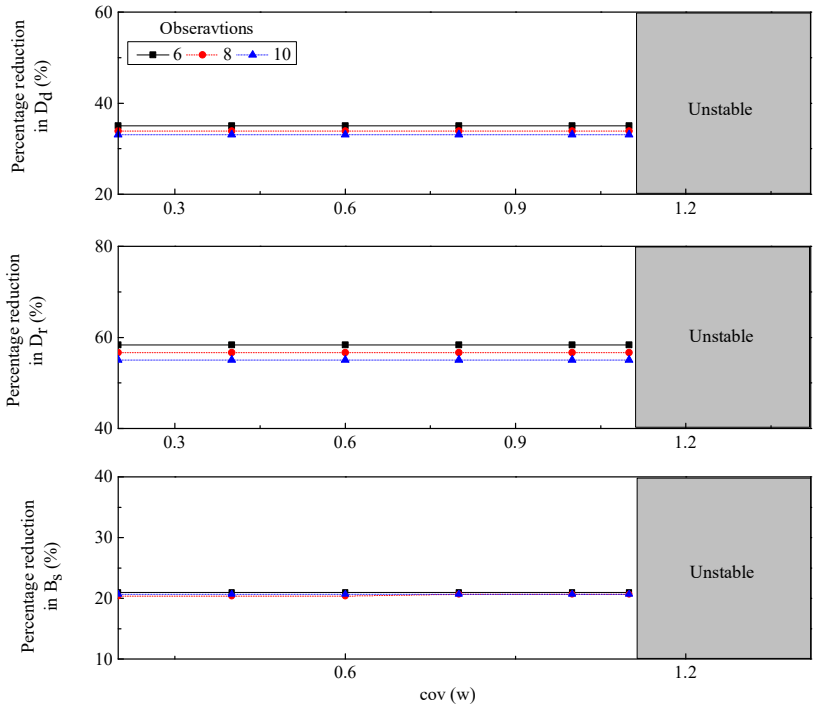

Figure 4-34: Variation of percentage reduction in different response quantities with covariance of excitation for bang bang for broadband excitation at $vv^T = 10^{-7}$ m^2/sec^4 (VB-1)

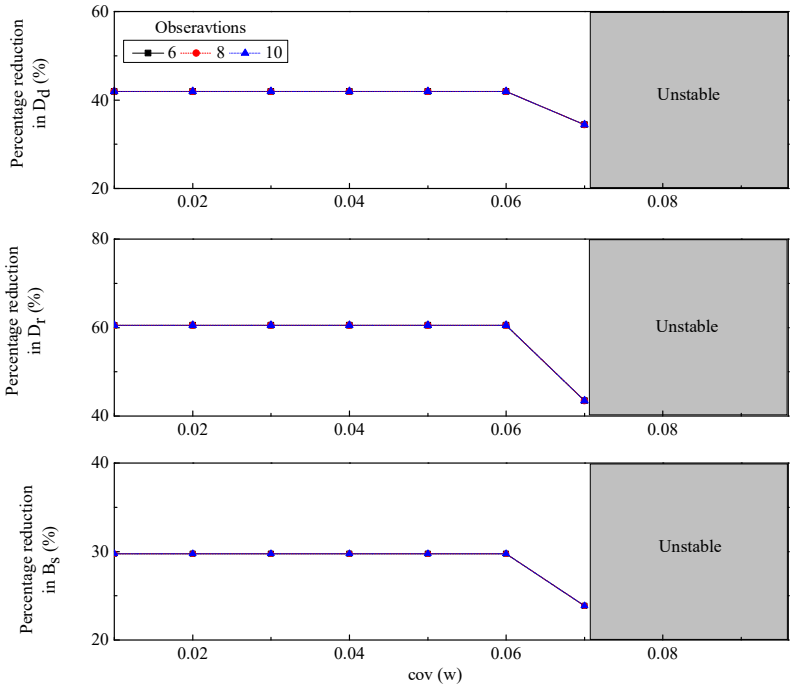

Figure 4-35: Variation of percentage reduction in different response quantities with covariance of excitation for white noise for bang bang corresponding to broadband excitation at $vv^T = 10^{-9}$ m^2/sec^4 (VB-2)

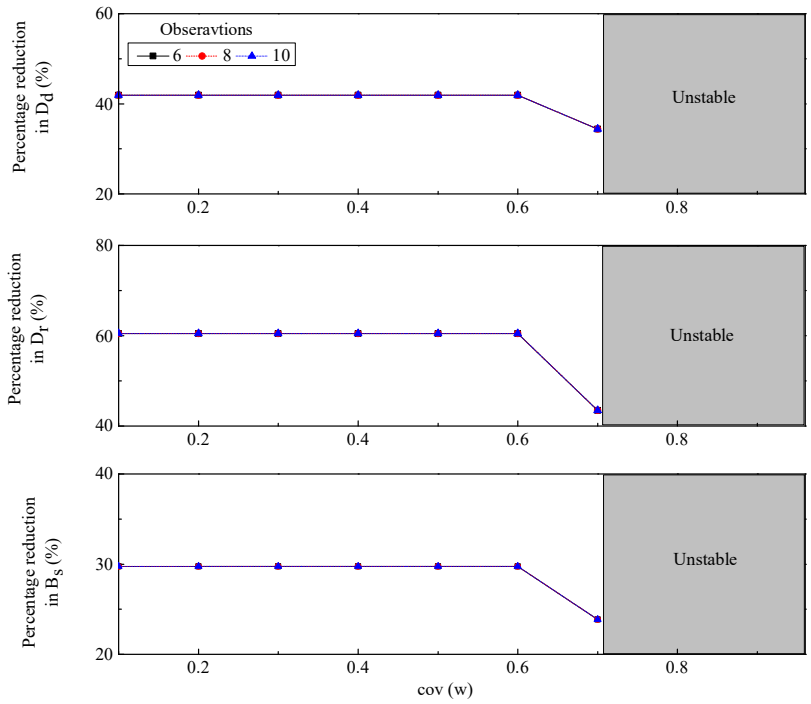

Figure 4-36: Variation of percentage reduction in different response quantities with covariance of excitation for white noise for bang bang corresponding to broadband excitation at $vv^T = 10^{-8}$ m^2/sec^4 (VB-2)

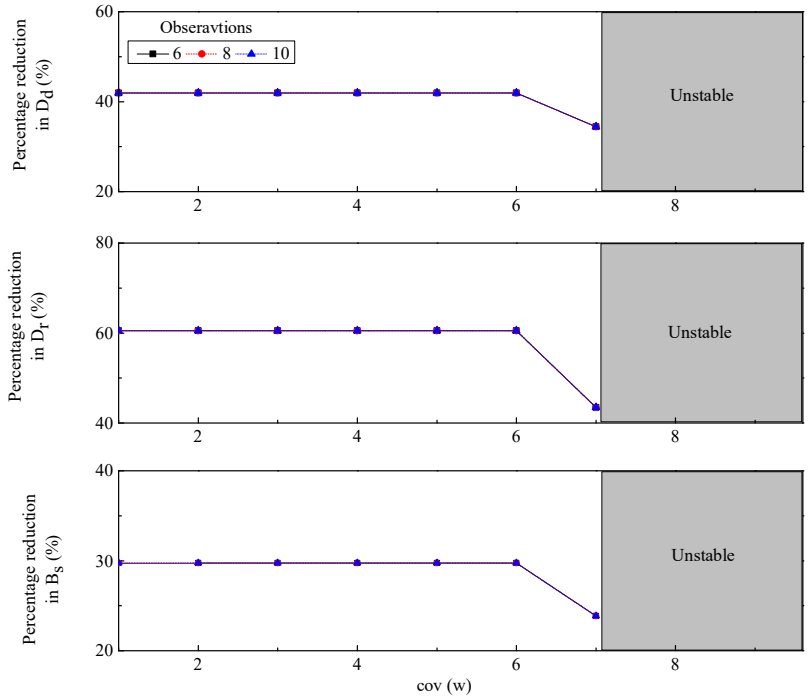

Figure 4-37: Variation of percentage reduction in different response quantities with covariance of excitation for white noise for bang bang corresponding to broadband excitation at $vv^T = 10^{-7}$ m^2/sec^4 (VB-2)

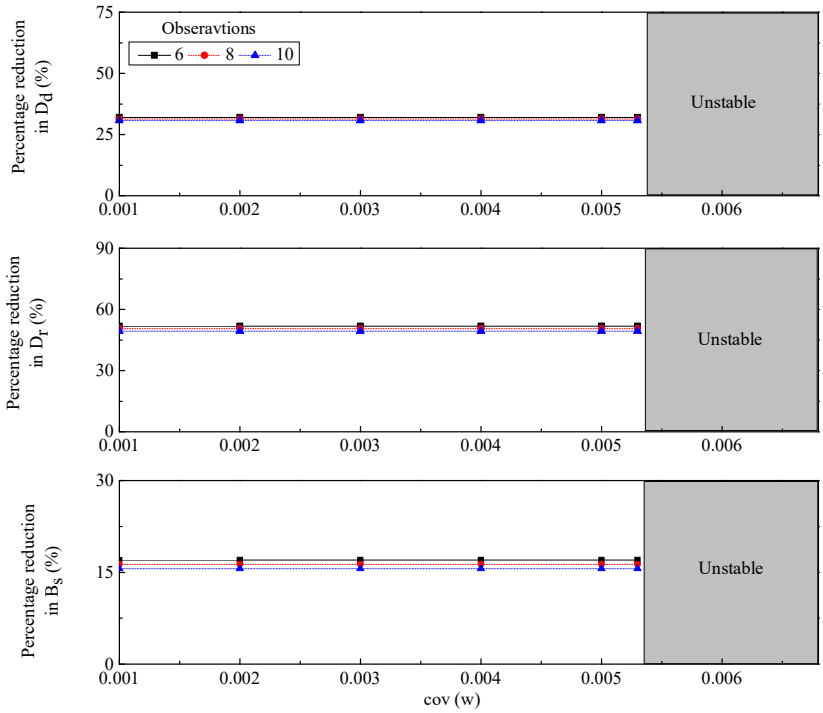

Figure 4-38: Variation of percentage reduction in different response quantities with covariance of excitation for bang bang for narrowband excitation at $vv^T = 10^{-9}$ m^2/sec^4 (VB-1)

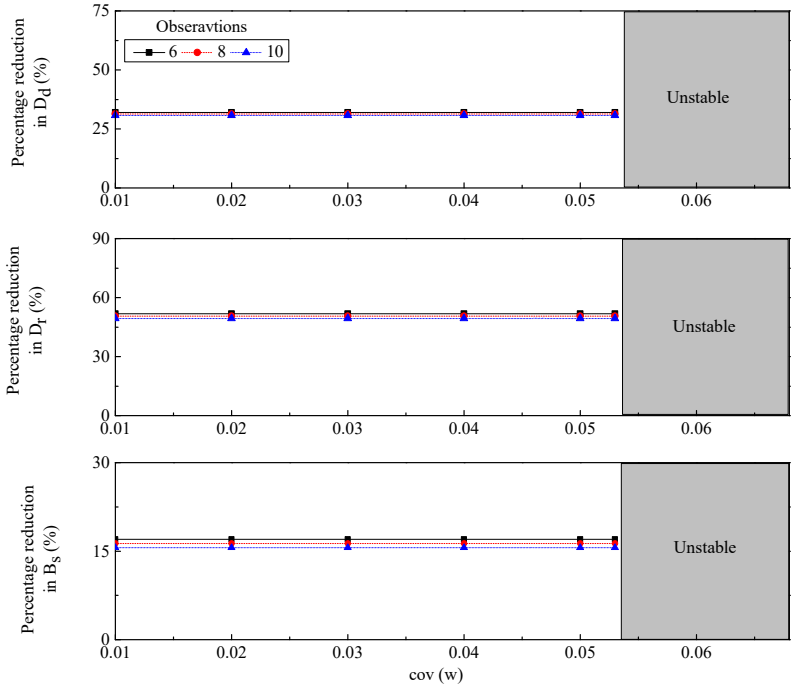

Figure 4-39: Variation of percentage reduction in different response quantities with covariance of excitation for bang bang for narrowband excitation at $vv^T = 10^{-8}$ m^2/sec^4 (VB-1)

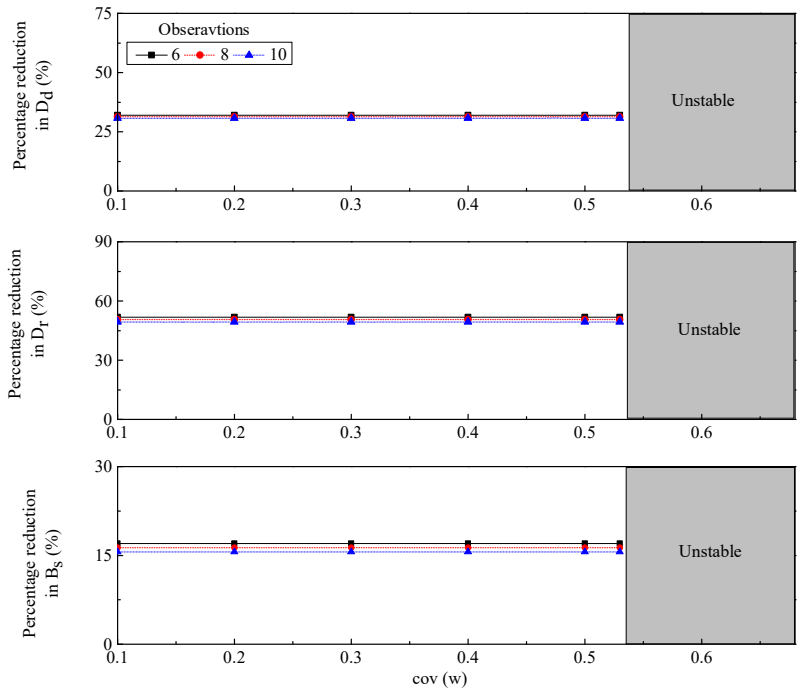

Figure 4-40: Variation of percentage reduction in different response quantities with covariance of excitation for bang bang for narrowband excitation at $vv^T = 10^{-7}$ m^2/sec^4 (VB-1)

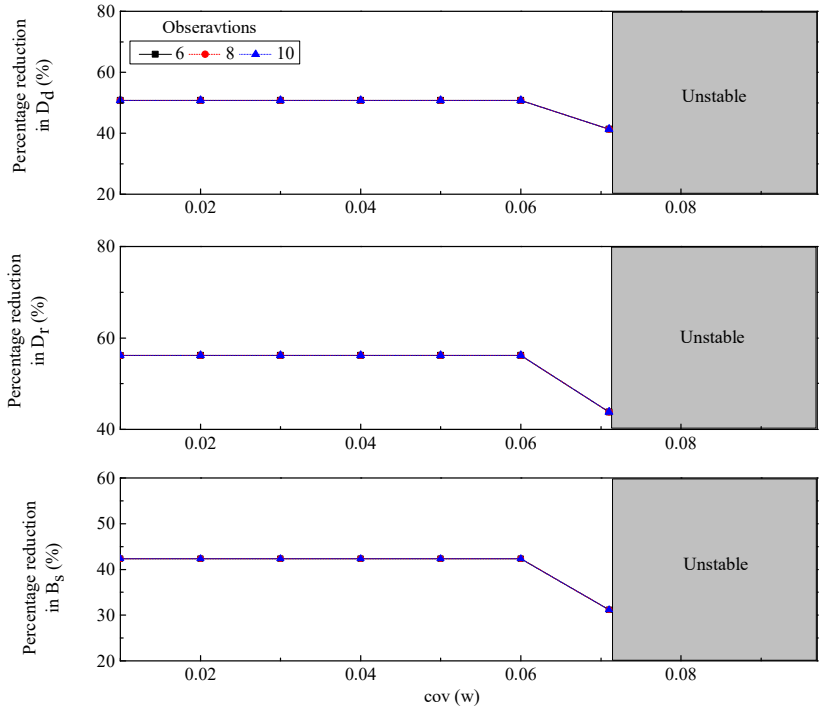

Figure 4-41: Variation of percentage reduction in different response quantities with covariance of excitation for white noise for bang bang corresponding to narrowband excitation at $vv^T = 10^{-9}$ m^2/sec^4 (VB-2)

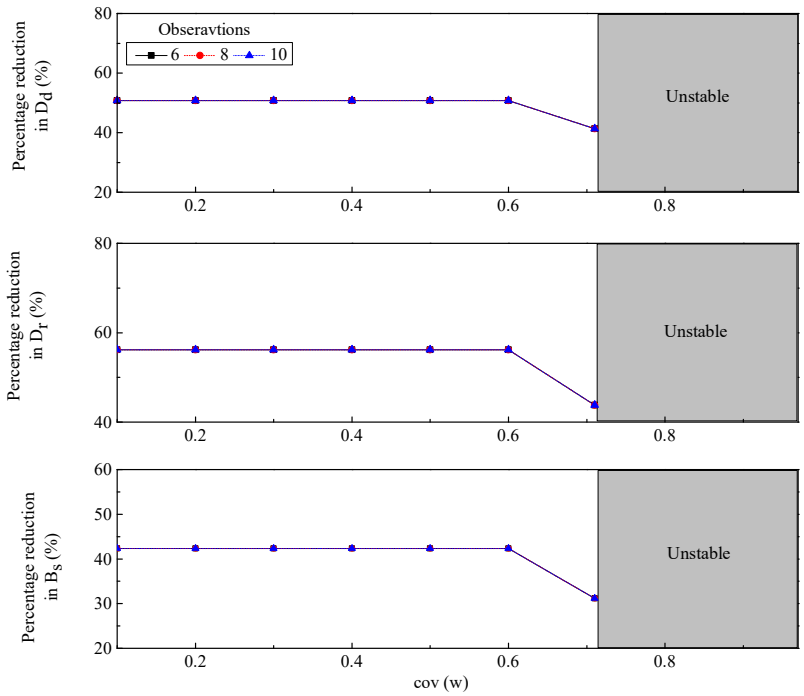

Figure 4-42: Variation of percentage reduction in different response quantities with covariance of excitation for white noise for bang bang corresponding to narrowband excitation at $vv^T = 10^{-8}$ m^2/sec^4 (VB-2)

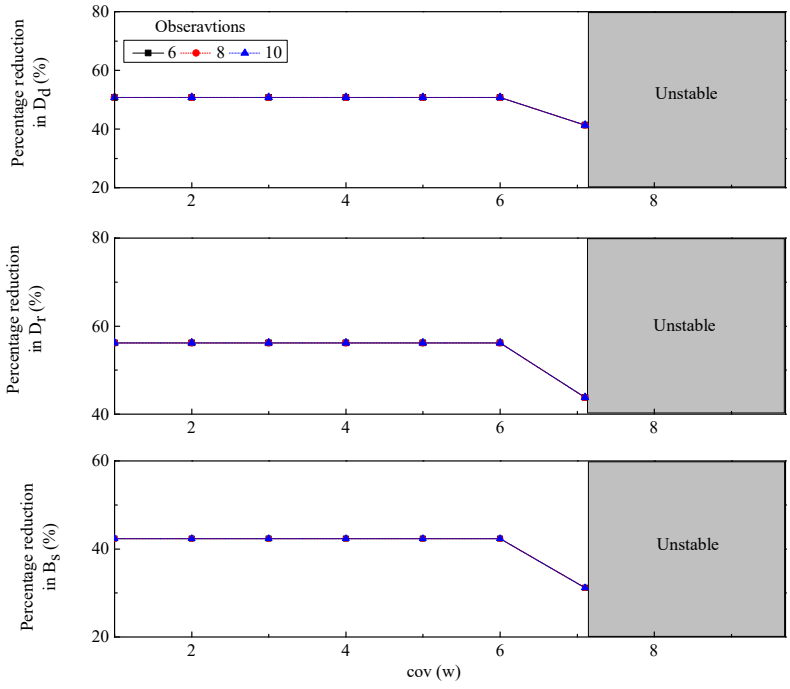

Figure 4-43: Variation of percentage reduction in different response quantities with covariance of excitation for white noise for bang bang corresponding to narrowband excitation at $vv^T = 10^{-7}$ m^2/sec^4 (VB-2)

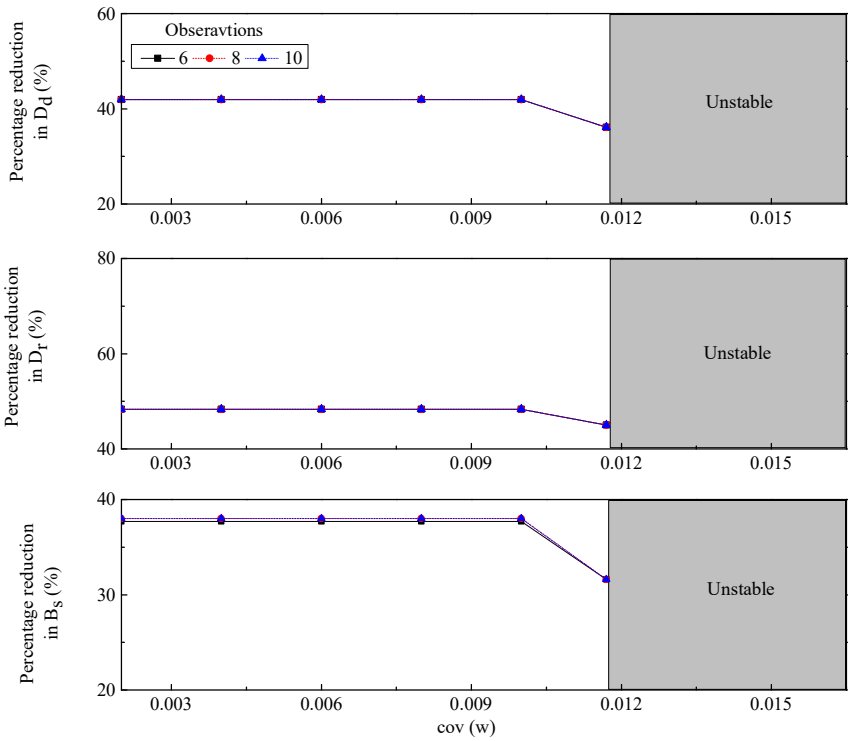

Figure 4-44-: Variation of percentage reduction in different response quantities with covariance of excitation for SMCCl for broaband excitation at $vv^T = 10^{-9}$ m^2/sec^4 (VB-1)

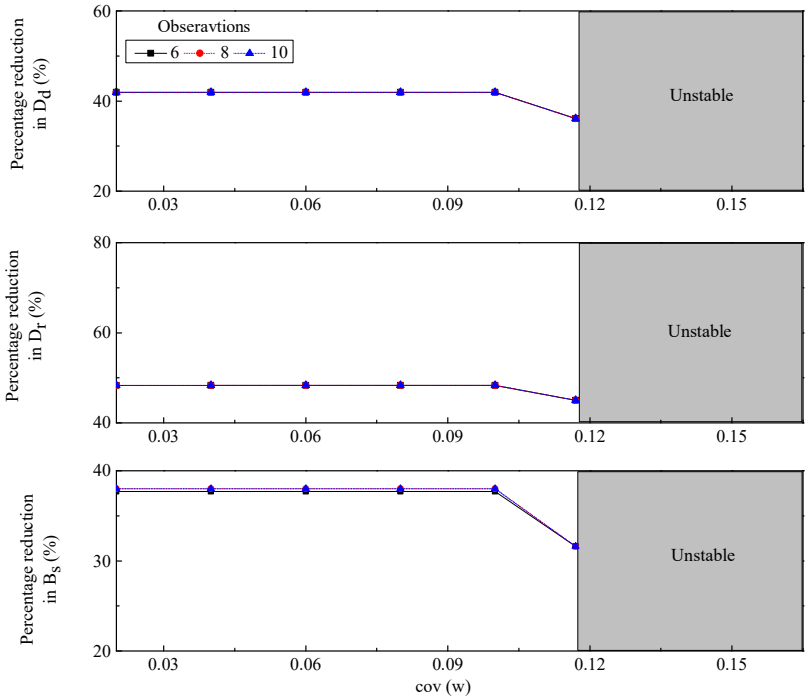

Figure 4-45: Variation of percentage reduction in different response quantities with covariance of excitation for SMCCl for broaband excitation at $vv^T = 10^{-8}$ m^2/sec^4 (VB-1)

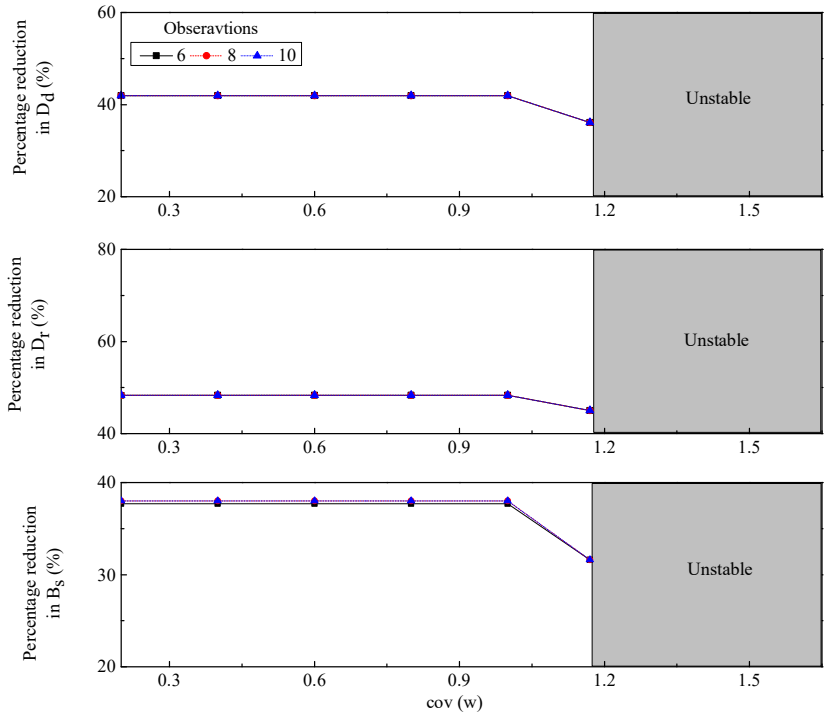

Figure 4-46: Variation of percentage reduction in different response quantities with covariance of excitation for SMCCl for broaband excitation at $vv^T = 10^{-7}$ m^2/sec^4 (VB-1)

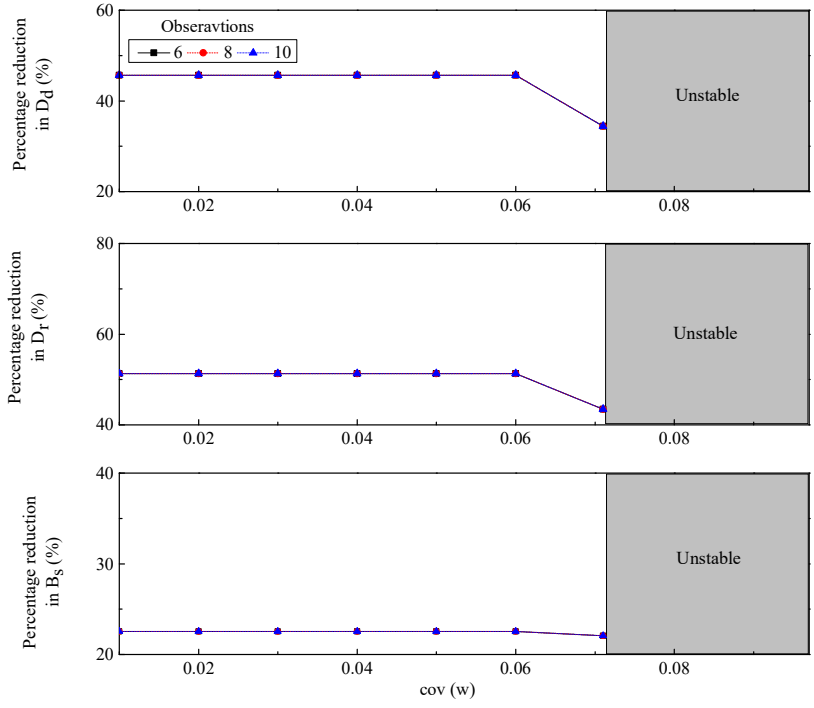

Figure 4-47: Variation of percentage reduction in different response quantities with covariance of excitation for white noise for SMCCl corresponding to broadband excitation at $vv^T = 10^{-9}$ m^2/sec^4 (VB-2)

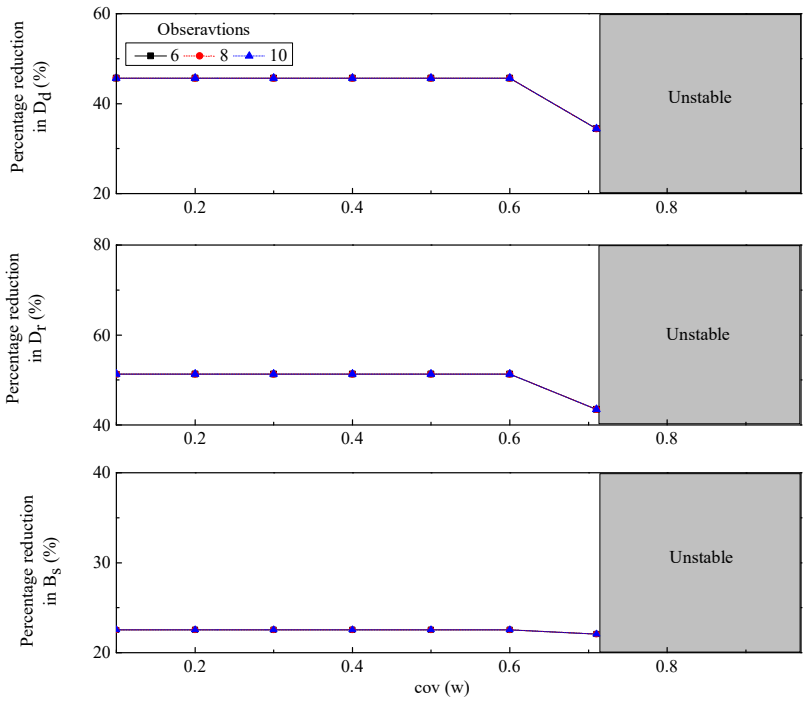

Figure 4-48: Variation of percentage reduction in different response quantities with covariance of excitation for white noise for SMCCl corresponding to broadband excitation at $vv^T = 10^{-8}$ m^2/sec^4 (VB-2)

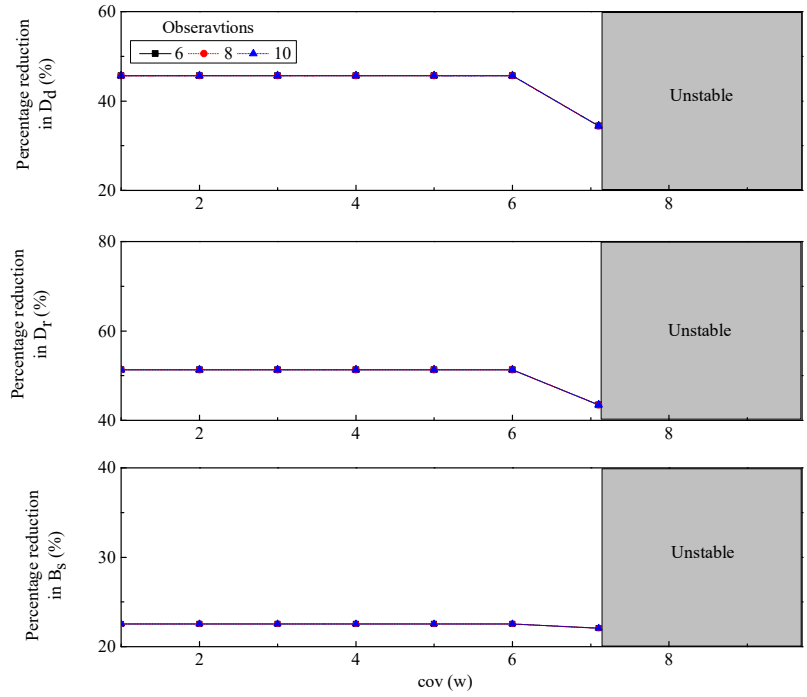

Figure 4-49: Variation of percentage reduction in different response quantities with covariance of excitation for white noise for SMCCl corresponding to broadband excitation at $vv^T = 10^{-7}$ m^2/sec^4 (VB-2)

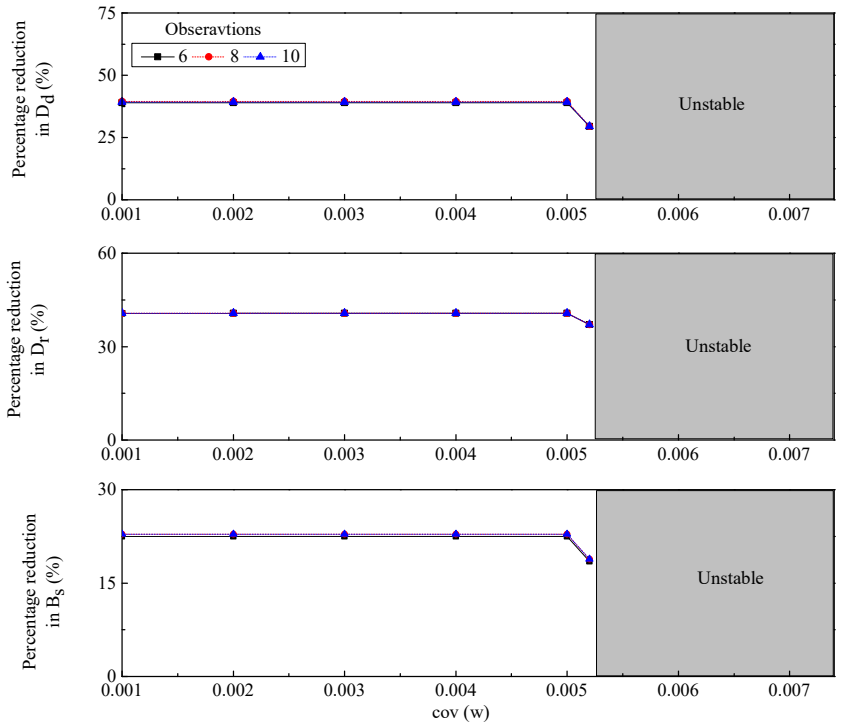

Figure 4-50: Variation of percentage reduction in different response quantities with covariance of excitation for SMCCl for narrowband excitation at $vv^T = 10^{-9}$ m^2/sec^4 (VB-1)

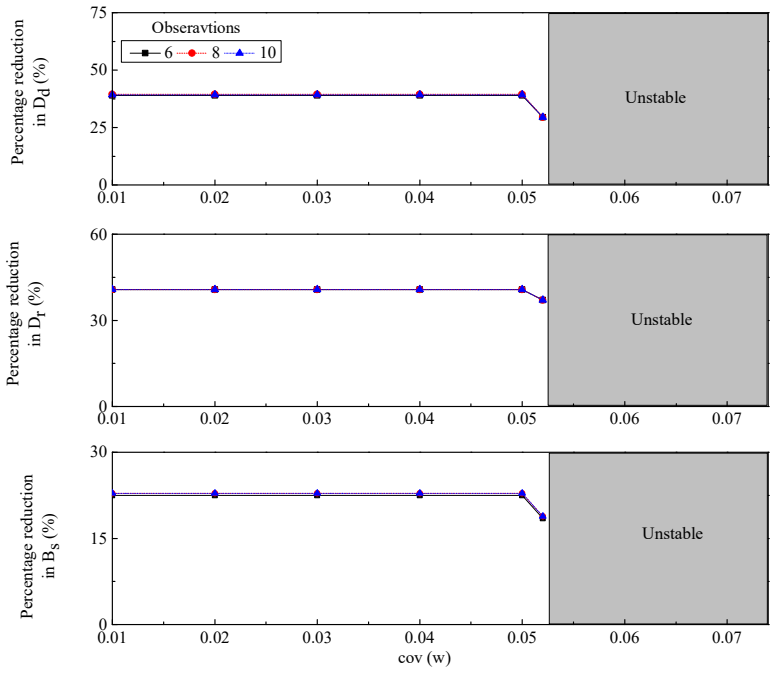

Figure 4-51: Variation of percentage reduction in different response quantities with covariance of excitation for SMCCl for narrowband excitation at $vv^T = 10^{-8}$ m^2/sec^4 (VB-1)

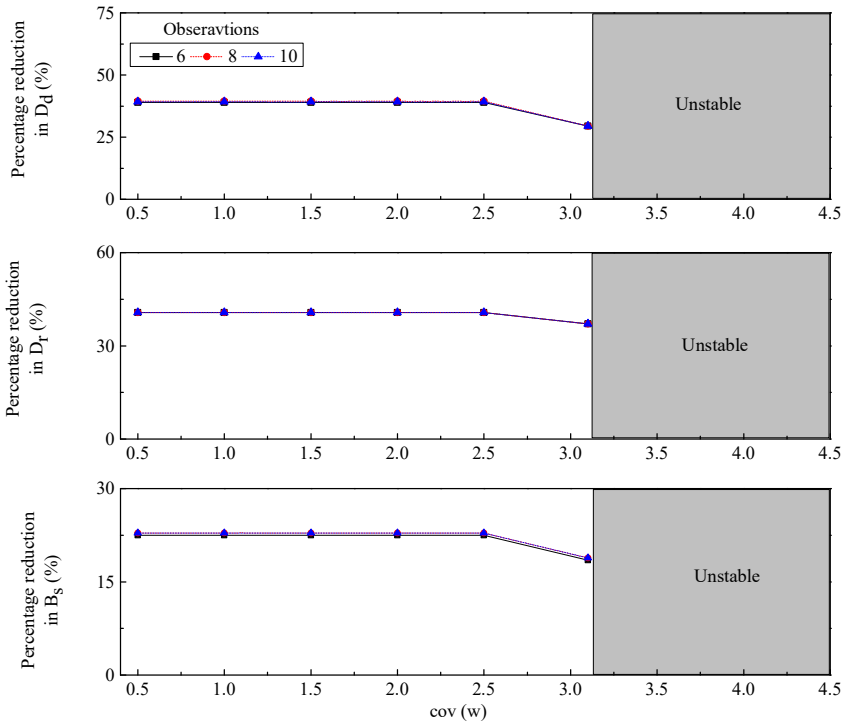

Figure 4-52: Variation of percentage reduction in different response quantities with covariance of excitation for SMCCl for narrowband excitation at $vv^T = 10^{-7}$ m^2/sec^4 (VB-1)

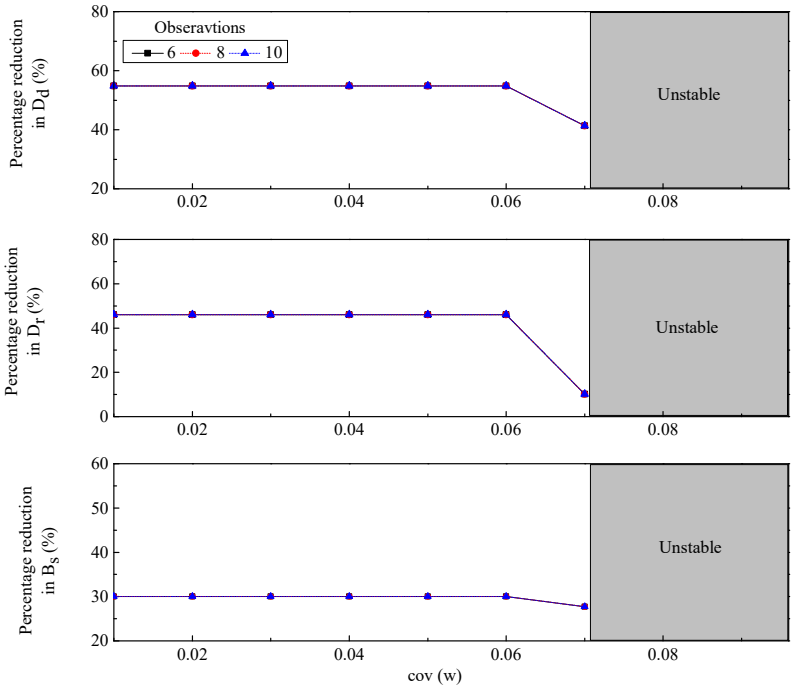

Figure 4-53: Variation of percentage reduction in different response quantities with covariance of excitation for white noise for SMCCl corresponding to narrowband excitation at $vv^T = 10^{-9}$ m^2/sec^4 (VB-2)

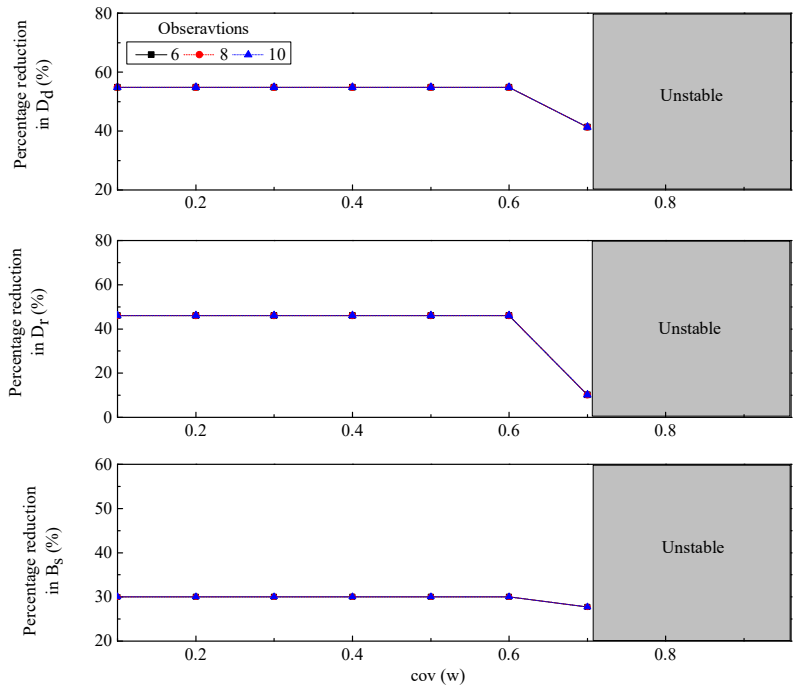

Figure 4-54: Variation of percentage reduction in different response quantities with covariance of excitation for white noise for SMCCl corresponding to narrowband excitation at $vv^T = 10^{-8}$ m^2/sec^4 (VB-2)

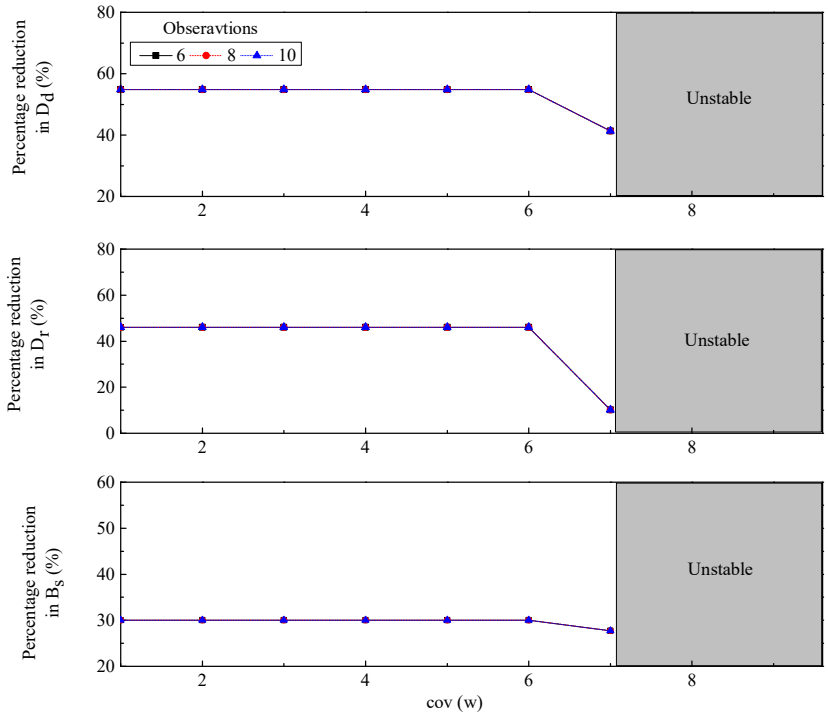

Figure 4-55: Variation of percentage reduction in different response quantities with covariance of excitation for white noise for SMCCl corresponding to narrowband excitation at $vv^T = 10^{-7}$ m^2/sec^4 (VB-2)

Chapter 5

Genetically Optimized Semi Active Control of Building Frames with Limited Number of MR Dampers and Sensors

5.1 Introduction

Optimum semi active control of structures using a limited number of MR dampers and sensors has a few distinct features compared to optimum active control using a limited number of actuators and sensors. The features include i) limitation of voltage which is applied to generate forces in MR Dampers, resulting in limitation on the maximum control force that could be applied on the structures, ii) need for good estimation of velocity from the measured state of the floors where MR dampers are located and iii) modelling the non-linear behaviour of MR dampers.

A very few studies are reported on the optimal placement of MR dampers. (Ok et al.,2008, Bharti et al. (2010), Uz and Hadi,2014). These studies do not consider the optimization problem as a combined problem of optimal placement of measurement sensors and MR dampers. Since forces generated in MR dampers primarily depend upon the velocities of the floors in which the MR dampers are located, correct estimation of the floor velocities from the measured states are required. Therefore, the measurement sensors should be located such that best estimate of the states of the floors where MR dampers are located can be made. This requires the optimization problem to be formulated as a combined problem of optimal placement of MR dampers and sensors.

The objective of the present study is to propose a computationally efficient control scheme, which is developed by considering both locations of MR dampers and measurement sensors as optimization variables for partially observed building frames under seismic excitation. In the proposed scheme, velocity sensors are invariably placed at the floors where the MR dampers are located and the rest of the sensors (velocity or displacement) are optimally placed in the frame. The reason for adopting this observation scheme is to capture the velocities of the floors where MR dampers are placed as accurately as possible in order to best estimate the damper forces using modified Bouc Wen model. Genetic Algorithm (GA) is employed for finding optimal locations of MR dampers and sensors. For optimization, a single objective GA with objective functions as base shear, top floor displacement and inter-story drift is used. The time histories of

voltage supplied to the MR dampers are determined using two standard control laws, namely, linear quadratic Gaussian (LQG) control with clipped optimal law and bang-bang control. Numerical results are obtained for two types of ground motions namely, (i) synthetically generated narrowband and broadband ground motions, and (ii) measured far field and near field ground motions. The results of the proposed scheme are compared with those of the optimal placement scheme of sensors (velocity or displacement) which are located in the frame without any consideration to the positions of the MR dampers. The efficiency of the optimal control scheme is evaluated by comparing its results with those of fully observed system using Linear Quadratic Regulator (LQR) with clipped optimal law.

5.2 Theory

Formulation of the optimum semi active control using a limited number of MR dampers and sensors is presented in two parts, namely, i) Semi active control using the MR damper for partially observed system and ii) Optimization procedure using genetic algorithm.

5.2.1 Semi active control using the MR damper

Semi active control strategies using MR dampers for partially observed system are developed based on separation principle, i.e. the state estimation and control algorithm are separately developed. Herein, clipped optimal law with LQR and LQG and Lypaunov control, i.e. bang-bang control is used for obtaining the control force in MR dampers. Modified Bouc-wen model is used to model the MR damper. The brief outline of modified Bouc-wen model, LQR, Kalman filter, clipped optimal law and bang bang control law has been given in Chapter 3

5.2.2 Optimization procedure using GA

Most of the earlier optimization techniques used for determining optimal locations of dampers/ actuators are based on gradient based techniques, weightage selection technique, iterative techniques and trial methods with trade off curves (Arbel,1981, Delorenzo,1990, Zhang and Soong,1992, Onoda and Hanawa,1993, Milman and Chu,1994, Wu et al.,1997, Brown et al.,1999, Shukla and Datta,1999, Singh and Moreschi,2001, Moita et al.,2006)]. The disadvantage of all the above stated optimization theories is that they treat the optimization problem as a continuous domain problem.

These approaches involve first solving the problem by treating all the variables as continuous and subsequently enumerating the neighbouring feasible discrete solutions to identify an optimum. In doing so, the original optimization problem is expanded into a large number of sub-optimization problems. Since the damper and sensor locations are spatially discrete, the optimization problem has discrete variables and therefore, cannot be solved using continuous domain optimization techniques. To overcome this difficulty, GA algorithm is used with integer representation (Dhingra and Lee,1995, Wongprasert and Symans,2004), to determine the optimal locations of sensors and dampers.

Four different characteristics of GA that differentiates it from the other optimization techniques are i) GA does not work with the parameters to be optimized rather it operates with a coding of the parameter set; ii) GA searches the genetic solution from a population of points and not around a single point; iii) that the GA does not use any derivative or auxiliary knowledge for optimization, rather it uses the knowledge of objective function and finally, iv) the GA uses probabilistic transition rules for the optimization instead of the deterministic rules used by other optimization algorithms.

As a consequence, GA has been widely used in finding optimal locations of sensors and control devices in active structural control. A brief outline of GA is included below for completeness. There is not much work reported in the literature for finding optimum locations of MR dampers and sensors in semi active control of structures. Use of GA for optimum control using limited number of MR dampers and sensors requires careful consideration of the following factors, which are duly considered in the formulation of the optimization problem.

i) Use of suitable sensors for state estimation

All three types of sensors, namely displacement, velocity and acceleration are now available for practical use. As a result, any type of sensors may be used for directly measuring any of the three response quantities mentioned above. Although acceleration sensors are popularly used for response measurements, the formulation for the partially observed state space equation deviates from the commonly used formulation incorporated in most software. For example, in the Simulink toolbox of Matlab, the **C** matrix in equation 3.10 uses displacements and velocities as the measured states of the system. Further, the standard conditions to be satisfied for controllability and stability conditions use **C** matrix in with displacements and velocities as measured quantities. Therefore, displacement and velocity sensors are used in the present study.

ii) Accurate estimation of the velocity of the floors where MR dampers are located

Since forces developed in the MR dampers are primarily governed by the velocities of the floors where the MR dampers are located, a good estimation of the velocities of those floors is crucial for best prediction of the control forces generated in MR dampers. Keeping this in view, two different strategies for the placement of sensors are adopted for the optimization problem, namely, the proposed strategy and the conventional strategy. In the proposed strategy (strategy1), out of the total number of sensors used, a number of velocity sensors equal to that of MR dampers are located at the floors where MR dampers are placed as necessary condition; the rest of the sensors are placed optimally in the structure. In the conventional strategy (strategy 2), no such constraint is imposed on the placement of sensors in the structure. Both strategies have their advantages and disadvantages which influence the subsequent factors considered in the optimization technique.

iii) Numbers of MR dampers and sensors used for effective application of GA

In the proposed strategy, the total numbers of variables for optimization is n_s ($n_s > n_m$) and in the second strategy, total number of variables for optimization is $n_m + n_s$ where, n_m and n_s are the numbers of MR dampers and sensors, respectively. Clearly, the first strategy is more effective from the point of the size of the variables used in the optimization problem. Since the efficiency of the GA is highly dependent on the number of variables used; the first strategy turns out to be computationally more efficient. In the second strategy, although the number of variables is more as compared to the first one, the optimization problem being an unconstrained becomes simpler.

iv) Stability and observability of the system as a whole during each trial in GA

In the present formulation, tournament selection, adaptive feasible mutation function and scattered crossover function are used. For each selection, the observability and controllability conditions (equation 3.12) are to be satisfied.

The matrix **A**, **B**, **E**, **C** and **D** should be such that the controllability condition is satisfied i.e.

i. The pair **A** and **E** is stabilizable.

ii. The pair **A** and **B** is stabilizable; pair **C** and **A** is detectable.

Further, the observability condition should also hold good

$$\begin{bmatrix} \mathbf{B} \\ \mathbf{D} \end{bmatrix} \mathbf{D}^{T} = \begin{bmatrix} \mathbf{O} \\ \mathbf{I} \end{bmatrix} \tag{5.1}$$

where **O** and **I** are the identity and null matrices.

For each selection, the **C** matrix change. The generated **C** matrix may not always satisfy the observability and controllability conditions. The GA terminates the current selection if such cases arise and attempts for new selections.

5.2.3 Genetic Algorithm

Genetic Algorithm (GA) is based on the Darwin's evolutionary theory of "survival of the fittest". GA is a metaheuristic optimization algorithm that is extensively used for solving the optimization problems in different fields of research. Robustness, parallel computation and constraint independence are some of the features of the GA that make it a one of the most powerful optimization technique in the engineering field. GA was initially proposed by Holland (Holland,1975a) and later developed by Goldberg (Goldberg and Holland,1988). Goldberg defined four different characteristics of GA that differentiates GA from the other optimization techniques. First is that the GA does not work with the parameters to be optimized rather it operates with a coding of the parameter set. Second is that the GA searches the genetic solution from a population of points and not around a single point. Third is that the GA does not use any derivative or auxiliary knowledge for optimization rather it uses the knowledge of the objective function and finally, the GA uses probabilistic transition rules for the optimization instead of the deterministic rules used by other optimization algorithms.

GA starts off by creating a random population of binary bits '0' and '1'. The binary bits are mapped to real design variables and are decoded as real values. The fitness of each decoded real value is evaluated using the objective (fitness) function. Based on the fitness values, the better individuals are selected and transferred into the mating pool for reproduction. The two mostly used selection algorithms are tournament selection and roulette wheel selection algorithms. Through the crossover and mutation operators, the selected individuals undergo reproduction. Hence, the genetic loop comprising of fitness

evaluation, selection, crossover and mutation is an iterative process and it continues until some convergence criteria is satisfied. The flow chart of the GA is given in Figure 5-1

Selection

The principle of "survival of fittest" state that the chance of survival is more for the individual which is well adapted to the environment. Keeping in view, the concept of natural selection was introduced in GA through the selection operator. Various kinds of selection mechanisms like tournament, roulette wheel, fitness proportionate selection, reward based selection etc. exist. For the study tournament selection is employed for selection.

In tournament selection, a few individuals are selected randomly from the current population. The selected individuals compete against each other and the one with the best fitness value is selected for crossover. The selection process continues until the size of selected individuals become equal to the size of initial population. Tournament selection is preferred over other selection algorithms because they can work on parallel architecture and are simple to code.

Crossover

In GA, the concept of reproduction through sexual mating is achieved through crossover operator. Different types of crossover mechanism like single point crossover, multi-point crossover (Eshelman et al.,1989), uniform crossover (Syswerda,1989) and cycle crossover (Oliver et al.,1987) exists. GA generally uses single point crossover. In a single point crossover, randomly two parents are selected from the population selected for mating. Then a crossover point is selected on both parents. All the data beyond the crossover point is swapped in both the parents, as a result, two new off springs are generated. Figure 5-2 shows an example of a single point crossover mechanism. Two binary strings 10100 and 00101are selected from the mating pool. The crossover point is randomly picked on the two points as shown in the figure. The data beyond the crossover point in both the parents is exchanged and the two new individuals 10101 and 00100 are generated.

Mutation

For a simple genetic algorithm, during the crossover operation no new information is created. During the continuous generation, the selected chromosomes become robust to

the problem environment and as a result, the chromosomes start resembling each other over time. Hence, it is a possibility that global optimized solution pre converges to local solution. To overcome the problem of premature convergence to local solution, a mutation operation is introduced. The mutation operation prevents the loss of gene information from the current population and sustains the diversity of gene information. The process of mutation is shown in Figure 5-3.

5.3 Numerical Study

For the study, the ten story linear shear type building frame of Chapter 3 is used. The building frame is subjected to the same two near field, two far field earthquakes and two artificially generated ground motions used in Chapter 3. Maximum numbers of MR dampers and sensors to be employed are taken as 5 and 7 respectively. The different combinations attempted in the study are shown in Table 5-1. In selecting the strategy for optimal placement of MR dampers and sensors to be adopted for the parametric study, the two strategies discussed in the theory are considered for comparison. Additionally, the results of the full state observation are studied side by side. Two control algorithms, i.e. clipped optimal control and bang bang control are used to obtain the control forces in MR dampers. The response quantities of interest are the top floor displacement (D_d), maximum inter story drift (D_r) and base shear (B_s).

For optimization using GA, several initial selections are tried, like any other optimization technique, in order to arrive at global maximum/minimum. Further, as in other numerical optimization techniques, GA may not converge to an optimum solution, especially satisfying controllability and observability conditions required in the present study. This problem is tackled by changing initial selections as mentioned above. For the numerical problem solved here, converged solutions are obtained in all cases. Because of the superiority of GA over classical optimization techniques claimed by other authors (Rao et al.,1991, Dhingra and Lee,1995, Furuya and Haftka,1995, Li et al.,2000, Abdullah et al.,2001, Ahlawat and Ramaswamy,2002, Li et al.,2004, Cha et al.,2013), no comparison of the results of GA with any other optimization technique is provided here.

5.3.1 Validation of the proposed control scheme

Experimental validation of the proposed control scheme is difficult to carry out as it requires huge experimental facility including the desired MR dampers. In the absence of the facilities required for preparing the experimental setup here, it is not possible to

validate the proposed method by experimental facility. However, numerical studies carried out using proposed scheme are compared with those of other similar theoretical problems. Two building frames of eleven (Mohajer Rahbari et al.,2013) and nine storey (Zahrai and Salehi,2014) are taken from the literature. In problem 1 (Mohajer Rahbari et al.,2013), three MR dampers are placed sequentially at the top three floors and the frame is subjected to the El Centro earthquake. In problem 2, two MR dampers are placed at the first and fifth floor and the frame is subjected to the Kobe earthquake. The time histories of voltage to be applied to the MR dampers are obtained using clipped optimal control along with LQR in the above studies. The same problems are solved with the help of the proposed control scheme using four velocity sensors. Table 5.2 compares the percentage reductions in top floor displacement, drift and acceleration obtained by the proposed control scheme with those reported in the literature (Mohajer Rahbari et al.,2013. Zahrai and Salehi,2014) It is seen from the table that the percentage reductions obtained by the proposed control scheme and other studies are of the same order. Note that in the other studies (Mohajer Rahbari et al.,2013. Zahrai and Salehi,2014), the problems are solved for fully observed state, whereas the proposed control scheme uses partially observed state with four measurement sensors. In spite of that, the agreement between the results of the two studies is excellent.

5.3.2 Selection of the control strategy

In selecting the strategy for optimal placement of MR dampers and sensors to be adopted for the parametric study, the two strategies discussed in the theory are considered for comparison. Additionally, the results of the full state observation are studied side by side. Two control algorithms, i.e. clipped optimal control and bang-bang control are used to obtain the control forces in MR dampers. The response quantities of interest are the top floor displacement (D_d), maximum inter story drift (D_r) and base shear (B_s). Response reductions for the three response quantities of interest for four real earthquakes and two artificial earthquakes are shown in Figs. 5.4-5 for bang bang. Similarly, response reductions for the three response quantities of interest for four real earthquakes and two artificial earthquakes for clipped optimal control algorithms are shown in Figs. 5.6-7. It is seen from the figures that both strategies 1 and 2 provide nearly the same reductions in responses quantities. For the full state observation, the percentage reductions in response quantities differ from those of strategies 1 and 2 by various degrees except for the El Centro earthquake. In certain cases, the percentage reductions for full state observation

are less as compared to strategies 1 and 2. This is the case because the full state observation provides actual states of the system which are different from the estimated states in strategies 1 and 2. Further, if clipped optimal law is adopted, the gain matrices for the two cases become different as the former uses LQR and the latter uses LQG. As a consequence, the time histories of the ideal control forces used as reference control forces to obtain the time history of on-off voltage are significantly different for the two cases (Figs. 5.8-9). However, because of limitation on maximum voltage which can be applied and clipping law, the time histories of actual MR damper forces generated are much lower than the reference control forces and do not differ significantly under some earthquakes (like El Centro and Spitak) for the two cases (ie., partially observed and fully observed cases). While for the bang-bang control, only the first factor (limitation on maximum voltage) influences, for the clipped optimal control both factors influence the time histories of control force generated in MR dampers. Typical time histories of control force generated in the MR damper located in the first floor are depicted in Figs. 10-11 which show that maximum control forces are almost the same for all cases for El Centro and Spitak earthquakes. As a result, the percentage reductions in response quantities are nearly the same for partially observed (strategies 1-2) and fully observed cases for these two earthquakes.

For further parametric study, strategy 1 is selected since the number of variables for optimization is less in strategy 1 as compared to strategy 2, thus requiring less computational effort. Further, the relative efficiency of strategy 1 is evaluated by finding the number of generations (iterations) required by GA for each objective function and compared with those for strategy 2 for all real earthquakes. The comparison is shown in Figs. 5.12-13. It is seen from the figures that the number of generations required by strategy 1 is almost half of that required for strategy 2. The parametric study investigates effects of i) the number of MR dampers and sensors, ii) placement of dampers and sensors, iii) algorithms used (clipped and bang bang) and iv) types of earthquakes on the reductions of response quantities of interest.

5.3.3 Optimum number of MR dampers

Figures 5.14-19 show the comparison between maximum percentage reductions in response quantities of interest for different numbers of MR dampers used for El Cenro, Victoria, Kobe, Spitak and artificially generated (broadband and narrowband) earthquakes for the two control algorithms used. It is observed from the figures that the

percentage reduction in different response quantities increases as the number of MR damper increases except for Kobe earthquake, for top floor displacement, the percentage reduction decreases beyond three MR dampers. However, beyond four MR dampers change in the percentage reduction is negligible for all earthquakes considered in the study. Further, even with three MR dampers results are close to those found with four MR dampers. For the above study, MR dampers and sensors are located optimally using strategy 1 and seven sensors (i.e. the maximum number of sensors) are used.

5.3.4 Optimum location of MR dampers

Optimum location of MR dampers for different cases is found to be sequential placement of MR dampers beginning from the first floor. The optimal locations remain the same for all types of earthquakes and for the two control algorithms.

5.3.5 Optimum number of sensors

Figures 5.20-37 show the percentage reductions obtained in different response quantities for two, three and four MR dampers for El Cenro, Victoria, Kobe, Spitak and artificially generated (broadband and narrowband) earthquakes for the two control algorithms used. It is seen from the figures that the number of dampers plus one is the optimal number of sensors for all response quantities of interest.

5.3.6 Optimum location of sensors

Tables 5.3-8 show optimal sensor locations for two, three and four MR dampers for bang bang and clipped optimal control algorithms for different earthquakes. Note that the numbers in the tables refer to displacement or velocity sensors placed at different floor levels. For example, 7 refer to displacement sensor placed at the seventh storey; 15 refer to velocity sensor placed at fifth storey. A pictorial view of optimum locations for the case of four sensors used for El Centro earthquake is shown in Figure 5.38 as illustration. It is seen from the tables that optimal sensor locations generally vary with the earthquake, the response quantity of interest and the control algorithm used. Hence, no unique solution for optimal sensor location exists.

5.3.7 Performance and limitation of the control algorithms used

From figures, it is evident that clipped optimal control algorithm provides a higher percentage reduction in response quantities. However, the difference between the performances of the two algorithms is not very significant because of the limitation of the

maximum voltage to be applied to generate actual MR damper force for controlling the structure. As mentioned in the theory, the time history of the on-off voltages for generating the MR damper control force is obtained either by clipping (clipped optimal control), the reference ideal force obtained using LQG/LQR algorithm or by using Heaviside function in the case of bang bang control. Thus, the control laws do not allow full control force to be developed in the MR dampers. Figures 5.8-9 show the time histories of ideal control force obtained using LQR/LQG algorithm for El Centro and Spitak earthquakes. This time histories of control forces are distinctly different from the time histories of control force developed in the damper. From the figures, it is seen that actual control forces developed in the MR damper are significantly lower than the actual time histories of control forces obtained by LQG/LQR algorithms. Because of these reasons, optimum control of responses using MR dampers is different and less as compared to active control using actuators. Further, the difference between the reductions of responses obtained by different algorithms is not found to be very large because of the limitation on maximum voltage that can be applied to MR dampers.

5.4 Conclusions

A computationally efficient optimal solution for semi active control of a partially observed ten story building frame using a limited number of MR dampers and measurement sensors is presented. Solutions are obtained for both simulated and real earthquake records. The optimal placement of the sensors and MR dampers is obtained by genetic algorithm. The Kalman filter is used for estimating the full state from the measured responses. Two control algorithms are employed for obtaining the time histories of voltages to be applied to the MR dampers namely, clipped optimal control and bang-bang control. Control of three response quantities is considered in the study, namely, top floor displacement, maximum inter storey drift and base shear. The results of the numerical study lead to the following conclusions:

- Optimum response reductions can be achieved by using a limited number of sensors and MR dampers.
- As the number of MR dampers is increased beyond a certain value, the response reduction tends to be stationary. For the ten-storey frame, the optimum number of MR dampers is found to be four for all earthquakes, all response quantities of interest and for both control algorithms.

- Optimum locations of sensors vary with earthquakes, response quantities of interest and control algorithms used.
- The proposed strategy of placement of sensors is computationally efficient and is recommended for optimum control using MR dampers; the optimum number of sensors is found to be equal to the number of MR dampers plus one.
- Optimum response reductions vary with the earthquakes; for some earthquakes, they could be very less. In the present study, a minimum reduction of responses is obtained for Kobe earthquake.
- Due to the limitation of maximum command voltage that can be applied to the MR dampers, the ideal control force predicted by LQR/LQG cannot be generated in the dampers and no significant difference is found between the response reductions obtained by different control algorithms.

Table 5-1: Various combinations of MR dampers and sensors used in the study

Maxm. No. (MR dampers)	**Maxm. No. (sensors)**	**Scheme (Strategy)**	**Control Algorithm**
3	5	Both	Both
2	2, 3, 4, 5, 6	First	Both
3	3, 4, 5, 6	First	Both
4	4,5,6	First	Both
5	5,6,7	First	Both

Table 5-2: Comparison of percentage reductions in responses obtained by the proposed control scheme and other studies

Response quantity	**Percentage reduction in problem 1**	**Percentage reduction by proposed scheme**	**Percentage reduction in problem 2**	**Percentage reduction by proposed scheme**
Top floor displacement	38.4%	42%		
Drift	38%	41%	21 %	20%
Acceleration	17.1%	20 %	15%	13%

Table 5-3: Optimum sensor locations for bang bang control algorithm for 2 MR dampers for different earthquakes

		3 sensors	4 sensors	5 sensors	6 sensors
Top floor displacement	El Centro	10 11 12	10 11 12 13	9 10 11 12 13	8 9 10 11 12 13
	Victoria	10 11 12	9 10 11 12	8 9 10 11 12	7 8 9 10 11 12
	Kobe	10 11 12	10 11 12 13	9 10 11 12 13	8 9 10 11 12 13
	Spitak	3 11 12	3 4 11 12	3 4 5 11 12	3 4 5 6 11 12
	Broadband	3 11 12	3 4 11 12	3 4 5 11 12	3 4 5 6 11 12
	Narrowband	10 11 12	10 11 12 13	9 10 11 12 13	8 9 10 11 12 13
Maximum drift	El Centro	10 11 12	10 11 12 13	9 10 11 12 13	8 9 10 11 12 13
	Victoria	10 11 12	9 10 11 12	8 9 10 11 12	7 8 9 10 11 12
	Kobe	11 12 14	10 11 12 14	9 10 11 12 14	8 9 10 11 12 14
	Spitak	3 11 12	3 4 11 12	3 4 5 11 12	3 4 5 6 11 12
	Broadband	10 11 12	10 11 12 13	9 10 11 12 13	8 9 10 11 12 13
	Narrowband	3 11 12	3 4 11 12	3 4 5 11 12	3 4 5 6 11 12
Base Shear	El Centro	10 11 12	10 11 12 13	9 10 11 12 13	8 9 10 11 12 13
	Victoria	10 11 12	9 10 11 12	8 9 10 11 12	7 8 9 10 11 12
	Kobe	10 11 12	10 11 12 13	9 10 11 12 13	8 9 10 11 12 13
	Spitak	3 11 12	3 4 11 12	3 4 5 11 12	3 4 5 6 11 12
	Broadband	10 11 12	9 10 11 12	8 9 10 11 12	7 8 9 10 11 12
	Narrowband	3 11 12	3 4 11 12	3 4 5 11 12	3 4 5 6 11 12

Table 5-4: Optimum sensor locations for clipped optimal control using LQG (LQGCl) algorithm for 2 MR dampers for different earthquakes

		3 sensors	4 sensors	5 sensors	6 sensors
Top floor displacement	El Centro	11 12 13	4 11 12 13	4 5 11 12 13	5 6 11 12 13 14
	Victoria	11 12 14	5 11 12 14	5 6 11 12 14	5 6 7 11 12 14
	Kobe	11 12 13	4 11 12 13	4 5 11 12 13	4 5 6 11 12 13
	Spitak	6 11 12	5 6 11 12	4 5 6 11 12	3 4 5 6 11 12
	Broadband	3 11 12	3 4 11 12	3 4 5 11 12	3 4 5 6 11 12
	Narrowband	10 11 12	9 10 11 12	8 9 10 11 12	7 8 9 10 11 12
Maximum drift	El Centro	11 12 17	4 11 12 13	4 5 11 12 13	5 6 11 12 13 14
	Victoria	11 12 20	11 12 13 20	11 12 13 14 20	11 12 13 14 15 20
	Kobe	11 12 17	9 10 11 12	8 9 10 11 12	7 8 9 10 11 12
	Spitak	11 12 17	11 12 13 18	9 10 11 12 17	11 12 13 14 15 18
	Broadband	11 12 17	11 12 13 17	11 12 13 14 17	11 12 13 14 15 17
	Narrowband	11 12 13	10 11 12 13	9 10 11 12 13	8 9 10 11 12 13
Base Shear	El Centro	11 12 14	11 12 13 14	11 12 13 14 15	11 12 13 14 15 16
	Victoria	11 12 17	11 12 13 17	11 12 13 14 17	11 12 13 14 15 17
	Kobe	11 12 13	4 11 12 13	4 5 11 12 13	4 5 6 11 12 13
	Spitak	10 11 12	10 11 12 13	8 9 11 12 13	8 9 10 11 12 13
	Broadband	11 12 13	10 11 12 13	9 10 11 12 13	8 9 10 11 12 13
	Narrowband	11 12 13	4 11 12 13	4 5 11 12 13	4 5 6 11 12 13

Table 5-5: Optimum sensor locations for bang bang control algorithm for 3 MR dampers for different earthquakes

		4 sensors	5 sensors	6 sensors
Top floor displacement	El Centro	4 11 12 13	4 5 11 12 13	4 5 6 11 12 13
	Victoria	4 11 12 13	4 5 11 12 13	4 5 6 11 12 13
	Kobe	4 11 12 13	4 5 11 12 13	4 5 6 11 12 13
	Spitak	4 11 12 13	4 5 11 12 13	4 5 6 11 12 13
	Broadband	11 12 13 14	11 12 13 14 15	11 12 13 14 15 16
	Narrowband	11 12 13 14	5 11 12 13 14	5 6 11 12 13 14
Maximum drift	El Centro	4 11 12 13	4 5 11 12 13	4 5 6 11 12 13
	Victoria	4 11 12 13	4 5 11 12 13	4 5 6 11 12 13
	Kobe	4 11 12 13	4 5 11 12 13	4 5 6 11 12 13
	Spitak	4 11 12 13	4 5 11 12 13	4 5 6 11 12 13
	Broadband	11 12 13 14	5 11 12 13 14	5 6 11 12 13 14
	Narrowband	11 12 13 14	11 12 13 14 15	11 12 13 14 15 16
Base Shear	El Centro	11 12 13 17	11 12 13 14 17	11 12 13 14 15 17
	Victoria	4 11 12 13	4 5 11 12 13	4 5 6 11 12 13
	Kobe	11 12 13 17	11 12 13 14 17	11 12 13 14 16 17
	Spitak	4 11 12 13	4 5 11 12 13	4 5 6 11 12 13
	Broadband	11 12 13 17	11 12 13 14 17	11 12 13 14 15 17
	Narrowband	11 12 13 17	11 12 13 14 17	11 12 13 14 15 17

Table 5-6: Optimum sensor locations for clipped optimal algorithm for 3 MR dampers for different earthquakes

		4 sensors	5 sensors	6 sensors
Top floor displacement	El Centro	11 12 13 17	11 12 13 14 17	11 12 13 14 15 17
	Victoria	11 12 13 17	11 12 13 14 17	11 12 13 14 15 17
	Kobe	11 12 13 14	5 11 12 13 14	5 6 11 12 13 14
	Spitak	11 12 13 14	5 11 12 13 14	5 6 11 12 13 14
	Broadband	11 12 13 14	11 12 13 14 15	11 12 13 14 15 16
	Narrowband	11 12 13 14	5 11 12 13 14	5 6 11 12 13 14
Maximum drift	El Centro	11 12 13 17	11 12 13 14 17	11 12 13 14 15 17
	Victoria	11 12 13 17	11 12 13 14 17	11 12 13 14 15 17
	Kobe	11 12 13 17	11 12 13 14 17	11 12 13 14 15 17
	Spitak	11 12 13 17	11 12 13 14 17	11 12 13 14 15 17
	Broadband	11 12 13 14	5 11 12 13 14	5 6 11 12 13 14
	Narrowband	11 12 13 14	11 12 13 14 15	11 12 13 14 15 16
Base Shear	El Centro	11 12 13 17	11 12 13 14 17	11 12 13 14 15 17
	Victoria	11 12 13 14	5 11 12 13 14	5 6 11 12 13 14
	Kobe	11 12 13 14	5 11 12 13 14	5 6 11 12 13 14
	Spitak	11 12 13 14	5 11 12 13 14	5 6 11 12 13 14
	Broadband	11 12 13 17	11 12 13 14 17	11 12 13 14 15 17
	Narrowband	11 12 13 17	11 12 13 14 17	11 12 13 14 15 17

Table 5-7: Optimum sensor locations for bang bang algorithm for 4 MR dampers for different earthquakes

		5 sensors	6 sensors
Top floor displacement	El Centro	5 11 12 13 14	5 6 11 12 13 14
	Victoria	5 11 12 13 14	5 6 11 12 13 14
	Kobe	5 11 12 13 14	5 6 11 12 13 14
	Spitak	5 11 12 13 14	5 6 11 12 13 14
	Broadband	10 11 12 13 14	9 10 11 12 13 14
	Narrowband	10 11 12 13 14	9 10 11 12 13 14
Maximum drift	El Centro	5 11 12 13 14	5 6 11 12 13 14
	Victoria	5 11 12 13 14	5 6 11 12 13 14
	Kobe	10 11 12 13 14	9 10 11 12 13 14
	Spitak	10 11 12 13 14	9 10 11 12 13 14
	Broadband	10 11 12 13 14	9 10 11 12 13 14
	Narrowband	5 11 12 13 14	5 6 11 12 13 14
Base Shear	El Centro	11 12 13 14 15	11 12 13 14 15 17
	Victoria	11 12 13 14 15	5 6 11 12 13 14
	Kobe	11 12 13 14 17	11 12 13 14 15 17
	Spitak	5 11 12 13 14	5 6 11 12 13 14
	Broadband	10 11 12 13 14	9 10 11 12 13 14
	Narrowband	10 11 12 13 14	10 11 12 13 14 15

Table 5-8: Optimum sensor locations for clipped optimal algorithm for 4 MR dampers for different earthquakes

		5 sensors	6 sensors
Top floor displacement	El Centro	11 12 13 14 17	11 12 13 14 15 17
	Victoria	11 12 13 14 15	11 12 13 14 15 16
	Kobe	11 12 13 14 15	6 11 12 13 14 15
	Spitak	11 12 13 14 15	6 11 12 13 14 15
	Broadband	11 12 13 14 17	11 12 13 14 15 17
	Narrowband	11 12 13 14 17	11 12 13 14 15 17
Maximum drift	El Centro	11 12 13 14 17	11 12 13 14 15 17
	Victoria	11 12 13 14 20	11 12 13 14 15 20
	Kobe	11 12 13 14 15	6 11 12 13 14 15
	Spitak	11 12 13 14 17	11 12 13 14 15 17
	Broadband	11 12 13 14 15	11 12 13 14 15 16
	Narrowband	11 12 13 14 15	11 12 13 14 15 16
Base Shear	El Centro	11 12 13 14 17	11 12 13 14 15 17
	Victoria	5 11 12 13 14	5 6 11 12 13 14
	Kobe	10 11 12 13 14	10 11 12 13 14 15
	Spitak	11 12 13 14 15	6 11 12 13 14 15
	Broadband	11 12 13 14 17	11 12 13 14 15 17
	Narrowband	11 12 13 14 17	11 12 13 14 15 17

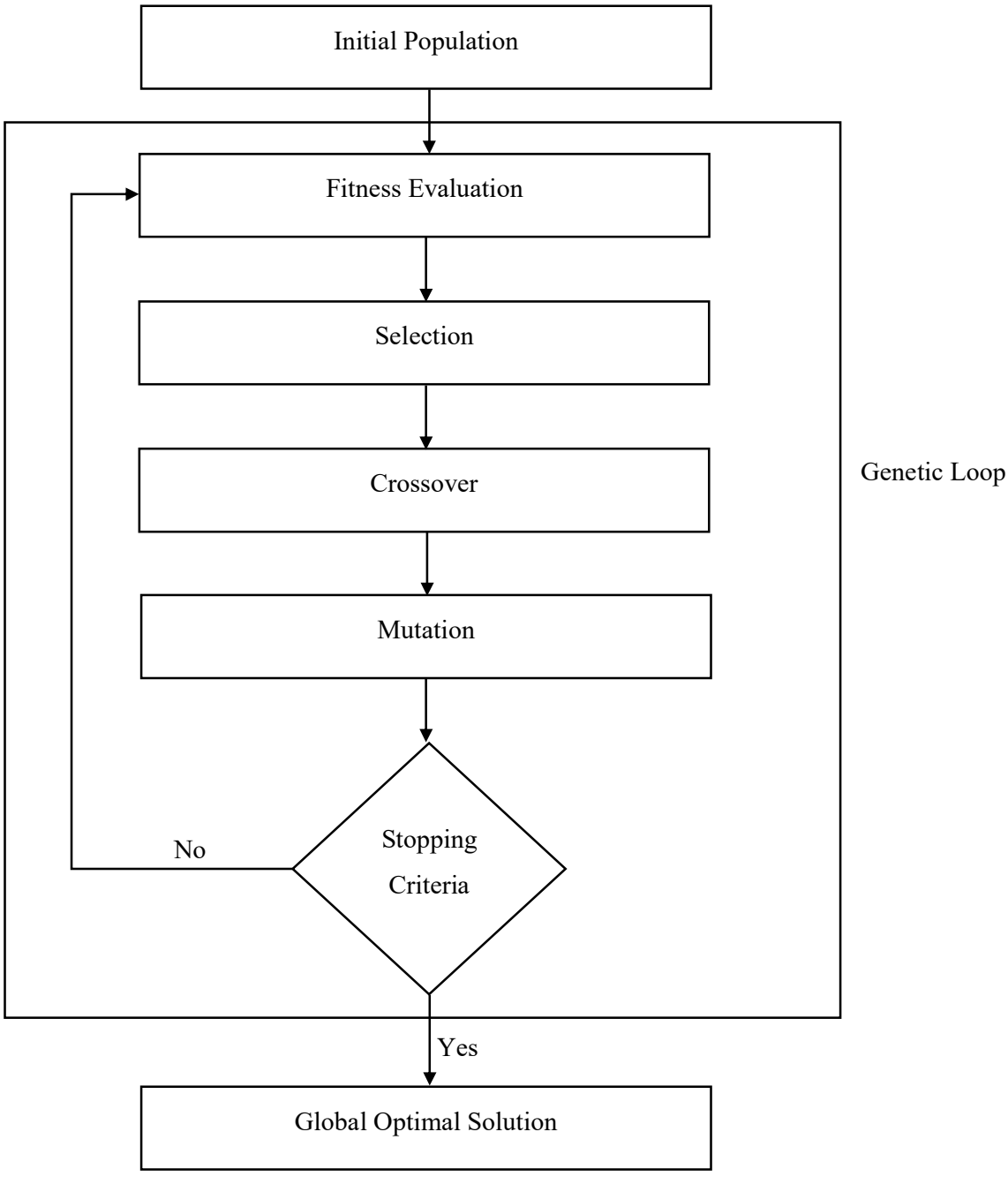

Figure 5-1: Flow chart of Genetic Algorithm

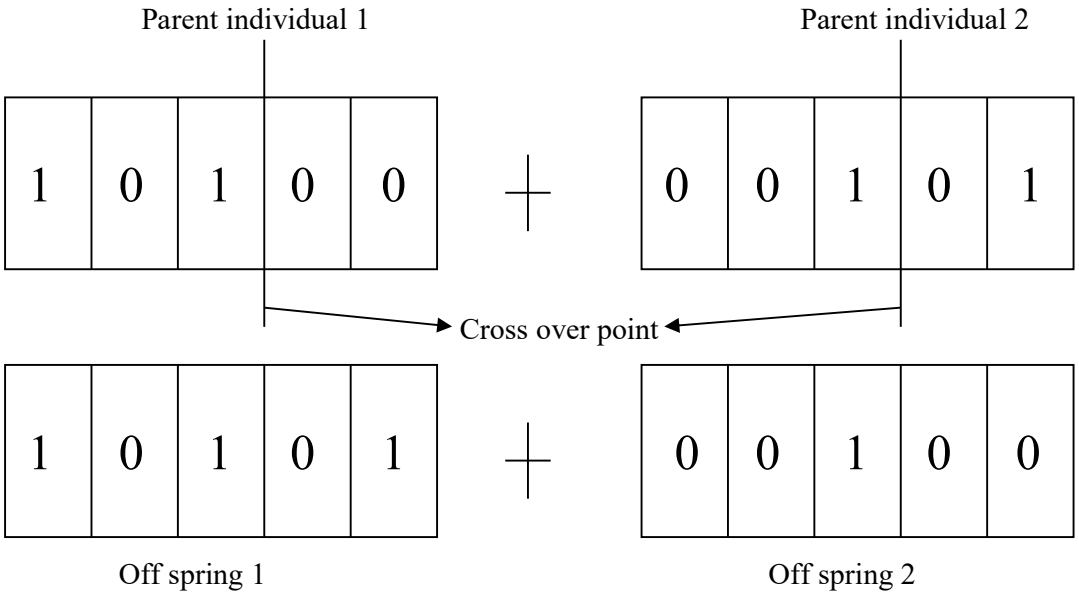

Figure 5-2: Flow chart for single point crossover

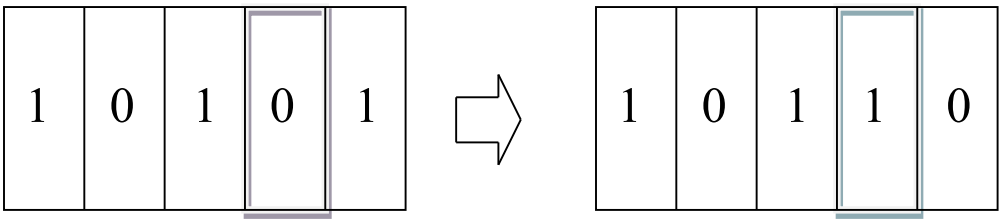

Figure 5-3: Mutation operation

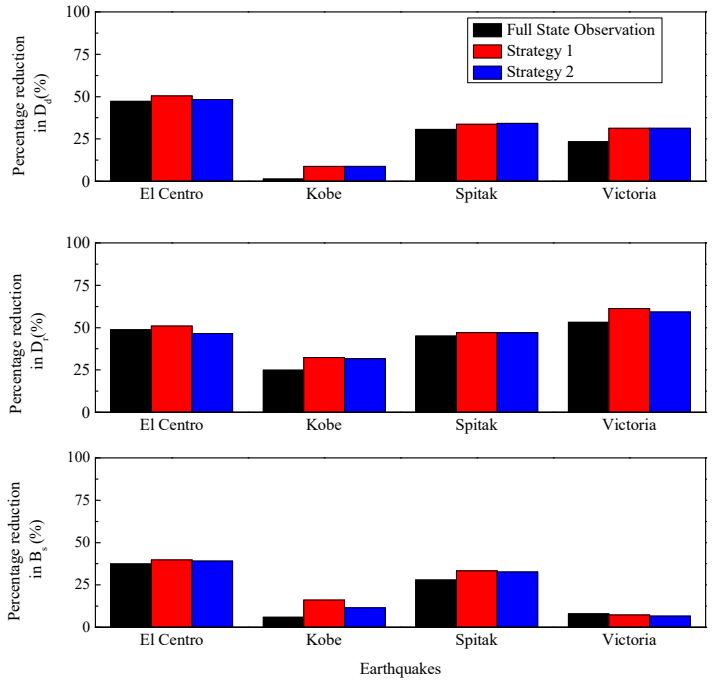

Figure 5-4: Comparison of percentage reductions in response quantities obtained by bang bang algorithm for optimally placed three MR dampers and five sensors for real earthquake records

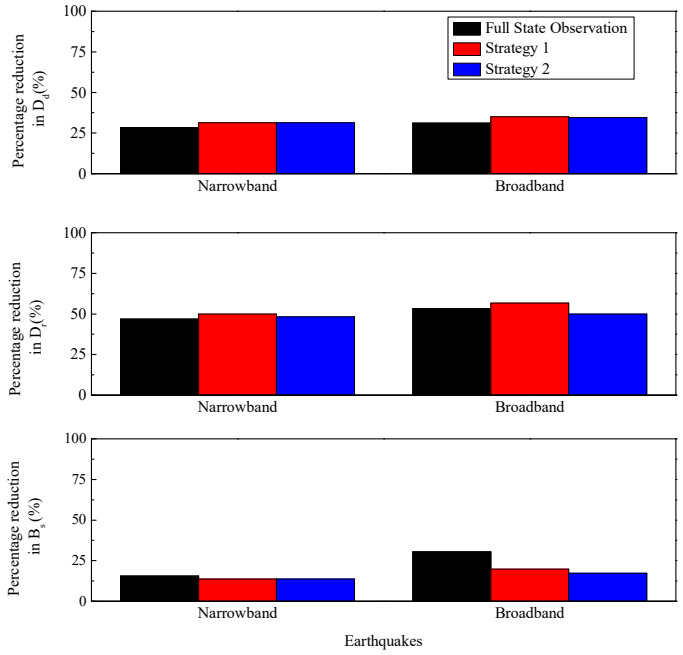

Figure 5-5: Comparison of percentage reductions in response quantities obtained by bang bang algorithm for optimally placed three MR dampers and five sensors for artificially generated earthquakes

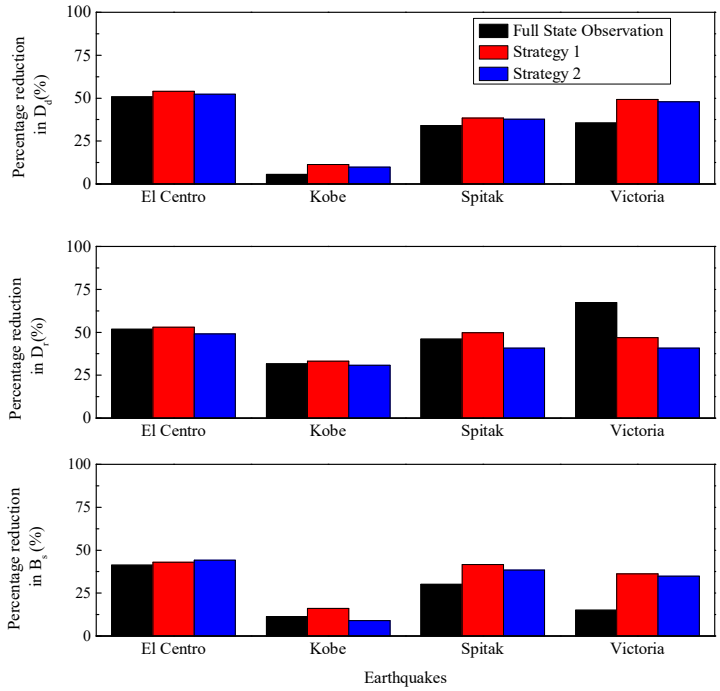

Figure 5-6: Comparison of percentage reductions in response quantities obtained by clipped on algorithm for optimally placed three MR dampers and five sensors for real earthquake records

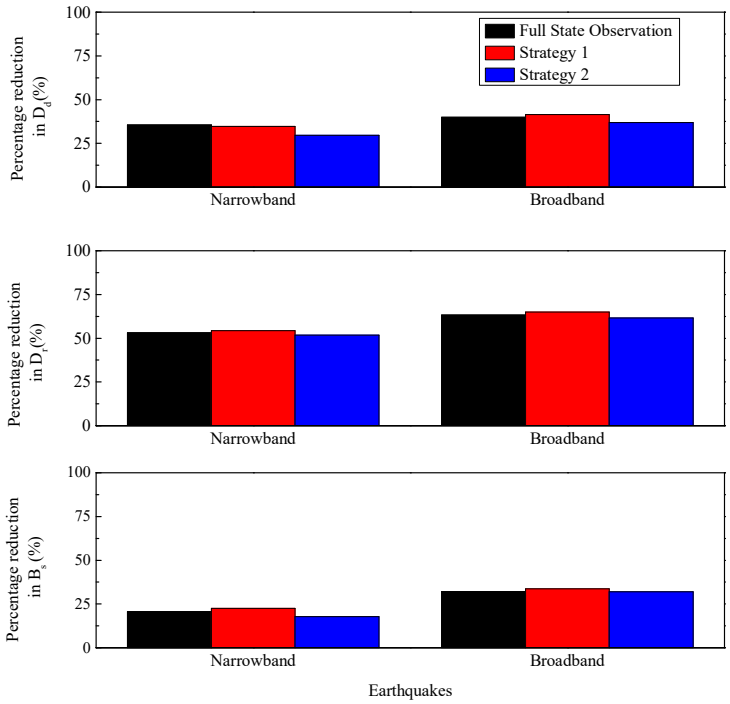

Figure 5-7: Comparison of percentage reductions in response quantities obtained by clipped on algorithm for optimally placed three MR dampers and five sensors for artificially generated records

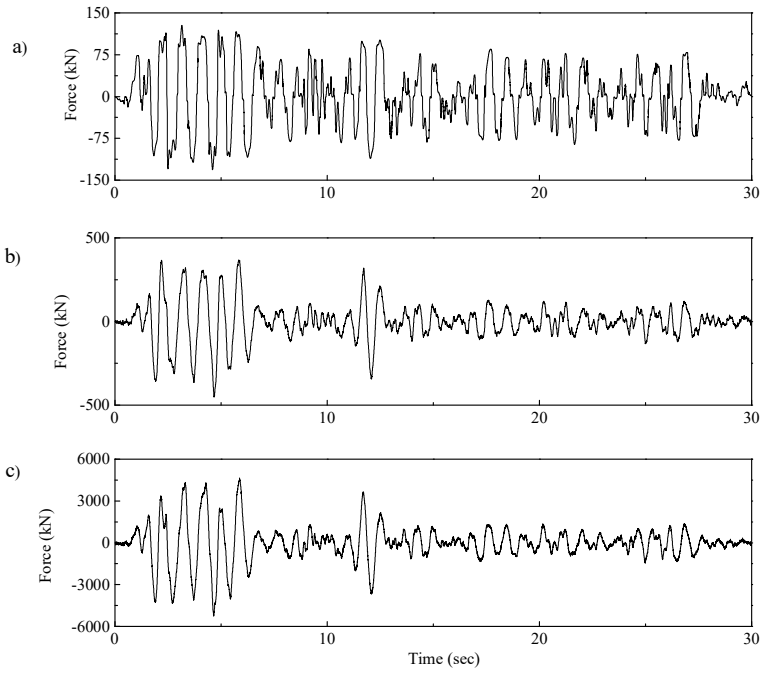

Figure 5-8: Comparison between control forces a) developed in MR damper at first storey with strategy 1; b) obtained by LQG, and c) obtained by LQR for El Centro earthquake

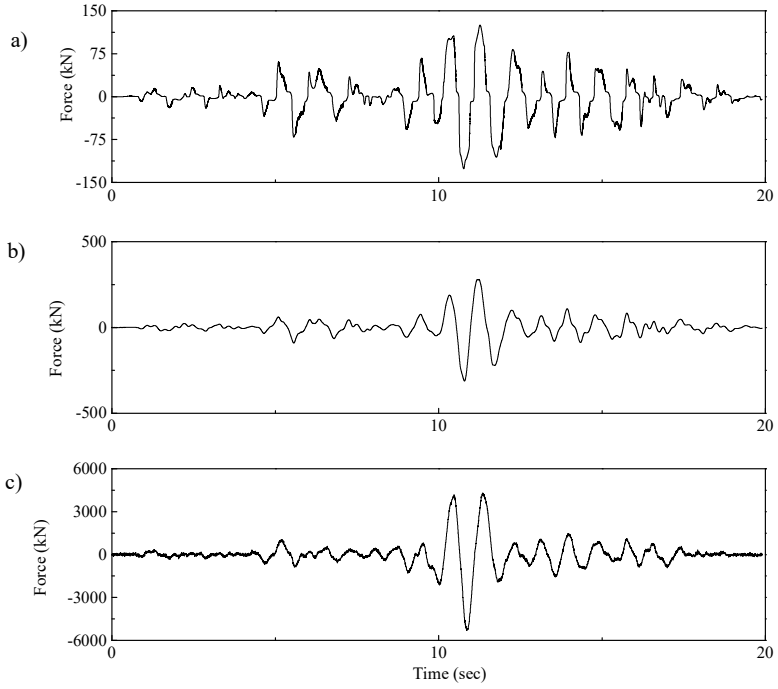

Figure 5-9: Comparison between control forces a) developed in MR damper at the first storey with strategy 1, b) obtained by LQG, and c) obtained by LQR for Spitak earthquake

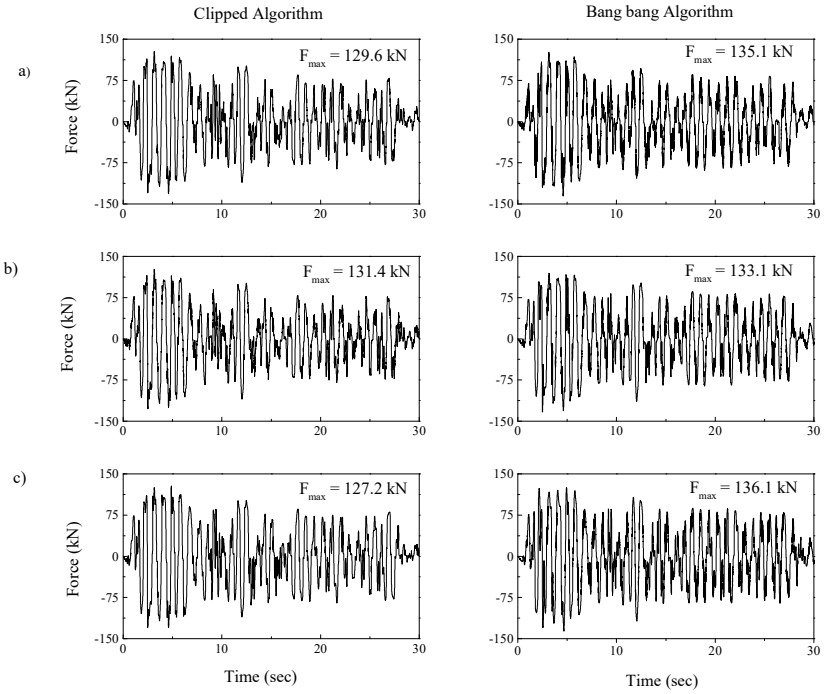

Figure 5-10: Comparison between control forces obtained through optimally placed three MR dampers and five sensors, a) full state observation b) strategy 1 and c) strategy 2 for El Centro earthquake

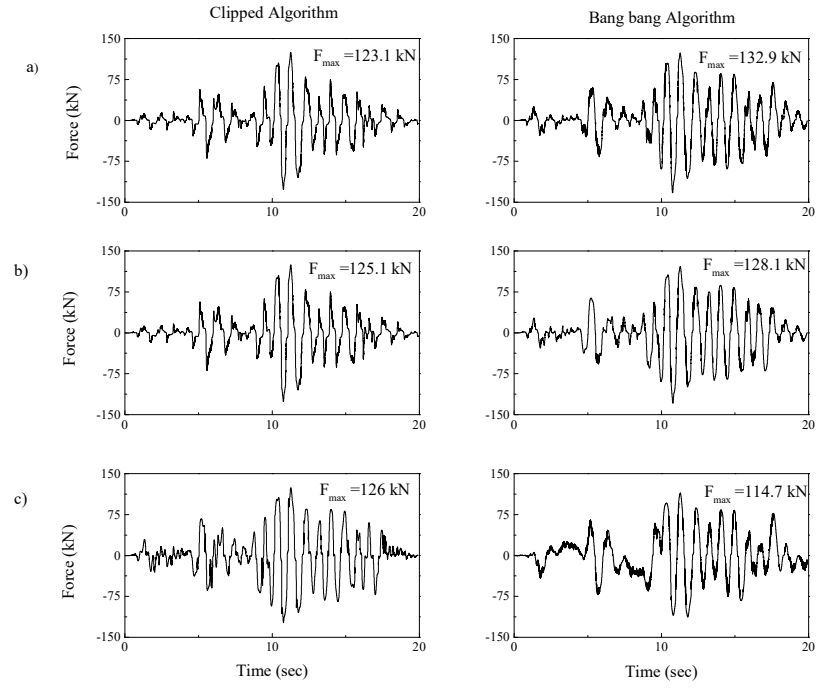

Figure 5-11: Comparison between control forces obtained through optimally placed three MR dampers and five sensors, a) full state observation b) strategy 1 and c) strategy 2 for Spitak earthquake

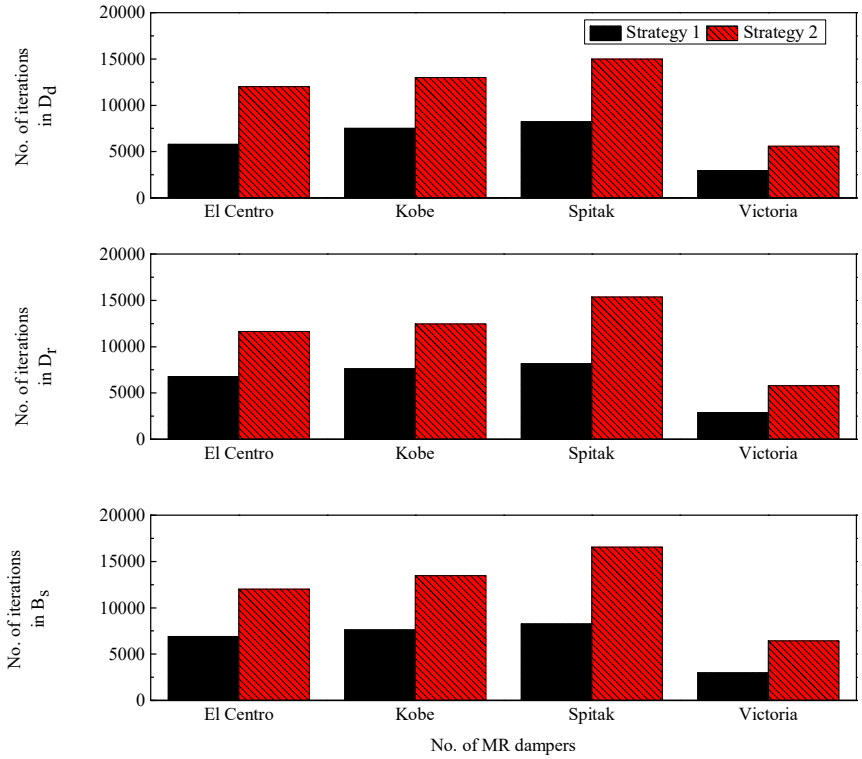

Figure 5-12: Number of iterations (generations) required by GA for each objective function for strategy 1 and 2 (clipped optimal control)

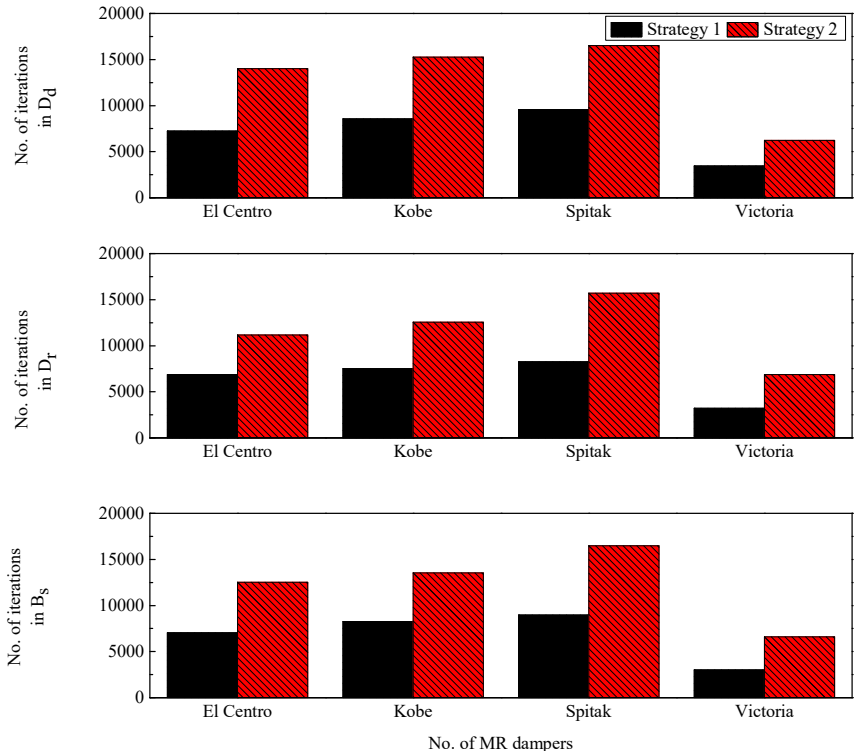

Figure 5-13: Number of iterations (generations) required by GA for each objective function for strategy 1 and 2 (bang bang control)

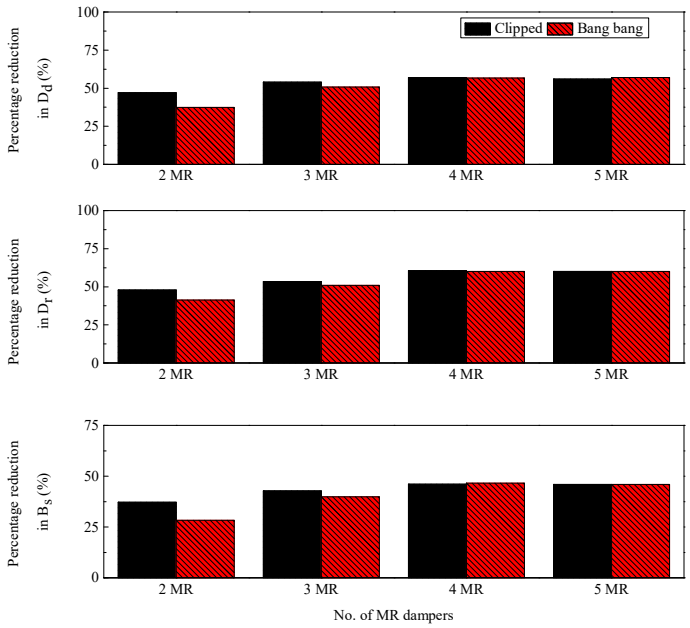

Figure 5-14: Comparison between maximum percentage reductions obtained by using different numbers of MR dampers for Victoria earthquake

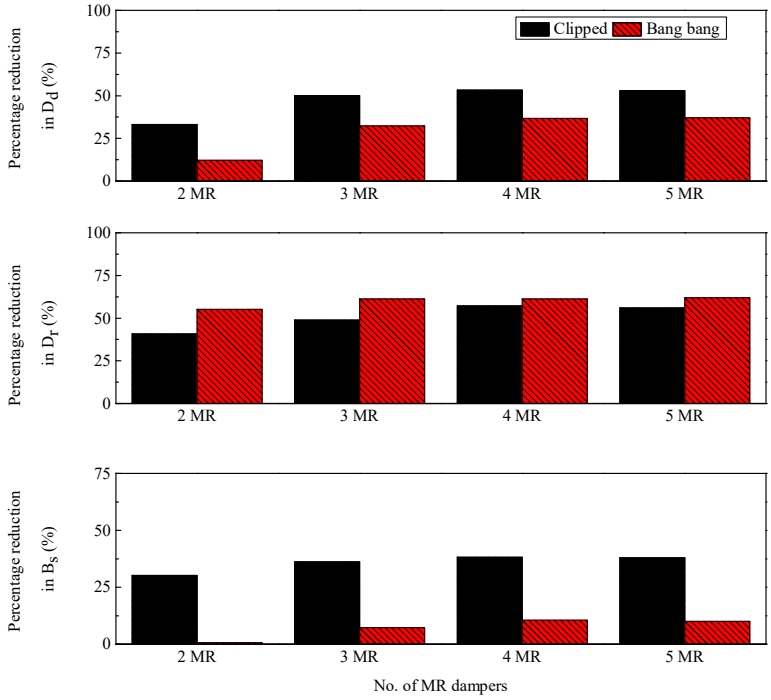

Figure 5-15: Comparison between maximum percentage reductions obtained by using different numbers of MR dampers for Victoria earthquake

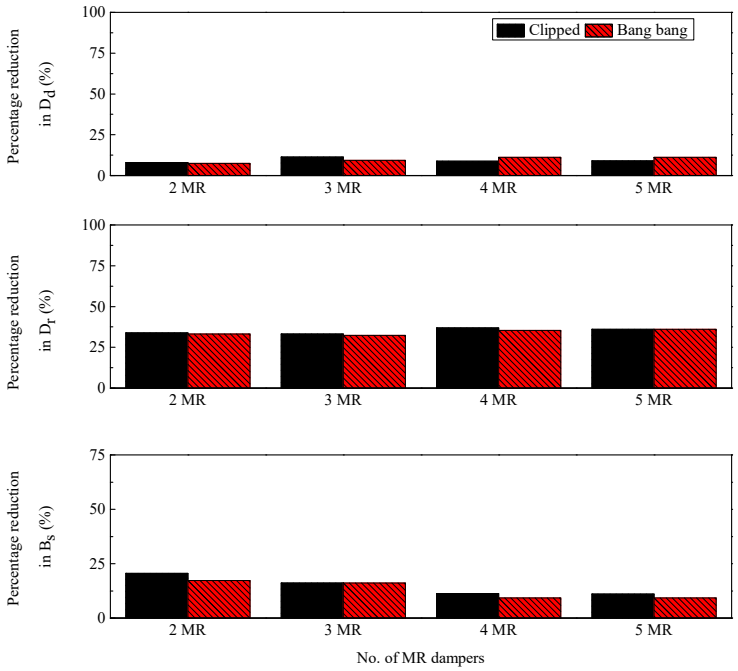

Figure 5-16: Comparison between maximum percentage reductions obtained by using different numbers of MR dampers for Kobe earthquake

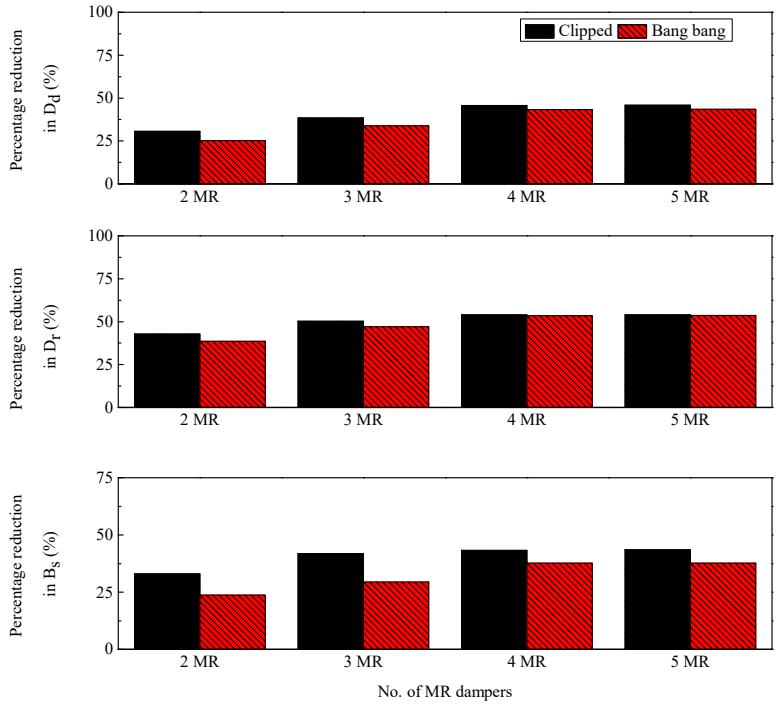

Figure 5-17: Comparison between maximum percentage reductions obtained by using different numbers of MR dampers for Spitak earthquake

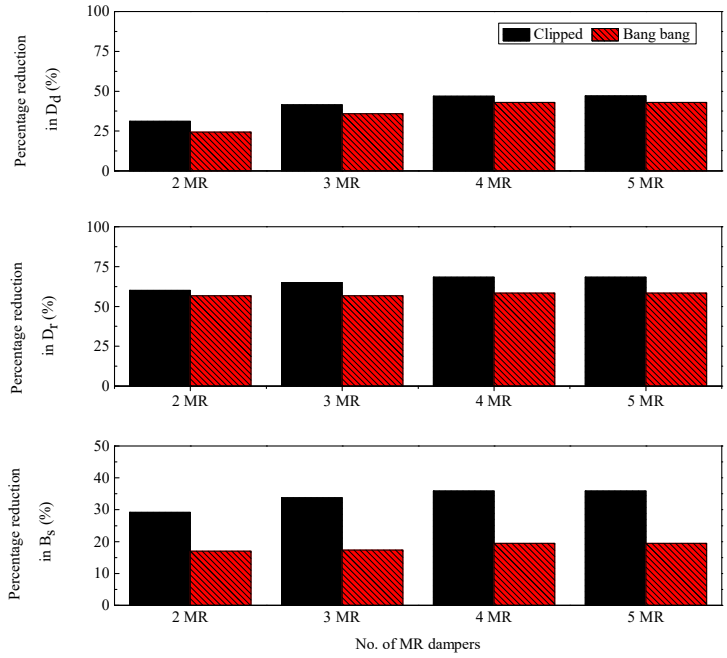

Figure 5-18: Comparison between maximum percentage reductions obtained by using different numbers of MR dampers (broadband excitation)

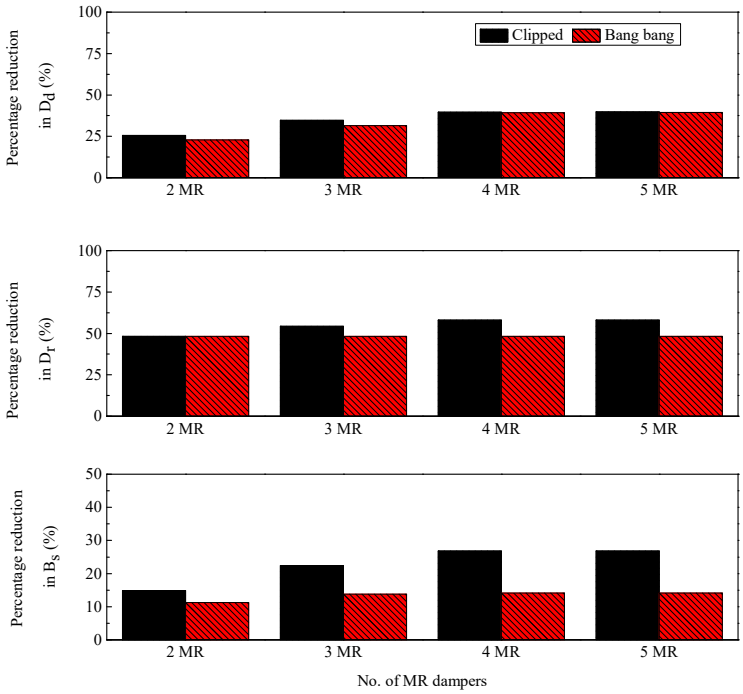

Figure 5-19: Comparison between maximum percentage reductions obtained by using different numbers of MR dampers (narrowband excitation)

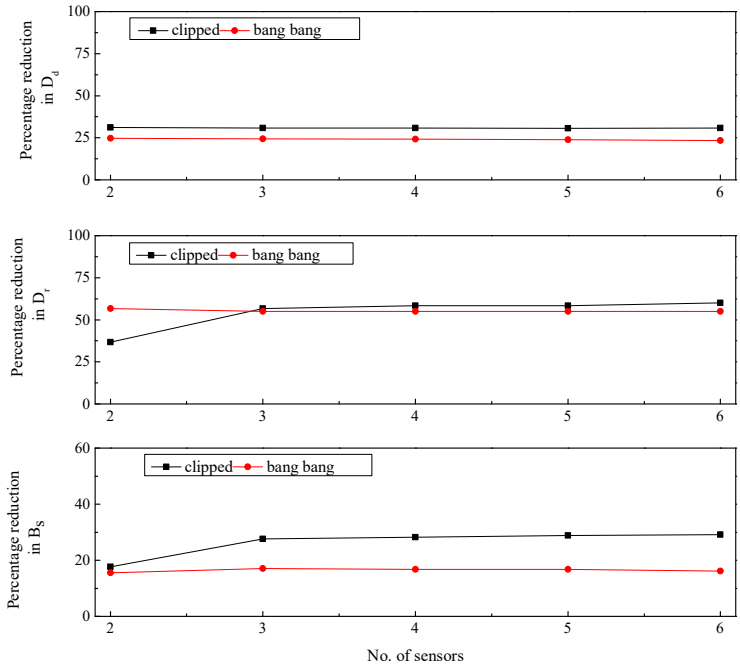

Figure 5-20: Percentage reduction obtained for different optimum sensor locations for 2 MR dampers subjected to broadband excitation for strategy 1

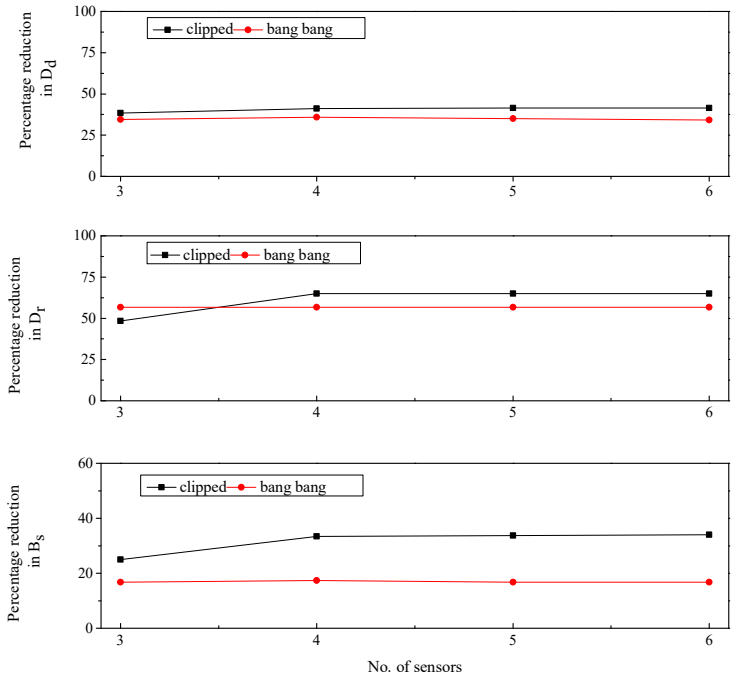

Figure 5-21: Percentage reduction obtained for different optimum sensor locations for 3 MR dampers subjected to broadband excitation for strategy 1

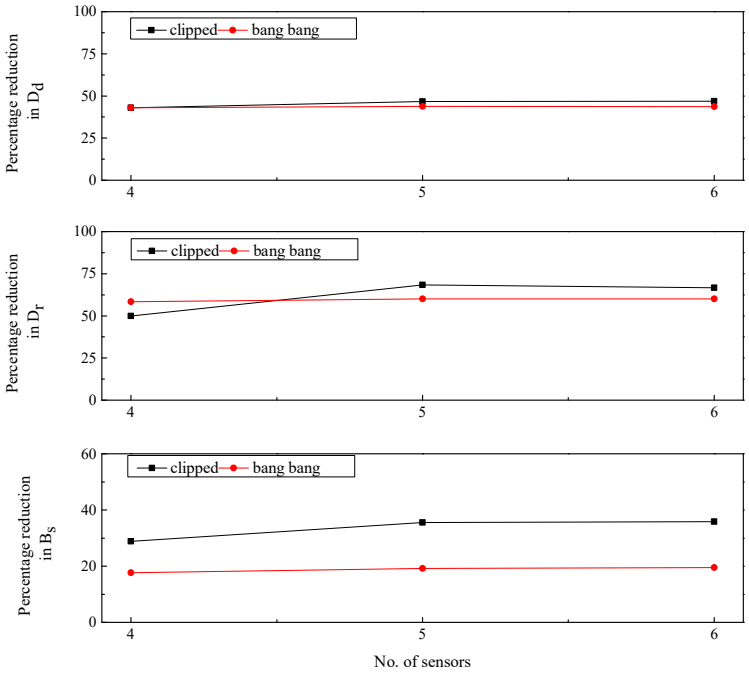

Figure 5-22: Percentage reduction obtained for different optimum sensor locations for 4 MR dampers subjected to broadband excitation for strategy 1

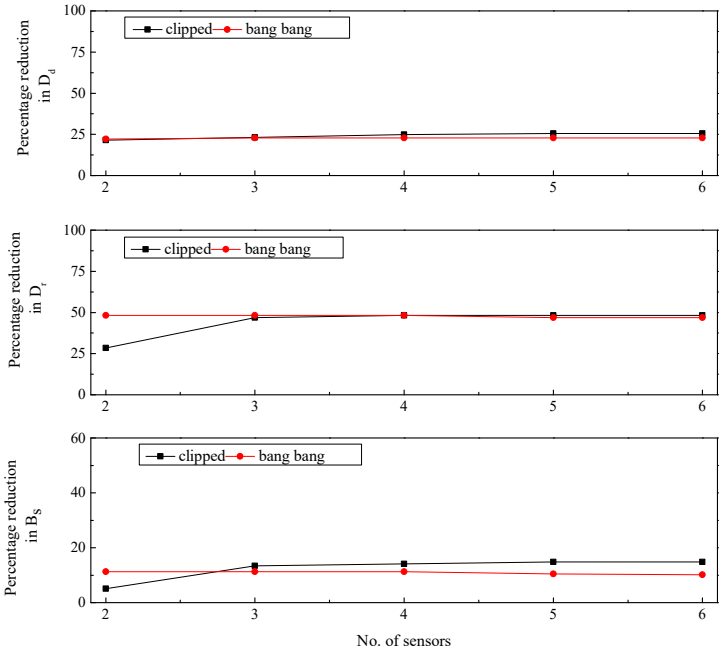

Figure 5-23: Percentage reduction obtained for different optimum sensor locations for 2 MR dampers subjected to broadband excitation for strategy 1

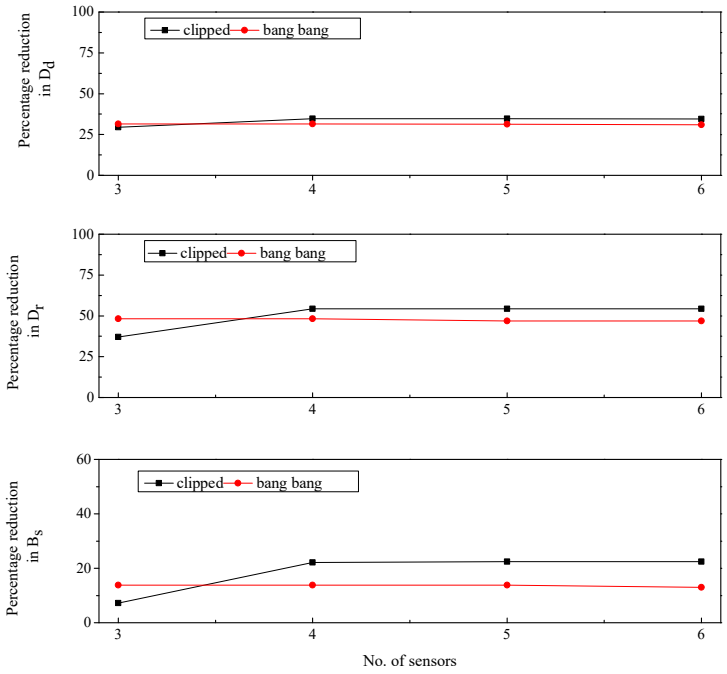

Figure 5-24: Percentage reduction obtained for optimum location of 3 MR dampers for narrowband earthquake for strategy 1

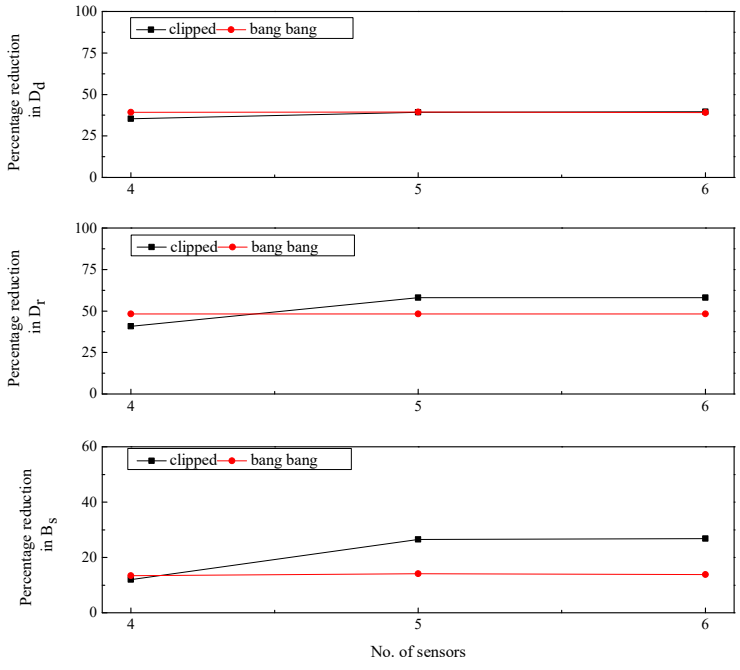

Figure 5-25: Percentage reduction obtained for optimum location of 4 MR dampers for narrowband earthquake for strategy 1

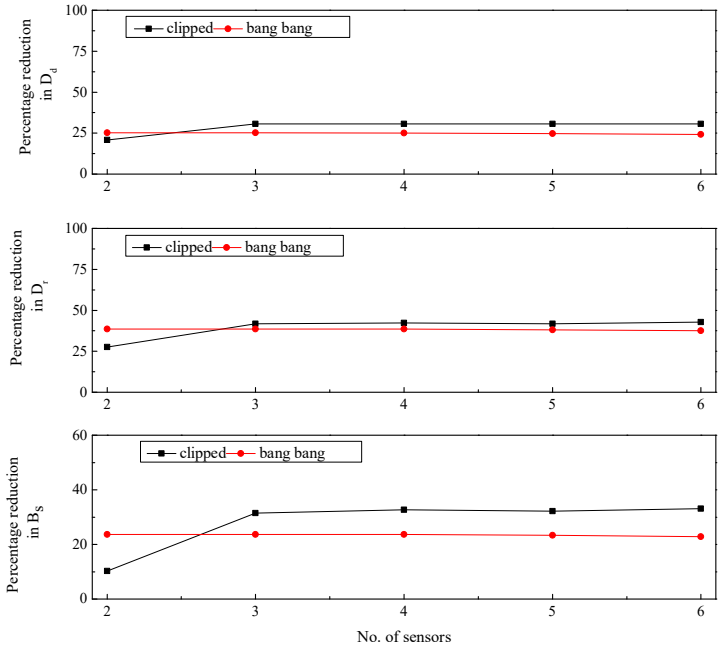

Figure 5-26: Percentage reduction obtained for optimum location of 2 MR dampers for Spitak earthquake for strategy 1

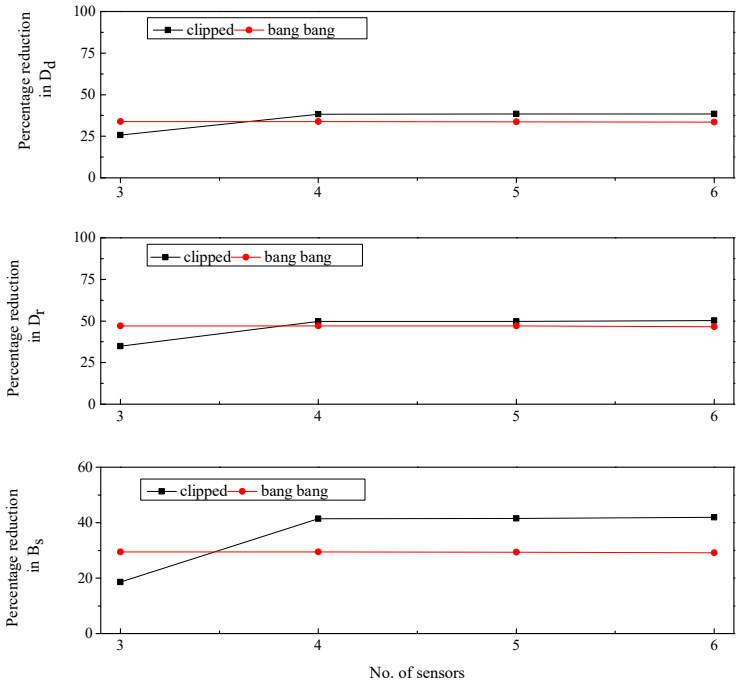

Figure 5-27: Percentage reduction obtained for optimum location of 3 MR dampers for Spitak earthquake for strategy 1

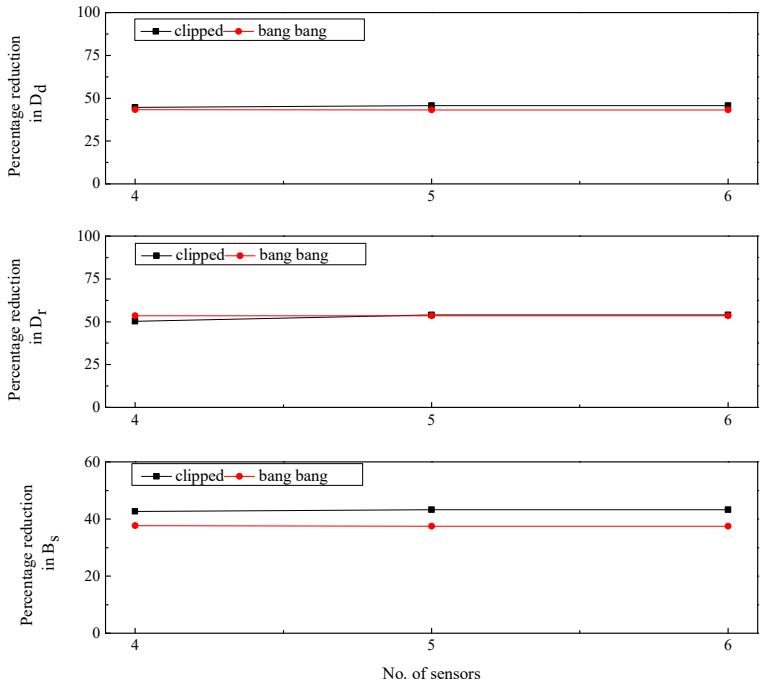

Figure 5-28: Percentage reduction obtained for optimum location of 4 MR dampers for Spitak earthquake for strategy 1

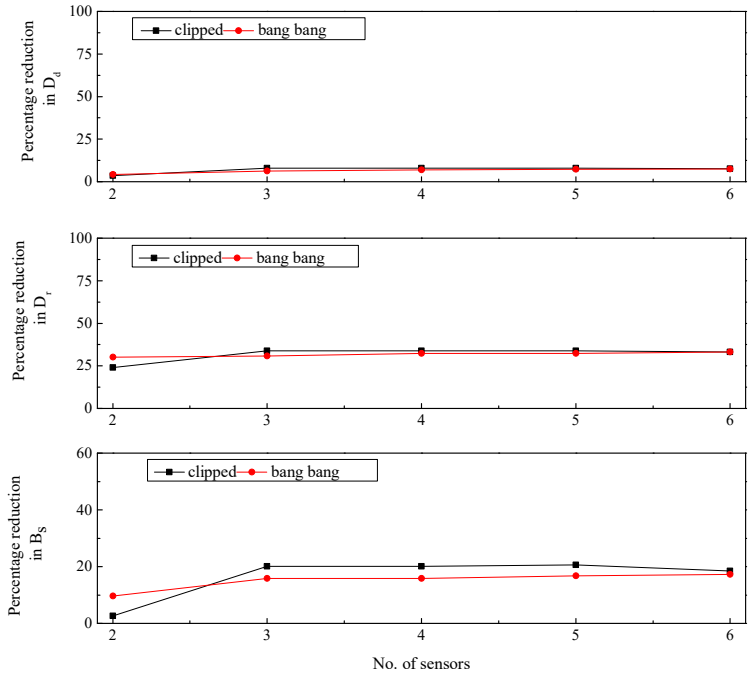

Figure 5-29: Percentage reduction obtained for optimum location of 2 MR dampers for Kobe earthquake for strategy 1

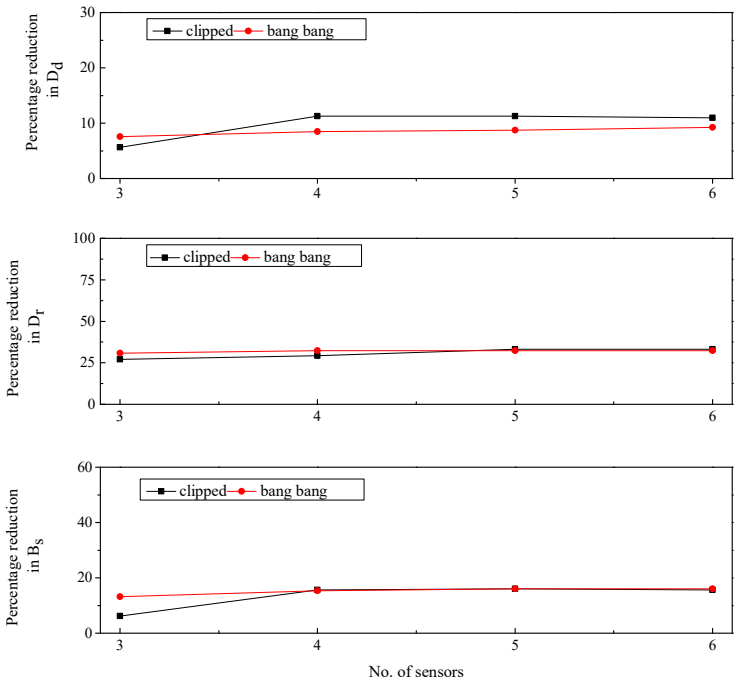

Figure 5-30: Percentage reduction obtained for optimum location of 3 MR dampers for Kobe earthquake for strategy 1

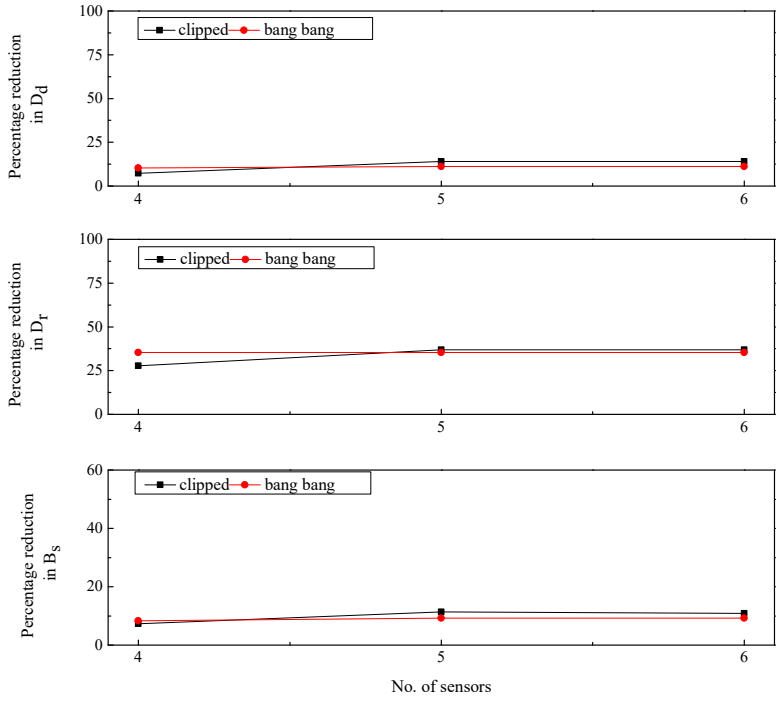

Figure 5-31: Percentage reduction obtained for optimum location of 4MR dampers for Kobe earthquake for strategy 1

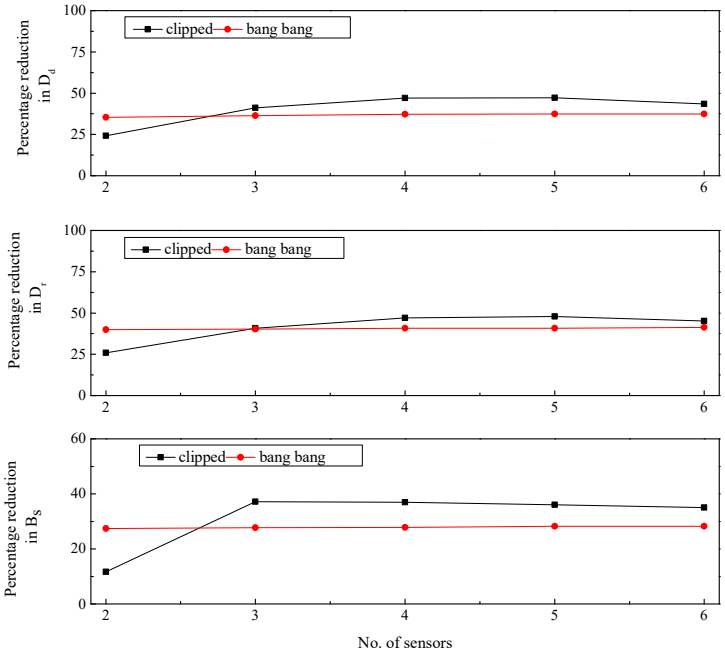

Figure 5-32: Percentage reduction obtained for optimum location of 2 MR dampers for El Centro earthquake for strategy 1

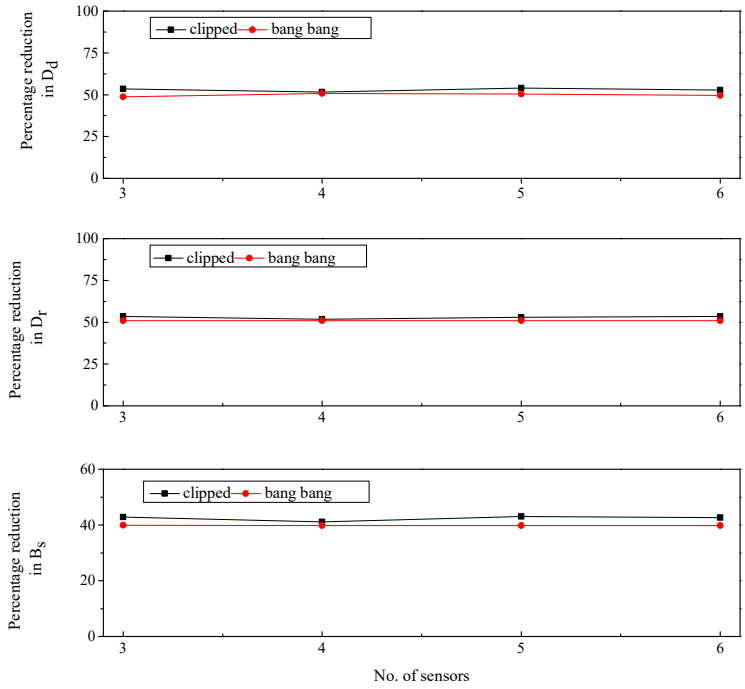

Figure 5-33: Percentage reduction obtained for optimum location of 3 MR dampers for El Centro earthquake for strategy 1

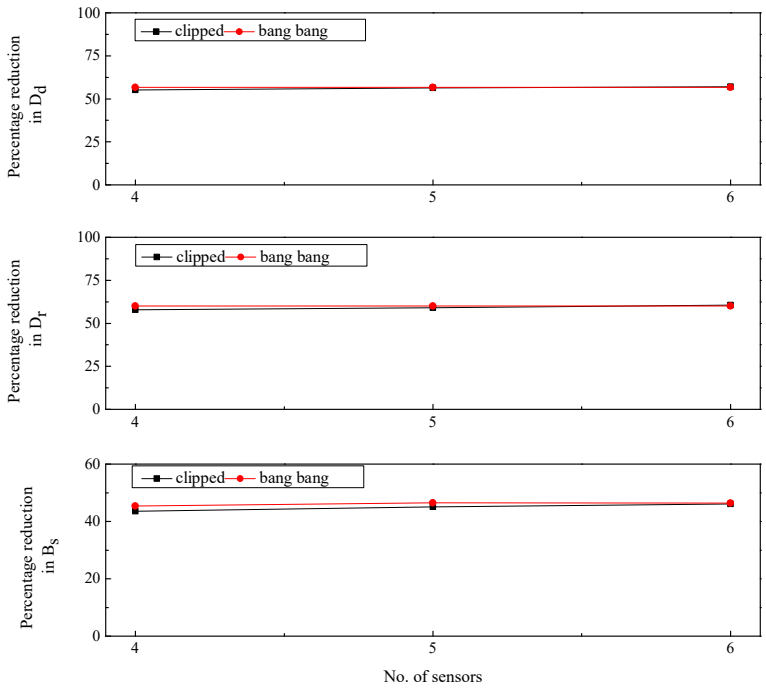

Figure 5-34: Percentage reduction obtained for optimum location of 4 MR dampers for El Centro earthquake for strategy 1

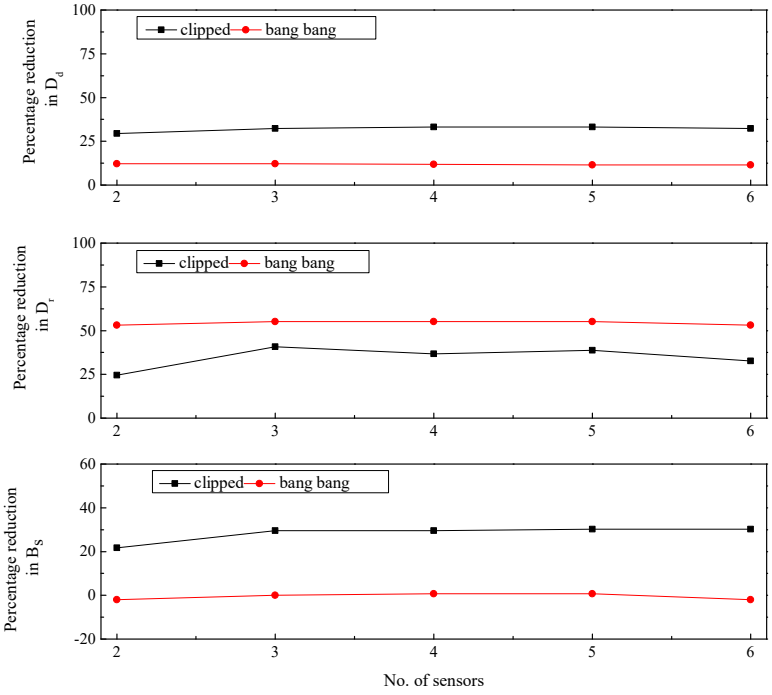

Figure 5-35: Percentage reduction obtained for optimum location of 2 MR dampers for Victoria earthquake for strategy 1

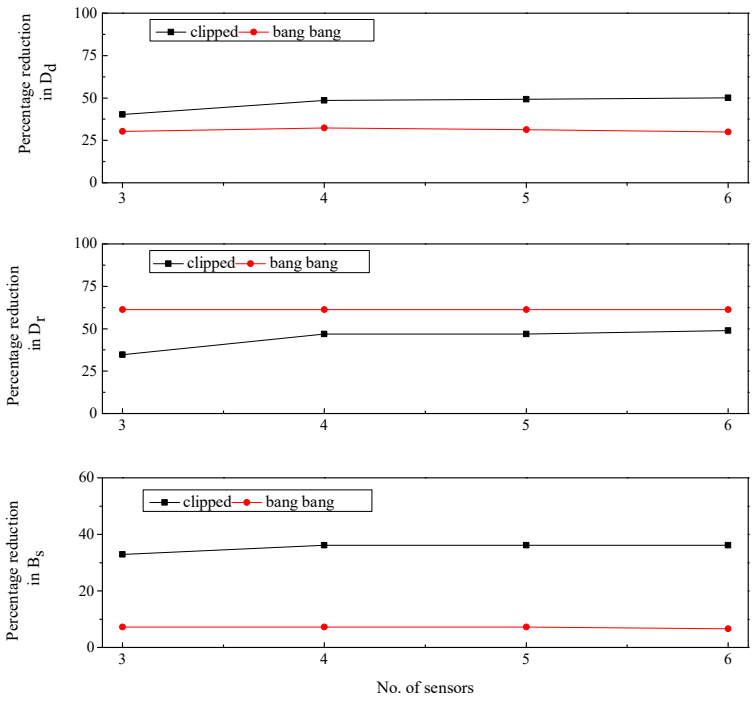

Figure 5-36: Percentage reduction obtained for optimum location of 3 MR dampers for Victoria earthquake for strategy 1

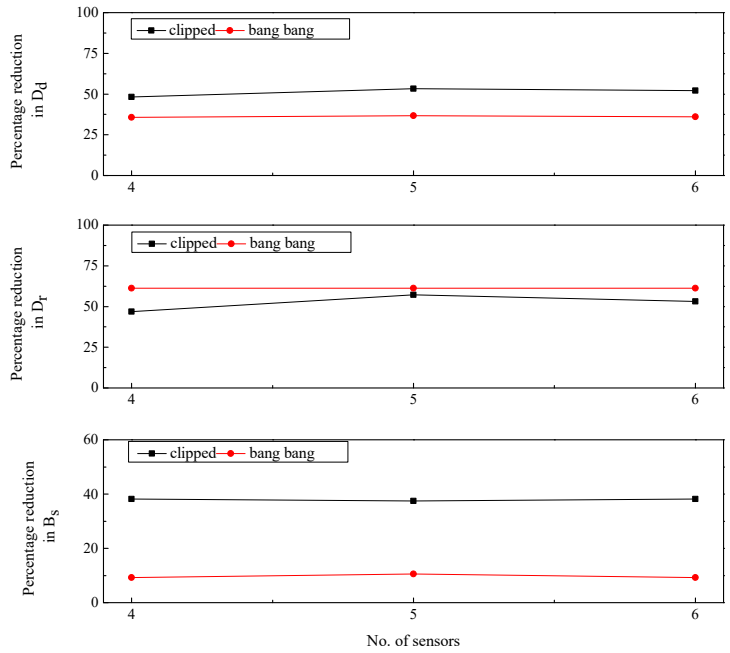

Figure 5-37: Percentage reduction obtained for optimum location of 4 MR dampers for Victoria earthquake for strategy 1

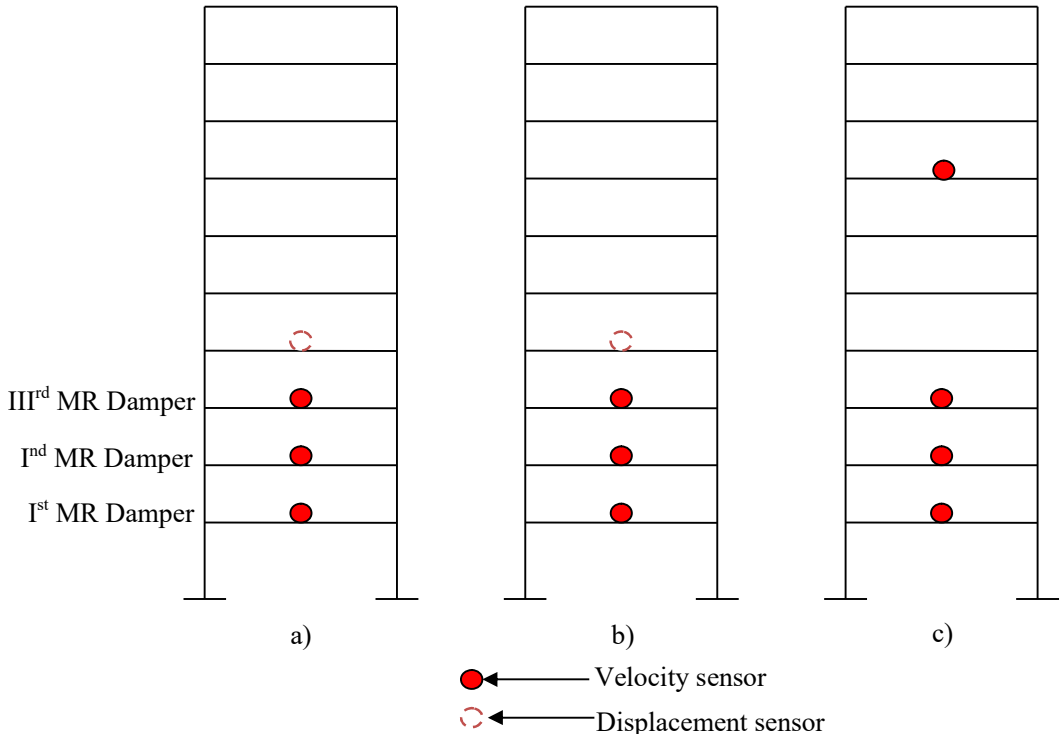

Figure 5-38: Pictorial view of optimal locations for the case of four sensors (for El Centro earthquake using bang bang control) for a) top floor displacement b) maximum drift and c) base shear

Chapter 6

Hybrid Control of Building Frame Using TMD and MR damper

6.1 Introduction

MR dampers for structural control are preferred because of their inherent stability and are fail safe as at the time of power failure they start behaving as passive dampers. However, due to the limitation of the maximum voltage that can be applied to the MR damper, there is a limitation on the maximum control force that can be achieved through the MR damper. As a result, the reduction in responses obtained through MR dampers is less as compared to similar configurations of active control systems. Moreover, even by increasing the number of MR dampers, not a substantial increase in reduction of responses is observed as shown in Chapter 5. Therefore, a hybrid system containing MR damper is justified.

In recent years, hybrid control strategy has gained considerable success in response reduction of structures and bridges. Various hybrid control systems have been formulated and studied comprising of hybrid mass dampers (HMDs), viscolelastic dampers (VEDs), active control systems and active or passive base isolation systems. They have been reviewed in chapter 2. Studies of hybrid control using MR dampers are relatively less. MR damper has been used in series with TMD called conventional semi active tuned mass damper (STMD) by different researchers (Kaveh et al.,2015, Bathaei et al.,2017) . The motivation behind this combination is that as MR dampers are very costly devices, therefore, addition of TMD may reduce their number. However, the effectiveness of a hybrid control system with different forms of the combination of MR damper and TMD has not been thoroughly investigated.

In this chapter, a few hybrid control strategies comprising of different types of combinations of MR dampers and TMDs are attempted in order to either reduce the number of MR dampers to be employed to obtain the comparable reductions in the responses or alleviate the response reductions substantially compared to the use of MR dampers alone. They include i) STMD at the top floor and one MR damper at the first floor (STMDMR); ii) TMD at the top floor and two MR dampers placed at first and second floor (TMDMR2); and iii) three MR dampers placed at bottommost three floors and a TMD at the top floor (TMDMR3). The response parameters investigated in the study are the maximum top floor displacement, maximum base shear, and maximum

inter-storey drift. Response reductions achieved with MR dampers alone are taken as the reference for comparison. Some of the control algorithms, namely LQR with clipped algorithm, VTC and passive on presented in previous chapters are used for obtaining the controlled responses.

6.2 Theoretical Formulation

Formulation of equation of motion for structure equipped with TMD and MR damper

The mathematical model of building frame equipped with TMD at the top floor and MR damper at bottom floors is shown in Figure 6.1(b). The equation of motion of this hybrid system consists of two parts: (i) equation of motion corresponding to the structural sway degrees-of-freedom of the frame and (ii) equation of motion for the TMD. Thus, for simulating the dynamic response of the building frame with a TMD at the top, the TMD is modelled as a hypothetical storey with structural properties of the TMD. The combined equation of motion is written as

$$[\mathbf{M_T}][\ddot{\mathbf{z}}]+[\mathbf{C_T}][\dot{\mathbf{z}}]+[\mathbf{K_T}][\mathbf{z}]=[\mathbf{G_T}][\mathbf{u}]-[\mathbf{M_T}][\mathbf{r}][\ddot{u}_g] \tag{6.1}$$

where, $\mathbf{M_T}$, $\mathbf{C_T}$, and $\mathbf{K_T}$ are the mass, damping and stiffness matrices of the combined system (building with MR damper and TMD), respectively; $\mathbf{u_T}$ is the MR damper force vector of size equal to the number of MR dampers employed; $\mathbf{G_T}$ is the damper location matrix of ones and zeroes; $\mathbf{z}$ is the displacement vector with respect to the ground; $\mathbf{r}$ is an influence coefficient vector; and $\ddot{\mathbf{u}}_\mathbf{g}$ is the earthquake ground acceleration. The matrices $\mathbf{M_T}$, $\mathbf{K_T}$, and $\mathbf{C_T}$ in this case can be expressed as

$$[\boldsymbol{M_T}]=\begin{bmatrix} m_1 & & & & & \\ & \ddots & & & & \\ & & \ddots & & & \\ & & & \ddots & & \\ & & & & m_n & \\ & & & & & m_{tmd} \end{bmatrix} \tag{6.2}$$

$$\left[\boldsymbol{K_T}\right]=\begin{bmatrix} k_1+k_2 & -k_1 & & & & \\ -k_1 & k_1+k_2 & -k_2 & & & \\ & & \cdots & & & \\ & & & \cdots & & \\ & & & -k_n & k_n+k_{\,tmd} & -k_{\,tmd} \\ & & & & -k_{\,tmd} & k_{\,tmd} \end{bmatrix} \tag{6.3}$$

$$\left[\boldsymbol{C_T}\right]=\begin{bmatrix} c_1+c_2 & -c_1 & & & & \\ -c_1 & c_1+c_2 & -c_2 & & & \\ & & \cdots & & & \\ & & & \cdots & & \\ & & & -c_n & c_n+c_{\,tmd} & -c_{\,tmd} \\ & & & & -c_{\,tmd} & c_{\,tmd} \end{bmatrix} \tag{6.4}$$

The tuning of the TMD will be derived from the chosen mass ration μ according to the design proposed by Den Hartog (1985) as follow :

$$m_{\,tmd}=\mu\times\sum_{i=1}^{n}m_{\,i} \tag{6.5}$$

$$f_{\,tmd}=\frac{f_{S1}}{\left(\mu+1\right)^2} \tag{6.6}$$

$$k_{\,tmd}=f_{\,tmd}{}^2\times m_{\,tmd} \tag{6.7}$$

$$c_{\,tmd}=\sqrt{\frac{3\mu}{8(\mu+1)^3}} \tag{6.8}$$

where $m_{\,tmd}$ is the mass of the TMD, f_{S1} is the first frequency of the structure, μ is the TMD the mass ration and $f_{\,tmd}$ is the frequency of the TMD. $k_{\,tmd}$ and $c_{\,tmd}$ are respectively the stiffness and the damping of the TMD device.

Formulation of equation of motion for semi active tuned mass damper (STMD) at top floor

Consider the equation of motion given in equation 6.1. When STMD is applied at the top floor (Fig. 6.1 (c)), the mass and stiffness matrix ($\mathbf{M_T}$ and $\mathbf{K_T}$) remains the same. However, the damping matrix is modified and is given by equation 6.9. All the other parameters are obtained by equations 6.5-8.

$$[\boldsymbol{C_T}] = \begin{bmatrix} c_1 + c_2 & -c_1 & & & & \\ -c_1 & c_1 + c_2 & -c_2 & & & \\ & & \cdots & & & \\ & & & \cdots & & \\ & & & -c_n & c_n & 0 \\ & & & & 0 & 0 \end{bmatrix} \tag{6.9}$$

The governing equation (Equation 6.1) is expressed in the state-space form as below:

$$\{\dot{\mathbf{X}}_\mathbf{T}\} = [\mathbf{A_T}]\{\mathbf{X_T}\} + [\mathbf{B_T}]\{\mathbf{U_T}\} + [\mathbf{E_T}]\{\ddot{\mathbf{u}}_\mathbf{g}\} \tag{6.10}$$

$$\mathbf{Y_V} = [\mathbf{C_T}]\{\mathbf{X_T}\} + [\mathbf{D_T}]\{\mathbf{U_T}\} + \mathbf{v} \tag{6.11}$$

where $\mathbf{X_T}' = \{\mathbf{z}\ z_T\ \dot{\mathbf{z}}\ \dot{z}_T\}$; $\mathbf{A_T}$ is a 2(n+1) x 2(n+1) matrix whose elements are function of structure's and TMD characteristics, $\mathbf{B_T}$ is a 2(n+1) x m damper force coefficient matrix, $\mathbf{E_T}$ is a 2(n+1) x 1 excitation coefficient matrix, $\mathbf{C_V}$ is a p x 2(n+1) measurement matrix, $\mathbf{D_T}$ is a p x m matrix of zeroes, $\mathbf{X_T}$ is a 2(n+1) x 1 state vector, $\mathbf{Y_T}$ is a p x 1 vector of measured outputs, $\mathbf{v}$ is a p x 1 measurement noise vector, z_T and $\dot{z}_T$ is the displacement and velocity of TMD mass, m is number of dampers, p is number of sensors and prime denotes transpose. Note that all the above matrices can be defined in similar way as defined in Chapter 3 for building frame equipped with MR dampers only.

Three standard semi-active control strategies are employed to obtain the voltage to be applied to the MR dampers, namely i) LQR with clipped optimal control (LQRCCl); ii) passive on and iii) VTC described in chapter 3. All the control algorithms used are given in Chapter 3, and therefore, are not repeated here.

6.3 Numerical Study

For the numerical study, the same ten story linear shear building frame of Chapter 3 is used. Firstly, the effect of TMD mass on response reduction is observed for three algorithms, namely, LQR with clipped algorithm (LQRCl), VTC and passive on for STMD placed at the top floor of the building. The TMD mass is varied from 2.5% to 15 % of the total weight of the building.Three earthquakes namely, El Centro, Kobe and Spitak are used for the study.

Figure 6.2 shows a comparison between the variations of percentage reductions of response quantities of interest with STMD mass obtained by passive on, LQRCl and VTC algorithm for the El Centro earthquake. It is seen from the figure that the reductions in responses increase with STMD mass until they reach a stationary value for LQRCl and VTC. For a mass ratio of about 12.5%, the stationary values are attained. Note the response reductions for the two algorithms are almost same. For passive on control, the reductions in responses increase with the STMD mass. Further, the reduction in responses obtained by passive on control is less as compared to the other two control algorithms i.e. LQRCl and VTC.

Figures 6.3-4 shows the same comparisons for Kobe and Spitak earthquakes, respectively. The trends of variations remain the same as those for the El Centro earthquake. Here, the stationary values of response reductions take place at about 10% mass ratio.

Since the passive on control provides inferior performance, two control algorithms LQRCl and VTC are used for further parametric studies. Three hybrid control strategies are considered, namely, i) STMD at the top floor and MR damper at the first floor (STMDMR); ii) TMD at the top floor and two MR dampers placed at first and second floor (TMD2MR); and iii) TMD at the top floor and three MR dampers placed at first, second and third floors (TMD3MR). Four cases of TMD mass are considered, namely 2.5% (Case I), 5% (Case 2), 10% (Case 3) and 15% (Case 4) of the total weight of the building for study.

Figures 6.5-6 show the percentage reductions in response quantities of interest for El Centro earthquake for four cases of TMD mass ratio. It is seen from the figures that at lower TMD mass (up to 5%) TMD2MR and TMD3MR give a better response reduction than STMDMR. However, at higher TMD mass (10% and 15%), response reductions are

in general greater for STMDMR. Further, the two control strategies (LQRCl and VTC) provide nearly the same response reductions.

Figures 6.7-8 show the same percentage of response reductions for Spitak earthquake. It is seen that the performance of STMD improves with increased mass ratio. However, its performance compared to the other two hybrid strategies remains in general less.

Figures 6.9-10 show the same percentage of reductions of responses for Kobe earthquake. Here, the trend of the results is similar to those observed for the El Centro earthquake. However, the response reductions are found to be less as compared to the El Centro earthquake.

The table 6.1-6.2 show the comparison between the response reductions achieved by different control strategies. It is observed from the tables that the performance of the hybrid control strategies is enhanced for higher values of the TMD mass ratio (comparison between the values for μ= 5% and 10% are shown in the tables). For STMD, maximum enhancement is obtained by increasing the TMD mass ratio from 5% to 10%. The increase in the percentage reduction in responses is about 45-60%. The maximum increase in percentage reduction is observed for base shear. So far as hybrid system using one MR damper and one TMD is concerned performance of STMD turns out to be better as compared to TMDMR i.e. one MR damper at the bottom floor and TMD at the top floor.

When a single TMD is added to two MR dampers placed at bottom two stories (2MR+TMD) the percentage reduction in drift and base shear are increased by about 15-25% for 5% mass of the TMD. When the TMD mass is increased to 10%, the percentage reduction in drift and base shear increases to 25% and 40% respectively. For the case of three MR dampers less benefit is obtained by putting a TMD at the top floor. For 5% TMD mass ratio, the increase in drift and base shear are 10 % to 12%. When the TMD mass ratio is increased to 10% percentage reduction in responses are increased by 15-20%. Thus, it is seen that the benefit of putting a single TMD at the top of the frame to make a hybrid system combined with MR dampers becomes less effective with an increase in the number of MR dampers. Further, the performance of STMD (which is a combination of single MR damper and TMD) positioned at the top of the frame, is found to be more than that of providing four MR dampers only especially for reductions in drift

and base shear for mass ratio of 10%. The tables also clearly show the saturation effect, i.e., beyond three MR dampers (only), the increase in the response reductions is marginal. The above observations hold good for both earthquakes and for the two control algorithms considered in the study.

6.4 Conclusions

The seismic control of a ten storey shear building frame is achieved using three hybrid control strategy, namely, STMD at the top floor and MR damper at the first floor (STMDMR); ii) TMD at the top floor and two MR dampers placed at first and second floor (TMD2MR); and iii) TMD at the top floor and three MR dampers placed at bottom three floors (TMD3MR). All three strategies use TMD and MR damper combined in different forms. The controlled responses are obtained for three earthquakes namely, El Centro, Spitak and Kobe using three control algorithms, i.e., LQRCl, VTC and passive-on. The response quantities of interest are top floor displacement, maximum interstory drift and base shear. The controlled responses are obtained by varying the TMD mass in order to study its effect on the response reductions. The results of the study lead to following conclusions:

i) There exists an optimum mass of TMD for STMD beyond which the response reductions become stationary. The optimum mass varies with the earthquake and the response quantity of interest.

ii) For STMD, LQR and VTC control algorithms perform far better than the passive on algorithm.

iii) The effectiveness of hybrid control strategy using a single TMD decreases as the number of MR dampers is increased; in the particular study, maximum enhancement in the percentage reduction of responses is achieved when a single MR damper in the form of STMD.

iv) The performance of hybrid system increases with the increase in the TMD mass ratio upto a certain mass value; this value is termed as an optimum TMD mass ratio.

v) A saturation effect is observed with respect to the number of MR dampers used; for this problem beyond three MR dampers, increase in the number of MR dampers marginally increases the response reduction.

vi) For the problem used here, a hybrid system of STMD provides nearly the same values of percentage reductions in drift and displacement and much increase in the percentage reduction of base shear if 10% mass ratio of TMD is used in the STMD; thus STMD appears to be a promising hybrid control system to be used in place of using only MR dampers.

Table 6-1: Comparison of peak response reductions in response quantities of interest for different control strategies for El Centro earthquake [M_1= 5% & M_2= 10%]

	LQRCl						VTC					
	D_d		D_r		B_s		D_d		D_r		B_s	
	M_1	M_2	M_1	M_2	M_1	M_2	M_1	M_2	M_1	M_2	M_1	M_2
STMD	35	53	36	57	33	58	36	53	38	57	36	60
TMDMR	29	35	39	43	27	34	30	36	40	43	27	35
MR	30		31		20		32		31		21	
2MR+TMD	39	45	49	53	38	42	41	45	49	52	40	43
2MR	43		42		30		43		43		31	
3MR+TMD	49	53	56	59	46	49	50	54	53	59	49	51
3MR	51		51		41		52		51		42	
4MR	53		53		43		54		54		45	

Table 6-2: Comparison of peak response reductions in response quantities of interest for different control strategies for Spitak earthquake [M_1= 5% & M_2= 10%]

	LQRCl						VTC					
	D_d		D_r		B_s		D_d		D_r		B_s	
	M_1	M_2	M_1	M_2	M_1	M_2	M_1	M_2	M_1	M_2	M_1	M_2
STMD	28	43	31	48	31	51	29	45	30	49	33	52
TMDMR	31	43	44	47	33	37	32	43	45	48	33	38
MR	36		38		20		37		21		38	
2MR+TMD	39	51	54	58	42	45	40	52	55	58	43	47
2MR	44		42		26		45		43		46	
3MR+TMD	45	53	57	60	46	50	47	54	59	62	48	52
3MR	51		47		30		53		48		53	
4MR	52		49		32		54		50		33	

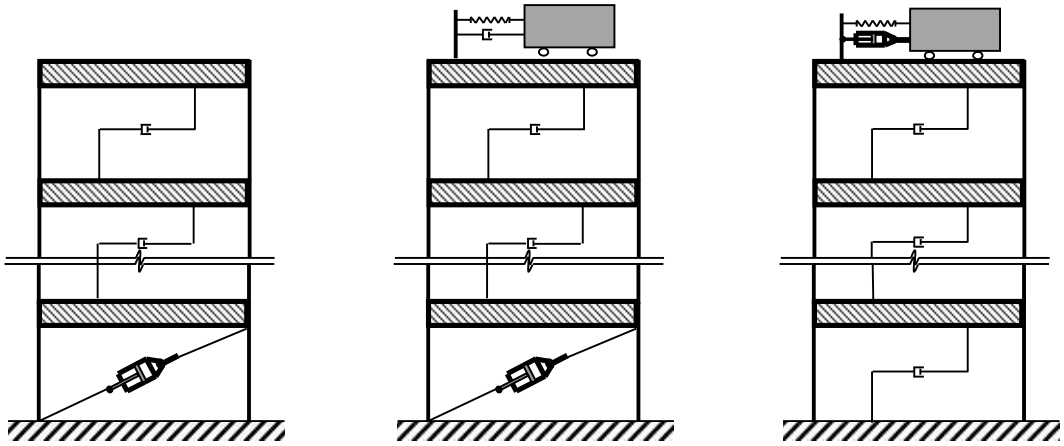

a) b) c)

Figure 6-1: (a) Structure with MR damper at bottom floor (b) Structure with a TMD at top and MR damper at bottom floor (c) Structure with a conventional MR-STMD

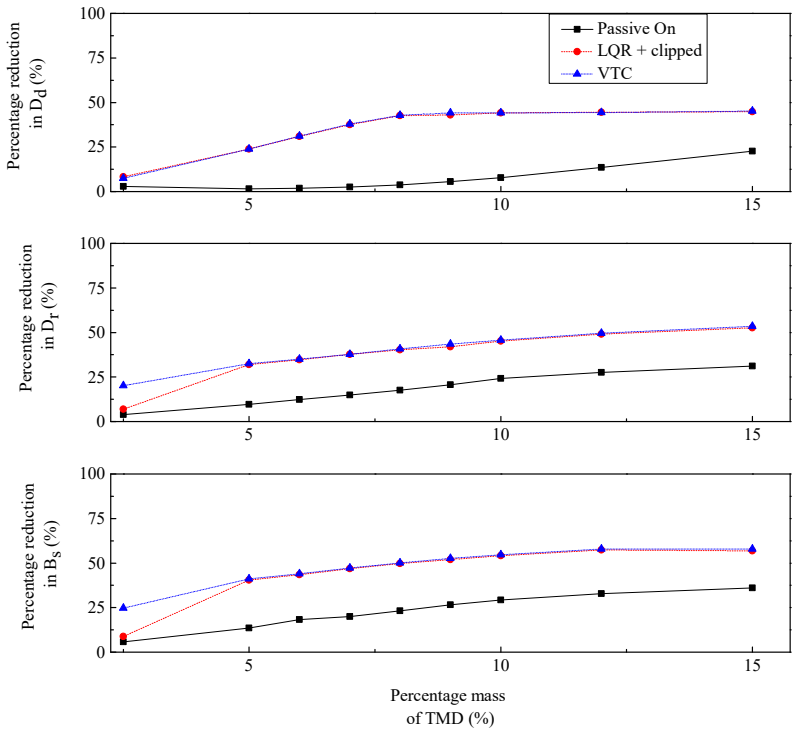

Figure 6-2: Variation of percentage reductions in response quantities with the mass of TMD for conventional STMD for different control algorithms (El Centro earthquake)

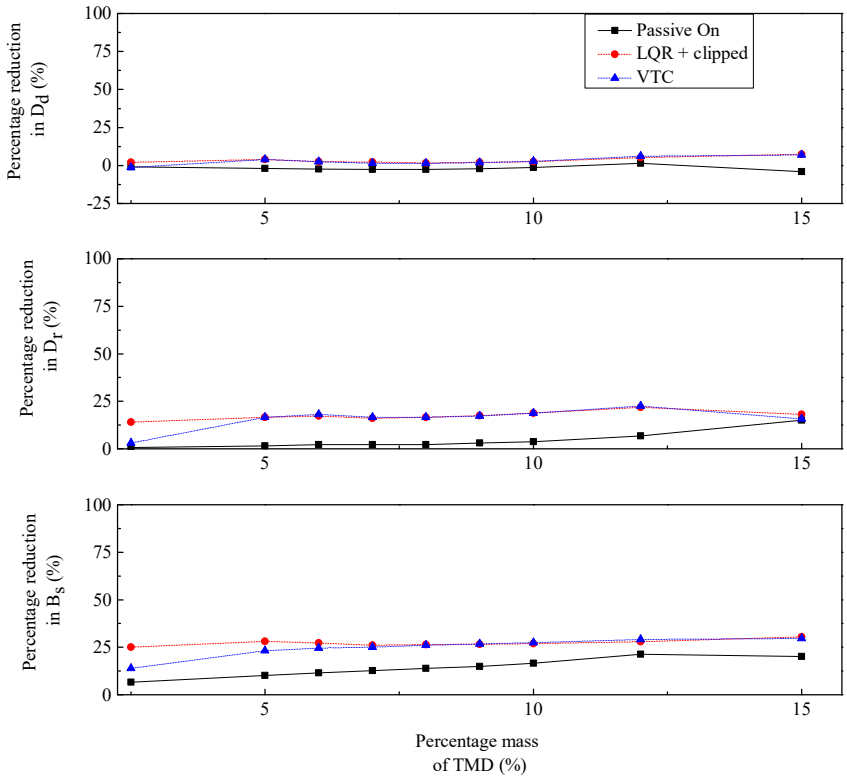

Figure 6-3: Variation of percentage reductions in response quantities with the mass of TMD for conventional STMD for different control algorithms (Kobe earthquake)

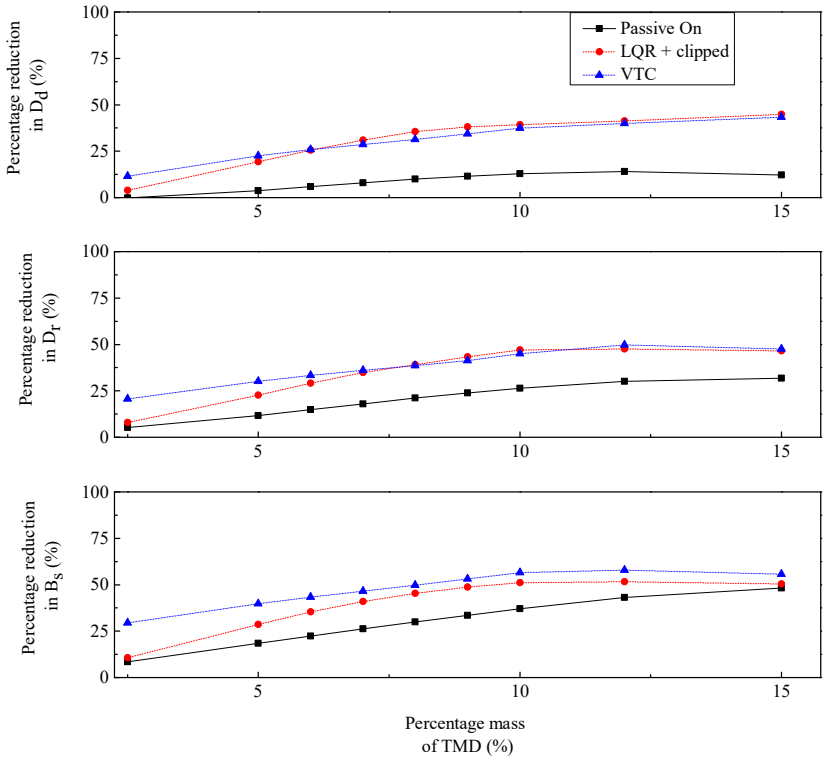

Figure 6-4: Variation of percentage reductions in response quantities with the mass of TMD for conventional STMD for different control algorithms (Spitak earthquake)

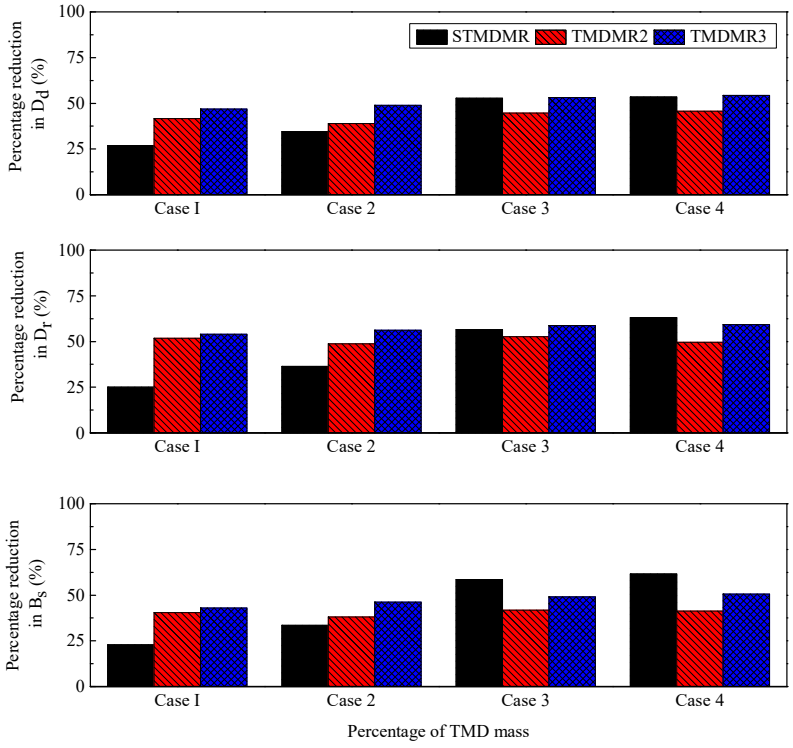

Figure 6-5: Percentage reductions in response quantities of interest for different TMD mass ratios (El Centro earthquake and LQRCl algorithm)

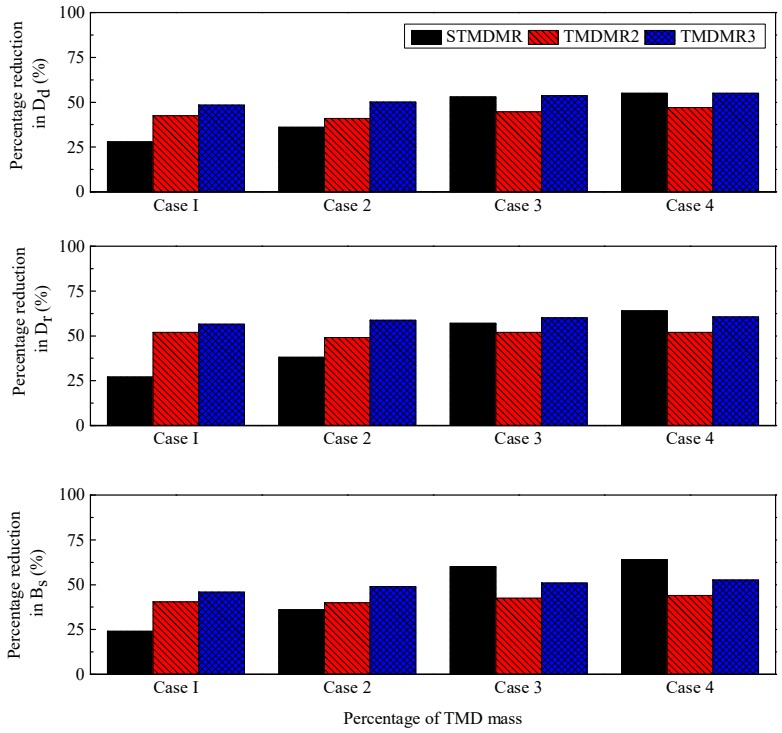

Figure 6-6: Percentage reductions in response quantities of interest for different TMD mass ratios (El Centro earthquake and VTC algorithm)

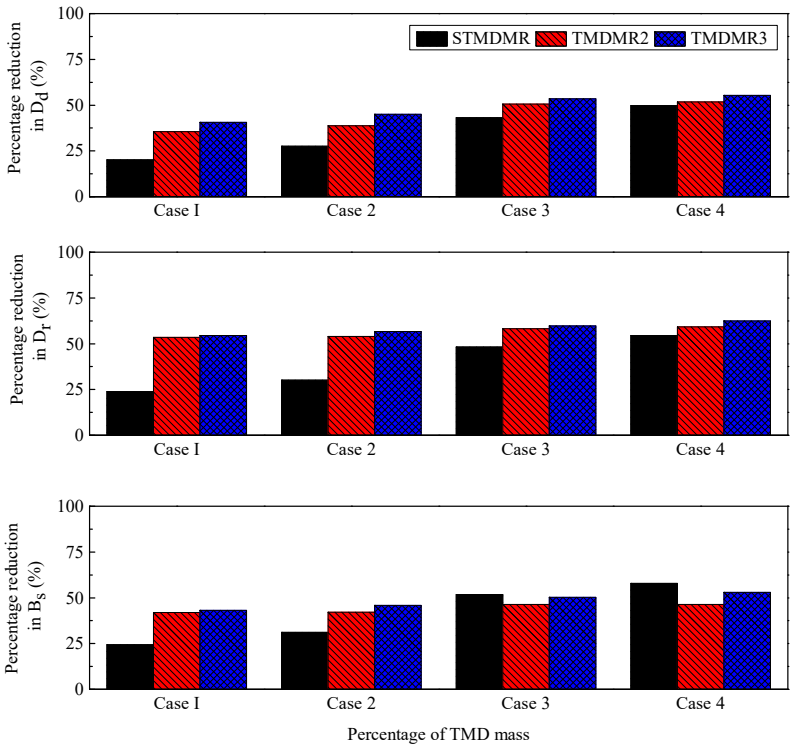

Figure 6-7: Percentage reductions in response quantities of interest for different TMD mass ratios (Spitak earthquake and LQRCl algorithm)

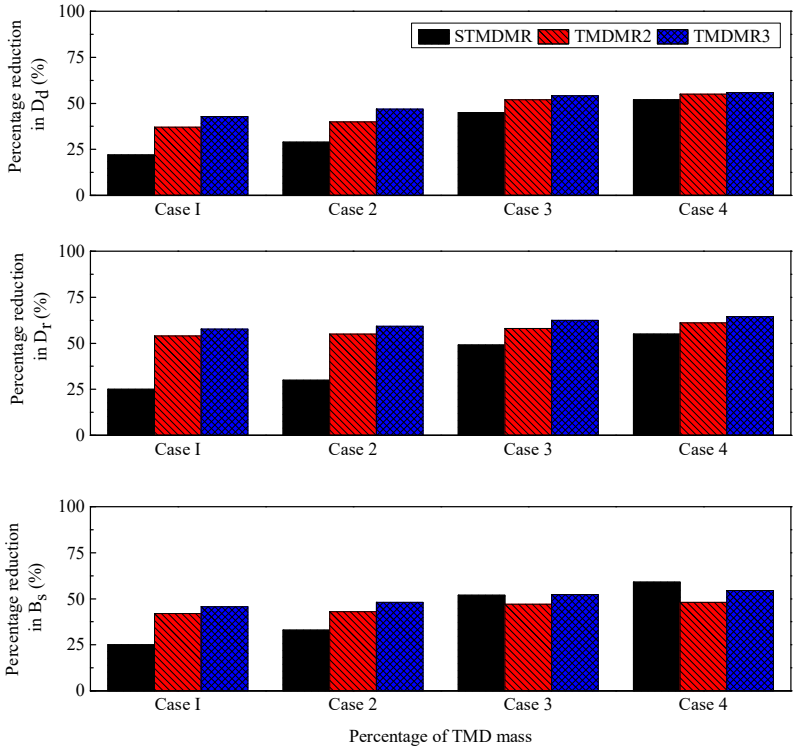

Figure 6-8: Percentage reductions in response quantities of interest for different TMD mass ratios (Spitak earthquake and VTC algorithm)

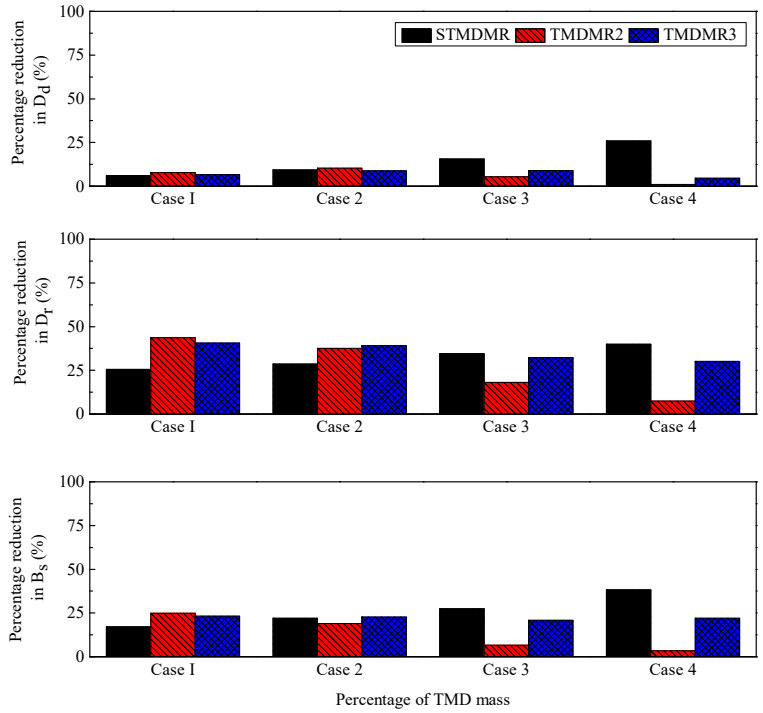

Figure 6-9: Percentage reductions in response quantities of interest for different TMD mass ratios (Kobe earthquake and LQRCl algorithm)

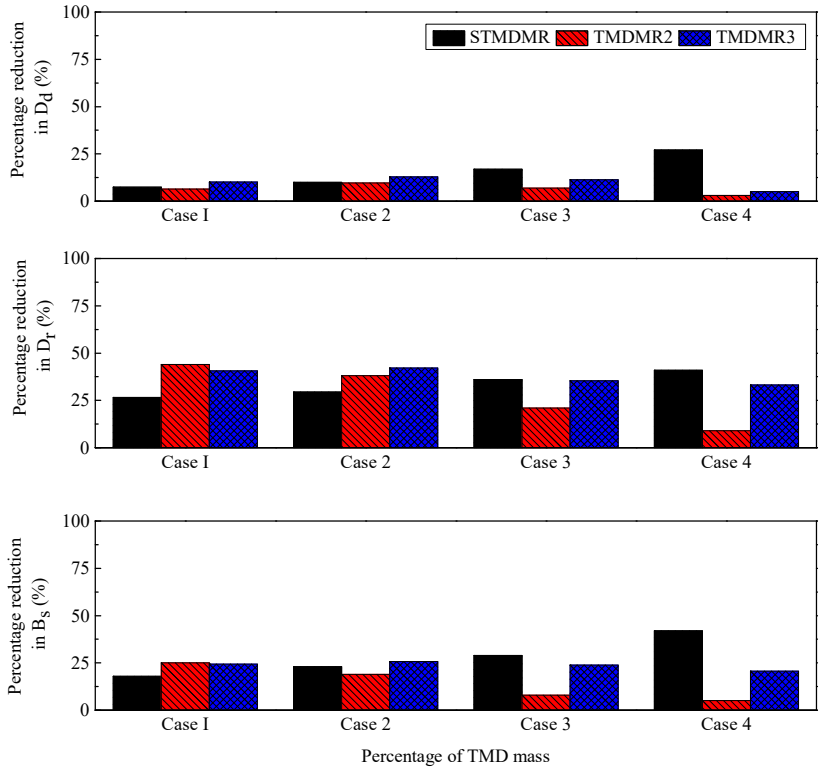

Figure 6-10: Percentage reductions in response quantities of interest for different TMD mass ratios (Kobe earthquake and VTC algorithm)

Chapter 7

Conclusions and Recommendations for Future Work

7.1 Conclusions

In the present work, a comprehensive study is carried on semi-active and hybrid control of building frames subjected to earthquake excitation. A new semi-active control strategy (VTC) for building frames using MR dampers subjected to both random excitations and real earthquake records is proposed. The controlled responses are compared with those of a few standard algorithms, namely, i) LQG and sliding mode algorithms applied in conjunction with clipped optimal control; ii) Bang-bang control and iii) Passive on control. Since the semi-active control using the MR damper is inherently nonlinear, a simulation procedure is adopted for random excitations to retain the full nonlinearity. The Kalman filter is used for estimating the states. Three response quantities of interest are considered in the study, namely, peak top floor displacement, maximum drift, and maximum base shear.

Further, a modified semi-active control of partially observed building frames under seismic excitation is presented. The new formulation incorporates more theoretical rigor in the analysis by making the input excitation to be Gaussian white with the help of a double filter incorporated in the structural system. Moreover, a sensitivity analysis is carried out which helps in selecting appropriate values of the covariance matrices, which are not known a priori, to be inputted to Kalman filter for state estimation for online applications. This is necessary for avoiding the onset of numerical instability in the control algorithm and hence, making it more robust. The results of the alternative formulation are compared with the conventional analysis in which the ground motion is directly used as an input to the base of the building frame. Three control algorithms, namely; LQGCl, SMCCL and bang bang are used for obtaining the time histories of the voltage to be applied to MR dampers.

A computationally efficient optimal solution for semi-active control of a partially observed ten story building frame using a limited number of MR dampers and measurement sensors is presented. Solutions are obtained for both simulated and real earthquake records. The optimal placement of the sensors and MR dampers is obtained by genetic algorithm. Two control algorithms are employed for obtaining the time histories

of voltages to be applied to the MR dampers namely, clipped optimal control and bang-bang control. Control of three response quantities is considered in the study, namely, top floor displacement, maximum inter storey drift, and base shear. The numerical studies are conducted on a ten-story building frame under a variety of earthquakes which include far field and near field earthquakes, and also simulated random ground motions.

For hybrid control, three hybrid control strategy, namely, STMD at the top floor and MR damper at the first floor (STMDMR); ii) TMD at the top floor and two MR dampers placed at first and second floor (TMD2MR); and iii) TMD at the top floor and three MR dampers placed at bottom three floors (TMD3MR). All three strategies use TMD and MR damper combined in different forms. The controlled responses are obtained for three earthquakes namely, El Centro, Spitak and Kobe using three control algorithms, i.e., LQRCl, VTC, and passive-on. The response quantities of interest are top floor displacement, maximum inter-story drift, and base shear. The controlled responses are obtained by varying the TMD mass in order to study its effect on the response reductions.

The following important conclusions can be drawn from the numerical studies carried out in different chapters:

i. In VTC algorithm, there is no need to estimate the full state for the prediction of control voltage and hence, it is a direct algorithm in the sense that no reference control force is required to predict the control voltage.
ii. The VTC control algorithm provides a maximum percentage reduction in the peak inter story drift amongst all control algorithms considered. Percentage reductions in other two response quantities obtained by VTC control algorithms are quite comparable to those of other algorithms.
iii. Response reduction per unit control force denoted by factor R is consistently higher for VTC algorithm for all earthquakes; from this consideration, VTC algorithm is most efficient among the algorithms considered in the study.
iv. Response reductions obtained by the proposed alternative formulation (VB-2) differ from those of the conventional formulation (VB-1) showing the need for improving the state estimation with more theoretical rigor; in general, the response

v. Critical covariance of excitation depends on the formulation (VB-1 and VB-2), and the covariance of noise; below the critical value, the response reductions are invariant of the value of the covariance matrix of excitation given as input to the Kalman filter. The covariance matrix of excitation inputted to the Kalman filter should be less than or equal to the critical covariance for numerical stability of the algorithm.

vi. Covariance of noise is to be set to a higher level in order to increase the critical covariance of excitation; thus, for the high anticipated PGA used in the design, adjusted covariance of noise is higher.

vii. For semi active control with MR damper, the differences in response reductions due to the change in formulation and in the parameters considered in the sensitivity analysis are narrowed down due to the limitation on maximum voltage that can be applied to the MR damper; in this sense, semi active control with MR damper merits an advantage.

viii. As the number of MR dampers is increased beyond a certain value, the response reduction tends to be stationary. For the ten-storey frame, the optimum number of MR dampers is found to be four for all earthquakes, all response quantities of interest and for both control algorithms.

ix. Optimum locations of sensors vary with earthquakes, response quantities of interest and control algorithms used.

x. The proposed strategy of placement of sensors is computationally efficient and is recommended for optimum control using MR dampers; the optimum number of sensors is found to be equal to the number of MR dampers plus one.

xi. Due to the limitation of maximum command voltage that can be applied to the MR dampers, the ideal control force predicted by LQR/LQG cannot be generated in the dampers and no significant difference is found between the response reductions obtained by different control algorithms.

xii. There exists an optimum mass of TMD for STMD beyond which the response reductions become stationary. The optimum mass varies with the earthquake and the response quantity of interest.

xiii. For STMD, LQR and VTC control algorithms perform far better than the passive on algorithm.

xiv. The effectiveness of hybrid control strategy using a single TMD decrease as the number of MR dampers is increased; in the particular study, maximum enhancement in the percentage reduction of responses is achieved when a single MR damper in the form of STMD.

xv. The performance of the hybrid system increases with the increase in the TMD mass ratio upto a certain mass value; this value is termed as an optimum TMD mass rato.

xvi. A saturation effect is observed with respect to the number of MR dampers used; for this problem beyond three MR dampers, increase in the number of MR dampers marginally increases the response reduction.

7.2 Recommendations of Future Work

As an extension of the present study and in order to have a better understanding and application of semi-active and hybrid control under seismic excitation, the following studies may be carried out:

- Development of semi-active control algorithm considering time delay and structural non-linearity.
- Study of the hybrid control scheme using a combination of MR dampers and other passive/active devices.
- Use of MR damper for controlling liquid storage tanks under earthquake excitation.
- Use of MR dampers for seismic control of secondary systems.
- Use of shared MR damper/STMD in coupled structures.

REFERENCES

Abdullah, M. M., A. Richardson and J. Hanif (2001). "Placement of sensors/actuators on civil structures using genetic algorithms." Earthquake engineering & structural dynamics 30(8): 1167-1184.

Adhikari, R. and H. Yamaguchi (1994). Adaptive control of nonstationary wind-induced vibration of tall buildings. Proc., First World Conf. Struct. Control, TA4.

Adhikari, R. and H. Yamaguchi (1997). "Sliding mode control of buildings with ATMD." Earthquake engineering & structural dynamics 26(4): 409-422.

Ahlawat, A. and A. Ramaswamy (2002). "Multi-objective optimal design of FLC driven hybrid mass damper for seismically excited structures." Earthquake engineering & structural dynamics 31(7): 1459-1479.

Akbay, Z. and H. Aktan (1991). Actively regulated friction slip devices. Proc., 6th Can. Conf. On Earthquake Engrg.

Arbel, A. (1981). "Controllability measures and actuator placement in oscillatory systems." International Journal of Control 33(3): 565-574.

Athans, M. (1971). "The role and use of the stochastic linear-quadratic-Gaussian problem in control system design." IEEE transactions on automatic control 16(6): 529-552.

Bathaei, A., S. M. Zahrai and M. Ramezani (2017). "Semi-active seismic control of an 11-DOF building model with TMD+ MR damper using type-1 and-2 fuzzy algorithms." Journal of Vibration and Control: 1077546317696369.

Bharti, S., S. Dumne and M. Shrimali (2010). "Seismic response analysis of adjacent buildings connected with MR dampers." Engineering Structures 32(8): 2122-2133.

Brown, A. S., S. Ankireddi and H. T. Yang (1999). "Actuator and sensor placement for multiobjective control of structures." Journal of Structural Engineering 125(7): 757-765.

Cai, C., W. Wu and M. Araujo (2007). "Cable vibration control with a TMD-MR damper system: experimental exploration." Journal of structural engineering 133(5): 629-637.

Cha, Y.-J., A. K. Agrawal, A. Friedman, B. Phillips, R. Ahn, B. Dong, S. J. Dyke, B. F. Spencer, J. Ricles and R. Christenson (2014). "Performance validations of semiactive controllers on large-scale moment-resisting frame equipped with 200-kN MR damper using real-time hybrid simulations." Journal of Structural Engineering 140(10): 04014066.

Cha, Y. J. and A. K. Agrawal (2013a). "Decentralized output feedback polynomial control of seismically excited structures using genetic algorithm." Structural Control and Health Monitoring 20(3): 241-258.

Cha, Y. J. and A. K. Agrawal (2013b). "Velocity based semi-active turbo-Lyapunov control algorithms for seismically excited nonlinear smart structures." Structural Control and Health Monitoring 20(6): 1043-1056.

Cha, Y. J., A. Raich, L. Barroso and A. Agrawal (2013). "Optimal placement of active control devices and sensors in frame structures using multi-objective genetic algorithms." Structural Control and Health Monitoring 20(1): 16-44.

Chang, C.-C. and L. Zhou (2002). "Neural network emulation of inverse dynamics for a magnetorheological damper." Journal of Structural Engineering 128(2): 231-239.

Cheng, H., W. Zhu and Z. Ying (2006). "Stochastic optimal semi-active control of hysteretic systems by using a magneto-rheological damper." Smart materials and structures 15(3): 711.

Cho, S.-W., B.-W. Kim, H.-J. Jung and I.-W. Lee (2005). "Implementation of modal control for seismically excited structures using magnetorheological dampers." Journal of Engineering Mechanics 131(2): 177-184.

Christenson, R., Y. Z. Lin, A. Emmons and B. Bass (2008). "Large-Scale Experimental Verification of Semiactive Control through Real-Time Hybrid Simulation " Journal of Structural Engineering 134(4): 522-534.

Clough, R. W. and J. Penzien (1975). Dynamics of structures.

Datta, T. (2003). "A state-of-the-art review on active control of structures." ISET Journal of earthquake technology 40(1): 1-17.

Delorenzo, M. L. (1990). "Sensor and actuator selection for large space structure control." Journal of Guidance, Control, and Dynamics 13(2): 249-257.

Den Hartog, J. P. (1985). Mechanical vibrations, Courier Corporation.

Dhingra, A. and B. Lee (1995). "Multiobjective design of actively controlled structures using a hybrid optimization method." International journal for numerical methods in engineering 38(20): 3383-3401.

Dong, L., Z. Ying and W. Zhu (2004). "Stochastic Optimal Semi-Active Control of Nonlinear Systems by Using MR Dampers." Advances in Structural Engineering 7(6): 485-494.

Dyke, S., B. Spencer, M. Sain and J. Carlson (1997). An experimental study of magnetorheological dampers for seismic hazard mitigation. Building to Last, ASCE.

Dyke, S., B. Spencer Jr, P. Quast, M. Sain, D. K. Jr and T. Soong (1996a). "Acceleration feedback control of MDOF structures." Journal of Engineering Mechanics 122(9): 907-918.

Dyke, S., B. Spencer Jr, M. Sain and J. Carlson (1996b). "Modeling and control of magnetorheological dampers for seismic response reduction." Smart materials and structures 5(5): 565.

Ehrgott, R. and S. Masri (1992). "Modeling the oscillatory dynamic behaviour of electrorheological materials in shear." Smart Materials and Structures 1(4): 275.

Eshelman, L. J., R. A. Caruana and J. D. Schaffer (1989). Biases in the crossover landscape. Proceedings of the third international conference on Genetic algorithms, Morgan Kaufmann Publishers Inc.

Feng, M. Q. (1993). "Application of hybrid sliding isolation system to buildings." Journal of Engineering Mechanics 119(10): 2090-2108.

Feng, M. Q., M. Shinozuka and S. Fujii (1993). "Friction-controllable sliding isolation system." Journal of engineering mechanics 119(9): 1845-1864.

Fisco, N. and H. Adeli (2011a). "Smart structures: part I—active and semi-active control." Scientia Iranica 18(3): 275-284.

Fisco, N. and H. Adeli (2011b). "Smart structures: part II—hybrid control systems and control strategies." Scientia Iranica 18(3): 285-295.

Furuya, H. and R. Haftka (1995). "Placing actuators on space structures by genetic algorithms and effectiveness indices." Structural optimization 9(2): 69-75.

Gamota, D. and F. Filisko (1991). "Dynamic mechanical studies of electrorheological materials: moderate frequencies." Journal of Rheology (1978-present) 35(3): 399-425.

Goldberg, D. E. and J. H. Holland (1988). "Genetic algorithms and machine learning." Machine learning 3(2): 95-99.

Hazaveh, N. K., J. G. Chase, G. W. Rodgers and S. Pampanin (2015). "Smart semi-active MR damper to control the structural response."

He, W., A. Agrawal and K. Mahmoud (2001). "Control of seismically excited cable-stayed bridge using resetting semiactive stiffness dampers." Journal of Bridge Engineering 6(6): 376-384.

Holland, J. (1975a). "Adaption in natural and artificial systems." Ann Arbor MI: The University of Michigan Press.

Holland, J. H. (1975b). Adaptation in natural and artificial systems: an introductory analysis with applications to biology, control, and artificial intelligence, U Michigan Press.

Housner, G., L. A. Bergman, T. K. Caughey, A. G. Chassiakos, R. O. Claus, S. F. Masri, R. E. Skelton, T. Soong, B. Spencer and J. T. Yao (1997). "Structural control: past, present, and future." Journal of engineering mechanics 123(9): 897-971.

Hu, R., H. Xiong, W. Jin and W. Zhu (2016). "Stochastic minimax semi-active control for MDOF nonlinear uncertain systems under combined harmonic and wide-band noise excitations using MR dampers." International Journal of Non-Linear Mechanics 83: 26-38.

Inaudi, J. A. (1997). "MODULATED HOMOGENEOUS FRICTION: A SEMI-ACTIVE DAMPING STRATEGY." Earthquake engineering & structural dynamics 26(3): 361-376.

Inaudi, J. A. and J. M. Kelly (1993). "Hybrid isolation systems for equipment protection." Earthquake engineering & structural dynamics 22(4): 297-313.

Jangid, R. and T. Datta (1995). "Seismic behaviour of base-isolated buildings: a state-of-the-art review." Proceedings of the Institution of Civil Engineers. Structures and buildings 110(2): 186-203.

Jansen, L. M. and S. J. Dyke (2000). "Semiactive control strategies for MR dampers: comparative study." Journal of Engineering Mechanics 126(8): 795-803.

Jiménez, R. and L. Álvarez-Icaza (2005). "LuGre friction model for a magnetorheological damper." Structural Control and Health Monitoring 12(1): 91-116.

Jin, G., M. K. Sain and B. F. Spencer (2002). Modeling MR-dampers: the ridgenet estimation approach. Proceedings of the 2002 American Control Conference (IEEE Cat. No. CH37301), IEEE.

Jing, C., Q. Weilian, Z. Nanlun and L. Hongsheng (2002). Structural Control Based on Panboolean Algebra. The 6th World Multi-Conference on SYSTEMICS, CYBERNETICS AND INFORMATICS.

Jung, H. J., K. M. Choi, B. F. Spencer and I. W. Lee (2006). "Application of some semi-active control algorithms to a smart base-isolated building employing MR dampers." Structural Control and Health Monitoring 13(2-3): 693-704.

Kang, J., H. S. Kim and D. G. Lee (2011). "Mitigation of wind response of a tall building using semi-active tuned mass dampers." The Structural Design of Tall and Special Buildings 20(5): 552-565.

Kaveh, A., S. Pirgholizadeh and O. K. Hosseini (2015). "Semi-active tuned mass damper performance with optimized fuzzy controller using CSS algorithm." Asian J. Civil Eng.(BHRC) 16(5): 587-606.

Kawatani, M., Y. Yamada, M. Shirnono and A. Mori (1994). Hybrid control of traffic-induced vibration of girder bridges. Proc., First World Conf. on Struct. Control, TA2.

Kelly, J. M. (1986). "Aseismic base isolation: review and bibliography." Soil Dynamics and Earthquake Engineering 5(4): 202-216.

Kim, H.-S., C. Chang and J.-W. Kang (2015). "Control performance evaluation of semi-active tmd subjected to various types of loads." International Journal of Steel Structures 15(3): 581-594.

Kim, H.-S., P. N. Roschke, P.-Y. Lin and C.-H. Loh (2006). "Neuro-fuzzy model of hybrid semi-active base isolation system with FPS bearings and an MR damper." Engineering structures 28(7): 947-958.

Kim, H. and H. Adeli (2004). "Hybrid feedback-least mean square algorithm for structural control." Journal of Structural Engineering 130(1): 120-127.

Lee-Glauser, G. J., G. Ahmadi and L. G. Horta (1997). "Integrated passive/active vibration absorber for multistory buildings." Journal of Structural Engineering 123(4): 499-504.

Leitmann, G. (1994). "Semiactive control for vibration attenuation." Journal of Intelligent Material Systems and Structures 5(6): 841-846.

Li, Q., D. Liu, J. Fang and C. Tam (2000). "Multi-level optimal design of buildings with active control under winds using genetic algorithms." Journal of Wind Engineering and Industrial Aerodynamics 86(1): 65-86.

Li, Q., D. Liu, J. Tang, N. Zhang and C. Tam (2004). "Combinatorial optimal design of number and positions of actuators in actively controlled structures using genetic algorithms." Journal of sound and vibration 270(4): 611-624.

Lin, P., L. Chung and C. Loh (2005). "Semiactive control of building structures with semiactive tuned mass damper." Computer-Aided Civil and Infrastructure Engineering 20(1): 35-51.

McClamroch, N. H. and H. Gavin (1995). Closed loop structural control using electrorheological dampers. American Control Conference, Proceedings of the 1995, IEEE.

Meirovitch, L. and T. J. Stemple (1997). "Nonlinear control of structures in earthquakes." Journal of engineering mechanics 123(10): 1090-1095.

Milman, M. H. and C.-C. Chu (1994). "Optimization methods for passive damper placement and tuning." Journal of Guidance, Control, and Dynamics 17(4): 848-856.

Mohajer Rahbari, N., B. Farahmand Azar, S. Talatahari and H. Safari (2013). "Semi-active direct control method for seismic alleviation of structures using MR dampers." Structural Control and Health Monitoring 20(6): 1021-1042.

Moita, J. M. S., V. M. F. Correia, P. G. Martins, C. M. M. Soares and C. A. M. Soares (2006). "Optimal design in vibration control of adaptive structures using a simulated annealing algorithm." Composite Structures 75(1): 79-87.

Nagarajaiah, S. (1994). Fuzzy controller for structures with hybrid isolation system. Proc., First World Conf. Struct. Control, TA2.

Nagarajaiah, S., M. A. Riley and A. Reinhorn (1993). "Control of sliding-isolated bridge with absolute acceleration feedback." Journal of engineering Mechanics 119(11): 2317-2332.

Nagashima, I., R. Maseki, Y. Asami, J. Hirai and H. Abiru (2001). "Performance of hybrid mass damper system applied to a 36-storey high-rise building." Earthquake engineering & structural dynamics 30(11): 1615-1637.

Ok, S.-Y., J. Song and K.-S. Park (2008). "Optimal design of hysteretic dampers connecting adjacent structures using multi-objective genetic algorithm and stochastic linearization method." Engineering structures 30(5): 1240-1249.

Oliver, I., D. Smith and J. R. Holland (1987). Study of permutation crossover operators on the traveling salesman problem. Genetic algorithms and their applications: proceedings of the second International Conference on Genetic Algorithms: July 28-31, 1987 at the Massachusetts Institute of Technology, Cambridge, MA, Hillsdale, NJ: L. Erlhaum Associates, 1987.

Onoda, J. and Y. Hanawa (1993). "Actuator placement optimization by genetic and improved simulated annealing algorithms." AIAA journal 31(6): 1167-1169.

Park, K.-S., H.-J. Jung and I.-W. Lee (2003). "Hybrid control strategy for seismic protection of a benchmark cable-stayed bridge." Engineering Structures 25(4): 405-417.

Rao, S. S., T.-S. Pan and V. B. Venkayya (1991). "Optimal placement of actuators in actively controlled structures using genetic algorithms." AIAA journal 29(6): 942-943.

Reinhorn, A. and M. A. Riley (1994). Control of bridge vibrations with hybrid devices. Proc., First World Conf. on Struct. Control, TA2.

Rodellar, J., A. Barbat and N. Molinares (1994). Response analysis of buildings with a new nonlinear base isolation system. Proc., First World Conf. on Struct. Control, TP1.

Rofooei, F. R. and I. G. Tadjbakhsh (1993). "Optimal control of structures with acceleration, velocity, and displacement feedback." Journal of engineering mechanics 119(10): 1993-2010.

Sack, R., C. Kuo, H. Wu, L. Liu and W. Patten (1994). Seismic motion control via semiactive hydraulic actuators. Proc., US 5th Nat. Conf. on Earthquake Engrg.

Sahasrabudhe, S. and S. Nagarajaiah (2005). "Experimental study of sliding base-isolated buildings with magnetorheological dampers in near-fault earthquakes." Journal of structural engineering 131(7): 1025-1034.

Saito, T., K. Shiba and K. Tamura (2001). "Vibration control characteristics of a hybrid mass damper system installed in tall buildings." Earthquake engineering & structural dynamics 30(11): 1677-1696.

Sarbjeet, S. and T. Datta (2000). "Nonlinear sliding mode control of seismic response of building frames." Journal of engineering mechanics 126(4): 340-347.

Sarbjeet, S. and T. Datta (2003). "Sliding mode control of building frames under random ground motion." Journal of earthquake engineering 7(01): 73-95.

Shing, P., M. Dixon, N. Kermiche, R. Su and D. Frangopol (1994). Hybrid control techniques for building structures. Proc. 1st World Conf. on Struct. Control.

Shukla, A. and T. Datta (1999). "Optimal use of viscoelastic dampers in building frames for seismic force." Journal of Structural Engineering 125(4): 401-409.

Singh, M. P. and L. M. Moreschi (2001). "Optimal seismic response control with dampers." Earthquake engineering & structural dynamics 30(4): 553-572.

Soneji, B. and R. Jangid (2007). "Passive hybrid systems for earthquake protection of cable-stayed bridge." Engineering structures 29(1): 57-70.

Soong, T. (1988). "State-of-the-art review: active structural control in civil engineering." Engineering Structures 10(2): 74-84.

Soong, T. and A. Reinhorn (1993). "An overview of active and hybrid structural control research in the US." The structural design of tall buildings 2(3): 193-209.

Spencer, B., S. Dyke, M. Sain and J. Carlson (1997). "Phenomenological model for magnetorheological dampers." Journal of engineering mechanics 123(3): 230-238.

Spencer Jr, B. and S. Nagarajaiah (2003). "State of the art of structural control." Journal of structural engineering 129(7): 845-856.

Spencer Jr, B., J. Suhardjo and M. Sain (1994). "Frequency domain optimal control strategies for aseismic protection." Journal of Engineering Mechanics 120(1): 135-158.

Stanway, R., J. Sproston and N. Stevens (1987). "Non-linear modelling of an electro-rheological vibration damper." Journal of Electrostatics 20(2): 167-184.

Sun, Q., L. Zhang, J. Zhou and Q. Shi (2003). "Experimental study of the semi-active control of building structures using the shaking table." Earthquake engineering & structural dynamics 32(15): 2353-2376.

Symans, M. D. and M. C. Constantinou (1997). "Seismic testing of a building structure with a semi-active fluid damper control system." Earthquake Engineering & Structural Dynamics 26(7): 759-777.

Symans, M. D. and M. C. Constantinou (1999). "Semi-active control systems for seismic protection of structures: a state-of-the-art review." Engineering structures 21(6): 469-487.

Symans, M. D. and S. W. Kelly (1999). "Fuzzy logic control of bridge structures using intelligent semi-active seismic isolation systems." Earthquake engineering & structural dynamics 28(1): 37-60.

Syswerda, G. (1989). "Uniform crossover in genetic algorithms."

Tamura, K., K. Shiba, Y. Inada and A. Wada (1994). Control gain scheduling of a hybrid mass damper system against wind response of tall buildings. Proc. of the First World Conference on Structural Control.

Terasawa, T. and A. Sano (2005). Fully adaptive vibration control for uncertain structure installed with MR damper. Proceedings of the 2005, American Control Conference, 2005., IEEE.

Tse, T. and C. Chang (2004). "Shear-mode rotary magnetorheological damper for small-scale structural control experiments." Journal of structural engineering 130(6): 904-911.

Tzan, S. R. and C. P. Pantelides (1994). "Hybrid structural control using viscoelastic dampers and active control systems." Earthquake engineering & structural dynamics 23(12): 1369-1388.

Uz, M. E. and M. N. Hadi (2014). "Optimal design of semi active control for adjacent buildings connected by MR damper based on integrated fuzzy logic and multi-objective genetic algorithm." Engineering Structures 69: 135-148.

Venini, P. and Y.-K. Wen (1994). Hybrid vibration control of MDOF hysteretic structures with neural networks. Proceedings of the First World Conference on Structures Control.

Wang, X. and F. Gordaninejad (2001). Dynamic modeling of semi-active ER/MR fluid dampers. SPIE's 8th Annual International Symposium on Smart Structures and Materials, International Society for Optics and Photonics.

Wongprasert, N. and M. Symans (2004). "Application of a genetic algorithm for optimal damper distribution within the nonlinear seismic benchmark building." Journal of Engineering Mechanics 130(4): 401-406.

Wu, B., J.-P. Ou and T. Soong (1997). "Optimal placement of energy dissipation devices for three-dimensional structures." Engineering Structures 19(2): 113-125.

Xia, P.-Q. (2003). "An inverse model of MR damper using optimal neural network and system identification." Journal of Sound and Vibration 266(5): 1009-1023.

Xu, Y., J. Chen, C. Ng and W. Qu (2005). "Semiactive seismic response control of buildings with podium structure." Journal of Structural Engineering 131(6): 890-899.

Xu, Y., W. Qu and J. Ko (2000). "Seismic response control of frame structures using magnetorheological/electrorheological dampers." Earthquake engineering & structural dynamics 29(5): 557-575.

Yang, G., B. Spencer, J. Carlson and M. Sain (2002). "Large-scale MR fluid dampers: modeling and dynamic performance considerations." Engineering structures 24(3): 309-323.

Yang, G., B. F. Spencer Jr, H.-J. Jung and J. D. Carlson (2004). "Dynamic modeling of large-scale magnetorheological damper systems for civil engineering applications." Journal of Engineering Mechanics 130(9): 1107-1114.

Yang, J.-N. (1975). "Application of optimal control theory to civil engineering structures." Journal of the engineering Mechanics Division 101(6): 819-838.

Yang, J., A. Danielians and S. Liu (1991). "Aseismic hybrid control systems for building structures." Journal of engineering mechanics 117(4): 836-853.

Yang, J., Z. Li and S. Liu (1992). "Control of hysteretic system using velocity and acceleration feedbacks." Journal of engineering mechanics 118(11): 2227-2245.

Yang, J., Z. Li, J. Wu and I. Hsu (1994a). "Control of sliding-isolated buildings using dynamic linearization." Engineering Structures 16(6): 437-444.

Yang, J., J. Wu, A. Reinhorn and M. Riley (1996). "Control of sliding-isolated buildings using sliding-mode control." Journal of Structural Engineering 122(2): 179-186.

Yang, J. N. and A. K. Agrawal (2002). "Semi-active hybrid control systems for nonlinear buildings against near-field earthquakes." Engineering Structures 24(3): 271-280.

Yang, J. N., J. Wu, A. Agrawal and Z. Li (1994b). Sliding mode control for seismic-excited linear and nonlinear civil engineering structures. Technical Report NCEER, US National Center for Earthquake Engineering Research. 94.

Yi, F., S. J. Dyke, J. M. Caicedo and J. D. Carlson (2001). "Experimental verification of multiinput seismic control strategies for smart dampers." Journal of Engineering Mechanics 127(11): 1152-1164.

Ying, Z., W. Zhu and T. Soong (2003). "A stochastic optimal semi-active control strategy for ER/MR dampers." Journal of Sound and Vibration 259(1): 45-62.

Yoshida, O. and S. J. Dyke (2004). "Seismic control of a nonlinear benchmark building using smart dampers." Journal of engineering mechanics 130(4): 386-392.

Yoshida, O., S. J. Dyke, L. M. Giacosa and K. Z. Truman (2003). "Experimental verification of torsional response control of asymmetric buildings using MR dampers." Earthquake engineering & structural dynamics 32(13): 2085-2105.

Yoshioka, H., J. Ramallo and B. Spencer Jr (2002). "“Smart” base isolation strategies employing magnetorheological dampers." Journal of engineering mechanics 128(5): 540-551.

Zahrai, S. and H. Salehi (2014). "Semi-active seismic control of mid-rise structures using magneto-rheological dampers and two proposed improving mechanisms." Iranian Journal of Science and Technology. Transactions of Civil Engineering 38(C1): 21.

Zhang, R.-H. and T. Soong (1992). "Seismic design of viscoelastic dampers for structural applications." Journal of Structural Engineering 118(5): 1375-1392.

Zhao, B., X. Lu, M. Wu and Z. Mei (2000). "Sliding mode control of buildings with base-isolation hybrid protective system." Earthquake engineering & structural dynamics 29(3): 315-326.

Zhu, W., M. Luo and L. Dong (2004). "Semi-active control of wind excited building structures using MR/ER dampers." Probabilistic engineering mechanics 19(3): 279-285.

BIO-DATA

The author is a regular PhD Research Scholar at Malaviya National Institute of Technology Jaipur, Jaipur (Rajasthan) since 2014. He obtained his Bachelor's Degree in Civil Engineering from M.B.M. Engineering College, Jodhpur (Rajasthan) in 2011. He completed his Master's Degree in Structural Engineering with dissertation on "**Seismic Response Prediction Using Artificial Neural Network**", from Malaviya National Institute of Technology Jaipur, Jaipur (Rajasthan) in 2013. His area of specialization is "Earthquake Engineering".

Following is the list of the publications from his Doctoral work

Conference

1. Vishisht Bhaiya, S. D. Bharti, M. K. Shrimali, "Observation Based Semi Active Control of Structures Using MR Dampers "**Sixteen World Conference on Earthquake Engineering** by IEA at Santigo, Chile / 1-13 / 2017
2. Vishisht Bhaiya, SD Bharti, M K Shrimali and TK Datta, "Performance of Semi Actively Controlled Building Frame Using MR Damper for Near Field Earthquakes" **10th Structural Engineering Convention** by SERC CSIR Chennai at Chennai / 1384-1388 / 2016

Journal

1. **Vishisht Bhaiya**, S. D. Bharti, M. K. Shrimali and T. K. Datta (2018), Genetic Algorithm Based Optimum Semi-Active Control of Building Frames Using Limited Number of Magneto-Rheological Dampers and Sensors. *Journal of Dynamic Systems, Measurement, and Control*, *140*(10), 101013.
2. **Vishisht Bhaiya**, SD Bharti, M K Shrimali and T K Datta (2016), "Effect of noises on the Active Optimal Control of Partially Observed Structures for White Random Ground Motion", Journal *of Noise Control Engineering* Volume :64 / 789-799 / 2016 ISBN: 9781498726740
3. Vishisht Bhaiya, S. D. Bharti, M. K. Shrimali and T. K. Datta, "Modified Seismic Semi-active Control of Partially Observed Systems Using MR Dampers", Soil Dynamics and Earthquake Engineering (Communicated)

4. Vishisht Bhaiya, S. D. Bharti, M. K. Shrimali and T. K. Datta, “Velocity Tracking Control Algorithm for Semi Active Control with MR Dampers”, Journal of Vibration and Control (Communicated)

5. Vishisht Bhaiya, S. D. Bharti, M. K. Shrimali and T. K. Datta, “Semi active Passive Hybrid Control of Building Frames Under Seismic Excitation”, Structures and Buildings, ICE (Communicated)